(1)

DEVELOPMENT OF A LEAST SQUARES TIME RESPONSE LOWER-ORDER EQUIVALENT SYSTEMS TECHNIQUE

THESIS

Clarke O. Manning
Captain, USAF

AFIT/GAE/ENY/90M-02

DEPARTMENT OF THE AIR FORCE
AIR UNIVERSITY
AIR FORCE INSTITUTE OF TECHNOLOGY

Wright-Patterson Air Force Base, Ohio

AFIT/GAE/ENY/90M-02

DEVELOPMENT OF A LEAST SQUARES TIME RESPONSE LOWER-ORDER EQUIVALENT SYSTEMS TECHNIQUE

THESIS

Clarke O. Manning
Captain, USAF

AFIT/GAE/ENY/90M-02

Approved for public release; distribution unlimited

AFIT/GAE/ENY/90M-02

DEVELOPMENT OF A LEAST SQUARES TIME RESPONSE LOWER-ORDER EQUIVALENT SYSTEMS TECHNIQUE

THESIS

Presented to the Faculty of the School of Engineering

of the Air Force Institute of Technology

Air University

in Partial Fulfillment of the

Requirements for the Degree of

Master of Science in Aerospace Engineering

Clarke O. Manning, B.S.

Captain, USAF

March 1990

Preface

This report represents the results of a year long research effort at the Air Force Institute of Technology, Wright-Patterson Air Force Base, Ohio, as well as three months of flight testing at the USAF Test Pilot School, Edwards Air Force Base, California. It has been an outstanding and challenging learning experience to be able to apply the theoretical basis of the AFIT thesis to the real world of flight testing.

I wish to express my gratitude to the many faculty members at the Air Force Institute of Technology who assisted in preparing this thesis. I am especially indebted to my thesis advisor Major (Dr.) Daniel Gleason and to Dr. Robert Calico for their ideas and advice on many difficult theoretical areas.

I am also deeply indebted to the members of the HAVE CONTROL test team, the Test Pilot School staff, and the CALSPAN Corporation who assisted in the flight testing. The members of the HAVE CONTROL test team included Capt Steve Lindsey, Capt Kurt Baum, Capt Rodney Liu, Capt Steve Thomas, and Capt Clarke Manning. The CALSPAN project pilots were John Ball and Russ Easter. I also wish to thank 1Lt Dan Ringenbach of the Air Force Flight Test Center Simulation Facility and SSGT Howard Burkett and Lorraine Hed of the USAF Test Pilot School for their assistance with the data acquisition system and data reduction.

Finally, I wish to thank my wife, Carrie, for her support throughout the two year AFIT/TPS program.

Clarke O. Manning

Table of Contents

Table of Contents (Concluded)

List of Figures

List of Figures (Continued)

Figure Page

List of Figures (Continued)

List of Figures (Continued)

List of Figures (Continued)

Figure Page

List of Figures (Concluded)

Figure Page

List of Tables

List of Tables (Concluded)

Table | Page

List of Abbreviations and Symbols

ABBREVIATION	DEFINITION
AFB	Air Force Base
AFFTC	Air Force Flight Test Center
AFIT	Air Force Institute of Technology
AOA	Angle of Attack, degrees
ARMA	Auto Regressive Moving Average
A/C	Aircraft
CAP	Control Anticipation Parameter, $g^{-1}sec^{-1}$
DAS	Data Acquisition System
DFCS	Digital Flight Control System
DFBW	Digital Fly-By-Wire
HOS	Higher Order System
HUD	Head-up Display
KCAS	Knots Calibrated Airspeed
KIAS	Knots Indicated Airspeed
LOES	Lower Order Equivalent System
LOS	Lower Order System
LONFIT	Longitudinal Frequency Response Curve Fit
LS	Least Squares
MACFIT	General Frequency Response Curve Fit
MIL-STD	Military Standard
OCM	Optimal Control Model
PHQR	Pilot Handling Qualities Rating

List of Abbreviations and Symbols (Continued)

ABBREVIATION	DEFINITION
PIO	Pilot Induced Oscillation
PR	Pilot Rating
SISO	Single Input-Single Output
S/N	Serial Number
TF	Transfer Function
TPS	Test Pilot School
USAF	United States Air Force
USAFTPS	USAF Test Pilot School
VSS	Variable Stability System

SYMBOL	DEFINITION
A	State matrix
A_{nz}	Gain of n_z/δ_e for aircraft, g/rad
A_θ	Gain of $\dot{\theta}/\delta_e$ for aircraft, rps/rad
B	Control matrix
cg	Center of gravity, percent chord
C	Output matrix
$Cost_f$	Frequency Domain Cost Function
$Cost_t$	Time Domain Cost Function
DB	Decibels
e	Error function
F	Discrete state matrix
F_s	Longitudinal Stick Force, pounds

List of Abbreviations and Symbols (Continued)

SYMBOL	DEFINITION
F_{es}	Longitudinal Stick Force, pounds
F_{as}	Lateral Stick Force, pounds
g	Acceleration of gravity, ft/sec^2
G	Discrete control matrix
H	Discrete output matrix
$H(z)$	Discrete transfer function matrix
I	Identity matrix
J	Cost Function
J_β	Change in cost function due to change in parameter vector
k	Discrete time step (k=1,2,3,...N)
K_{fs}	Gain of feel system TF, in/lb
K_{gr}	Gain of actuator TF, rad/in
K_{nz}	Gain of n_z/F_s LOES, g/lb
K_p	Gain of pugoid LOES, rps/lb
K_{sp}	Gain of short period LOES, rps/lb
K_θ	Gain of $\dot{\theta}/F_s$ (short period) LOES, rps/lb
L_α	Lift curve slope, sec^{-1}
M	Mach number
M	Sum of squares mismatch function
M_α	Pitching moment in body axis due to α
M_q	Pitching moment in body axis due to q
M_u	Pitching moment in body axis due to u
M_w	Pitching moment in body axis due to w

List of Abbreviations and Symbols (Continued)

SYMBOL	DEFINITION
$M_{\delta e}$	Pitching moment in body axis due to δ_e
n	Normal load factor, g
n_z	Normal load factor, g
q	Perturbed pitch rate, rps
rps	Radians per second
R	Set of real numbers (matrix space)
s	Laplace transform variable
t, T	Time, sec
T_a	Actuator time constant, sec^{-1}
T_{h1}	n_z/F_s numerator term, sec^{-1}
t_m	Least squares match time, sec
T_n	Undamped natural period, sec
T_{nz1}	n_z/F_s numerator term, sec^{-1}
T_{nz2}	n_z/F_s numerator term, sec^{-1}
t_r	Rise time of ramp input, sec
$T_{\theta 1}$	Phugoid numerator term, sec^{-1}
$T_{\theta 2}$	Short period numerator term, sec^{-1}
u	Perturbed forward speed in the body axis, ft/sec
u	Input (or control) vector
u(k)	Discrete input vector
U_o	Equilibrium forward speed, feet/sec
v, V	Velocity, ft/sec
w	Perturbed downward speed in the body axis, ft/sec

List of Abbreviations and Symbols (Continued)

SYMBOL	DEFINITION
WT1	Weighting function in calculation of $cost_f$
WT2	Weighting function in calculation of $cost_f$
w_o	Equilibrium downward speed, ft/sec
x	State vector
X_q	Longitudinal force in body axis due to q
X_u	Longitudinal force in body axis due to u
X_w	Longitudinal force in body axis due to w
$X_{\delta e}$	Longitudinal force in body axis due to δ_e
y	Output vector
y(k)	Discrete output vector
z	Discrete Laplace transform variable
Z_α	Vertical force in body axis due to α
Z_q	Vertical force in body axis due to q
Z_u	Vertical force in body axis due to u
Z_w	Vertical force in body axis due to w
$Z_{\delta e}$	Vertical force in body axis due to δ_e
α	Angle of attack, degrees
β	Perturbed sideslip angle, deg
β, β, β^o,	Parameter vectors
β_{LS}	Least squares estimate of parameter vector
δ_e	Elevator deflection, rad
δ_{es}	Longitudinal control stick deflection, rad
Φ	Roll angle in the body axis, deg

SYMBOL	DEFINITION
Φ	Phase angle, rad
ω_d	Dutch roll natural frequency, rps
ω_e	Equivalent natural frequency, rps
ω_{fs}	Feel system natural frequency, rps
ω_n	Discrete frequencies (n = 1,2,3,...), rps
ω_{nz}	Numerator natural frequency (n_z/δ_e), rps
ω_p	Phugoid natural frequency, rps
ω_{sp}	Short period natural frequency, rps
ω_{180}	Open loop frequency at 180 degrees phase, rps
ω_{BW}	Bandwidth frequency, rps
τ	Equivalent time delay, sec
τ_e	Equivalent time delay, sec
τ_θ	Equivalent time delay, sec
τ_p	Phase delay, sec
TD	Actual time delay, sec
τ_r	Roll mode time constant, sec
τ_1	Pre-filter HOS dynamics first order numerator time constant, sec
τ_2	Pre-filter HOS dynamics first order denominator time constant, sec
θ	Perturbed pitch angle in the body axis, deg
θ_o	Equilibrium pitch angle, deg
ζ_d	Dutch roll damping ratio
ζ_e	Equivalent damping ratio

List of Abbreviations and Symbols (Concluded)

SYMBOL	DEFINITION
ζ_{fs}	Feel system damping ratio
ζ_{nz}	Numerator damping ratio (n_z/δ_e)
ζ_p	Phugoid damping ratio
ζ_{sp}	Short period damping ratio

Abstract

The most widely accepted method for specifying flying qualities of highly-augmented aircraft is the low-order equivalent systems technique. This technique matches the frequency response of a high-order system (HOS) with a lower-order equivalent system (LOES). The LOES is generally in the form of a "classical" (unaugmented) aircraft so that comparisons with the classical data base can be made. Most LOES research has been accomplished using frequency response matching, however there are also methods available for matching the time responses of the HOS and LOES. Time response matching is an attractive option for flight test applications since all that is required is output versus input data.

This thesis develops and tests a Least Squares LOES time response matching program. The program was tested analytically at the Air Force Institute of Technology, Wright-Patterson AFB, OH. During the analytical testing, a HOS was modeled using an A-4D aircraft with servo-actuator and feel system dynamics. Lower order equivalent parameters were calculated using the Least Squares program and the results were compared to those obtained using a frequency response matching program (LONFIT). Various flight conditions and feel system dynamics were used to change the HOS dynamics and the effects of these changes on the two matching techniques were investigated.

The Least Squares LOES program was also tested during a flight test program at the USAF Test Pilot School, Edwards AFB,

CA. During this test a variable stability NT-33A aircraft operated by the CALSPAN Corporation was used to model the higher-order aircraft dynamics. Thirteen configurations were tested using system identification and offset landing tasks. The configurations were chosen to span Level 1, 2, and 3 flying qualities by varying ω_{sp}, ζ_{sp}, and pre-filter dynamics. The LOES Least Squares program was used to predict the flying qualities of the configurations based on MIL-STD-1797 guidance for equivalent ζ_{sp}, ω_{sp}, and τ_{θ}. Parameter identification was also accomplished using the actual flight test output versus input data. The results of the flying qualities predictions were compared to predictions given by Hoh's Bandwidth method for specifying flying qualities.

DEVELOPMENT OF A LEAST SQUARES TIME RESPONSE LOWER-ORDER EQUIVALENT SYSTEMS TECHNIQUE

I. Introduction

Background

The use of complex augmentation systems for modern airplanes has necessitated the development of various methods for predicting and analyzing their flying qualities. The Military Specification for Flying Qualities of Piloted Airplanes, MIL-F-8785B (1) was developed in the 1960's for unaugmented airplanes and did not account for high-order augmentation systems. As a result, some modern airplanes were designed without direct benefit of the guidelines of MIL-F-8785B since these guidelines were not considered to be applicable. MIL-F-8785C (2), published in 1980, did acknowledge the existence of high-order systems and the current specification, MIL-STD-1797 (3) includes detailed recommendations of methods for specifying the flying qualities of these systems. MIL-STD-1797 states that the preferred method for specifying flying qualities of highly augmented aircraft is the low-order equivalent systems approach. This approach makes use of the substantial data base that exists for unaugmented "classical" aircraft and retains the requirements of MIL-F-8785.

Hodgkinson (4) demonstrates the need for equivalent systems by first reviewing conventional methods for specifying flying qualities. In the past, the short term pitch rate dynamics were typically represented by a linear second order response to stick

force. This representation, known as the short period approximation, is shown in equation 1.

$$\frac{\dot{\theta}}{F_s} = \frac{K_\theta(s + 1/T_{\theta 2})}{(s^2 + 2\zeta_{sp}\omega_{sp}s + \omega_{sp}^2)} = \frac{(1/T_{\theta 2})}{[\zeta_{sp};\omega_{sp}]} \qquad (1)$$

Texts such as McRuer et al. (5) define all of the terms in this function using aerodynamic characteristics, aircraft speed, inertia, etc. This expression ignores high-order terms such as structural modes, stick dynamics, and the interaction of other aerodynamic modes of motion such as the phugoid. The effects of these terms were considered small, as were the effects of linearization; or if they were significant, they could be considered separately. Thus, this transfer function defined a well-accepted "simulation space". That is, the parameters K_θ, $1/T_{\theta 2}$, ζ_{sp}, and ω_{sp} provided all the information necessary to simulate the short period response of the aircraft. Additionally, these parameters appear (explicitly or implicitly) in MIL-F-8785 and in MIL-STD-1797 meaning that they also define a well-accepted "specification space" for short term pitch dynamics. For past aircraft, the dimension of the simulation space and specification space was the same.

Transfer functions required to simulate modern aircraft dynamics have grown in complexity. Figure 1, for example, shows the pitch rate transfer function which emerged during the development of the F-18 digital flight control system. Even with the same simplifying assumptions used in equation 1, the simulation

space required to describe short-term pitch rate dynamics for the F-18 has 89 dimensions! Using the same approach as in the past, this means that a 89-dimensional specification space would be required to specify the longitudinal short period dynamics! Clearly, another approach is needed.

$$\frac{\dot{\theta}}{F_S} = \frac{[-0.5;127]\ [-0.3;83]\ [-0.07;61]\ [1;0.9]\ [1;1]\ [1;1.2]}{(0.5)\ (0.8)\ (0.9)\ [1;1.1]\ (2)\ [1;2.4]\ [0.7;4.1]\ (3.4)}$$

$$\times \frac{[1;2.3]\ [1;2.8]\ (4)\ [0.1;53]\ (13)\ (14)\ [0.4;34]\ [0.34;46]}{(3.7)\ (6.7)\ [0.2;53]\ [1;13]\ [0.4;33]\ [0.7;20]\ [0.3;42]}$$

$$\times \frac{[0.55;39]\ [1;22]\ [0.7;37]\ [0.9;34]\ [0.9;34]\ (35)}{[0.9;16]\ [0.6;27]\ [0.3;66]\ [0.4;85]\ [0.4;105]\ [0.9;47]}$$

$$\times \frac{1}{[0.3;140]\ [0.4;180]\ [0.7;102]\ (72)\ [0.5;228]\ (112)\ [0.6;279]}$$

$$\times \frac{1}{[0.8;329]\ (259)\ [0.9;378]\ [1;410]}$$

$$\times \text{TERMS DUE TO DIGITAL SYSTEM}$$

Figure 1. Modern High-Order Response (Reference 4)

Since it is impractical to change the MIL Standard requirements to correspond to the complexity of these high-order systems, analytical tools have emerged so that high-order systems can be specified in fewer dimensions. Several methods are

presented in MIL-STD-1797 including the low-order equivalent systems approach, which approximates high-order responses with low-order responses; the Neal-Smith method, which uses a mathematical model of the pilot; and the bandwidth method, which takes simple frequency response measurements. If the gain parameter is specified separately, the equivalent system of equation 1 has a three-dimensional specification space. The Neal-Smith and bandwidth methods are two-dimensional. Human pilots process these systems to produce a one-dimensional specification of flying qualities - the Cooper-Harper rating.

The Low-Order Equivalent System Method

The low-order equivalent system method provides an order reduction by matching (in a least squares sense) the frequency response of the high-order system (HOS) to that of a low-order equivalent system (LOES). The LOES pitch rate and normal load factor transfer function forms to be used for the matching are given in MIL-STD-1797 as follows:

$$\frac{\dot{\theta}}{F_s} = \frac{K_\theta s(s + 1/T_{\theta 1})(s + 1/T_{\theta 2})e^{-\tau s}}{(s^2 + 2\zeta_p\omega_p s + \omega_p{}^2)(s^2 + 2\zeta_{sp}\omega_{sp}s + \omega_{sp}{}^2)} \qquad (2)$$

$$\frac{n_z}{F_s} = \frac{K_n(s + 1/T_{h1})e^{-\tau s}}{(s^2 + 2\zeta_p\omega_p s + \omega_p{}^2)(s^2 + 2\zeta_{sp}\omega_{sp}s + \omega_{sp}{}^2)} \qquad (3)$$

These expressions are linearized, reduced-order models of the actual aircraft response. The MIL-Standard states that in most

cases the phugoid and short period modes are sufficiently separated that further order reduction is possible (i.e. for the pitch rate LOES) as follows:

$$\text{Phugoid:} \quad \frac{\dot{\theta}}{F_s} = \frac{K_p(s + 1/T_{\theta 1})}{(s^2 + 2\zeta_p\omega_p s + \omega_p{}^2)} \qquad (4)$$

$$\text{Short Period:} \quad \frac{\dot{\theta}}{F_s} = \frac{K_{sp}(s + 1/T_{\theta 2})e^{-\tau s}}{(s^2 + 2\zeta_{sp}\omega_{sp} s + \omega_{sp}{}^2)} \qquad (5)$$

Equations 4 and 5 are universally recognized as pitch rate models of phugoid and short period dynamics and may normally be used in place of the three-degree-of-freedom equations over their appropriate respective frequency ranges. The normal load factor LOES can be reduced in the same manner. General guidelines regarding when to use the two-degree-of-freedom versus the three-degree-of-freedom equations are discussed in more detail in chapter II.

Computer programs accomplish the frequency response matching by varying the LOES parameters so as to minimize an error function between the HOS and LOES over the frequency range of interest. This frequency range is defined by MIL-STD-1797 as follows:

ω_1 - Normally 0.1 rad/sec but > ω_p

ω_2 - Normally 10.0 rad/sec but > the resulting equivalent ω_{sp} and $1/T_{\theta 2}$

and, the general form of the error function is:

$$M = \Sigma (\Delta G)^2 + K \Sigma (\Delta \Phi)^2$$

$$= \Sigma (G_{HOS} - G_{LOES})^2 + K \Sigma (\Phi_{HOS} - \Phi_{LOES})^2 \qquad (6)$$

where: M is the sum-of-squares "mismatch" function

G is the amplitude in decibels

Φ is the phase angle in radians

K is a weighting factor

ΔG and $\Delta \Phi$ are calculated at discrete frequencies between ω_1 and ω_2 evenly spaced on a logarithmic scale. Note that the mismatch function is not well defined unless the number of discrete frequencies is specified. For this reason, 20 frequencies are generally used, or else M is normalized by 20/n where n is an arbitrary number of frequencies selected for the match (6). This will be seen in chapter III where the error function for the computer programs LONFIT and MACFIT is defined. The weighting factor K is generally specified at approximately 0.017. This gives approximately the same importance to one decibel of gain mismatch as to eight degrees of phase mismatch (7).

Mismatch Criteria

Because low-order equivalent systems are only an approximation to the actual high-order system there is a need to define acceptable versus unacceptable levels of mismatch between the two (i.e. how "good" does the match have to be for the equivalent system to provide an acceptable approximation?) The need to define

acceptable mismatch criteria is often cited as a fundamental drawback of the equivalent system technique. Other criteria such as the Neal-Smith and bandwidth methods simply use the response of the high-order system and do not involve a matching process. Therefore it is said that the question of mismatch does not arise, which is an advantage. Hodgkinson (4) argues that any method for specifying high-order systems involves a reduction in dimension which means that some high-order effects are ignored. These effects are quantified as "mismatch" for low-order equivalent systems, but can be similarly quantified for the Neal-Smith and bandwidth methods using the concept of a "minimum order system." In fact, the more a specification method reduces the dimension (i.e. the lower the order of its minimum order system) the larger the mismatch can be.

Regarding the specification of acceptable mismatch criteria, MIL-STD-1797 states the following:

> There is currently insufficient data to place definitive requirements on mismatch between the HOS and LOES. It should be noted, however, that the question of mismatch is inherent in any n-dimensional specification of an m-dimensional response, when $n < m$. (3)

Hodgkinson and Johnston (8) addressed the question of mismatch with the USAF/CALSPAN NT-33 aircraft in an investigation of longitudinal and lateral dynamics during landing. The flying qualities of various high-order systems and their low-order equivalents were compared. Pilot ratings were used to determine how closely the LOES must approximate the HOS to be a valid flying qualities prediction tool. It was found that rather large

analytical mismatch values proved unnoticeable to the pilots. The report concludes with a tentative guideline of a mismatch value of 200 or less as a LOES criterion for representative augmented dynamics. This guideline is also quoted in MIL-STD-1797. This guideline is considerably more lenient than the previous "limit" of 10 which was based solely on the visual appearance of the frequency response mismatch.

Another study used by the MIL-Standard to define acceptable mismatch criteria was conducted by Hodgkinson and Wood (9). These investigations compared pilot rating differences between pairs of configurations in previous NT-33 experiments. Each pair of configurations consisted of an unaugmented, low-order aircraft response and a high-order system formed by adding terms to the low-order response. From these comparisons, mismatch envelopes of "maximum unnoticeable added dynamics" were derived (figure 2). MIL-STD-1797 states that mismatches between the HOS and the LOES in excess of the values shown in figure 2 would be cause to suspect that the equivalent parameters may not accurately predict pilot opinion.

Equivalent Time Delay

Equivalent system studies by DiFranco, Neal-Smith, and MCAIR (10,11,12) determined that the specification space of classical systems is insufficient to adequately model most high-order systems. This is true primarily because the phase lags of the high-frequency modes are not accounted for. Since the major effect

of these high-frequency modes (i.e. frequencies well beyond the crossover frequency) is an equivalent time delay, the solution to the problem is to add an equivalent time delay term to the low-order system. (This is the e^{-TS} term shown in equations 2,3, and 5).

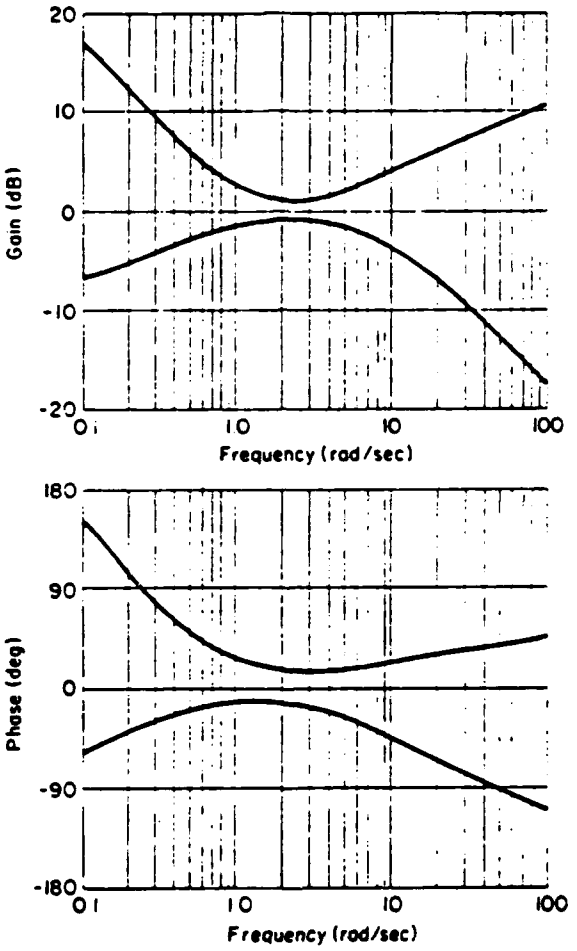

Figure 2. Envelopes of Maximum Unnoticeable Added Dynamics (Reference 3)

Equivalent time delay can be used to model the effects of many different flight control components such as stick prefilters, feel systems, actuators, and structural filters. The DiFranco and Neal-Smith investigations (10,11) found that these time-delays - - -

consistently degraded pilot ratings down. Time delay therefore has a significant effect on flying qualities and must be included in any viable equivalent system model. This adds one extra dimension to the specification space in the MIL-Standards.

Problems Encountered in LOES Methods

The encouraging results from equivalent systems techniques hold much promise for their ability to specify flying qualities of highly sophisticated aircraft. There are, however, a few unresolved questions to be addressed concerning the LOES approach. The most significant question is on the definition of "equivalence" itself. In some cases it has been shown that the LOES parameters are not necessarily equivalent to their classical counterparts. Before discussing this point further, it will be helpful to review the MIL-Standard requirements for longitudinal equivalent system parameters.

The requirements on equivalent pitch time delay (τ_θ) and on equivalent short period damping (ζ_{sp}) are straightforward and are specified as follows (3):

Equivalent Time Delay and Short Period Damping Ratio Criteria:

Level	Allowable Delay	Allowable ζ_{sp} Limits
1	0.10 (sec)	0.35-1.30
2	0.20 (sec)	0.25-0.35 or 1.30-2.00
3	0.25 (sec)	< 0.25 or > 2.00

The requirements on equivalent short period natural frequency (ω_{sp}) are given in terms of the control anticipation parameter (CAP) defined as CAP = $\omega_{sp}^2/(n/\alpha)$ where $n/\alpha = (V/g)(1/T_{\theta 2})$. CAP is

approximately equal to the ratio of initial pitching acceleration to steady state normal acceleration. Because of the time lapse before reaching steady state, the pilot needs an earlier indication of the response to control inputs. Both the initial and final responses must be neither too sensitive nor too insensitive to the commanded flight-path changes. The requirements on CAP are listed below (3):

Equivalent Short Period Natural Frequency Criteria:

Level	Allowable CAP Limits ($g^{-1}sec^{-1}$)
1	0.28-3.60
2	0.16-0.28 or 3.60-10.00
3	< 0.16 or > 10.00

The ζ_{sp} and CAP requirements shown above are for category A (rapid maneuvering, precision tracking, or precise flight-path control) flight phases only. For a more complete discussion of these requirements, the interested reader is referred to MIL-F-8785C (2) or to MIL-STD-1797 (3).

The available data base of HOS flying qualities piloted evaluations is currently quite limited. The Neal-Smith (11) and Landing Approach High-Order System "LAHOS" (13) studies are the most widely recognized. Fortunately, this small quantity of data covers quite a large range of flight conditions and tasks. The Neal-Smith investigation provides good examples of both the encouraging results from the LOES method as well as problems that have been encountered. Of the 51 configurations flown in the Neal-Smith program, 41 were either unaugmented or included only first or second order lags. The flying qualities of 28 of these were

correctly predicted by the LOES method. The remaining ten configurations had (possibly unrealistic) lead/lag combinations, and only five of these were predicted accurately. For the five that failed, the equivalent dynamics (ζ_{sp}, ω_{sp}, $1/T_{\theta 2}$, and τ_θ) predicted level 1 flying qualities but were rated level 2 by the pilots.

There are two potential methods for dealing with lead/lag systems like those in the Neal-Smith study. Unfortunately, neither is physically very appealing and, in each, there is an underlying question as to the universality of the equivalent systems approach.

Redefine Limits on ζ_{sp}

If the minimum allowable ζ_{sp} for level 1 were increased from 0.35 to 0.50, four of the five configurations would meet the requirements (i.e. predict level 2). But applying this restriction to unaugmented aircraft as well is unappealing since the lower ζ_{sp} boundary is well supported by flight test data for classical aircraft. The alternative is to specify two sets of requirements - one for unaugmented aircraft and one for augmented aircraft. This is especially unattractive since it is an admission that "ζ_e" is not equivalent to ζ_{sp} and "equivalent systems" is a misnomer. Additionally, specifying two sets of requirements presents the problem of defining the specific level of augmentation at which the requirements would change over. For example, should the addition of a simple high-frequency stick filter (whose only major effect is to increase τ) suddenly mean that the airplane must meet a more

stringent damping requirement?

Redefine τ

Three of the four low ζ_{sp} violators discussed above also had $\tau = 0$ and it was found that a better LOES fit could have been obtained for these three cases if τ were allowed to be less than zero. This illustrates another fundamental problem with the LOES approach. The problem is in interpreting the significance of negative time delay or time lead. Physically, it might be considered to represent a high-order system which is too abrupt (i.e. the system responds τ seconds before the input is made or has finite magnitude at zero time). Unfortunately, the concept of a system responding prior to an input (i.e. a non-causal system) is not very appealing physically and it raises some question as to whether or not the equivalent systems approach is universally applicable.

Another important question regarding the LOES approach is whether or not all LOES parameters should be freed in the matching process. Specifically, it is argued that the pitch numerator term $1/T_{\theta 2}$ (which is approximately equal to L_α) should be held at the basic aircraft value. The rationale behind keeping it fixed is that L_α is determined by wing size and planform which are dimensions that can not be varied for a particular aircraft. In LOES studies where L_α has been freed, however, the results have produced large changes in L_α from the basic aircraft values (3). Again, this raises questions as to the "equivalence" of the LOES

parameters. For example, how is the equivalent L_α to be interpreted if it is significantly higher (or lower) than the basic aircraft value?

It should be mentioned that despite the problems discussed in this section, the LOES approach to the analysis of highly augmented aircraft continues to show promise. The success obtained with HOS flight tests (11,13) has shown that the pitch short period equivalent dynamics are relatable to their classical counterparts for most cases. An additional important finding resulting from LOES studies is the significant role that equivalent time delay can play in the degradation of both longitudinal and lateral flying qualities (8,10,11.12).

The LOES approach, as defined in this chapter, is accomplished by minimizing the frequency response error (equation 6) between the HOS and the LOES. Most research in this area has been accomplished using this type of frequency response matching, however there are also methods available for matching the time response of the HOS and the LOES. In certain applications, matching the time response may be an attractive option since the HOS does not need to be modeled in the frequency domain. Instead, all that is required is the time history of HOS input and response. This approach, therefore, may be especially well suited to flight test system identification requirements. Shafer (14), for example, has conducted investigations using maximum likelihood estimation and the input/output time histories of flight test data. Her studies used data from the highly augmented F-8 digital fly-by-wire (DFBW)

aircraft to create a LOES model of the aircraft's longitudinal system response. Shafer reported encouraging results in that the dynamics of the HOS were excellently matched by the maximum likelihood technique. Further investigations using this technique are in progress.

Another possible advantage to time response matching is that the time response is a measure of the real world behavior (i.e. it is a measure of how the aircraft actually "flies"). Thus, matching in the time domain would apparently ensure a LOES that "flies" more like the HOS. A fundamental question in this regard however, is whether or not a good match in the time domain corresponds to a good match in the frequency domain. The answer to this question is important if the final step of the matching technique is the extraction of frequency response data (ζ_{sp}, ω_{sp}, $1/T_{\theta 2}$, and τ_{θ}) in order to take advantage of the classical data base.

The purpose of this thesis is to develop and test a time response matching technique adaptable to flight test parameter identification requirements. The technique will be compared to a frequency response matching program, Hoh's Bandwidth method, and actual pilot ratings. Comparisons between the techniques will be based on mathematical analysis such as fidelity of matching and differences between LOES parameters, as well as subjective analysis such as problems encountered during matching and adaptability to flight test data analysis techniques.

II. High-Order Control Systems

It has been known for some time that control system dynamics, as well as open-loop airplane dynamics, effect the handling qualities of the closed-loop pilot and airplane combination. Prior to the late 1960's, however, most handling qualities investigations were concerned primarily with the effects of variations in certain open-loop airplane parameters. The control system characteristics were, in general, held constant and their effect on airplane response to pilot inputs was not investigated. By making the control system sufficiently "fast" compared to the open-loop airplane, it was assumed that the effects of the control system dynamics could be neglected. With this simplifying assumption, the handling qualities were described in terms of the following open-loop airplane parameters:

(1) The short period frequency (ω_{sp}) and damping ratio (ζ_{sp})

(2) The pitch attitude numerator term (L_α) and the response ratio (n/α)

(3) The maneuvering stick force gradient (F_s/n)

The above airplane parameters can be used to adequately describe handling qualities if the effects of the control system are not too significant. In recent years, however, complex flight control systems have become increasingly common. These systems, with various types of feedback and feedforward loops, may introduce significant time delay and/or additional dynamic modes which have natural frequencies close to the airplane's short

period frequency. When this is the case, the airplane's flying qualities can become completely unacceptable even if the short period mode itself is well behaved.

The increased complexity of flight control systems has been a direct result of increased aircraft performance. Prior to the 1940's, the flight and loading envelopes of most airplanes were limited enough that stick force per g (F_s/n) could be kept within reasonable limits. The control systems were generally low-inertia mechanical systems, with restoring and damping forces derived from aerodynamic hinge moments. The dynamics of these control systems were quite fast compared to the aircraft dynamics, and there was little coupling between the aircraft and control system modes. Friction and freeplay could cause significant control system lag for small control inputs, however, resulting in control problems during precision maneuvers.

As airplane performance increased, it became difficult to keep maneuvering forces (F_s/n) within reasonable limits. The high stick forces due to increased elevator hinge moments were overcome by the introduction of aerodynamic devices such as spring tabs, horn balances, and set back control surfaces. In order to minimize variations in F_s/n, normal acceleration bobweights were often employed.

As performance was increased even further, it became necessary to resort to hydraulic actuator controls to overcome the increased hinge moments. The use of hydraulic powered control introduced another control system problem: there was no feedback

of control surface hinge moments to the stick for feel. To make the aircraft "feel right" to the pilots, feel springs were added. Pilots normally fly by physical association between applied force and maneuvering response. At low dynamic pressure, the predominant cue is pitch rate and, at high dynamic pressure the predominant cue is acceleration. Without feel devices, the maneuvering response cues were still present, but the stick "flopped" around the cockpit, and the need for force producers at the controls became critical. Feel springs were able to solve part of the problem, especially at low dynamic pressure, and the bobweight was able to provide additional force at the control stick during high g maneuvering flight.

The problem with feel springs, hydraulic actuators, bobweights, and other control augmentation systems is that they may introduce unwanted dynamics into the flight control system. This in turn may lead to control difficulties during maneuvering flight and in some cases lead to severe oscillations of the aircraft. From an equivalent systems standpoint, the control system dynamics may cause difficulties in the matching process. The aircraft dynamics may be changed by the presence of the control system to the point that it is no longer possible to match the system to conventional low-order forms. These matching difficulties seem to be compounded when the control system dynamics are "close" to the aircraft dynamics and there is coupling between the control system and aircraft roots.

The next sections of this chapter develop high-order control

and aircraft systems that are typical of systems currently in use on modern high-performance fighters. This will be accomplished using feel system and servo-actuator dynamics combined with conventional aircraft dynamics (A-4D). Since the primary purpose for modeling these high-order systems is to compare equivalent systems methods, the intent here is not to create overly complex systems. There are certainly other causes of high-order effects besides feel systems and servo-actuators (i.e. stability augmentation, model following, structural dynamics, bobweights, etc.) that will not be considered here. The available data base for HOS flying qualities piloted evaluations is currently quite limited, but some of the most widely recognized programs have used a feel system and actuator to model the high-order effects. The development presented here is adapted from these sources (10,11).

Control System Block Diagram

A block diagram of the open-loop airplane control through a feel system and actuator is shown in figure 3. As illustrated in the diagram, control is initiated by the pilot applying a control force (F_s) to the stick. Through the dynamics of the elevator feel system, this force results in a stick displacement (δ_{es}) which is an input to the elevator actuator. The elevator deflection (δ_e) is a function of the actuator dynamics, and commands the response of the airplane as determined by the airplane dynamics.

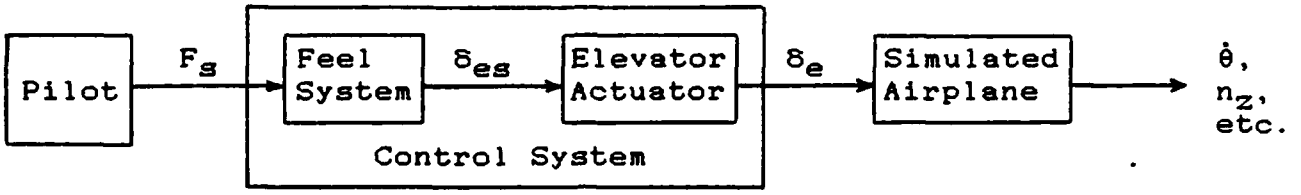

Figure 3. Block Diagram of Open-Loop Airplane Control

The overall aircraft response to pilot-applied stick-force inputs can be represented as a transfer function which is the product of the transfer function of the feel system, actuator, and airplane. Thus, the pitch rate ($\dot{\theta}$) and normal acceleration (n_z) transfer functions for stick force inputs (F_s) can be expressed as follows:

$$\frac{\dot{\theta}(s)}{F_s(s)} = \frac{\dot{\theta}(s)}{\delta_e(s)} \times \frac{\delta_e(s)}{\delta_{es}(s)} \times \frac{\delta_{es}(s)}{F_s(s)} \qquad (7)$$

$$\frac{n_z(s)}{F_s(s)} = \frac{n_z(s)}{\delta_e(s)} \times \frac{\delta_e(s)}{\delta_{es}(s)} \times \frac{\delta_{es}(s)}{F_s(s)} \qquad (8)$$

The parameters of each of the elements (feel system, actuator, and airplane) in the above transfer functions can be varied independently during ground or in-flight simulations to assess the effects on handling qualities of various combinations of these elements. A detailed description of each of these elements is given in the following sections.

Feel System Dynamics

The feel system dynamics can be approximated reasonably well with a "spring-mass-damper system" as shown by Biezad (15). This model results in the following second-order transfer function:

$$\frac{\delta_{es}}{F_s} = \frac{K_{fs}\omega_{fs}^2}{s^2 + 2\zeta_{fs}\omega_{fs}s + \omega_{fs}^2} \qquad (9)$$

The natural frequency and damping ratio (ω_{fs} and ζ_{fs}) determine the dynamics of the feel system and can be varied independently of the aircraft dynamics to evaluate their effects on aircraft response. The natural frequency ω_{fs} can be varied from approximately 6 to 31 rad/sec which effectively selects "slow" to "fast" feel system response times. During the matching process, ω_{fs} was varied from 6 rad/sec ("close" to the aircraft roots) to 31 rad/sec ("far" from the aircraft roots). This was done to investigate the effects of control system/aircraft coupling on equivalent systems techniques.

The damping ratio ζ_{fs} was varied from 0.45 to 1.00 to determine values which would provide the desired HOS time response characteristics. With the "slow" feel system, it was found that a value of ζ_{fs} = 1.00 resulted in the greatest coupling between the control system and aircraft roots. The "moderate" feel system, and ζ_{fs} = 1.00, resulted in a relatively uncoupled (pure time delay) HOS response. Since the intent was not to evaluate changes in the damping ratio from one configuration to another, and

because ζ_{fs} = 1.00 was found adequate to provide the desired coupled and uncoupled response characteristics, ζ_{fs} was held constant at 1.00 for all HOS configurations.

A complete specification of the feel system requires specification of the steady-state spring gradient $(F_s/\delta_{es})_{ss}$. Applying the final value theorem for Laplace transforms to eq. 9 gives the steady-state spring gradient for a step input as $(F_s/\delta_{es})_{ss} = 1/K_{fs}$. During the matching process, the feel system gain was held constant at K_{fs} = 0.046 which corresponds to a steady-state spring rate of 21.7 lbs/in. This is a typical value of the spring gradient for fighter "up and away" evaluations (11).

The variation in feel system response time is illustrated in figure 4 which compares "moderate" (ω_{fs} = 18.5 rad/sec) and "slow" (ω_{fs} = 6 rad/sec) feel systems. In each case, the response is shown for a step input with ζ_{fs} = 1.00 and K_{fs} = 0.046. To demonstrate the spring gradient calibration, a step input of F_s = 21.7 lbs is used which results in the correct steady-state output of $(\delta_{es})_{ss}$ = 1.00 in.

Servo-Actuator Dynamics

The servo-actuator dynamics can be approximated by a first-order "lag" response as shown by Biezad (15) and Roskam (16). The transfer function used to represent the servo-actuator is shown below:

$$\frac{\delta_e}{\delta_{es}} = \frac{K_{gr}}{T_a s + 1} \qquad (10)$$

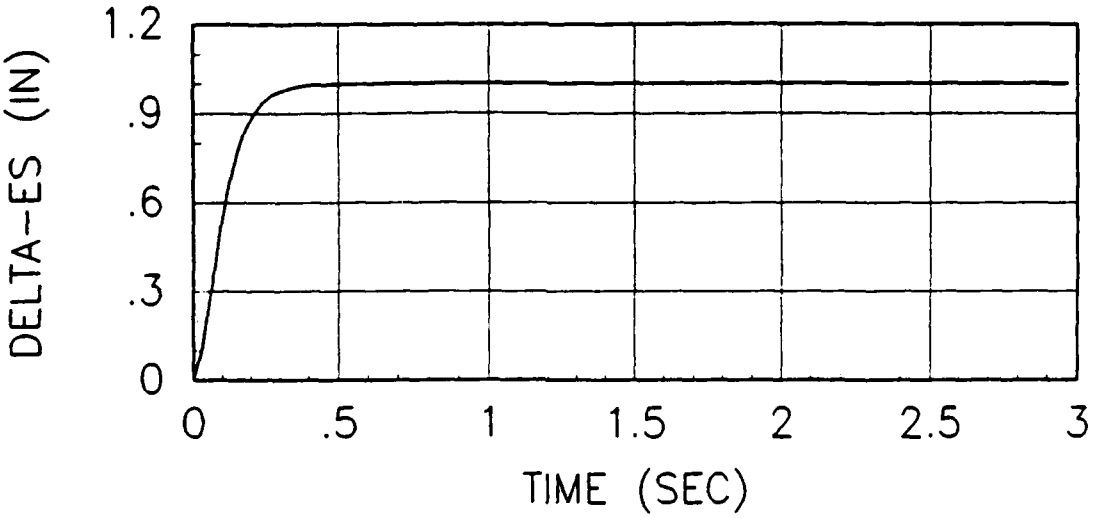

(a) Moderate Feel System Response (ω_{fs} = 18.5 rad/s)

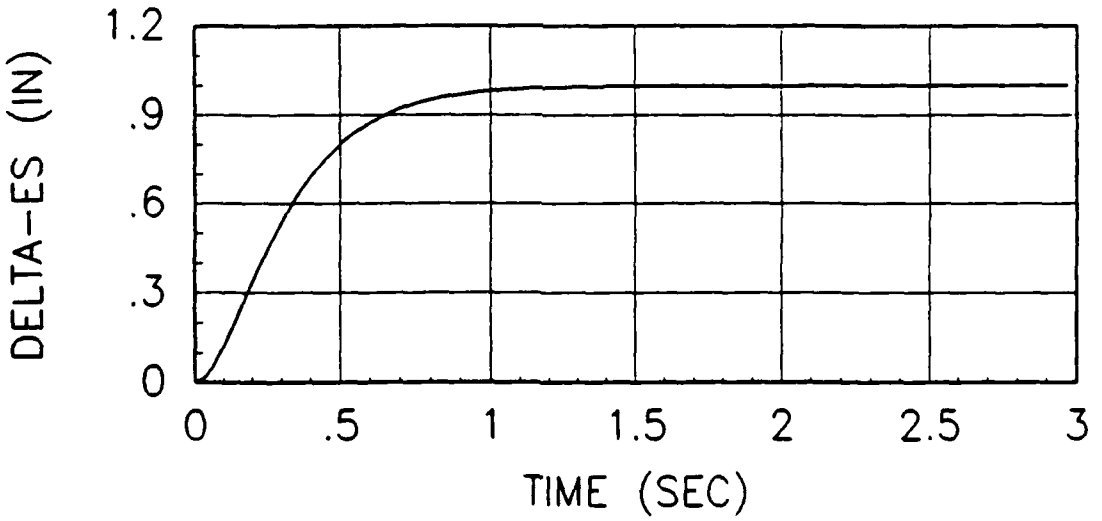

(b) Slow Feel System Response (ω_{fs} = 6.0 rad/s)

Figure 4. Feel System Response Characteristics (step input F_s = 21.7 lbs, ζ_{fs} = 1.00, and K_{fs} = 0.046 in/lb)

The time constant T_a determines the speed of the actuator response. Although a value of $1/T_a = 20$ is often used, this may be an optimistic view for the dynamic performance of most actuators. In a study by Gentry and Pujara (17), for example, an elevator actuator from the YF-16 was modeled using an equivalent system method over a frequency range of 0.1 to 10.0 rad/sec (as suggested for use with MIL-F-8785C). This equivalent system approach resulted in a more conservative and realistic first-order model of $13/(s + 13)$. For the matching techniques used in this thesis, therefore, the servo-actuator time constant was fixed at $1/T_a = 13$. Variations in the control system roots were accomplished only by changing the feel system's natural frequency (ω_{fs}).

Elevator-to-Stick-Force Gearing

The gain K_{gr} shown in equation 10 represents the elevator-to-stick-force gearing selection which determines the stick force per g (F_s/n) for a particular configuration. In flying qualities evaluations, the selection of elevator-to-stick-force gearing can be difficult for the pilot because it requires a compromise between the conflicting demands of satisfactory initial forces for good precision tracking capability, and satisfactory steady forces for gross fighter maneuverability. Consider, for example, configurations with initial response characteristics that are described as sluggish or slow, either because of low ω_{sp} or control system lags. In these configurations, the pilot will use

large initial inputs to "overdrive the airplane" in order to achieve the desired response. This calls for a high elevator-to-stick-force gearing to keep the initial forces reasonable. These same configurations, however, may have an unpredictable final response because the airplane tends to "dig in". These characteristics demand low elevator gearing to provide adequate g protection during the gross fighter maneuvers; and thus, a compromise gearing selection is required. Configurations with initial response characteristics described as abrupt or too sensitive, on the other hand, require the opposite gearing compromise. Because the initial forces for these configurations are considered "too light" by the pilot, a low elevator gearing is required to prevent inadvertent inputs. Such a gearing selection, however, tends to produce steady forces that are too high for the gross fighter maneuvers; and thus, the opposite compromise is required.

In the Neal-Smith evaluations (11), the pilots, when faced with a compromise in the elevator gearing selection, were not willing to vary F_s/n over a very large range. In general, the pilots would not compromise their ability to pull large load factors (i.e. achieve satisfactory gross maneuverability) even if the resulting F_s/n was not compatible with the initial forces required for precision tracking. The values of F_s/n selected by the pilots in the Neal-Smith study ranged from approximately 4.5 to 7 lbs/g although a few excursions (as low as 3 and as high as 14 lbs/g) were noted in some parts of the program.

Based on the findings of the Neal-Smith report, the gain K_{gr} was selected to give a stick force per g of 6 lbs/g during the equivalent systems matching. To find the required value of K_{gr}, the stick force per g was calculated using the short period approximation for n_z/F_s given by eq. 11.

$$\frac{n_z}{F_s} = \frac{K_{fs}\omega_{fs}^2}{s^2 + 2\zeta_{fs}\omega_{fs}s + \omega_{fs}^2} \times \frac{K_{gr}}{T_a s + 1} \times \frac{K_{nz}(s^2 + 2\zeta_{nz}\omega_{nz}s + \omega_{nz}^2)}{s^2 + 2\zeta_{sp}\omega_{sp}s + \omega_{sp}^2} \quad (11)$$

The steady state value of n_z/F_s for a step input was used to determine the required gain. Using eq. 11, the final value theorem for Laplace transforms, and solving for the gain gives the following:

$$K_{gr} = \frac{\omega_{sp}^2 (n_z/F_s)_{ss}}{K_{fs}K_{nz}\omega_{nz}^2} \quad (12)$$

Eq. 12 was used to calculate the gain needed for a stick force per g of 6 lbs/g. This resulted in a value of K_{gr} = 0.2710 rad/in for flight condition 1 and a value of K_{gr} = 0.0498 rad/in for flight condition 2. (See a description of flight conditions 1 and 2). To check that these values of gain were correct, they were used in eq. 11 along with the other appropriate parameters for flight conditions 1 and 2. The time response was then calculated for a step input of F_s = 6.0 lbs. Figure 5 shows that the step input results in the desired steady state value of 1.0 g in each case.

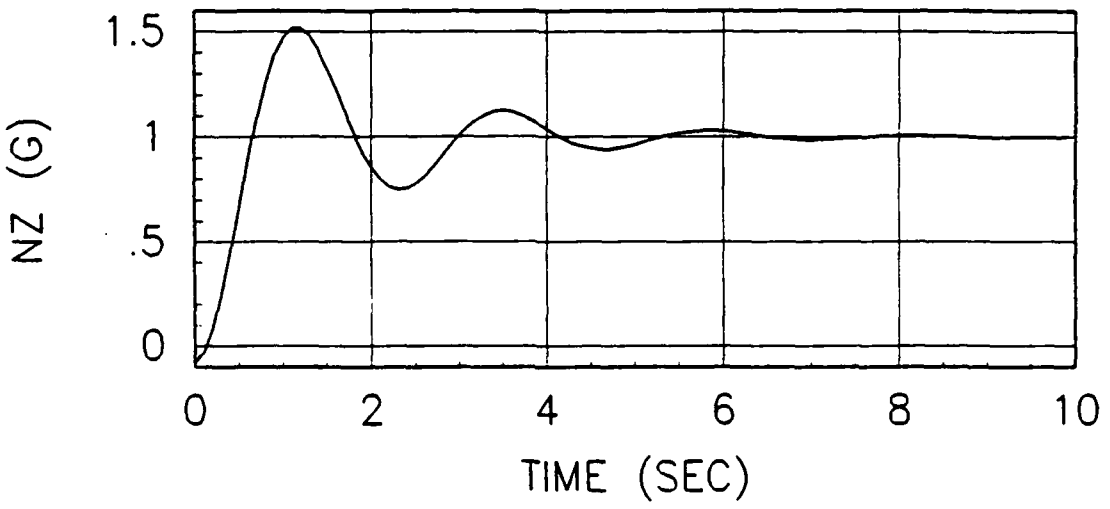

(a) Flight Condition 1, K_{gr} = 0.2710

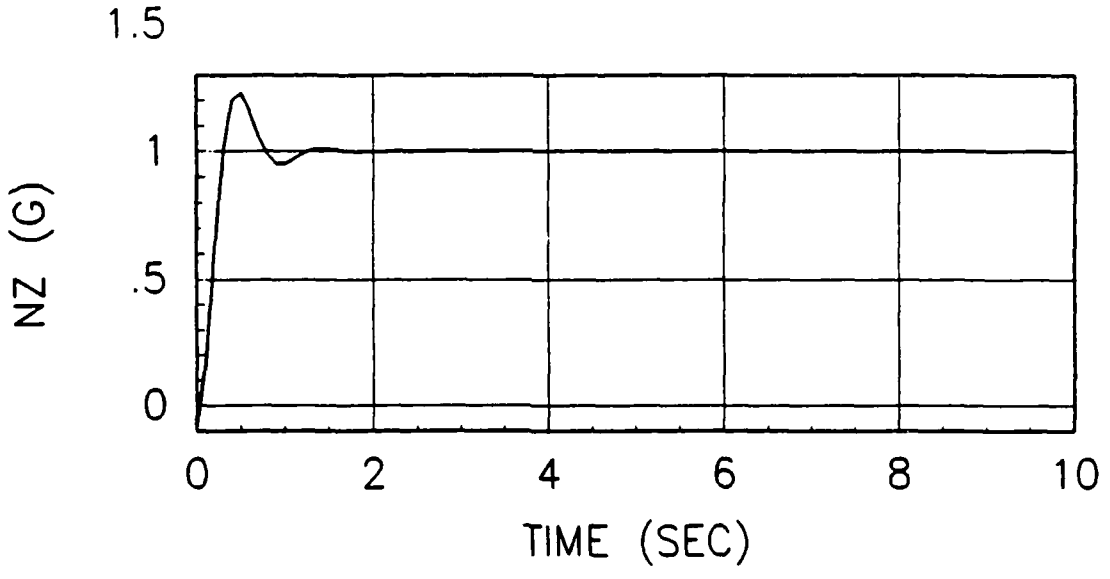

(b) Flight Condition 2, K_{gr} = 0.0498

Figure 5. Elevator Gearing Calibration (n_z/F_s response for step input of F_s = 6.0 lbs)

Longitudinal Airplane Dynamics

The mathematical models used to simulate longitudinal aircraft response to elevator inputs are developed by McRuer et al. (5). The derivation begins with the equations of motion describing how the aircraft deviates from trimmed, steady-state cruising flight when affected by small aerodynamic perturbations or limited control inputs and results in the following fourth-order transfer functions for pitch rate and normal acceleration:

$$\frac{\dot{\theta}}{\delta_e} = \frac{A_\theta s(s + 1/T_{\theta 1})(s + 1/T_{\theta 2})}{(s^2 + 2\zeta_p\omega_p s + \omega_p{}^2)(s^2 + 2\zeta_{sp}\omega_{sp}s + \omega_{sp}{}^2)} \qquad (13)$$

$$\frac{n_z}{\delta_e} = \frac{A_{nz}s(s + 1/T_{nz2})(s^2 + 2\zeta_{nz}\omega_{nz}s + \omega_{nz}{}^2)}{(s^2 + 2\zeta_p\omega_p s + \omega_p{}^2)(s^2 + 2\zeta_{sp}\omega_{sp}s + \omega_{sp}{}^2)} \qquad (14)$$

Equations 13 and 14 are the universally accepted 3 degree of freedom transfer functions used for describing longitudinal aircraft response to elevator control inputs. For most flight conditions, the phugoid and short period natural frequencies (ω_p and ω_{sp}) are sufficiently separated that their dynamic modes are relatively uncoupled (table I). Because of this, equations 13 and 14 can be simplified into the short period and phugoid approximations which are valid over their respective frequency ranges. Generally, the phugoid response of an aircraft is very slow compared to the short period response (i.e. $\omega_p << \omega_{sp}$). In an approximate sense, the phugoid mode describes the long-term translatory motions of the aircraft's center of mass, whereas the

short period mode describes rotations about the center of mass.

The short period approximation involves setting the variation in forward velocity u equal to zero with the assumption that it is relatively insignificant in the short period mode and that the two degrees of freedom α and θ are dominant. McRuer, et al. state:

> "...for frequencies above the phugoid the two degree of freedom, short period transfer functions are very good approximations in both amplitude and phase. Furthermore, the two- and three degree of freedom time responses in w and θ are in excellent agreement for times shorter than about 10 sec." (5)

Table I

Values of ω_p and ω_{sp} at Various Flight Conditions*

Mach No	Alt (ft)	Wt (lbs)	ω_p (rps)	ω_{sp} (rps)
0.20	0	22.058	0.1520	1.558
0.85	0	17,578	0.0696	7.350
0.40	15,000	17,578	0.0980	2.450
0.60	15,000	17,578	0.0635	3.690
0.50	35,000	17,578	0.0861	1.941
0.70	35,000	17,578	0.0752	2.770

*Data taken from McRuer (5) for the A-4D aircraft with c.g. location at 0.25 % c.

Thus, the short period characteristics are dominant during the time immediately following an initial perturbation (1-10 seconds) after which the phugoid characteristics begin to take over. For flying qualities specification, the primary interest is in the aircraft's short period response characteristics. This is evidenced by the extensive requirements in MIL-STD-1797 for short-term pitch response (para 4.2.1.2 - 99 pages) compared to the relatively sparse requirements for long-term pitch response (para 4.2.1.1 - 4 pages). Also, MIL-STD-1797 requires that equivalent

systems be matched over a frequency range of 0.1 to 10 rad/sec which, for typical flight conditions, corresponds to the frequency range in which the short period mode is dominant. For these reasons, equivalent systems techniques will often use the appropriate short period transfer functions as the low-order equivalent systems. The low-order equivalent systems used by program LONFIT for example (chapter III) are derived from the short period approximations for $\dot{\theta}/\delta_e$ and n_z/δ_e. The primary advantage of this approach is that it provides less complicated low-order systems to work with and, because well-accepted short period forms are used, the transfer functions give meaningful short period parameters when matched to the high-order systems.

MIL-STD-1797 suggests using the 3 degree of freedom transfer functions (eqs. 13 and 14) in equivalent systems work but states that in <u>most cases</u> the phugoid and short period modes are sufficiently separated that "within appropriate respective frequency ranges" the 2 degree of freedom approximations can be used. The requirements state that

> "While no specific guidance on the lower frequency bound of the matching region is offered, the phugoid and short period are generally separated by at least a factor of 10, which should be adequate to consider them separately. The assumption of widely separated phugoid and short period modes breaks down at low values of static stability (i.e., $M_\alpha = 0$) such as for conventional aircraft with extreme aft center of gravity locations and on most STOL configurations." (3)

The flight conditions and associated aircraft parameters chosen to represent the basic aircraft dynamics during the equivalent systems matching are shown in table II. These data are taken from McRuer, et al. (5) for the A-4D aircraft.

Table II

Flight Conditions and Associated Aircraft Parameters

Flt Cond	Alt (ft)	Mach No.	V_{To} (fps)	q (psf)
1	35,000	0.70	681	171
2	0	0.85	950	945

Flight Condition 1		Flight Condition 2	
ζ_{sp}	= 0.2250	ζ_{sp}	= 0.4360
ω_{sp}	= 2.7700	ω_{sp}	= 7.3500
ζ_p	= 0.1177	ζ_p	= 0.2260
ω_p	= 0.0752	ω_p	= 0.0696
A_θ	= -11.33	A_θ	= -64.00
$1/T_{\theta 1}$	= 0.0091	$1/T_{\theta 1}$	= 0.0287
$1/T_{\theta 2}$	= 0.4280	$1/T_{\theta 2}$	= 2.0800
A_{nz}	= 2.1353	A_{nz}	= 12.0590
$1/T_{nz1}$	= 0.0000	$1/T_{nz1}$	= 0.0000
$1/T_{nz2}$	= -0.0023	$1/T_{nz2}$	= 0.0268
ζ_{nz}	= 0.0260	ζ_{nz}	= 0.0461
ω_{nz}	= 6.8800	ω_{nz}	= 18.0500

These flight conditions were chosen primarily because of the values of ω_{sp} as will be explained in the following section. Note that in both flight conditions the natural frequencies ω_p and ω_{sp} are sufficiently separated (i.e. by a factor of 10 or more) so that the short period and phugoid modes can be considered separately. Also, since ω_p is less than 0.1, the short period mode will be dominant in the frequency range of interest (0.1 to 10 rad/sec). The short period approximation should therefore be appropriate to use during the equivalent systems matching process. This will be true as long as the control system roots do not cause unfavorable coupling effects with ω_{sp} thereby degrading the equivalent systems matching ability.

HOS Configurations

The effect of control system dynamics is to raise the order of the airplane response to pilot inputs. The airplane responses (eqs. 13 and 14) are fourth order responses for elevator control inputs. The additional dynamics of the elevator response to control stick displacements (servo-actuator) and the control stick response to control stick forces (feel system) will increase the order of the overall airplane response to control stick forces. In addition, the feel system and actuator roots may be near the airplane roots. Increased order and closeness of roots can alter the responses of the airplane to stick force inputs, affect the pilot's closed loop control, and change the airplane's flying qualities.

Studies of many different types of flight control systems have shown that most systems have certain similar effects on the airplane's overall maneuvering characteristics. In general, it can be said that a flight control system will do one of two things to the overall aircraft response: 1) introduce a "pure" time delay without changing the basic shape of the time response, or 2) introduce time delay and change the shape of the time response. The first case (pure time delay) is characterized by control system roots with relatively high natural frequencies compared to the aircraft roots. This type of control system will have a "fast" or at least "moderately fast" response compared to the basic aircraft response. The second case is characterized by

insufficient separation of the flight control system and airplane roots which causes a change in the basic aircraft response characteristics. This type of control system will have a "slower" response because of its lower natural frequency. In either case, the time delay, if it becomes excessive, is generally cited by pilots as the most objectionable characteristic of flight control systems.

In theory, the equivalent system matching process should be relatively straightforward for a high-order system with pure time delay. In this type of system, the natural frequencies of the control system roots are high compared to the aircraft roots and their effects can be neglected in the frequency band of interest (0.1 to 10 rad/sec). The only source of mismatch, therefore, is from the high-frequency phase contributions of the control system roots; and this can be approximated by a time delay. In the DiFranco (10) high-order system evaluations, for example, it was found that the frequency and damping ratio of the equivalent systems were very close to the airplane's short period characteristics when the control system roots were high relative to ω_{sp}. Thus, the high-order systems could be closely matched to equivalent second-order systems (i.e. the short period approximation) using a time delay term.

In the second type of high-order system, the time response has been altered because the control system roots are close to the aircraft roots. This type of system may not match well to a lower-order equivalent system because of the combined effects of

the aircraft and control system roots. One of the conclusions reported in the DiFranco evaluations for example states the following:

> "With higher-order control system dynamics, the airplane short period response to step stick force inputs can be reasonably well represented by a time delay and an equivalent second-order response...This simplified representation is poorest when the lowest frequency of the control system is near the airplane short period frequency." (10)

This problem was also reported in the Neal-Smith evaluations which tested various configurations with the control system roots close to the aircraft roots. Comparing the pure time delay type of high-order system with the systems used in their study, the report states that: "Since the control system dynamics studied in the present experiment significantly alter the shape of the airplane response to pilot inputs, determining an equivalent system is a more difficult proposition." The report goes on to state that because of the practical difficulties associated with the equivalent systems approach, a pilot-in-the-loop analysis was used instead (11).

Based on the results of these investigations, it was concluded that to adequately evaluate equivalent systems matching techniques it would be necessary to use high-order systems representative of both types discussed above. The aircraft and feel system parameters were therefore chosen to simulate high-order systems with "fast" response times (resulting in pure time delay) and high-order systems with "slow" response times (resulting in time delay plus change in time response). The flight conditions and parameters selected for these systems are

summarized in table III.

Table III

High-Order System Configurations					
HOS Designation	Flight Condition	HOS Type	K_{gr} (rad/in)	ω_{fs} (rad/s)	ω_{sp} (rad/s)
HOS_1 ($\dot{\theta}/F_s$)	1	Uncoupled	0.2710	18.5	2.77
HOS_2 (n_z/F_s)	1	Uncoupled	0.2710	18.5	2.77
HOS_3 ($\dot{\theta}/F_s$)	2	Coupled	0.0498	6.0	7.35
HOS_4 (n_z/F_s)	2	Coupled	0.0498	6.0	7.35

(K_{fs} = 0.046 in/lb and $1/T_a$ = 13 rad/s for all HOS configurations)

Note that for clarity throughout the equivalent systems matching process, the high order systems with pure time delay will be designated as HOS_1 ($\dot{\theta}/F_s$) and HOS_2 (n_z/F_s) and the higher-order systems with coupling between the control system and aircraft dynamics will be designated as HOS_3 ($\dot{\theta}/F_s$) and HOS_4 (n_z/F_s) as listed in table III. Although ω_{fs} will be varied throughout the range of 6 to 31 rad/sec resulting in a variety of other HOS configurations (as explained in chapter III) the HOS_1 - HOS_4 configurations will be the primary (baseline) systems used throughout the frequency domain and time domain comparisons.

The high-order configurations were chosen because of the relative values of $1/T_a$, ω_{fs}, and ω_{sp}. The dynamics of HOS_1 and HOS_2, for example, are the result of the relatively low short period frequency of the aircraft (ω_{sp} = 2.77) together with the relatively high natural frequency of the feel system (ω_{fs} = 18.5)

and corner frequency of the servo ($1/T_a$ = 13). This combination provides good separation between the control system and aircraft roots and results in a relatively uncoupled, pure time delay, high-order system response. The magnitude plots for HOS_1 and HOS_2 (figures 6a and 7a) show that the dynamics of the feel system and servo are essentially removed from the frequency range of interest (0.1 to 10 rad/sec). The only difference between the basic aircraft and the HOS, in this frequency range, is an increase in gain for the HOS equal to $(K_{fs}K_{gr}\omega_{fs}^2)/T_a$. The HOS_1 and HOS_2 phase plots (figures 6b and 7b) show the phase lags of the control system dynamics which correspond to the time delay. Figure 8 compares the time responses of HOS_1 and HOS_2 with the corresponding basic aircraft responses. The time responses are shown for a step input to the HOS of F_s = 5 lbs and an equivalent step input to the aircraft of δ_e = 3.57 deg. Note that the time responses of the high-order systems show a time delay but have essentially the same shape as the basic aircraft responses.

The HOS_3 and HOS_4 dynamics are influenced by the relatively high short period frequency of the aircraft (ω_{sp} = 7.35) combined with the relatively low natural frequency of the feel system (ω_{fs} = 6.0). This combination gives very little separation between the aircraft and control system roots and results in a coupled high-order system response. Compared with the HOS_1 and HOS_2 Bode plots, the HOS_3 and HOS_4 plots (figures 9 and 10) show the presence of ω_{fs} within the 0.1 to 10 rad/sec frequency band and indicate increased phase lags corresponding to a greater time

delay. The greater time delay is expected because of the relatively slow feel system response at ω_{fs} = 6.0 rad/sec. The presence of ω_{fs} within the 0.1 to 10 rad/sec frequency band results in coupling effects between the control system and aircraft dynamics. Figure 11 shows the time responses of HOS_3 and HOS_4 compared to the corresponding basic aircraft responses. The time responses are for a step input to the HOS of F_s = 5 lbs and an equivalent step input to the aircraft of δ_e = 0.66 deg. Note that the HOS_3 and HOS_4 time responses show an increase in time delay (compared to HOS_1 and HOS_2) as well as a change in the basic shape of the time response.

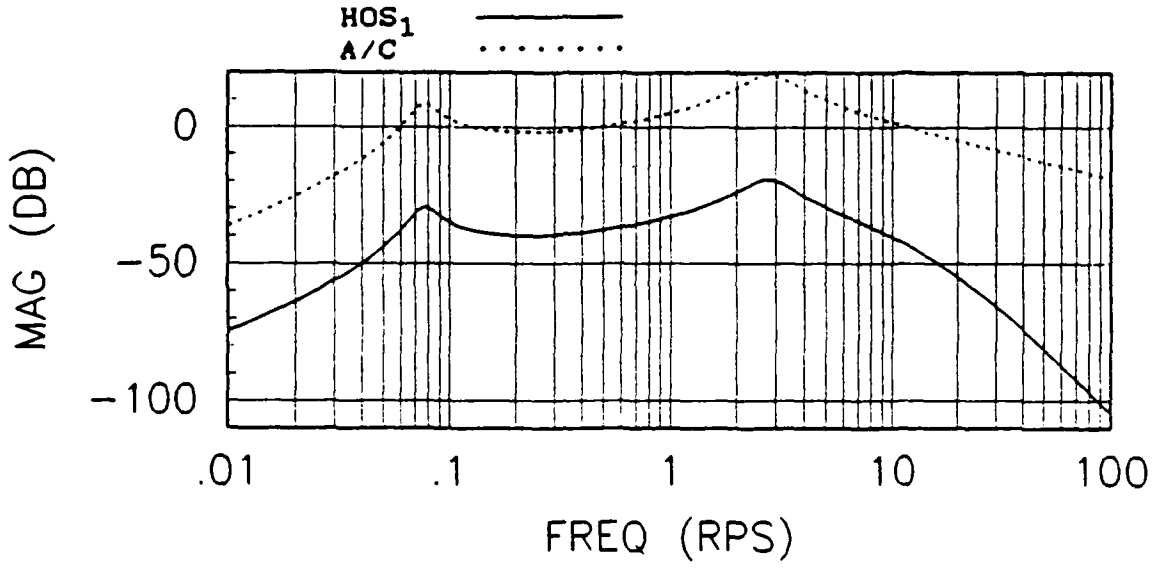

(a) Magnitude

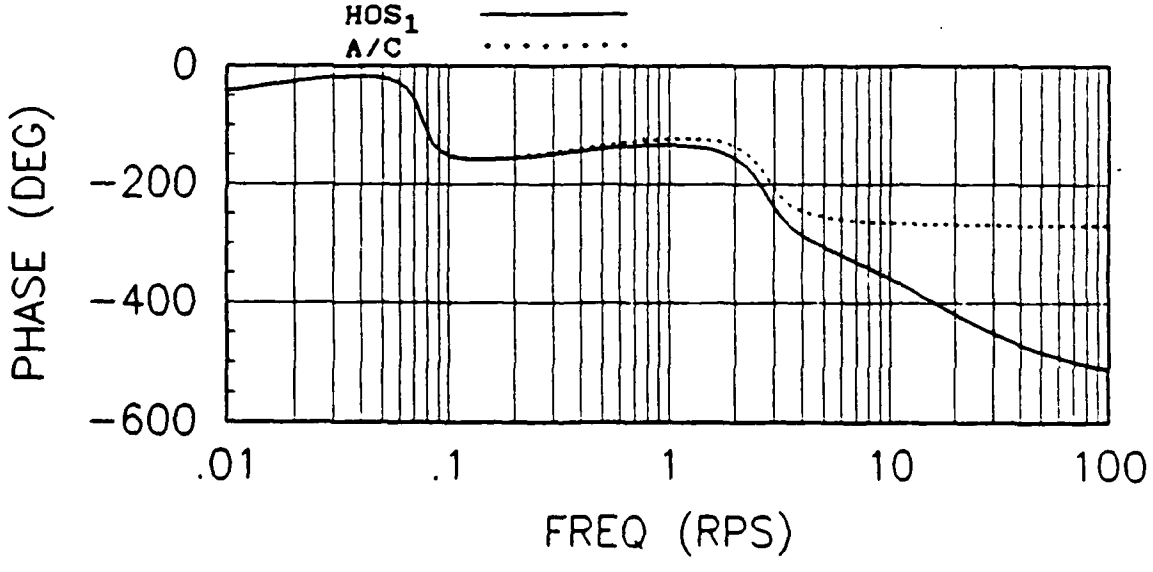

(b) Phase

Figure 6. Frequency Response Comparison, HOS_1 and Basic Aircraft (Flight Condition 1 and ω_{fs} = 18.5 rad/sec)

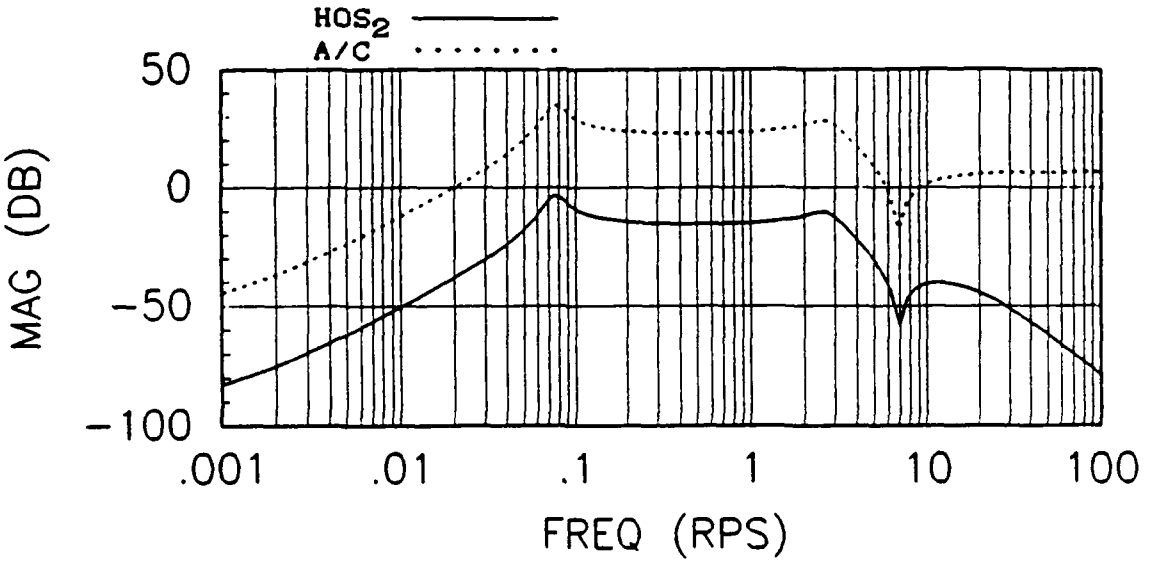

(a) Magnitude

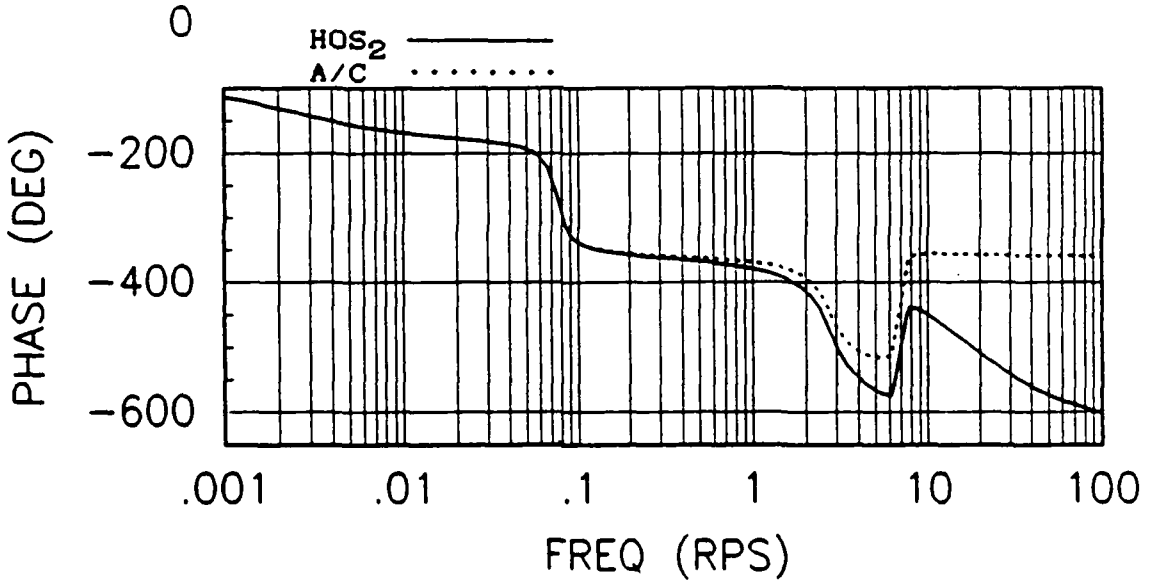

(b) Phase

Figure 7. Frequeny Response Comparison, HOS_2 and Basic Aircraft (Flight Condition 1 and ω_{fs} = 18.5 rad/sec)

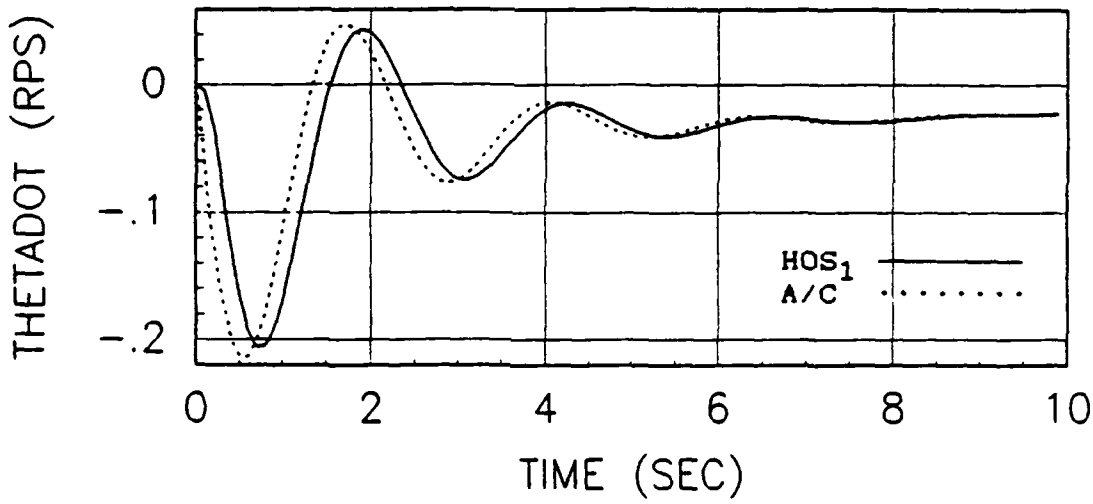

(a) HOS_1 versus Basic Aircraft
(Flight Condition 1 and ω_{fs} = 18.5 rad/s)

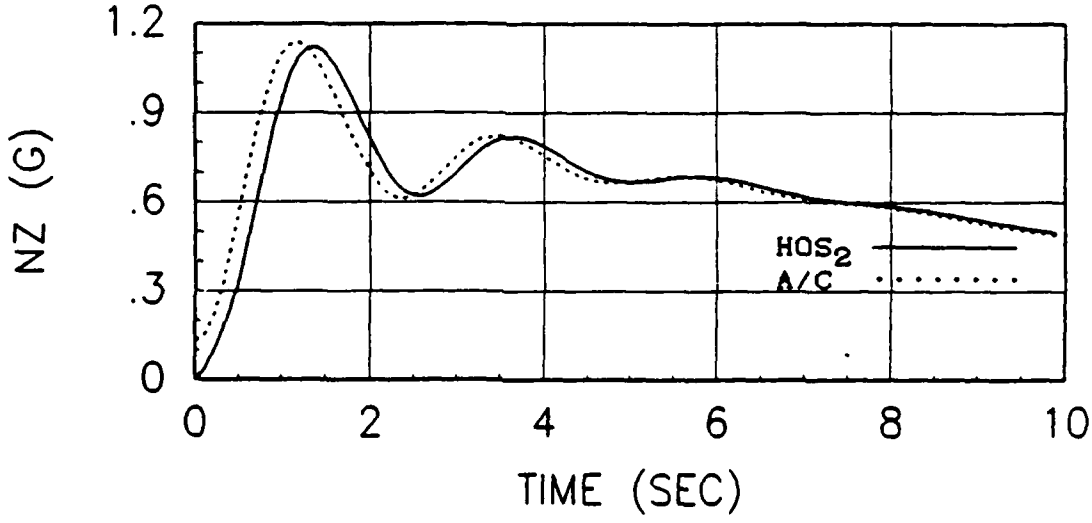

(b) HOS_2 versus Basic Aircraft
(Flight Condition 1 and ω_{fs} = 18.5 rad/s)

Figure 8. Time Response Comparisons (step input F_s = 5.0 lbs to HOS and equivalent step input δ_e = 3.57 deg to A/C)

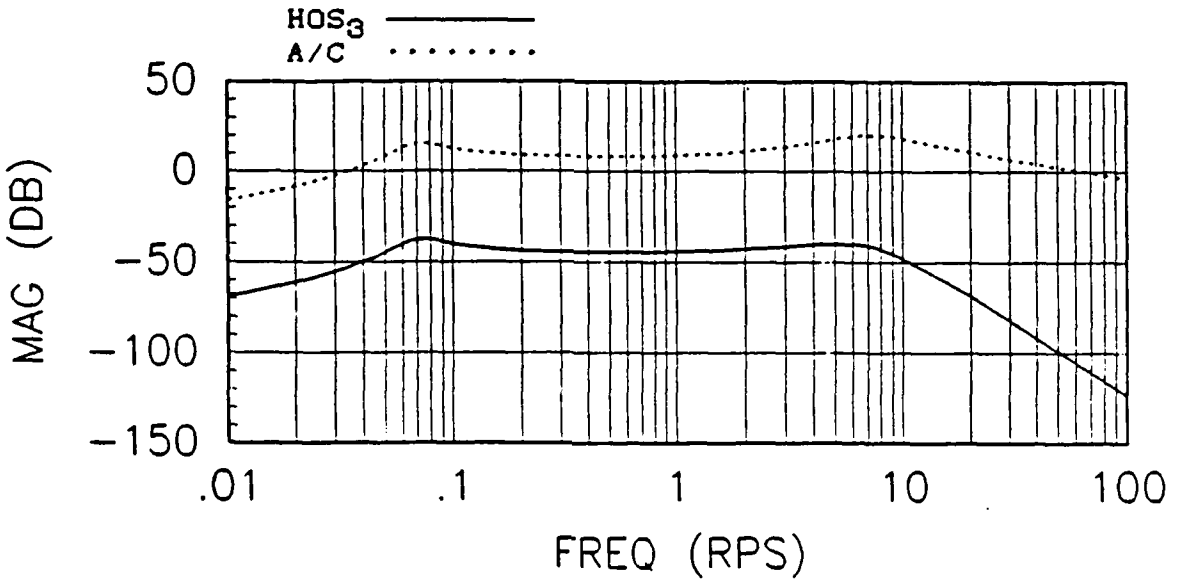

(a) Magnitude

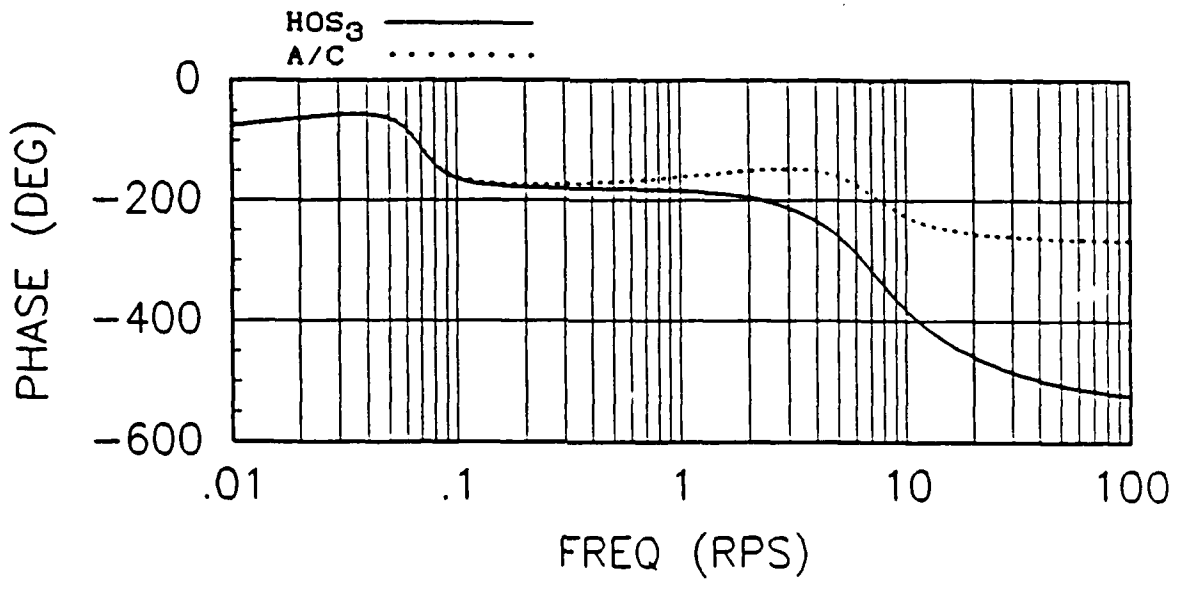

(b) Phase

Figure 9. Frequeny Response Comparison, HOS_3 and Basic Aircraft (Flight Condition 2 and ω_{fs} = 6.0 rad/sec)

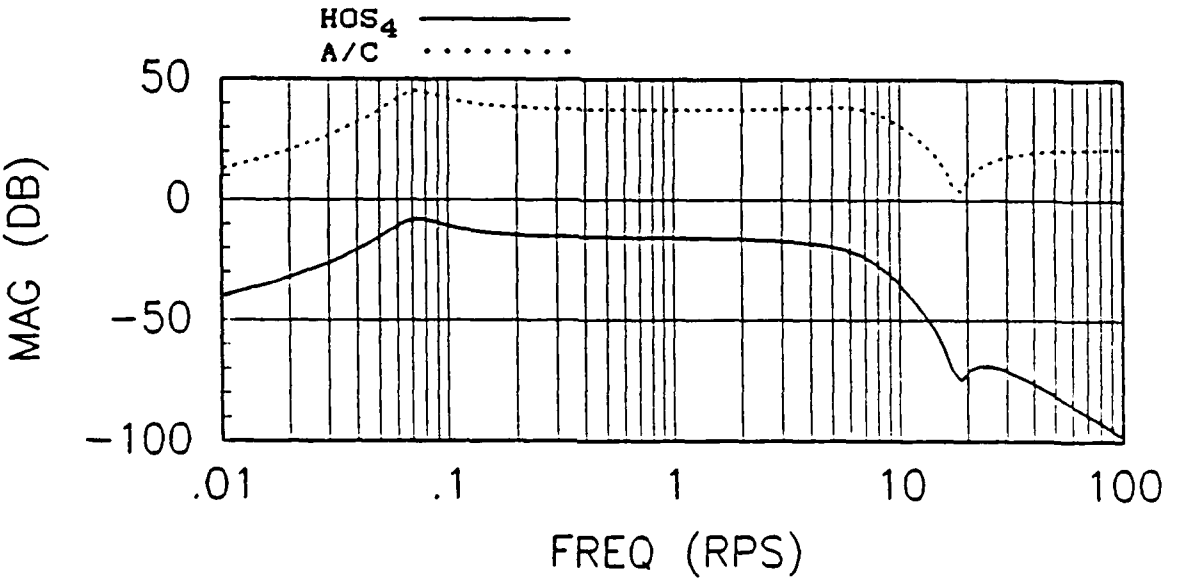

(a) Magnitude

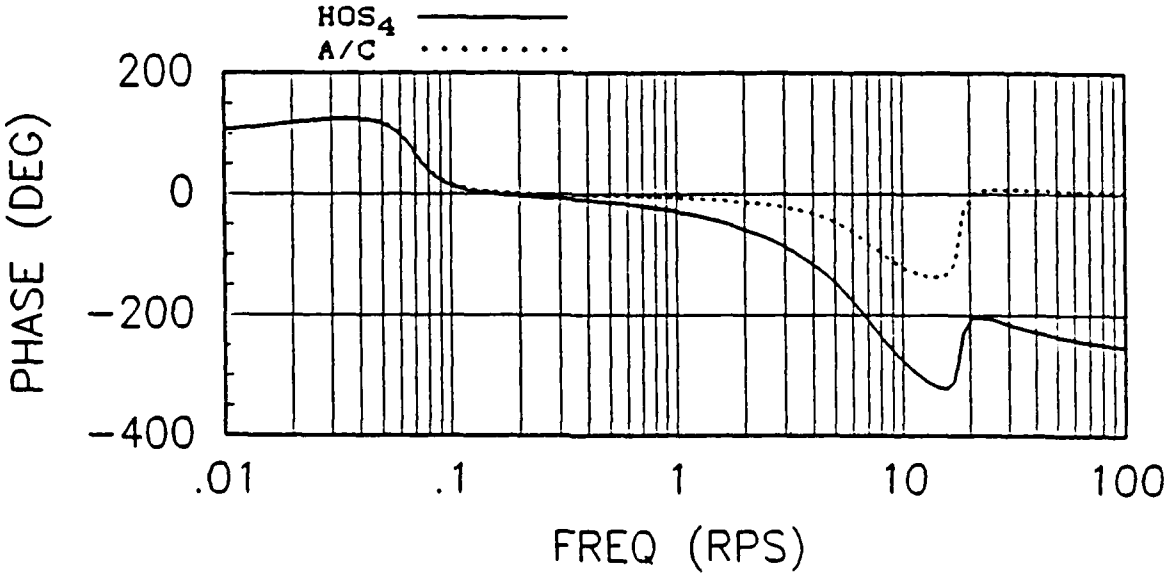

(b) Phase

Figure 10. Frequeny Response Comparison, HOS_4 and Basic Aircraft (Flight Condition 2 and ω_{fs} = 6.0 rad/sec)

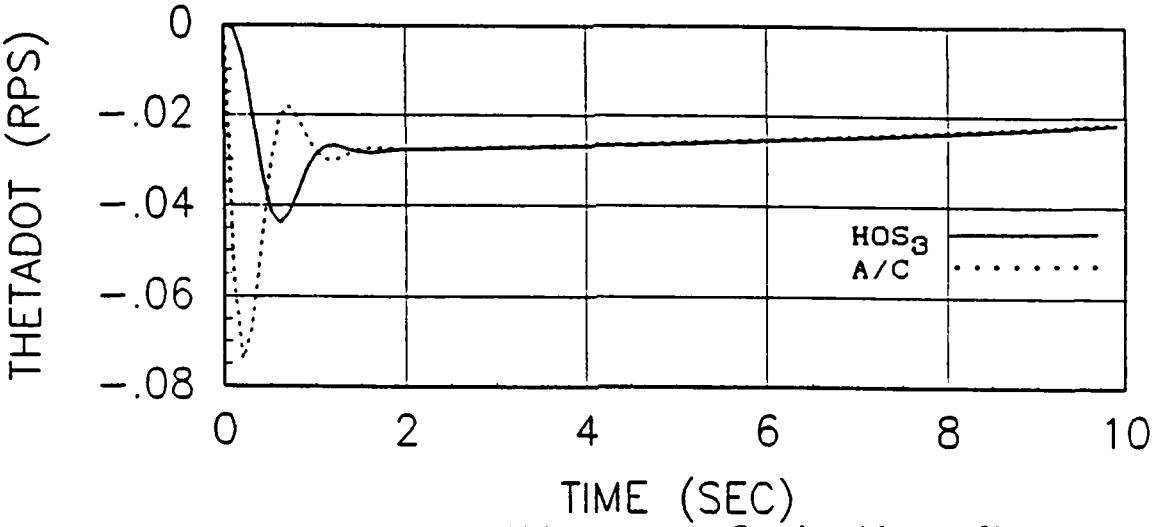

(a) HOS_3 versus Basic Aircraft
(Flight Condition 2 and ω_{fs} = 6.0 rad/s)

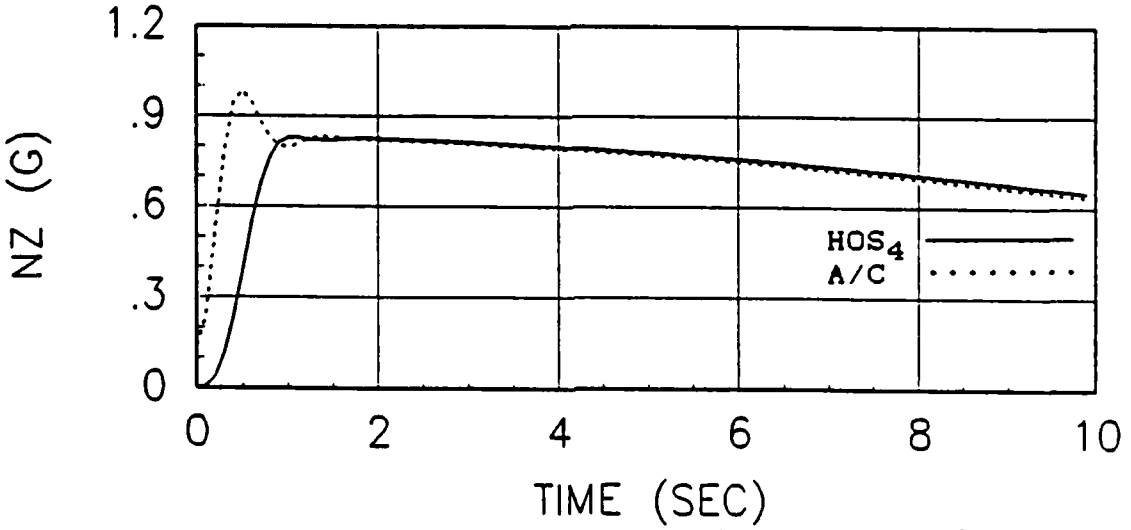

(b) HOS_4 versus Basic Aircraft
(Flight Condition 2 and ω_{fs} = 6.0 rad/s)

Figure 11. Time Response Comparisons (step input F_s = 5.0 lbs to HOS and equivalent step input δ_e = 0.66 deg to A/C)

III. Frequency Response Computer Matching

Computer Programs

The frequency domain matching was accomplished using the computer programs LONFIT and MACFIT (18,19). These programs, developed by McDonnell Douglas, are applicable to MIL-F-8785C para 3.2.2.1.1 (short period frequency and acceleration sensitivity) and para 3.2.2.1.2 (short period damping) requirements (2).

LONFIT matches high-order pitch rate and normal acceleration transfer functions with the following equivalent low-order systems:

$$\frac{\dot{\theta}}{F_s} = \frac{K_\theta(s + L_\alpha)e^{-s\tau}}{s^2 + 2\zeta_{sp}\omega_{sp}s + \omega_{sp}^2} \qquad (15)$$

$$\frac{n_z}{F_s} = \frac{K_{nz}e^{-s\tau}}{s^2 + 2\zeta_{sp}\omega_{sp}s + \omega_{sp}^2} \qquad (16)$$

where the parameters K_θ, K_{nz}, L_α, ζ_{sp}, ω_{sp}, and τ are determined by simultaneously matching the frequency response of the above transfer functions to those of the airframe plus flight control system (high-order system).

LONFIT is configured for longitudinal systems only and the equivalent low-order forms are restricted to the specific transfer functions of equations 15 and 16. MACFIT, on the other hand, is a general purpose matching program which can accept arbitrary HOS and LOES forms. Although LONFIT (due to the pre-chosen LOES

forms) is somewhat easier to use, MACFIT has the advantage of versatility in cases where the structure of LONFIT is inadequate.

LONFIT and MACFIT both use a Rosenbrock multivariable search algorithm to match Bode plots of the low-order and high-order systems by minimizing the weighted sum of the squares of the differences in magnitude and phase angle between the systems at n discrete frequencies. The following cost function is minimized:

$$cost_f = 20/n \sum_{\omega_1}^{\omega_n} WT1(\Delta gain)^2 + WT2(\Delta phase)^2 \qquad (17)$$

where: $cost_f$ is a frequency domain mismatch function
$WT1 = 1.0$
$WT2 = 0.01745$
$\Delta gain = gain_{HOS} - gain_{LOS}$ (in decibels)
$\Delta phase = phase_{HOS} - phase_{LOS}$ (in degrees)
and n is the number of frequencies

To begin the matching process, the coefficients (or roots) of the HOS numerator and denominator are required as input. The user then has the flexibility to specify initial values for the LOS parameters, which parameters the program may vary, the number of frequencies (n), the frequency range, the number of iterations, whether or not to include time delay, and whether or not to permit the resulting transfer functions to be unstable.

The subscript *f* in equation 17 is used to denote that "$cost_f$" is a measure of the mismatch in the frequency domain. Because it will be necessary to compare time domain and frequency domain matching in this study, it will be helpful to define a second cost function "$cost_t$" which will be used to measure the mismatch of the

HOS and LOES time responses. $Cost_t$ will be defined as follows:

$$cost_t = 1/k \sum_{t_1}^{t_k} (\Delta thetadot)^2 \qquad (18)$$

where: $cost_t$ is a time domain mismatch function
$\Delta thetadot = \dot{\theta}_{HOS} - \dot{\theta}_{LOS}$ (in degrees)
and k is the number of discrete data points

The time response ($\dot{\theta}$) in equation 18 is calculated using a step input of 5 lbs. Although $cost_t$ has been defined using the mismatch in $\dot{\theta}$ a similar definition could be used for n_z mismatch. In this thesis, however, comparisons between time domain and frequency domain LOES matching techniques will only be made for the $\dot{\theta}$ matching results. The time response mismatch has been defined such that the magnitude of $cost_t$ will be much less (i.e. on the order of 100 less) than the magnitude of $cost_f$ for a given HOS/LOES mismatch. This has been done to avoid the temptation of making direct comparisons between the magnitudes of $cost_f$ and $cost_t$. For example, a time domain mismatch of $cost_t < 200$ can <u>not</u> be used as a guideline for a "good" match as is generally the case for $cost_f$.

<u>Matching Strategy</u>

The HOS_1 and HOS_2 transfer functions derived in chapter II were matched to the corresponding LOS_1 and LOS_2 forms shown in eqs. 15 and 16 using the program LONFIT. The following matching strategy was taken primarily from the LONFIT users guide (18) although it has been modified somewhat for this particular

example.

(1) A frequency range of 0.1 to 10 rad/sec was used in accordance with MIL-F-8785C equivalent systems criteria and is intended to cover the frequency range of major interest to the pilot. The number of discrete frequencies (n) was set to 20 as suggested in the LONFIT users guide.

(2) L_α, ζ_{sp}, and ω_{sp} were initially set equal to their high-order system values (taken from the short-period roots of the basic aircraft transfer function). Initial values of gain and time delay were arbitrarily set to 1.0 and 0.1 respectively.

(3) To investigate the effects of L_α and time delay the HOS frequency response was matched by varying gain, ζ_{sp}, and ω_{sp} with the following combinations of L_α and time delay:

HOS_1 Matching			HOS_2 Matching		
	L_α	Time Delay		Time Delay	LOS Form
LOS_{1A}	Fixed	No	LOS_{2A}	No	LONFIT
LOS_{1B}	Fixed	Yes	LOS_{2B}	Yes	LONFIT
LOS_{1C}	Free	No	LOS_{2C}	No	MACFIT
LOS_{1D}	Free	Yes	LOS_{2D}	Yes	MACFIT

(4) The LOS_{2C} and LOS_{2D} matches were carried out using program MACFIT and a second order numerator, second order denominator form for the equivalent n_z/F_s low-order system. This is because the LONFIT form of eq. 16, which is an abbreviated form of the short-period approximation, did not match well with the high-order n_z/F_s transfer function. The complete short-period approximation was therefore used and produced good results. (This is explained further in the section on HOS_2 matching).

HOS_1 Matching

The $\dot{\theta}/F_s$ high-order system (HOS_1) was matched to the LOS_{1A} - LOS_{1D} equivalent systems using the first three steps outlined above. The resulting LOS parameters and $cost_f$ functions are shown Table IV. The cost function trends seen in Table IV demonstrate that increasing the the number of free variables (i.e. increasing the dimension space of the low-order system) generally results in a better match to the high-order system. Based on these results, the logical approach to achieving the best match would apparently be to free all the available parameters. The problem with this approach, however, is that questions can arise regarding the meaning of some free variables. Disagreement continues in the flying qualities community, for example, as to whether the parameter L_α should be fixed at the basic aircraft value or be determined by the match (3). The rationale behind keeping it fixed is that L_α is determined by wing size and planform which are dimensions that can not be varied significantly for a particular aircraft. It is argued, therefore, that L_α should be kept constant at the basic aircraft value. Furthermore, in studies where it has been allowed to vary, the results have produced unreasonable fluctuations in L_α from one configuration to another. The point is that even though the lowest cost function is achieved by freeing all the parameters, this may not be the best overall approach if ambiguity arises regarding the meaning of some terms.

Table IV

$\dot{\theta}/F_s$ Matching Results
Flight Condition 1 and ω_{fs} = 18.5 rad/s (HOS_1)

System	L_α		$K_\theta(A_\theta)$	ζ_{sp}	ω_{sp}	L_α	τ	$cost_f$
A-4D*	-	-	(-11.33)	0.225	2.770	0.428	-	--
LOS_{1A}	Fixed	No	-0.117	0.180	2.435	0.428	0	441
LOS_{1B}	Free	No	-0.099	0.128	2.617	0.786	0	374
LOS_{1C}	Fixed	Yes	-0.133	0.238	2.601	0.428	0.164	82
LOS_{1D}	Free	Yes	-0.120	0.193	2.686	0.595	0.156	60

* Basic A-4D aircraft parameters (without feel system and servo dynamics) taken from McRuer (5).

For some equivalent system configurations there may be no choice but to vary all the parameters. To achieve an acceptable match for the longitudinal high-order systems in the Neal-Smith evaluations, for example, the report stated that all parameters, including L_α, had to be varied (11). In the present example, however, an excellent match was obtained using the LOS_{1C} configuration with L_α fixed.

Magnitude, phase angle, and time response comparisons between HOS_1 and the LOS_{1C} and LOS_{1D} configurations are shown in Figures 12-14. To obtain the phase angle and time response plots it was necessary to represent the time delay term, $e^{-s\tau}$, by poles and zeros directly. This was done using a first order Pade' approximation as shown below:

$$e^{-s\tau} = \frac{1 - s\tau/2}{1 + s\tau/2} \qquad (19)$$

The effect of time delay can be seen in Figure 15 which compares the phase mismatch between HOS_1 and LOS_{1C} both with and without the Pade' approximation. Figure 15b which does have the Pade' approximation for e^{-sT} illustrates that equivalent time delay approximates the phase lags of the high-frequency terms quite well.

Figure 16 shows the corresponding time domain comparisons between HOS_1 and LOS_{1C} for a step input of F_s = 5 lbs. Figures 15a and 16a do not have the time delay term and illustrate that a poor match in the high-frequency region corresponds to a poor match in the transient time response region. On the other hand, Figures 15b and 16b, which both include time delay, show that a good match in the high-frequency region corresponds to a good match in the transient time response region. These results demonstrate the initial value theorem for Laplace transforms. This theorem states that the behavior of $f(t)$ in the neighborhood of $t = 0$ is related to the behavior of $sF(s)$ in the neighborhood of $s = \infty$. This behavior is clearly evident in Figures 15 and 16.

HOS_2 Matching

The n_z/F_s high-order system for flight condition 1 and ω_{fs} = 18.5 (HOS_2) was matched to LOS_{2A} and LOS_{2B} using program LONFIT and the first three steps outlined in the matching strategy. The resulting LOS parameters and cost functions are shown in Table V. The time delay was again applied using a first order Pade' approximation to obtain magnitude and phase comparisons for these

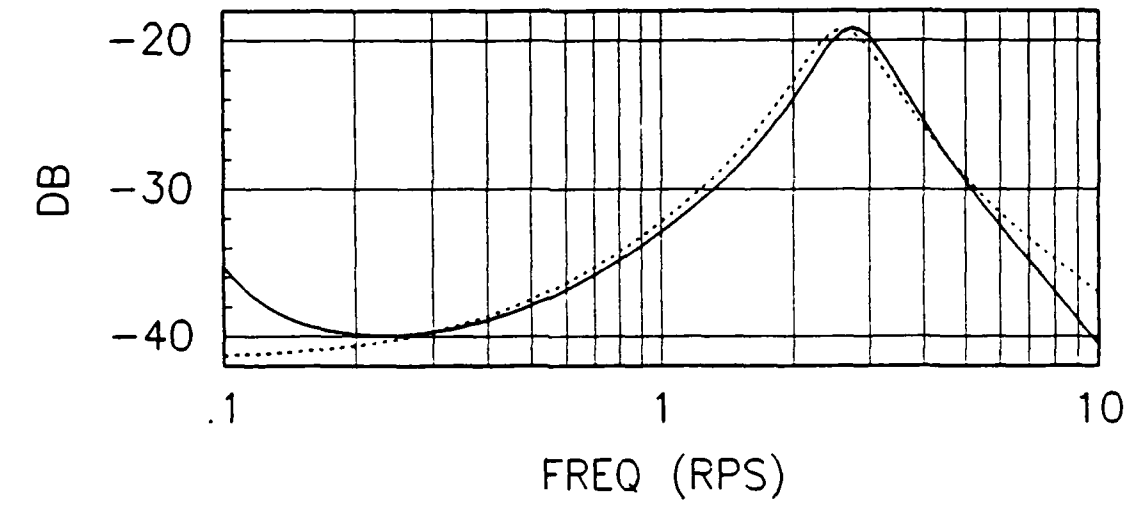

(a) Magnitude

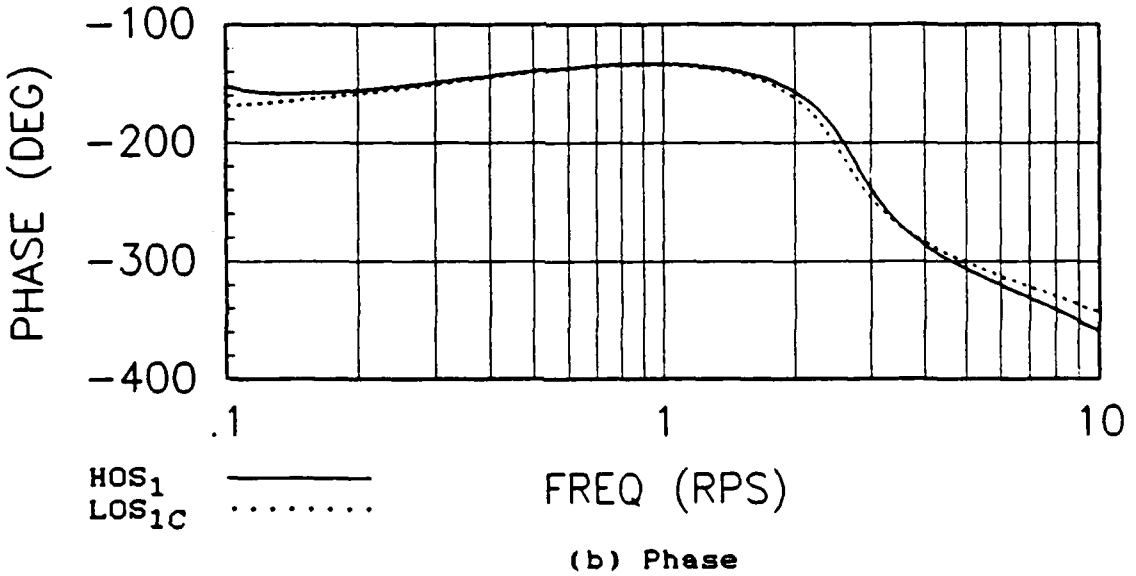

(b) Phase

Figure 12. Frequency Response Comparison, HOS_1 vs LOS_{1C} ($Cost_f$ = 82)

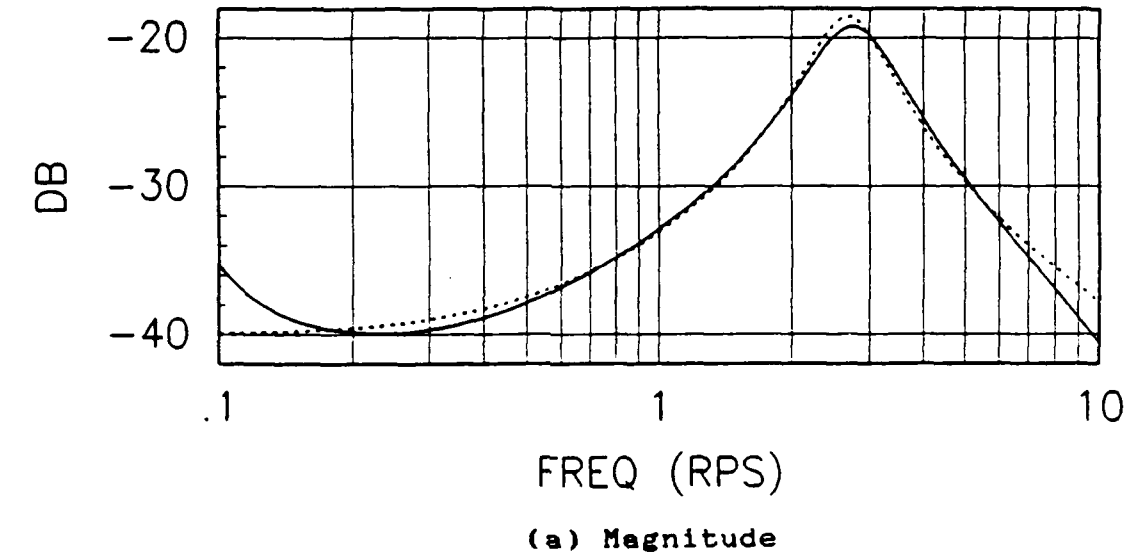

(a) Magnitude

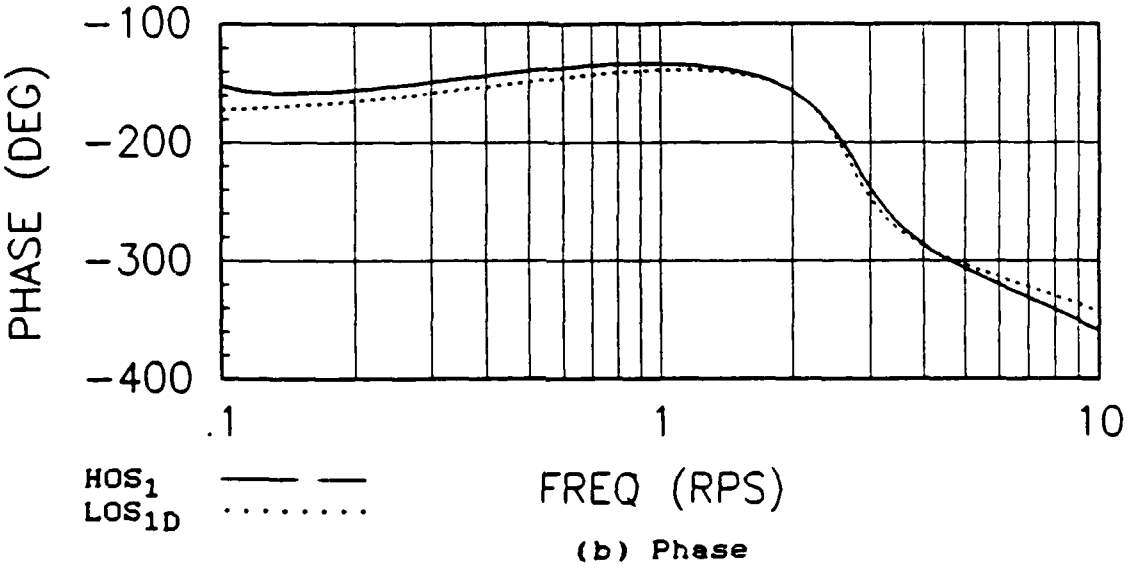

(b) Phase

Figure 13. Frequency Response Comparison, HOS_1 vs LOS_{1D} ($Cost_f$ = 60)

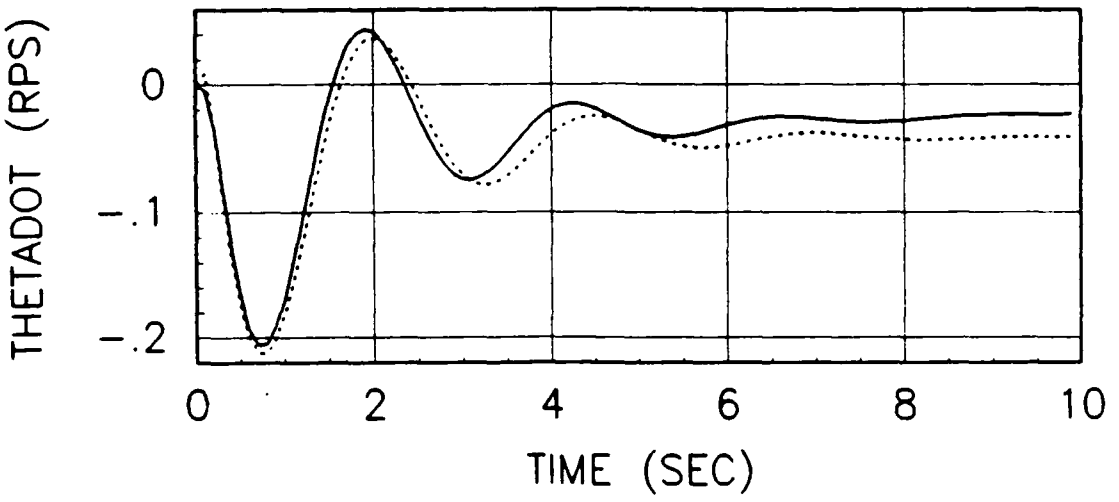

(a) HOS_1 vs LOS_{1C}

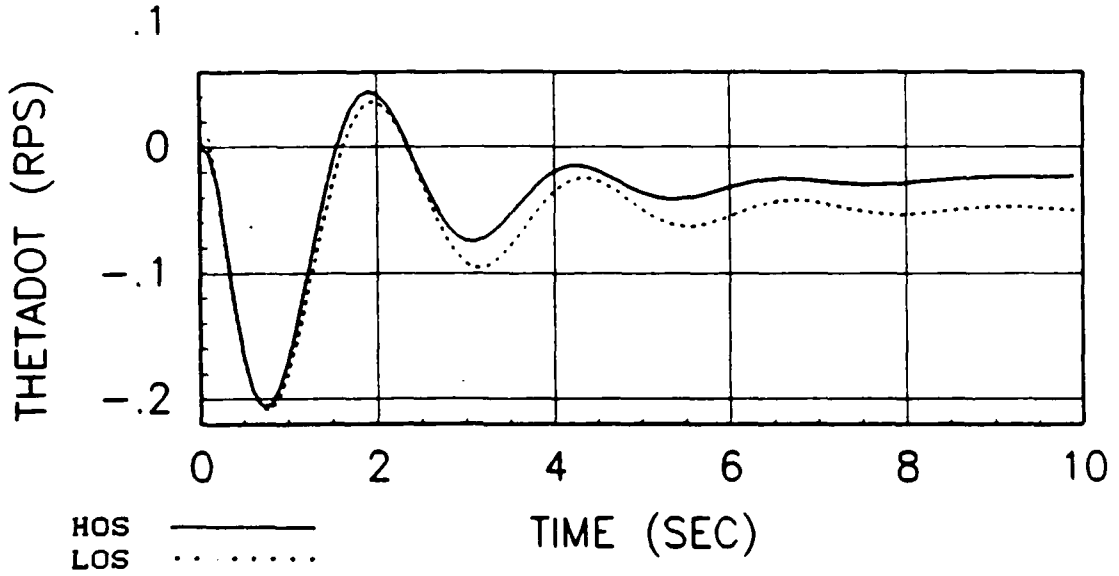

(b) HOS_1 vs LOS_{1D}

Figure 14. Time Response Comparisons (Step Input F_s = 5 lbs)

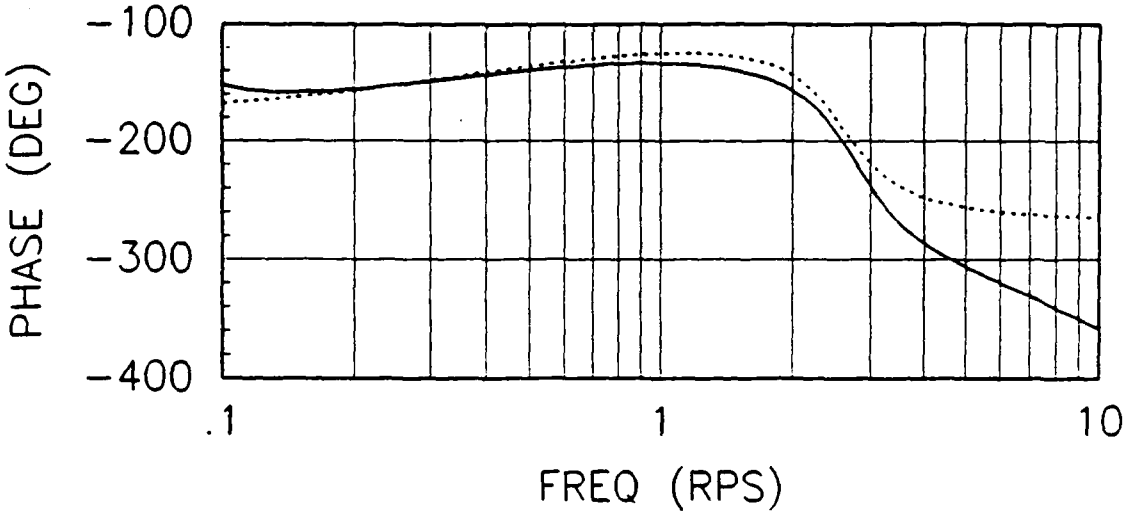

(a) LOS_{1C} without Pade Approximation

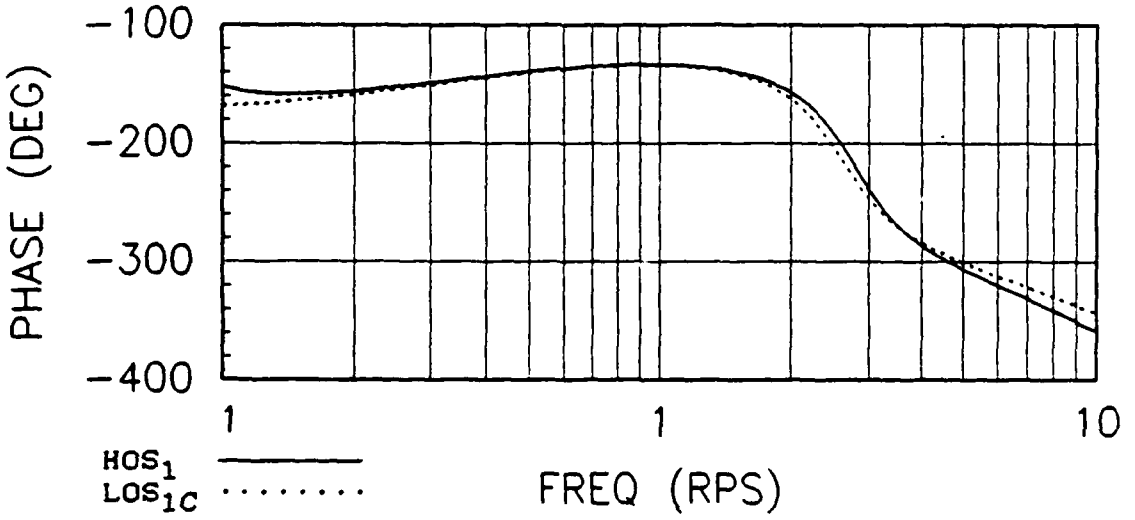

(b) LOS_{1C} with Pade Approximation

Figure 15. LOS_{1C} Phase Angle Comparisons - Effects of Time Delay

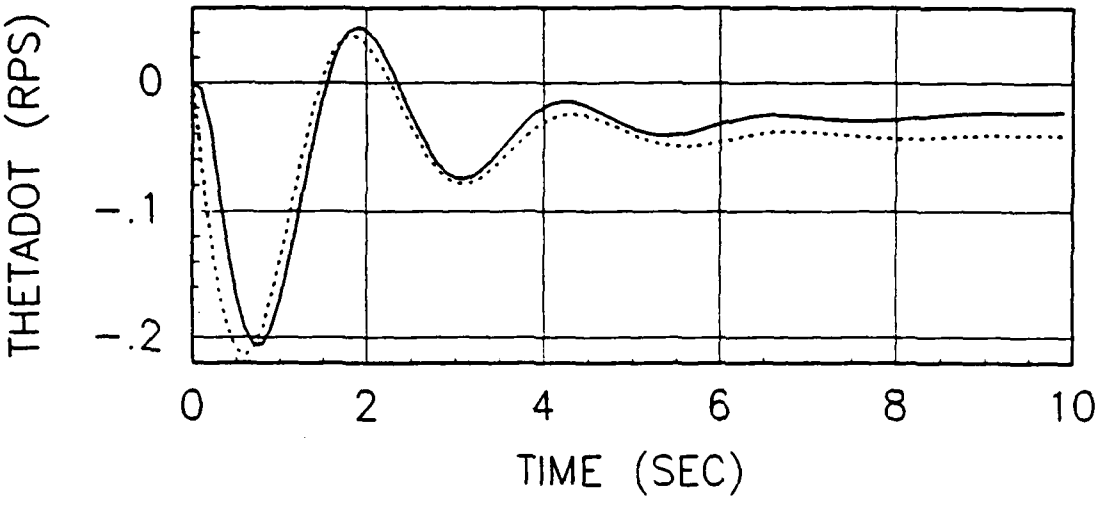

(a) LOS_{1C} without Pade Approximation

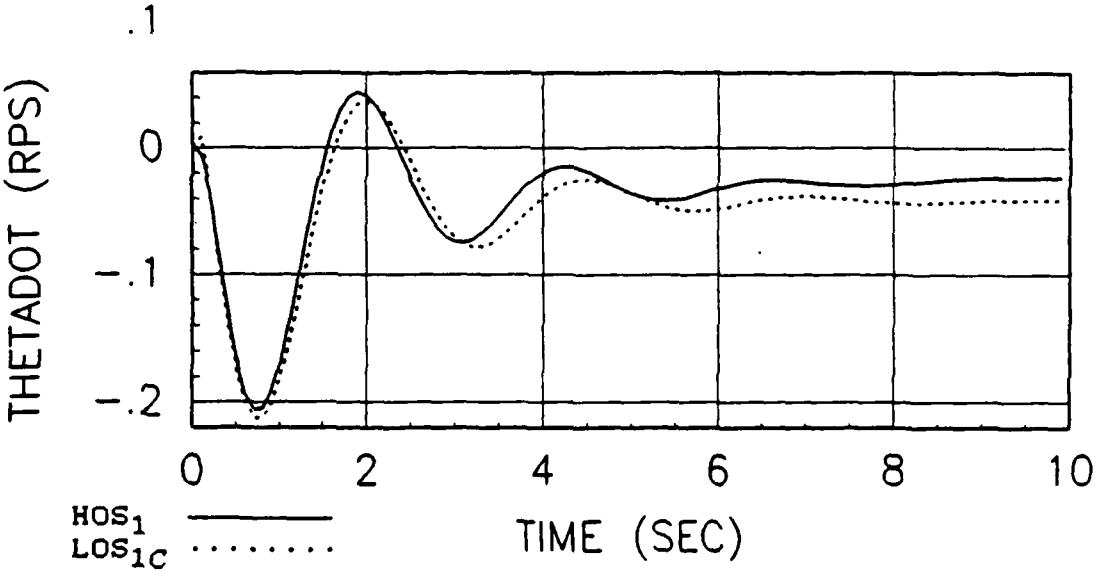

(b) LOS_{1C} with Pade Approximation

Figure 16. LOS_{1C} Time Response Comparisons - Effects of Time Delay (Step Input F_s = 5 lbs)

configurations. These plots (Figures 17 and 18) and the corresponding cost functions in Table V show a relatively poor match for the LOS_{2A} and LOS_{2B} systems.

Table V

n_z/F_s Matching Results
Flight Condition 1 and ω_{fs} = 18.5 (HOS_2)

System	LOS Form	K_{nz} (A_{nz})	ζ_{nz}	ω_{nz}	ζ_{sp}	ω_{sp}	τ	$cost_f$
A-4D*	-	(2.135)	0.026	6.880	0.225	2.770	-	-
LOS_{2A}	LONFIT	0.749	-	-	0.254	2.166	0	679
LOS_{2B}	LONFIT	0.713	-	-	0.229	2.110	-0.074	604
LOS_{2C}	MACFIT	0.176	0.104	7.790	0.193	2.386	0	394
LOS_{2D}	MACFIT	0.174	0.022	6.999	0.238	2.601	0.161	87

* Basic A-4D aircraft parameters (without feel system and servo dynamics) taken from McRuer (5).

The results of the LOS_{2A} and LOS_{2B} matching show that a better match is obtained when time delay is used but only if it is allowed to be negative. The question of whether or not to allow negative time delay has come up in piloted evaluations. Equivalent systems data from the Neal-Smith program (11) show that three of the five lead/lag systems that incorrectly predicted flying qualities (i.e. predicted level 1 but were rated level 2) could have produced a better match if τ was allowed to be less than zero. The Neal-Smith program, however, did not allow negative time delay and τ was set to zero for these configurations. In an analysis of these data, Mitchell and Hoh (20) argue that if τ was allowed to be negative the correlation

between predicted flying qualities and pilot ratings could have been improved for these configurations.

Although negative time delay did improve the match of the LOS_{2B} configuration, the improvement still did not result in a "good" match to the high-order system. The mismatch seen in Figures 17 and 18 suggests that a more fundamental system change (other than time delay) is needed. The problem is in the basic form of the low-order equivalent system used by LONFIT. This form, with a simple gain in the numerator, is an approximation to the short period approximation for n_z/δ_e. Although this approximation is commonly used in equivalent systems studies, McRuer, et al. (5) show that this approximation is valid only at frequencies below the numerator break frequencies as shown below:

$$\frac{n_z}{\delta_e} = \frac{1/g(M_{\delta e}Z_\alpha - M_\alpha Z_{\delta e})}{s^2 + 2\zeta_{sp}\omega_{sp}s + \omega_{sp}^2}, \quad s < \frac{1}{T_{nz2}}, \frac{1}{T_{nz3}}, \text{ or } \omega_{nz} \qquad (20)$$

Thus, the LOS_{2A} and LOS_{2B} systems do not match well to the high-order system because of the quadratic numerator term at ω_{nz} = 6.88 rad/sec. The frequency range of interest (0.1 to 10 rad/sec) lies above this numerator break frequency and eq. 20 is therefore not a good approximation in this case. For frequencies above the break frequencies, McRuer, et al. (5) state that the full short period approximation (eq. 21) should be used.

$$\frac{n_z}{\delta_e} = \frac{K_{nz}(s^2 + 2\zeta_{nz}\omega_{nz}s + \omega_{nz}^2)}{s^2 + 2\zeta_{sp}\omega_{sp}s + \omega_{sp}^2} \qquad (21)$$

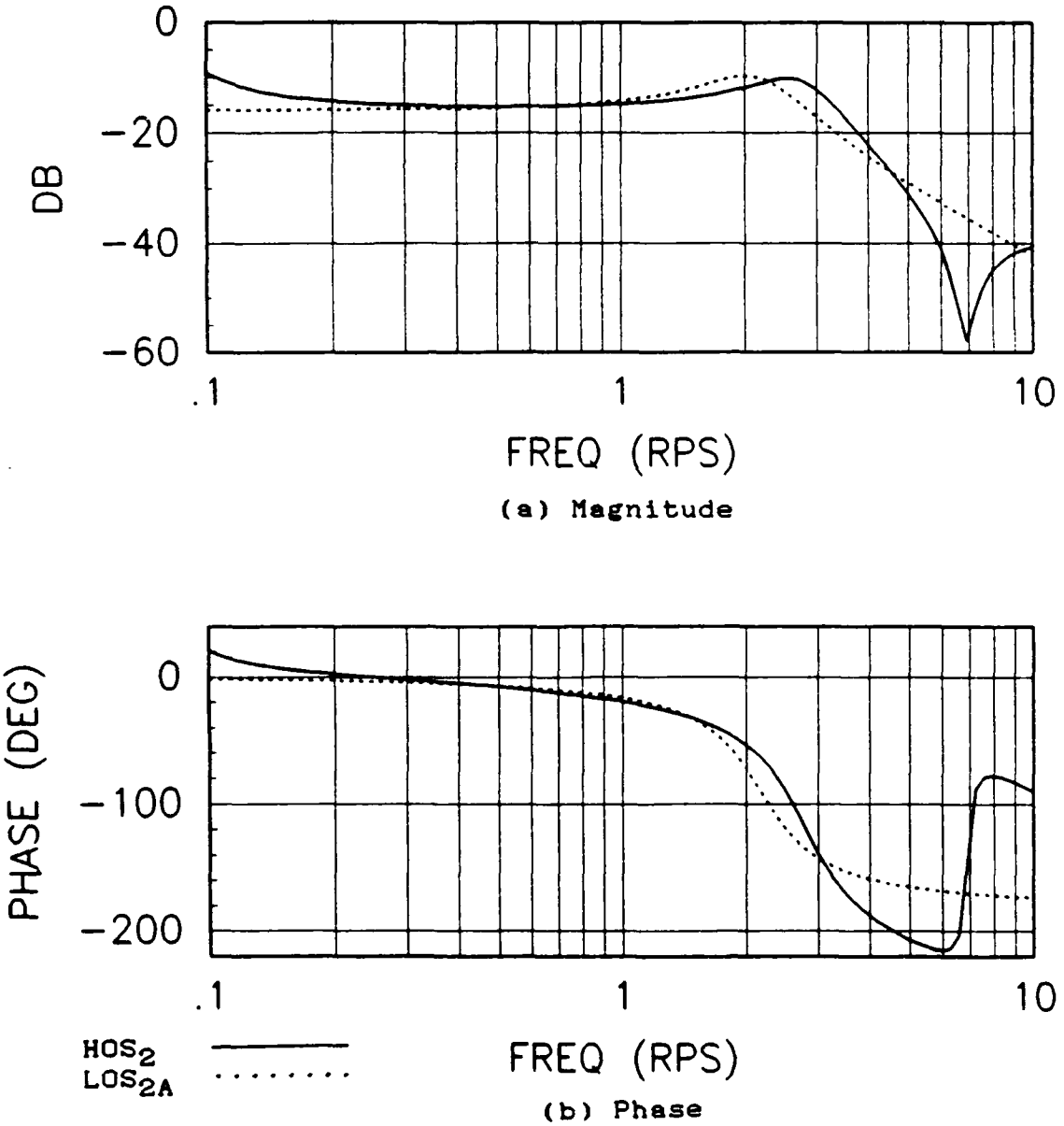

Figure 17. Frequency Response Comparison, HOS_2 vs LOS_{2A} ($Cost_f$ = 713)

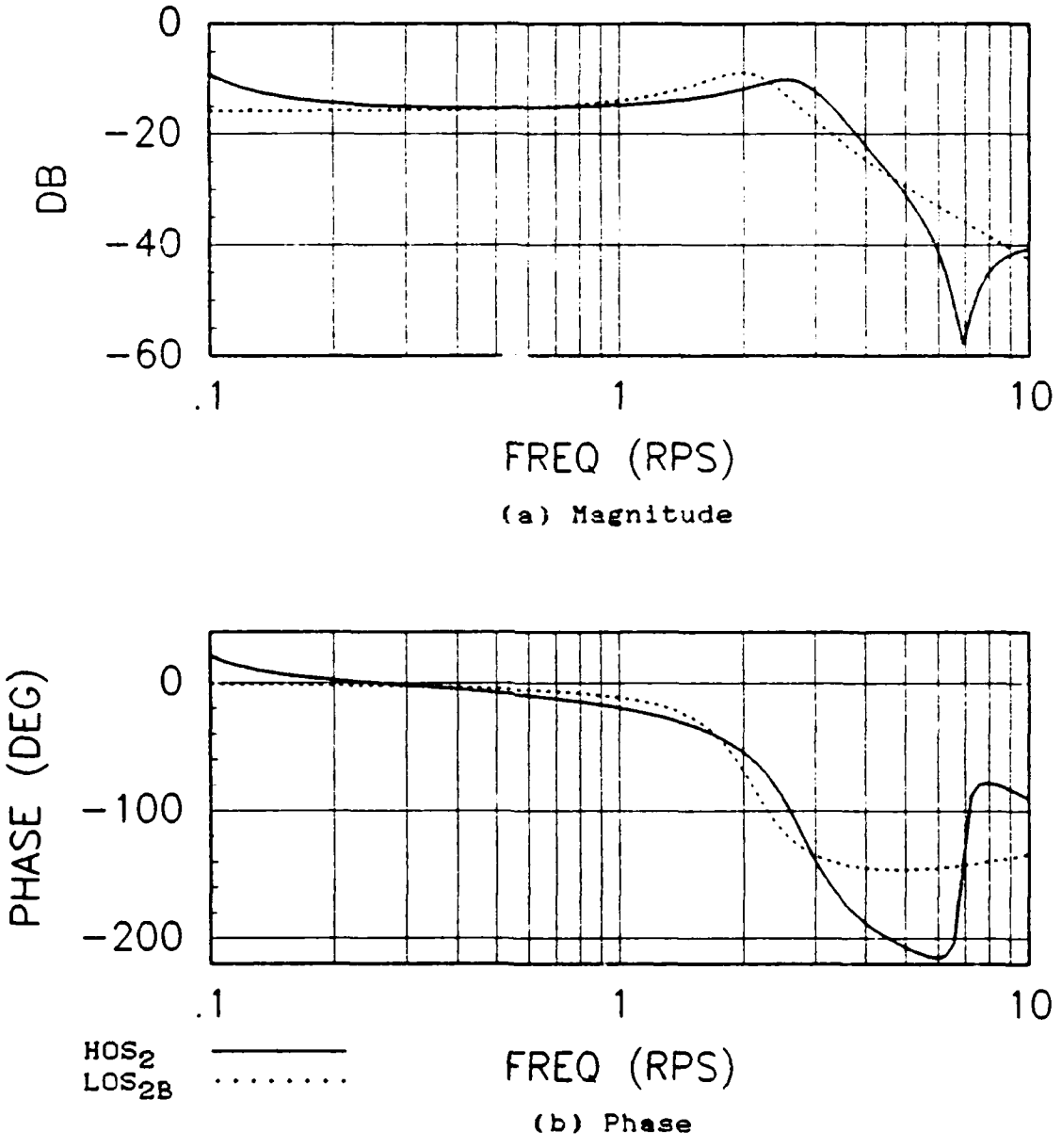

Figure 18. Frequency Response Comparison, HOS_2 vs LOS_{2B} ($Cost_f$ = 634)

Equation 21 was used as the low-order equivalent form for the LOS_{2C} and LOS_{2D} systems and matched to HOS_2 using program MACFIT. On MACFIT, this simply involved specifying a second order numerator and second order denominator as the "guess" for the low-order system form. The excellent results (Table V and Figures 19-21) show that the full short period approximation is indeed an appropriate low-order system to use for this situation.

The difficulties encountered during the Nz/F_s matching demonstrate the "guess work" involved in certain parts of the matching process. The fundamental problem, for example, became one of finding the best low-order system to use. The form typically used in equivalent system work (eq. 16) was found to be inadequate and a higher-order system (eq. 21) was required. Since the higher-order system improved the match, a logical question which follows is whether or not an even better LOS form exists. Certainly, a better match is possible as the order of the equivalent system is increased, but carrying this process too far may defeat the purpose of the equivalent system approach. That is, the existing data base for flying qualities parameters is for classical (unaugmented) airplane systems and a certain amount of mismatch must be tolerated in order to get the high-order system into one of these low-order forms. Among the classical forms, however, there may be several options to choose from (as we have seen in this example) and so the approach is not always straightforward. The individual performing the match must consider what LOES parameters are desired and decide what level of

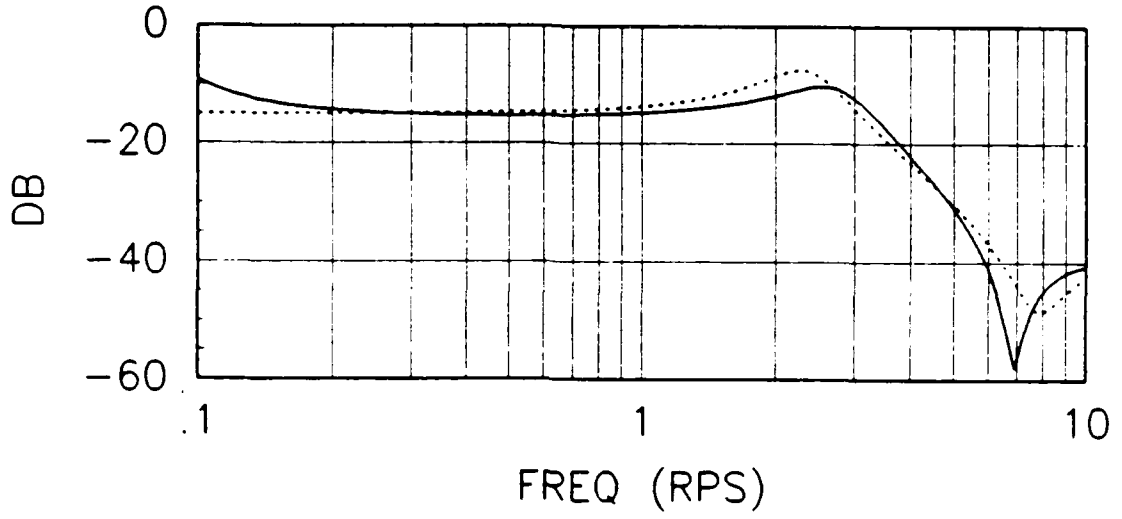

(a) Magnitude

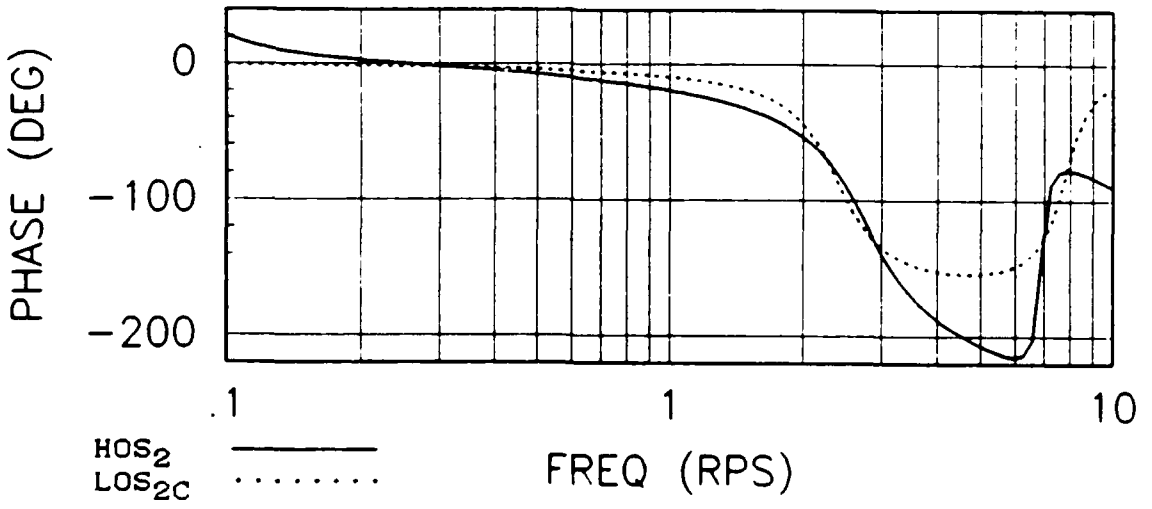

(b) Phase

Figure 18. Frequency Response Comparison, HOS_2 vs LOS_{2C} ($Cost_f$ = 384)

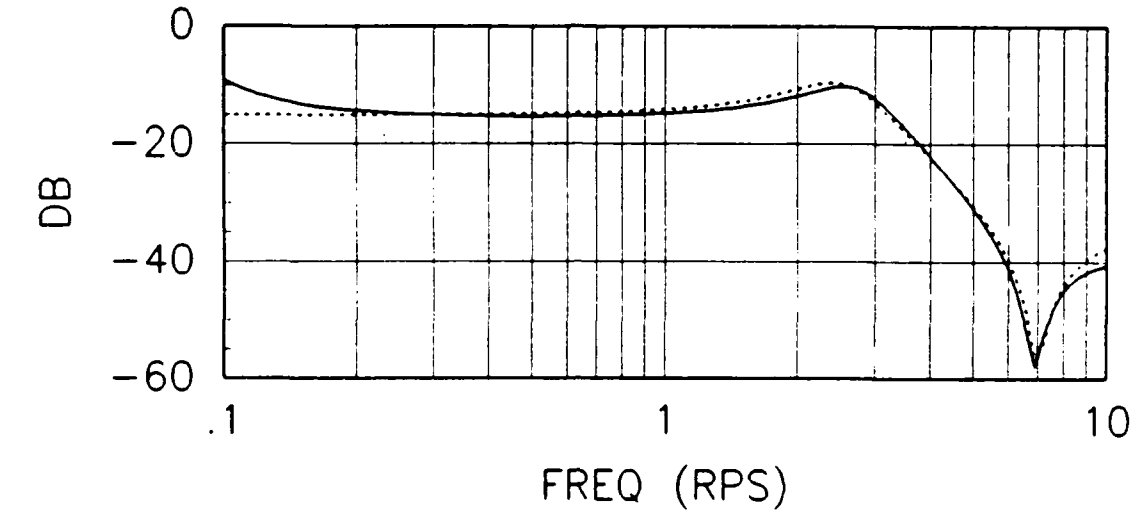

(a) Magnitude

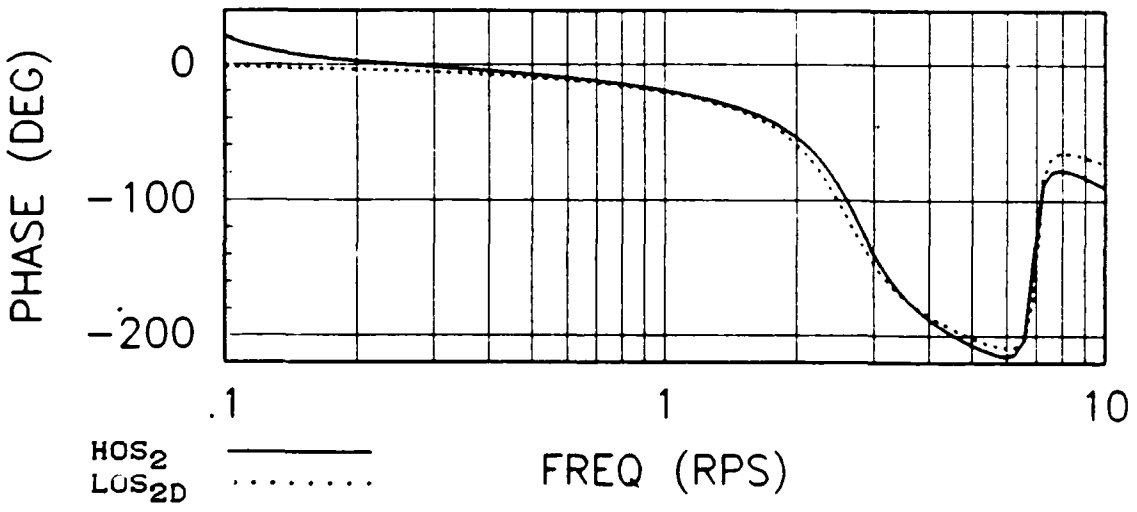

(b) Phase

Figure 20. Frequency Response Comparison, HOS_2 vs LOS_{2D} ($Cost_f$ = 87)

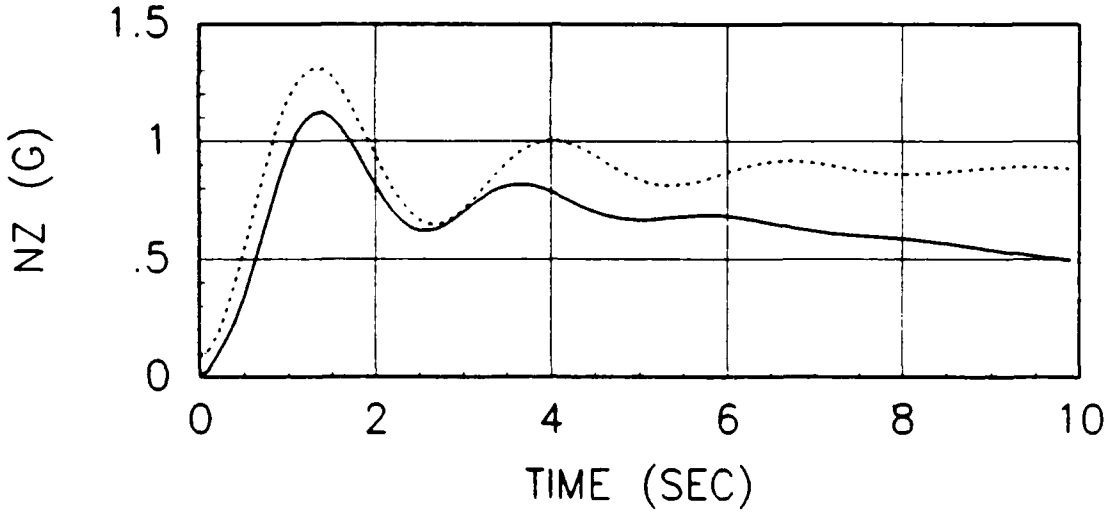

(a) HOS_2 vs LOS_{2C}

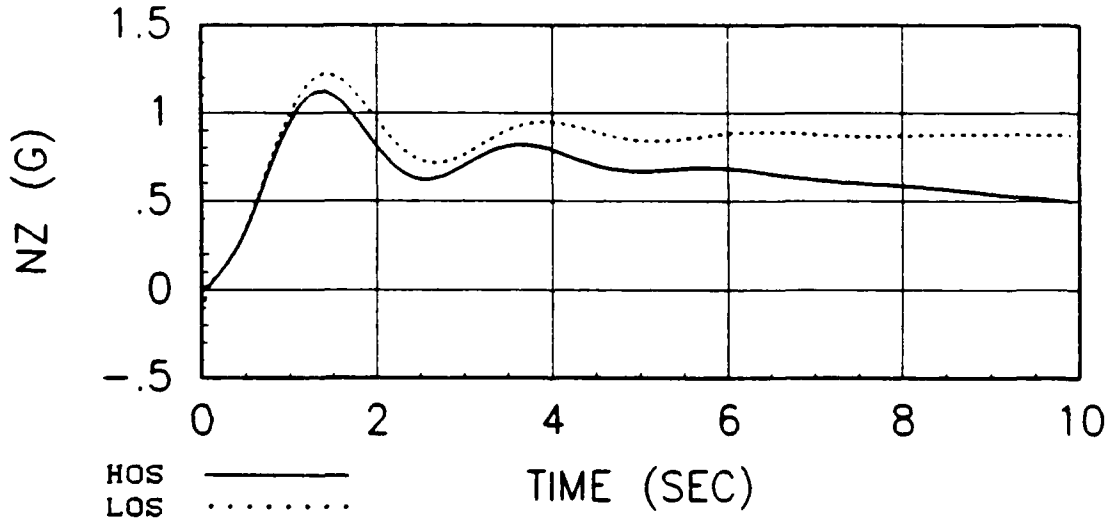

(b) HOS_2 vs LOS_{2D}

Figure 21. Time Response Comparisons (Step Input F_s = 5 lbs)

mismatch is acceptable. With these constraints in mind the LOS form can be chosen from the available options.

HOS_3 and HOS_4 Matching

The $\dot{\theta}/F_s$ and n_z/F_s high-order systems for flight condition 2 and ω_{fs} = 6.0 (HOS_3 and HOS_4) were matched, using the first three steps outlined in the matching strategy, to the following low-order systems:

HOS_3 Matching			HOS_4 Matching		
	L_α	Time Delay		Time Delay	Los Form
LOS_{3A}	Fixed	No	LOS_{4A}	No	LONFIT
LOS_{3B}	Free	No	LOS_{4B}	Yes	LONFIT
LOS_{3C}	Fixed	Yes			
LOS_{3D}	Free	Yes			

The resulting LOS parameters and $cost_f$ functions for the $\dot{\theta}/F_s$ (HOS_3) matching are shown in Table VI. Note that the relatively slow feel system dynamics (ω_{fs} = 6.0) of these HOS configurations

Table VI
$\dot{\theta}/F_s$ Matching Results
Flight Condition 2 and ω_{fs} = 6.0 (HOS_3)

System	L_α	Time Delay	K_θ (A_θ)	ζ_{sp}	ω_{sp}	L_α	τ	$cost_f$
A-4D*	-	-	(-64.00)	0.436	7.350	2.080	-	-
LOS_{3A}	Fixed	No	-0.030	0.449	3.194	2.080	-	511
LOS_{3B}	Free	No	-0.016	0.251	4.837	9.616	-	274
LOS_{3C}	Fixed	Yes	-0.059	0.720	4.524	2.080	0.220	58
LOS_{3D}	Free	Yes	-0.027	0.359	5.887	8.197	0.168	33

* Basic A-4D aircraft parameters (without feel system and servo dynamics) taken from McRuer (5).

resulted in a significant increase in time delay. Low-order equivalent systems without a time delay approximation therefore did not match well to these high-order systems.

The equivalent system parameters and $cost_f$ functions for the n_z/F_s (HOS_4) matching are shown in Table VII. Since ω_{nz} = 18.05 rad/sec for these configurations (which is well above the 0.1 to 10 rad/sec frequency band), eq. 20 shows that the simple LOES form used by LONFIT should be adequate to approximate the short period dynamics. The excellent results obtained using LONFIT show that this approximation is indeed valid. Thus, there is no need to use the full short period approximation (and program MACFIT) as was the case for flight condition 1 where ω_{nz} = 6.88 rad/sec. Magnitude, phase, and time response plots for LOS_{3C} and LOS_{4B} are shown in Figures 22-24.

Table VII

n_z/F_s Matching Results
Flight Condition 2 and ω_{fs} = 6.0 (HOS_4)

System	LOS Form	K_{nz} (A_{nz})	ζ_{sp}	ω_{sp}	τ	$cost_f$
A-4D*	-	(12.059)	0.436	7.350	-	-
LOS_{4A}	LONFIT	1.679	0.460	3.066	0	457
LOS_{4B}	LONFIT	2.888	0.694	4.076	0.196	80

* Basic A-4D aircraft parameters (without feel system and servo dynamics) taken from McRuer (5).

A cursory comparison between the "pure" time delay high-order systems of HOS_1 and HOS_2 and the time delay plus change in time

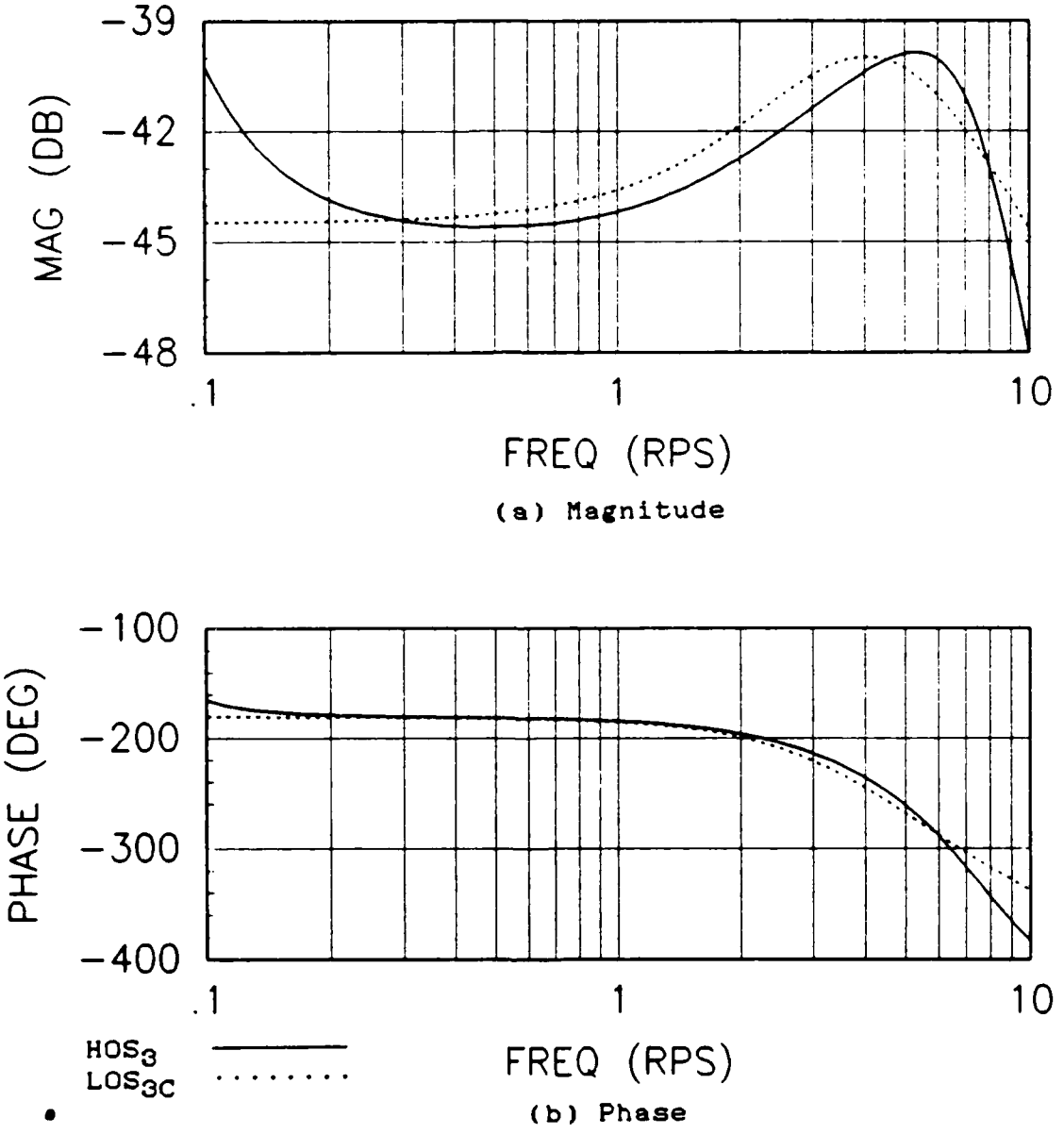

Figure 22. Frequency Response Comparison, HOS_3 vs LOS_{3C} ($Cost_f$ = 61)

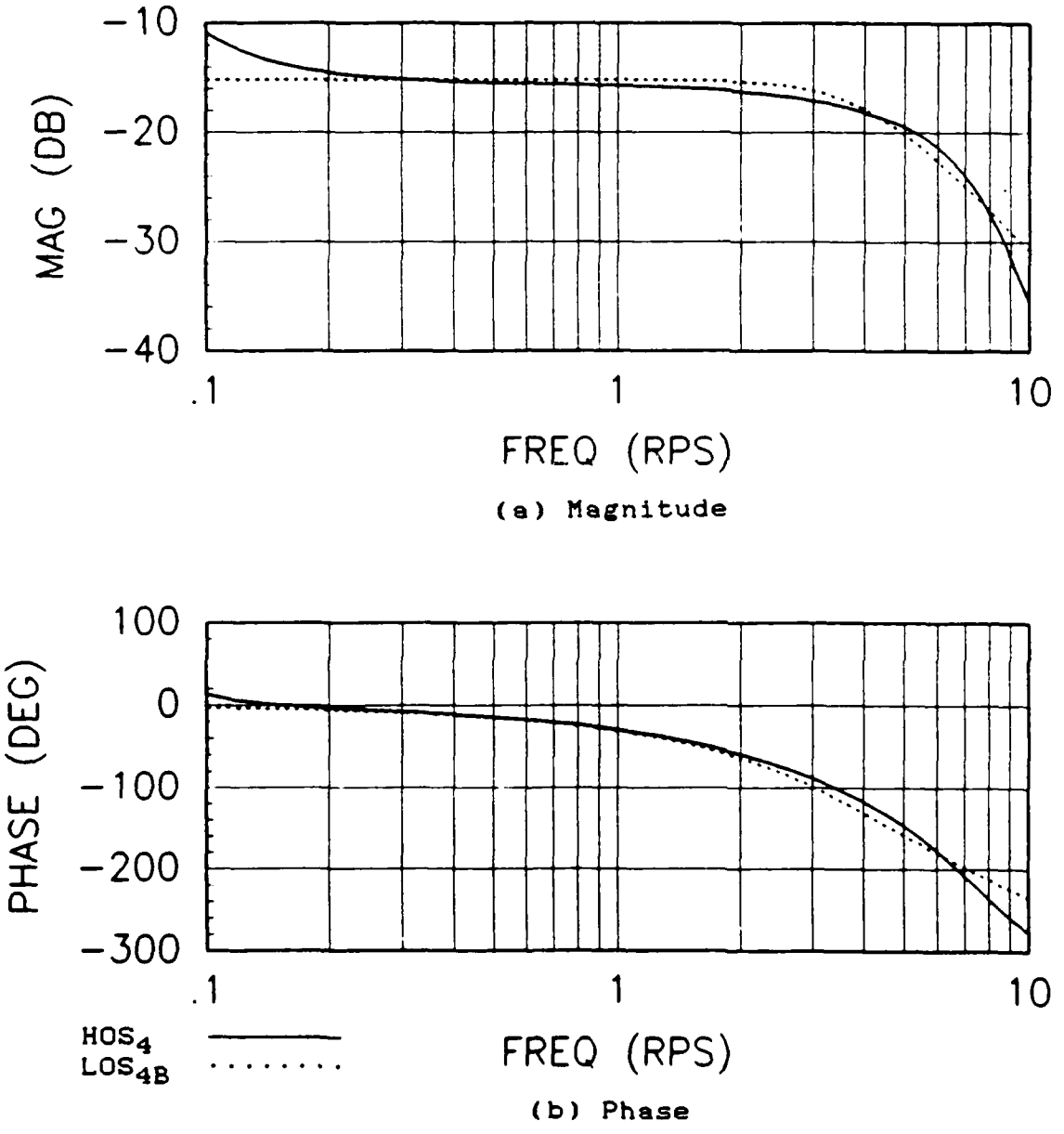

Figure 23. Frequency Response Comparison, HOS_4 vs LOS_{4B} ($Cost_f$ = 87)

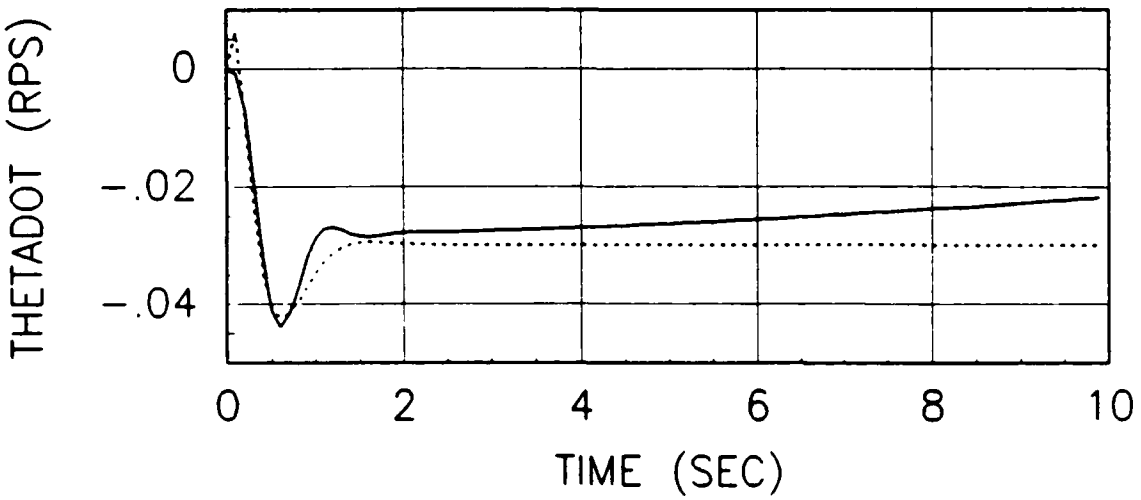

(a) HOS_3 vs LOS_{3C}

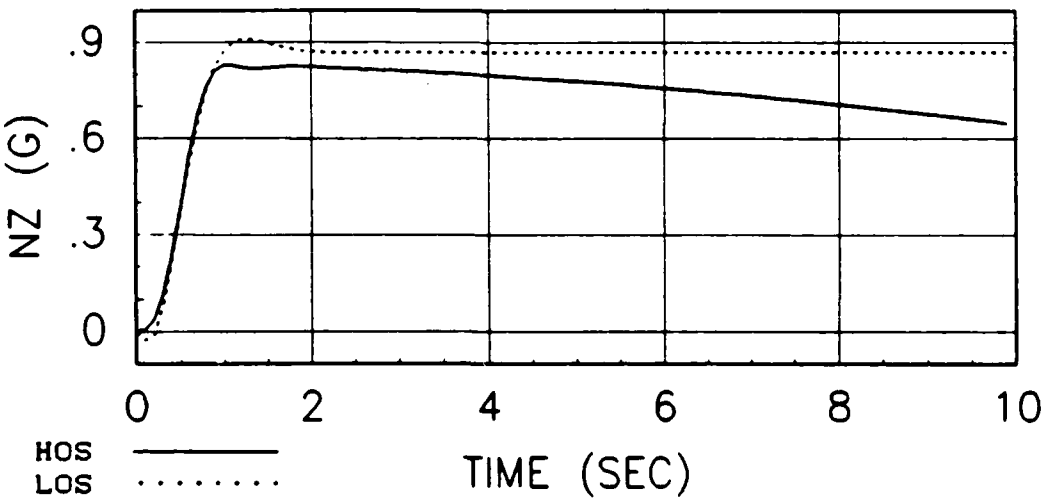

(b) HOS_4 vs LOS_{4B}

Figure 24. Time Response Comparisons (Step Input F_s = 5 lbs)

response systems of HOS_3 and HOS_4 does not show any significant differences between the coupled and uncoupled systems as was expected. In fact, considering only the $cost_f$ functions, the coupled systems (HOS_3 and HOS_4) actually matched better than the uncoupled systems (HOS_1 and HOS_2) since the former had slightly lower $cost_f$ functions - indicating a closer frequency domain match. The $cost_f$ functions, however, were all below 100 for the best matches which, from a flying qualities perspective, indicates an excellent match. The HOS_1 - HOS_4 systems, therefore, have been useful in providing a detailed look at the matching process but have provided only a limited look at the effects of coupling between the control system and aircraft dynamics. For this reason, a more complete range of control system dynamics was investigated. The results of this analysis are given in the following section.

Effects of Control System Dynamics

To investigate the effects of coupling between the control system and aircraft dynamics on equivalent systems matching techniques, the feel system natural frequency ω_{fs} was varied throughout the range of 6 to 31 rad/sec for each flight condition. This was done using the pitch rate $\dot{\theta}/F_s$ high-order system with L_α both fixed and free which resulted in a total of 12 HOS and 24 LOES configurations. The tabulated results of this matching are given in Appendix A, and selected plots of the data are presented here for consideration. The results of this matching demonstrate

trends associated with the movement of the control system roots and illustrate some of the problems in equivalent systems matching when there is coupling between the control system and aircraft dynamics.

In general, the results of this matching show that as the feel system's natural frequency is moved away from the aircraft's natural frequency a better equivalent system match is possible. This fact is perhaps best demonstrated by Figures 25 and 26 which show the cost functions versus ω_{fs} for both flight conditions. The fact that a better match is possible with a "faster" control system is not surprising. With sufficiently fast control system dynamics, the HOS configuration responds more like the basic aircraft (without control system); and, it is precisely this basic aircraft form (i.e. the short period approximation in this case) that is being matched to the high-order response.

Figures 27-29 show that the high-order systems do indeed behave more like the basic aircraft as the control system dynamics are made faster. Figures 27 and 28 show that the equivalent short period parameters, ω_{sp} and ζ_{sp}, approach their basic aircraft values as ω_{fs} is increased; and, Figure 29 shows the expected result that the equivalent time delay is reduced as ω_{fs} is increased.

In addition to increased mismatch, another limitation associated with coupling between the control system and aircraft roots was in the "behavior" of the matching programs themselves. The problem, encountered during the computer matching, was that

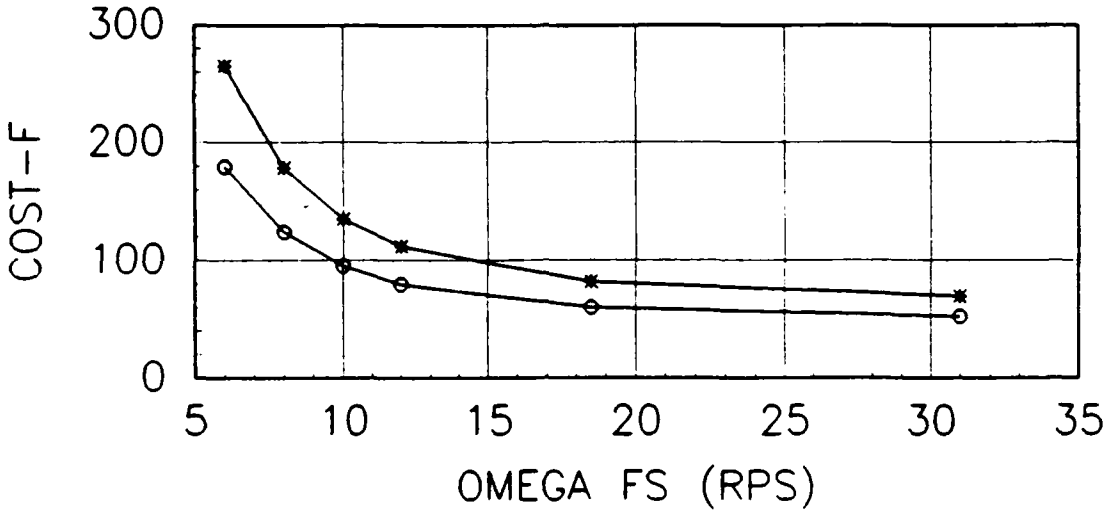

(a) Frequency Domain Cost Functions

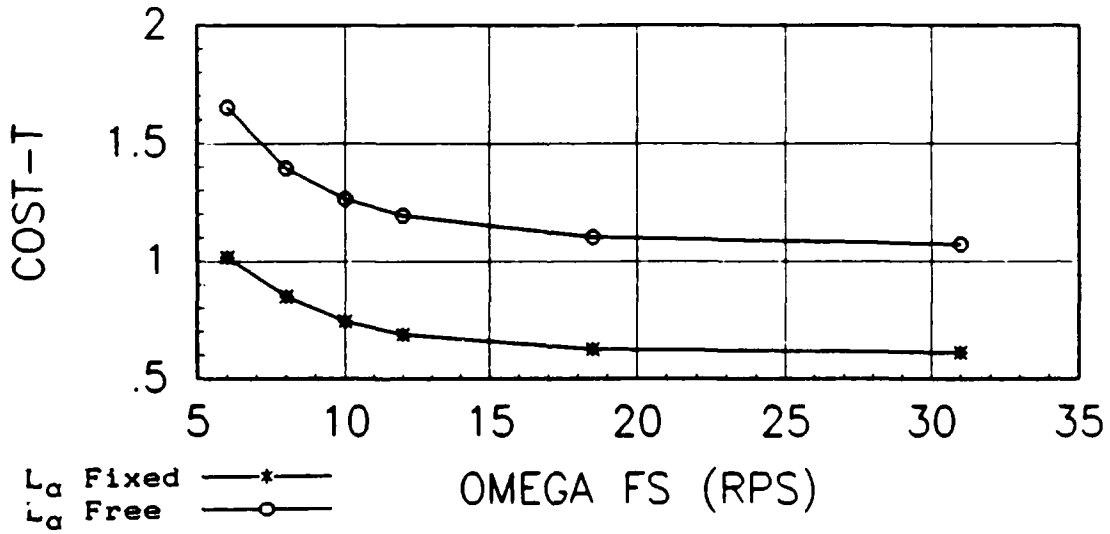

(b) Time Domain Cost Functions

Figure 25. Cost Functions versus ω_{fs} - Flight Condition 1

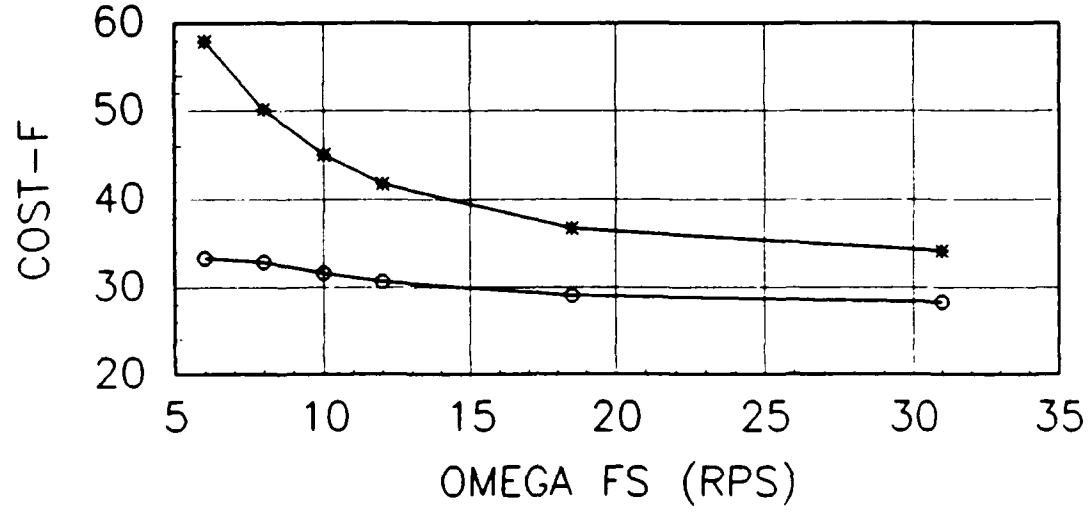

(a) Frequency Domain Cost Functions

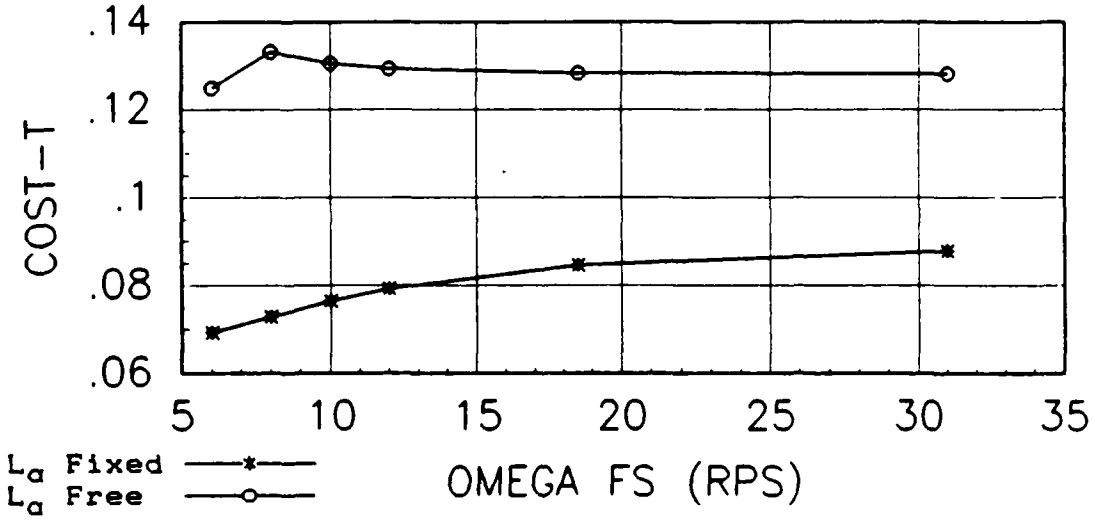

(b) Time Domain Cost Functions

Figure 26. Cost Functions versus ω_{fs} - Flight Condition 2

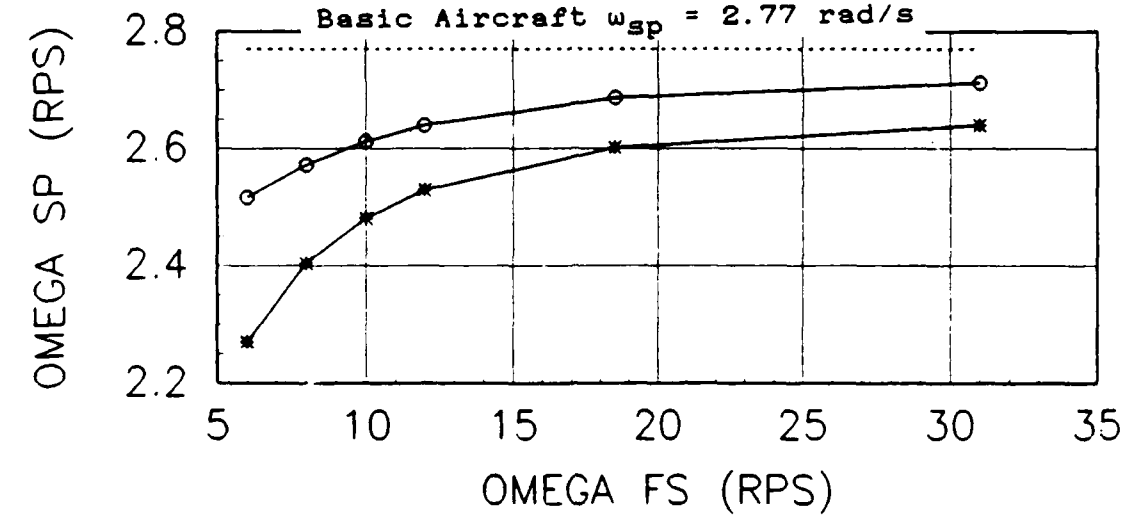

(a) Flight Condition 1

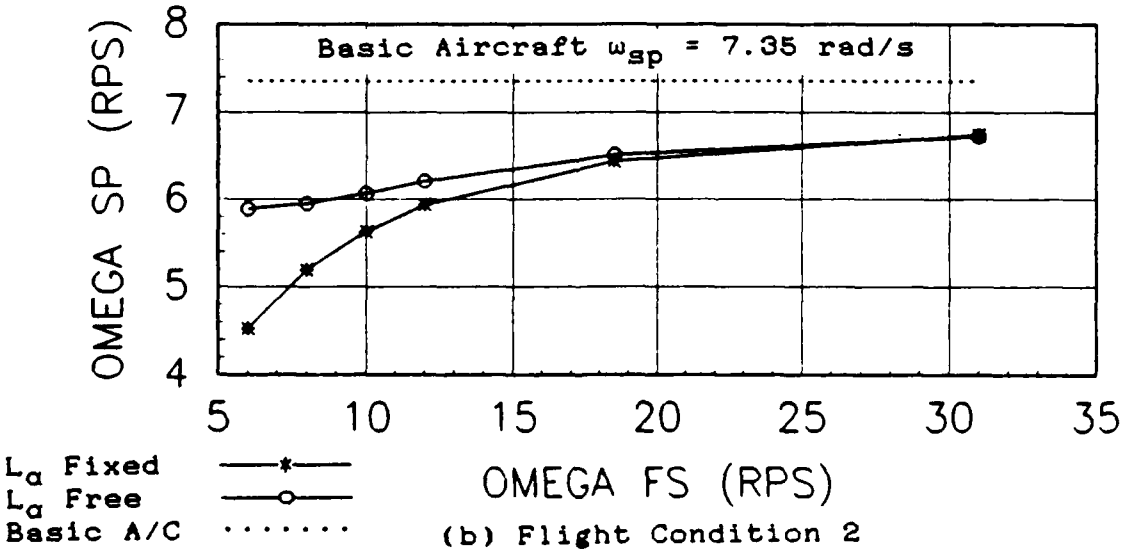

(b) Flight Condition 2

Figure 27. Equivalent ω_{sp} versus ω_{fs}

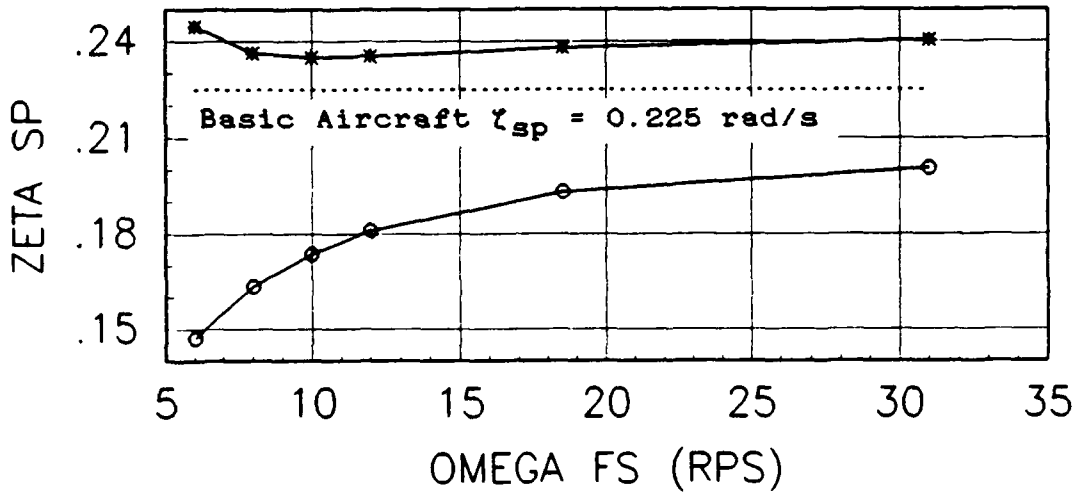

(a) Flight Condition 1

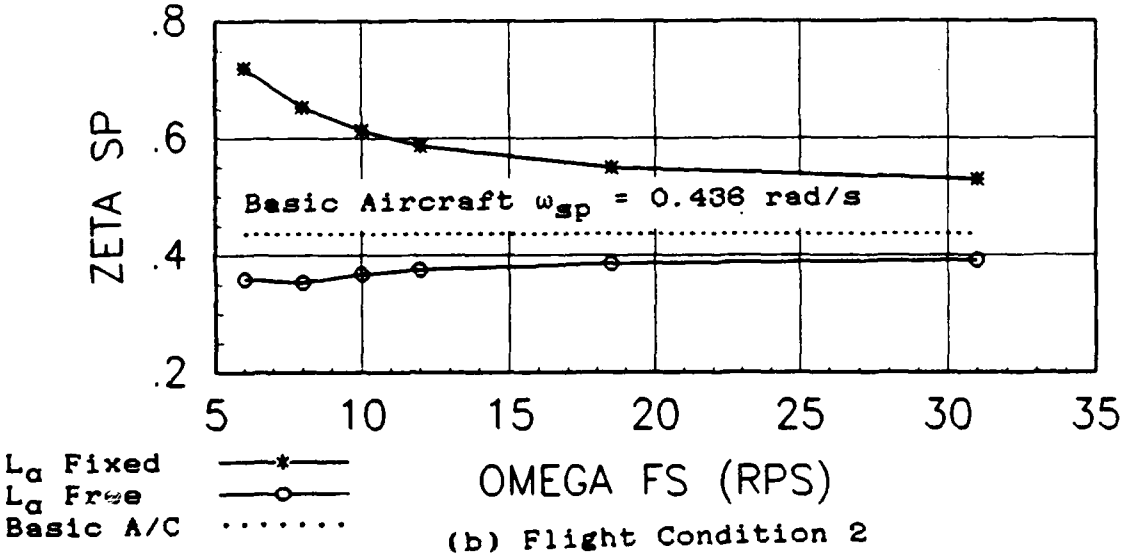

(b) Flight Condition 2

Figure 28. Equivalent ζ_{sp} versus ω_{fs}

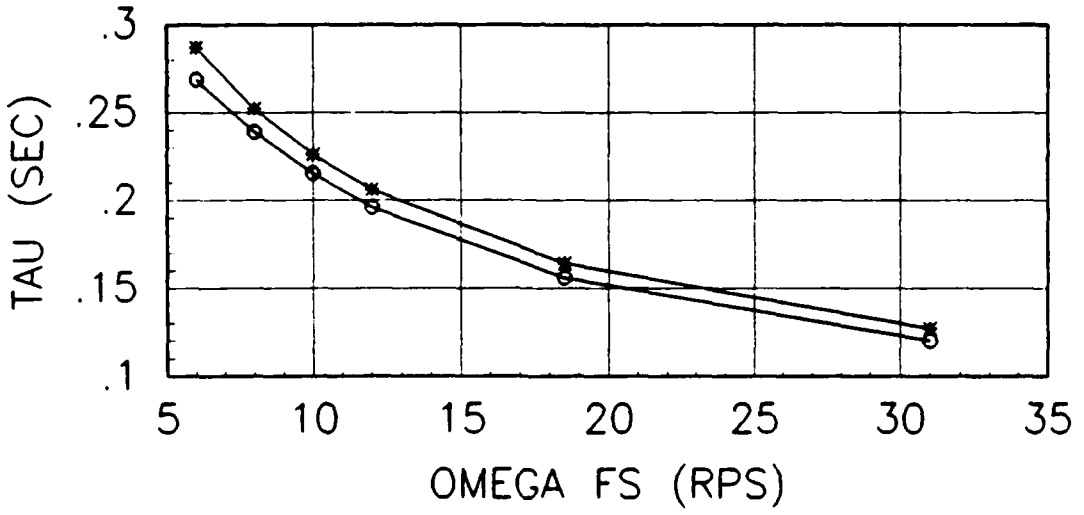

(a) Flight Condition 1

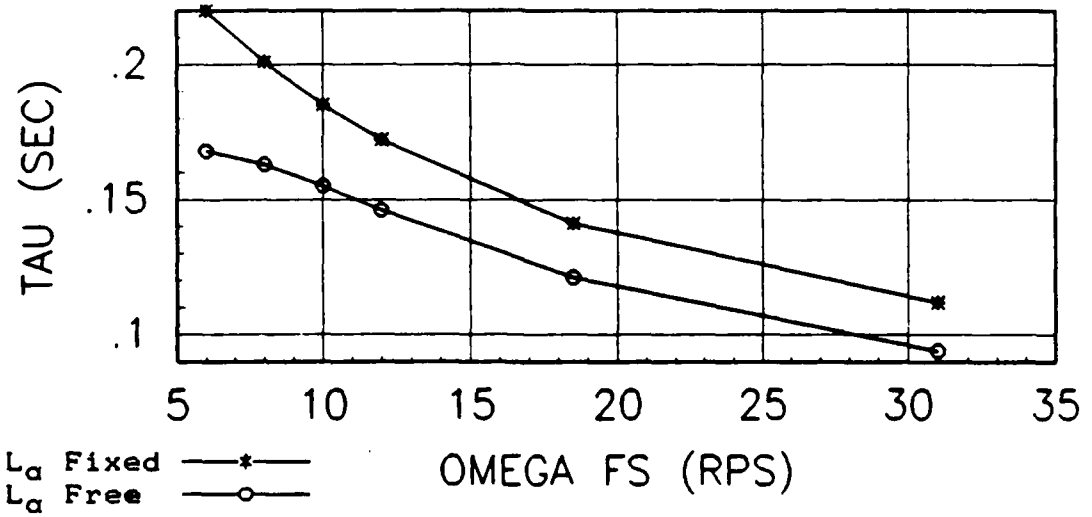

(b) Flight Condition 2

Figure 29. Equivalent Time Delay (τ_θ) versus ω_{fs}

the search vector (i.e. the vector made up of the matching variables) stopped at "local" minimums. Changing the initial condition vector slightly would generally solve the problem by allowing the search vector to bypass the local minimum and arrive at a smaller minimum which gave the desired best match. In most cases, it was apparent when a local minimum was encountered because the equivalent system parameters would take on extreme values, $cost_f$ would be unreasonably high, and (in some cases) the low-order equivalent system would have an unstable time response. In some cases, however, it was difficult to determine if a local minimum had been encountered, or if there was some other problem precluding a good match. For configurations with coupling between the control system and aircraft roots the programs had a greater tendency to arrive at a local minimum. In these configurations, the programs were more sensitive to variations in the initial condition vector, and the input initial conditions had to be closer to the correct final values in order to arrive at the best match.

A comparison of the L_α-free versus L_α-fixed matching data raises questions regarding the meaning of equivalent L_α. Figure 30 shows that the equivalent L_α approaches the aircraft value for configurations with fast control system dynamics, and assumes considerably higher values for configurations with slow control system dynamics. These results not only raise questions regarding the meaning of equivalent L_α but also raise questions regarding the meaning of the other equivalent parameters in the same LOS

configuration. Consider, for example, the HOS_3 configuration with flight condition 2 and ω_{fs} = 6.0 (Table VI and Figure 30b). For this configuration, the equivalent L_α of 8.197 is unreasonably high given that the basic aircraft value is 2.08. The value of L_α = 8.197 is a value picked by the matching routine that produced the best mathematical match but is not necessarily representative of the actual stability derivative of the high-order system. For the same HOS configuration, ζ_{sp} is nearly doubled and there are significant changes in ω_{sp} and τ between the L_α-fixed and L_α-free configurations. The question is, which set of parameters (L_α, ζ_{sp}, ω_{sp}, and τ) actually characterizes the HOS short period dynamics; or, are the actual HOS characteristics somewhere in between the two extremes? The fact that both sets of equivalent parameters give an excellent match to the HOS indicates that they both characterize the HOS dynamics. If that is the case, however, which set of parameters should be related to the requirements of MIL-F-8785C in order to specify and predict flying qualities? Figures 27-30 show that this "dilemma" is greatest (i.e. there is the greatest change in equivalent parameters between the L_α-fixed and L_α-free configurations) when the control system dynamics are the slowest.

Considerable insight could be gained through a simulator or flight test program set up to evaluate a large number of L_α-fixed and L_α-free configurations. The configurations should be similar to the example discussed above in which there is a significant change in equivalent parameters between the L_α-fixed and L_α-free

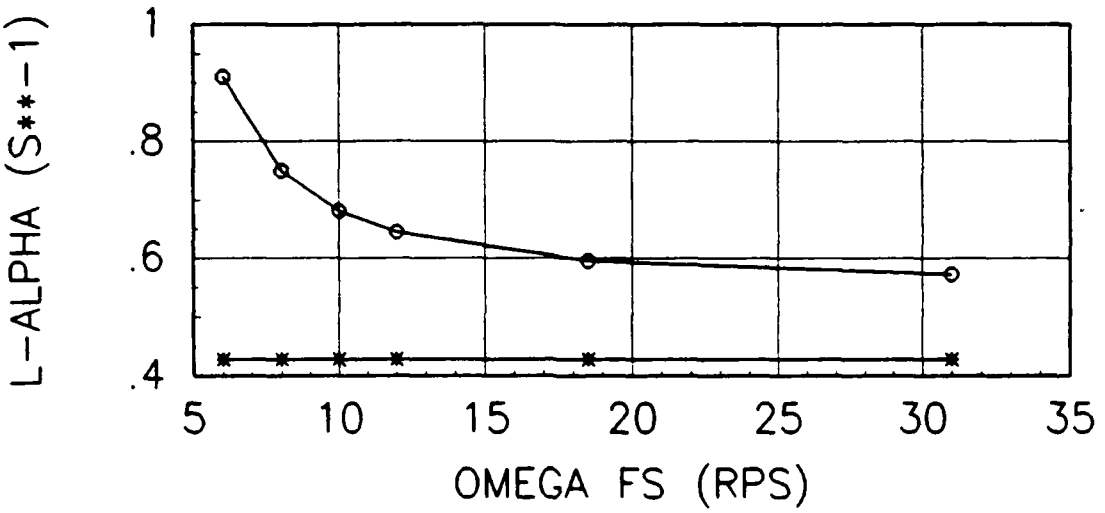

(a) Flight Condition 1

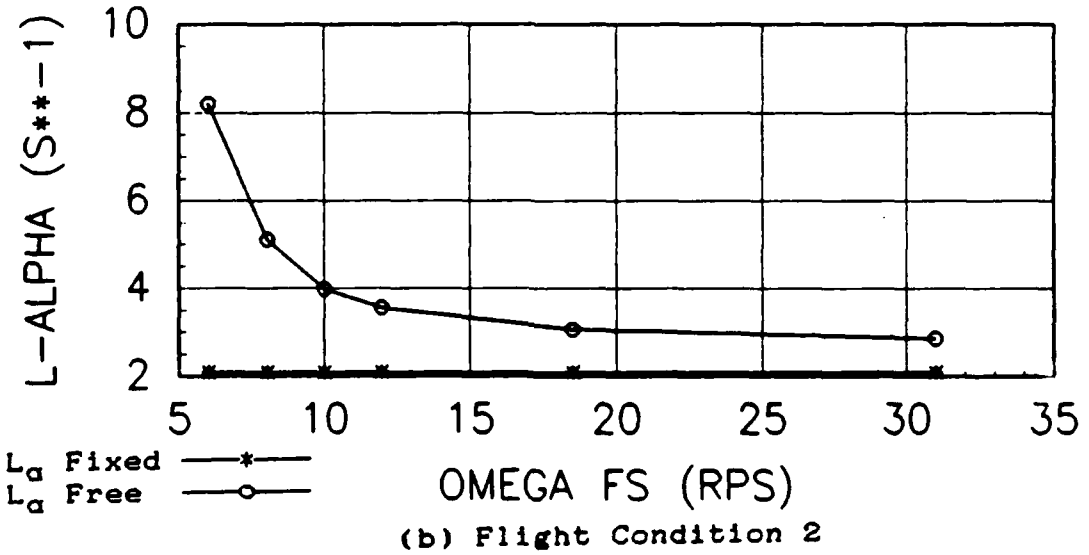

(b) Flight Condition 2

Figure 30. Equivalent L_α versus ω_{fs}

configurations. If the results of such evaluations show that over a large range of flight conditions and control system dynamics, the HOS flying qualities are best characterized by the L_α-fixed parameters, this would lend credence to the idea that L_α should be fixed during equivalent system matching. On the other hand, such evaluations could show that L_α should be free during equivalent system matching, or that there are certain configurations for which L_α should be free, etc.

The NT-33 piloted evaluations conducted by Neal-Smith (11) evaluated a total of 51 HOS configurations, many with significant coupling between the control system and aircraft dynamics. The report states that reasonable correlation between pilot rating data and equivalent systems data was achieved by plotting the product $\omega_{sp}T_{\theta 2}$ against the time delay τ. Due to numerous problems with the equivalent systems approach however, the authors developed a pilot-in-the-loop analysis that was used instead. In summary of the equivalent systems matching results, the report states the following:

> Although the correlation of the PR data with this equivalent system approach is reasonable, several limitations should be noted...In the region of low $\omega_{sp}T_{\theta 2}$ values (say $\omega_{sp}T_{\theta 2} < 2.5$), large trade-offs between $T_{\theta 2}$ and ω_{sp}, or in some cases between ζ_{sp} and ω_{sp}, can be made with little discernible difference in the accuracy of the analog match achieved. In the present experiment, this problem occurred for those configurations having $\dot{\theta}$ responses with little or no overshoot (configurations with low ω_{sp} or large control system lags)...The important point to note is that this lack of precision occurs in an area of primary practical importance, since the lower $\omega_{sp}T_{\theta 2}$ boundary would represent a design limit on aft center-of-gravity travel for many airplanes. (11)

Some of the problems quoted in the Neal-Smith report are

similar to the problems found in this study. The L_α-fixed and L_α-free configurations also had "large trade-offs" between the parameters with "little discernible difference in the accuracy of the analog match." As in the Neal-Smith study, these "trade-offs" were especially apparent in configurations with large control system lags.

The Neal-Smith report also states the following with regard to equivalent time delay determination: "Accurate determination of the time delay τ is often difficult; and for time delays greater than 0.1 sec, small variations in τ can mean significant changes in PR" (11). Similarly, in the HOS_3 matching discussed above, τ varied from 0.168 to 0.220 between the L_α-fixed and L_α-free configurations (Table VI) and there is some question as to which value is the "correct" one to use for specifying flying qualities.

The discussion of these problems is not meant to imply that equivalent systems techniques are not suitable for specifying flying qualities. Despite the limitations of the equivalent systems method it will continue to be used in flying qualities work and the requirements in MIL-F-8785C regarding equivalent systems are well documented. The purpose here is to point out some of the limitations of the method and discuss the areas that need more work. By discussing these problems for both the frequency domain and time domain techniques it will be possible to make subjective as well as objective comparisons between the two methods. The objective comparisons will be based on mathematical

differences (i.e. mismatch comparisons), and the subjective comparisons will be based on the consideration of problems such as those discussed in this section.

IV. Time Response Computer Matching

The time response matching theory discussed in this chapter is a least squares technique taken from Franklin and Powell (22) and adapted for use in flight test system identification work. The final product of the time response matching is a lower order equivalent system (LOES) which is a second order approximation of a higher order system (HOS).

To begin the time domain matching the higher order system is first expressed in state space form using vector notation as follows:

$$\dot{x} = Ax + Bu \qquad (22)$$

$$y = Cx$$

where $A \in R^n$, $B \in R^m$, and C is chosen to give the desired output y. Note that n equals the number of states and m equals the number of inputs for the HOS.

The first step in the time domain matching requires discrete HOS input and output data. To develop a discrete aircraft model from the continuous model, equation 22 is integrated over a sampling time T to yield (21):

$$x[(k+1)T] = F(T)x(kT) + G(T)u(kT) \qquad (23)$$

where the matrices:

$$F(T) = e^{AT}$$

$$G(T) = \int_0^T e^{A\tau} d\tau B$$

and u is assumed constant over the sampling interval. Equation 23 forms a discrete aircraft model which gives the aircraft states x at time T_{k+1} in terms of the state x and input u at the previously sampled time T_k. Equation 23 will be referred to in shortened form as follows:

$$x(k+1) = Fx(k) + Gu(k) \qquad (24)$$
$$y(k+1) = Hx(k+1)$$

where the H matrix can be chosen to give the desired output y.

One appealing aspect of the least squares time response matching technique is that the discrete data can be experimentally derived. This means that input versus output time histories of the HOS are all that is required to extract a low-order equivalent model. This technique, therefore would seem to be well suited for flight test data collection and parameter identification requirements. For the present development, however, the HOS has been analytically modeled so that equation 24 can be used to generate "synthetic" flight test data.

ARMA Canonical Form

At this point it will be necessary to introduce the Auto Regressive Moving Average (ARMA) canonical state space form. This canonical representation has one feature especially appropriate for identification, and will be used to develop the least squares matching technique in the next section. For a complete discussion

of the ARMA and other canonical forms, the interested reader is referred to Franklin and Powell (22).

To introduce the ARMA canonical form, consider the discrete transfer function matrix $H(z)$ which can be derived from the state space matrices using the following relation:

$$H(z) = Y(z)/U(z) = H(zI - F)^{-1}G \qquad (25)$$

Equation 25 implies that for a given set of state matrices F, G, and H there is a unique transfer function representation $H(z)$. Note, however, that for a given transfer function matrix there is not a unique set of state matrices. In general, there may be many combinations of F, G, and H that have the same transfer function. Thus, the definition of the state is not unique and can be selected in such a way which makes the task of system identification as easy as possible. The standard way to do this is to define the state so that F, G, and H are in accordance with one of the canonical forms for transfer functions. For the least squares system identification presented in the next section, the ARMA canonical form will be used.

To look at a specific example of the ARMA representation, suppose the state equations represent a single input/single output (SISO) system. The transfer function matrix would then reduce to a scalar and, for a third-order system may be represented by the following equation:

$$H(z) = \frac{b_1 z^{-1} + b_2 z^{-2} + b_3 z^{-3}}{1 - a_1 z^{-1} - a_2 z^{-2} - a_3 z^{-3}} \qquad (26)$$

The ARMA canonical form for equation 26 has six states and is given by the matrices:

$$F = \begin{bmatrix} a_1 & a_2 & a_3 & b_1 & b_2 & b_3 \\ 1 & 0 & 0 & 0 & 0 & 0 \\ 0 & 1 & 0 & 0 & 0 & 0 \\ 0 & 0 & 0 & 0 & 0 & 0 \\ 0 & 0 & 0 & 1 & 0 & 0 \\ 0 & 0 & 0 & 0 & 1 & 0 \end{bmatrix} \qquad G = \begin{bmatrix} 0 \\ 0 \\ 0 \\ 1 \\ 0 \\ 0 \end{bmatrix} \qquad (27)$$

$$H = [a_1 \; a_2 \; a_3 \; b_1 \; b_2 \; b_3]$$

The system described by equation 27 is seen to have six states to describe a third-order transfer function and thus to be "nonminimal." In fact, the F matrix can be shown to have three poles at z = 0 that are not observable for any values of a_i or b_i. However, the system does have one remarkable property: the state is given by

$$x_k = [y_{k-1} \; y_{k-2} \; y_{k-3} \; u_{k-1} \; u_{k-2} \; u_{k-3}]^T \qquad (28)$$

In other words, the state is exactly given by the past inputs and outputs. Thus, if the set of u_k and y_k are known, the state is known also since it is merely a listing of the six members of the set. All the "action" takes place in the output equation which is

$$\begin{aligned} y_k &= Hx_k \\ &= a_1 y_{k-1} + a_2 y_{k-2} + a_3 y_{k-3} + b_1 u_{k-1} \\ &\qquad + b_2 u_{k-2} + b_3 u_{k-3} \end{aligned} \qquad (29)$$

There is actually no need to carry any other equation along since the state equations are trivially related to this output equation.

Least Squares and Equation Error

Before discussing the actual least squares matching technique, a definition of "goodness" of fit will be made using the concept of equation error. To begin with, a parameter vector β will be defined as

$$\beta = [a_1 \; a_2 \; a_3 \; b_1 \; b_2 \; b_3]^T \qquad (30)$$

where the a_i and b_i are the coefficients of the discrete transfer function (equation 26). Next, imagine that a set of input sample values u(k) and a set of corresponding output sample values y(k) are observed, and that these come from a plant which may be described by the transfer function (equation 26) for some "true" value of the parameters, β^o. The identification problem is to compute from these u(k) and y(k) an estimate $\hat{\beta}$ which is a "good" approximation of β^o. To do this, it is necessary to define some idea of "goodness of fit" of a proposed value of β to the true β^o. Because, by the very nature of the problem, β^o is unknown, it is unrealistic to define a direct parameter error between β and β^o. The error must be defined in a way which can be computed from the u(k) and y(k). Three criteria which have been proposed and studied extensively are known as equation error, output error, and

output-prediction error.

Equation error (the method to be used in the present development) requires the complete equations of motion in a state variable description. In general, consider the continuous time state description with parameter vector β which can be written as follows:

$$\dot{x} = f(x,u;\beta) \qquad (31)$$

First, it is assumed that the form of the vector functions f are known but not the parameters β^o, which describe the plant. Next, it is assumed that it is possible to measure not only the controls u but also the states x and the state derivatives $\dot{x}$. Thus, <u>everything</u> is known about the equations except for the particular parameter values. An error can therefore be defined by the extent to which these equations of motion fail to be true for a specific value of β when used with the specific actual data x_a, $\dot{x}_a$, and u_a. The error is written as

$$\dot{x}_a - f(x_a,u_a;\beta) = e(t;\beta) \qquad (32)$$

and $e(t,\beta^o) = 0$ where β^o are the true plant parameters. The vector $e(t,\beta)$ are the equation errors, and are used to form a nonnegative cost function:

$$J(\beta) = \int_0^T e^T(t;\beta)e(t;\beta)dt \qquad (33)$$

With the cost function defined, a search over β is made until $\hat{\beta}$ is found such that $J(\hat{\beta}) = 0$, at which time the parameter set $\hat{\beta}$ is equivalent to β^o. If a unique parameterization has been selected, then only one parameter set will make $e(t,\beta^o) = 0$ and thus $\hat{\beta} = \beta^o$.

The assumption that enough instruments are available to measure the total state and all state derivatives is a strong assumption and often not realistic in continuous model identification. However, in discrete linear models there is one case where it is immediate, and that is the case of an ARMA model. The reason for this is not hard to find: in an ARMA model the state is no more than recent values of input and output! To be more explicit about it, the linear discrete-model equation error can be written:

$$x_a(k+1) - Fx_a(k) - Gu_a(k) = e(k;\beta) \qquad (34)$$

where F and G are functions of the parameters β. Substituting the values from equation 27, the ARMA model, gives the following:

$$\begin{bmatrix} x_1 \\ x_2 \\ x_3 \\ x_4 \\ x_5 \\ x_6 \end{bmatrix}_{k+1} - \begin{bmatrix} a_1 & a_2 & a_3 & b_1 & b_2 & b_3 \\ 1 & 0 & 0 & 0 & 0 & 0 \\ 0 & 1 & 0 & 0 & 0 & 0 \\ 0 & 0 & 0 & 0 & 0 & 0 \\ 0 & 0 & 0 & 1 & 0 & 0 \\ 0 & 0 & 0 & 0 & 1 & 0 \end{bmatrix} \begin{bmatrix} x_1 \\ x_2 \\ x_3 \\ x_4 \\ x_5 \\ x_6 \end{bmatrix}_k - \begin{bmatrix} 0 \\ 0 \\ 0 \\ 1 \\ 0 \\ 0 \end{bmatrix} u(k) = \begin{bmatrix} e_1 \\ e_2 \\ e_3 \\ e_4 \\ e_5 \\ e_6 \end{bmatrix}_k \qquad (35)$$

When the substitution from equation 28 is made it is found that for any β (i.e. for any values of a_i and b_i) the elements of

equation error are all zero except e_1. This element of error is given by:

$$x_1(k+1) - a_1x_1(k) - a_2x_2(k) - a_3x_3(k) - b_1x_4(k) - b_2x_5(k) - b_3x_6(k) = e_1(k;\beta) \quad (36)$$

or, from equation 28:

$$y_a(k) - a_1y_a(k-1) - a_2y_a(k-2) - a_3y_a(k-3) - b_1u_a(k-1) - b_2u_a(k-2) - b_3u_a(k-3) = e_1(k;\beta) \quad (37)$$

The discrete cost function becomes:

$$J(\beta) = \sum_{k=0}^{N} e_1^{\,2}(k;\beta) \quad (38)$$

Again, the subscript a has been placed on the observed data to emphasize the fact that these are actual data which were produced via the plant with parameter values β^o and in equations 36-38 an error results because β differs from β^o.

Least Squares Matching Technique:

To begin the discussion of the least squares matching technique, consider the ARMA model and equation error which leads to equation 37, repeated below for the nth-order case. (The subscript a is understood but omitted here).

$$y(k) - a_1y(k-1) - a_2y(k-2) - \cdots - a_ny(k-n)$$
$$- b_1u(k-1) - \cdots - b_nu(k-n) = e_1(k;\beta) \qquad (39)$$

Next, assume that the following set of inputs and outputs have been observed

$$[u(0),u(1),u(2),\ldots,u(N),y(0),y(1),\ldots,y(N)] \qquad (40)$$

from which it is desired to compute values for

$$\beta = [a_1 \cdots a_n \; b_1 \cdots b_n]^T \qquad (41)$$

which will best fit the observed data. Since y(k) depends on past data back to n periods earlier, the first error that can be formed is e(n;β). Suppose a vector of errors is defined by writing equation 39 over and over for k = n, n+1, ..., N. The results would be

$$\begin{aligned} y(n) &= x^T(n)\beta + e(n;\beta) \\ y(n+1) &= x^T(n+1)\beta + e(n+1;\beta) \\ &\vdots \\ y(N) &= x^T(N)\beta + e(N;\beta) \end{aligned} \qquad (42)$$

where the definition of the state of the ARMA model is

$$x(k) = [y(k-1)\; y(k-2)\ldots u(k-1)\ldots u(k-n)]^T \qquad (43)$$

To make the error even more compact, another level of matrix notation is used by defining the following:

$$Y(N) = [y(n)\ y(n+1)...y(N)]^T$$
$$X(N) = [x(n)\ x(n+1)...x(N)]^T$$
$$e(N;\beta) = [e(n)\ e(n+1)...e(N)]^T \qquad (44)$$

Note that X(N) is a matrix with 2n columns and N-n+1 rows. In terms of these definitions, the equation error can be written as

$$Y = X\beta + e(N;\beta) \qquad (45)$$

Least squares is a prescription that one should take that value of β which makes the sum of the squares of the e(k) as small as possible. In terms of equation 42 the cost function to be minimized is defined as

$$J(\beta) = \sum_{k=n}^{N} e^2(k;\beta) \qquad (46)$$

and in terms of equation 45 this is

$$J(\beta) = e^T(N;\beta)e(N;\beta) \qquad (47)$$

It is desired to find $\hat{\beta}_{LS}$, the least squares estimate of β^o, which is that β having the property

$$J(\hat{\beta}_{LS}) \leq J(\beta) \qquad (48)$$

But $J(\beta)$ is a quadratic function of the 2n parameters in β, and from calculus, a necessary condition on $\hat{\beta}_{LS}$, is that the partial derivatives of J with respect to β at $\beta = \hat{\beta}_{LS}$ should be zero. This is done as follows:

$$\begin{aligned} J(\beta) &= e^T e \\ &= Y - X\beta^T(Y - X\beta) \\ &= Y^T Y - \beta^T X^T Y - Y^T X\beta + \beta^T X^T X\beta \end{aligned} \qquad (49)$$

and applying the rules developed for derivatives of scalars with respect to vectors, the following is obtained:

$$J_\beta = \partial J/\partial\beta = -2Y^T X - 2\beta^T X^T X \qquad (50)$$

Taking the transpose of equation 50 and letting $\beta = \hat{\beta}_{LS}$, the result must be zero. This gives

$$X^T X\hat{\beta}_{LS} = X^T Y \qquad (51)$$

These equations are called the "normal equations" of the problem, and their solution will provide the desired least squares $\hat{\beta}_{LS}$.

Whether or not the equations have a unique solution depends mainly on how β was selected and what input signals u(k) were used. Consider first the selection of β and the "nonuniqueness"

of state space representations. If the state space model of equation 24 represented a third order system, for example, then equation 24 would have 15 parameters (nine elements in F and three elements each in G and H). Recall, however, that only six elements are needed to completely describe the input-output dependency (i.e. equation 26). This means that the state variable description has nine parameters that are in some sense redundant and may be chosen rather arbitrarily. If the 15 element β were used, the resulting normal equations could not have a unique solution. To obtain a unique parameter set a canonical form having a minimal number of parameters, such as the observer or ARMA forms must be selected. By way of definition, a parameter β having the property that one and only one value of β makes $J(\beta)$ a minimum is said to be "identifiable." Two parameters having the property that $J(\beta_1) = J(\beta_2)$ are said to be "equivalent."

As to the selection of the inputs u(k), consider first an extreme case. Suppose u(k) = c, a constant, for all k (i.e. a step function input). Now consider equation 42 again for the third order case to be specific. The errors are

$$\begin{aligned} &y(3) - a_1y(2) - a_2y(1) - a_3y(0) - b_1c - b_2c - b_3c = e(3) \\ &\quad\vdots \\ &y(N) - a_1y(N-1) - a_2y(N-2) - a_3y(N-3) - b_1c - b_2c - b_3c = e(N) \end{aligned} \qquad (52)$$

It is obvious that in equation 52 the parameters b_1, b_2, and b_3 always appear as the sum $b_1+b_2+b_3$ and that separation of them is not possible when a constant input is used. Somehow the constant

u fails to "excite" all the dynamics of the plant. This problem has been studied extensively by Astrom and Bohlin (23) and the property of "persistently exciting" has been defined by them to describe a sequence of u(k) which fluctuates enough to avoid the possibility that only linear combinations of elements of β will show up in the error and normal equations. Without going into more detail at this point, an input is said to be persistently exciting if the lower right (n x n)-matrix component of X^TX (which depends only on u(k)) is nonsingular.

Assuming that the u(k) are persistently exciting and that the β are identifiable (and consequently that X^TX is nonsingular), then the explicit least squares solution can be written as follows:

$$\hat{\beta}_{LS} = (X^TX)^{-1}X^TY \qquad (53)$$

Extracting the Continuous Model:

The parameters in $\hat{\beta}_{LS}$ describe a low-order discrete model (i.e. equation 26) of the high-order system. The next step in the matching process is the extraction of a low-order continuous model from the discrete model. The discrete transfer function represented by $\hat{\beta}_{LS}$ and equation 26 is first converted into a discrete state space form as follows:

$$\tilde{F} = \begin{bmatrix} a_1 & 1 & 0 \\ a_2 & 0 & 1 \\ a_3 & 0 & 0 \end{bmatrix} \qquad \tilde{G} = \begin{bmatrix} b_1 \\ b_2 \\ b_3 \end{bmatrix} \qquad (54)$$

$$\tilde{H} = [1 \quad 0 \quad 0]$$

The tilda denotes the low-order equivalent state matrices.

Equation 54 is known as the observer canonical form. Note, however, that any state space representation of the transfer function could be used at this point. This is because the final step will be a conversion back to a continuous transfer function form. Thus, the state space form (which is not unique) is used only as an intermediate step to obtain the final transfer function form (which is unique). Since the final transfer function is unique, any state space representation should give the same result.

To obtain the continuous transfer function form, the discrete state space model of equation 54 must first be converted to a continuous state space model. A straightforward and accurate method for this has been developed by Sinha and Lastman (24). The technique begins with an initial estimate $\tilde{A}_o$ for the $\tilde{A}$ matrix based on the derived $\tilde{F}$ matrix:

$$\tilde{A}_o T = 0.5(\tilde{F}-\tilde{F}^{-1}) \qquad (55)$$

The technique then begins its iterative phase by computing an estimated $\tilde{F}$ matrix $\tilde{F}_j$ as follows:

$$\tilde{F}_j = \exp(\tilde{A}_j T) \qquad (56)$$

where j is the iteration counter. Note that $\tilde{F}_j$ is what the $\tilde{F}$ matrix should be if $\tilde{A} = \tilde{A}_j$. The next iterative step is to correct the estimate of $\tilde{A}_j T$ for the difference between $\tilde{F}$ and $\tilde{F}_j$.

$$\tilde{A}_{j+1}T = \tilde{A}_jT + \tilde{F}^{-1}(\tilde{F}-\tilde{F}_j) \qquad (57)$$

The technique iterates between these last two equations until $\tilde{A}_{j+1}T$ is sufficiently close to $\tilde{A}_jT$. The estimated stability matrix $\tilde{A}$ is then $\tilde{A}_{j+1}$. The estimated control matrix $\tilde{B}$ is found from:

$$\tilde{B} = [(\tilde{A}_{j+1})^{-1}(\exp(\tilde{A}_{j+1}T)-I]^{-1}\tilde{G} \qquad (58)$$

The Sinha and Lastman technique provides extremely accurate results in extracting the continuous $\tilde{A}$ and $\tilde{B}$ matrices for most applications. For the technique to work however, the inverted matrices in equations 57 and 58 must be full rank. For this study, a trial run using the known short period stability derivatives for the A-4D resulted in accuracies of 10^{-14} for the $\tilde{A}$ matrix but only about 10^{-3} for the $\tilde{B}$ matrix. It was found that the problem was in the estimated stability matrix which was close to being singular (determinant close to zero) and equation 58 required that this matrix ($\tilde{A}_{j+1}$) be inverted. Because of this problem, an alternative method for extracting the control matrix was found.

In cases where the stability matrix is singular, an alternative technique is to extract the control matrix based on the power series expansion of the matrix exponential function e^{AT} which is given by

$$e^{AT} = I + AT + (A^2T^2)/2! + \cdots \qquad (59)$$

The technique is based on the definition of the discrete control matrix $\tilde{G}$. From equation 23 we have

$$\tilde{G} = \int_0^T e^{\tilde{A}\tau} d\tau \tilde{B} \qquad (60)$$

which can be written as a power series using equation 59 as follows:

$$\tilde{G} = \int_0^T (I + \tilde{A}\tau + \tilde{A}^2\tau^2/2! + \cdots) d\tau \tilde{B} \qquad (61)$$

After integrating and inverting, we have the following:

$$\tilde{B} = (T + \tilde{A}T^2/2 + \tilde{A}^2T^3/3*2 + \cdots)^{-1}\tilde{G} \qquad (62)$$

This gives a method for estimating the control matrix $\tilde{B}$ which does not require the stability matrix $\tilde{A}$ to be full rank. Thus, by substituting the estimated $\tilde{A}$ matrix obtained from the Sinha and Lastman technique into equation 62 the estimated control matrix $\tilde{B}$ was obtained for the A-4D short period example discussed above. In addition, because the power series can be carried out as far as desired, the accuracy of this method exceeds the accuracy of the Sinha and Lastman technique. For the A-4D short period example

the $\tilde{B}$ matrix was estimated with an accuracy of 10^{-14}, a significant improvement over the previous results. For this reason, the Sinha and Lastman technique was used to extract the $\tilde{A}$ matrices and the alternative technique, based on the power series expansion of e^{AT}, was used to extract the $\tilde{B}$ matrices throughout the least squares matching.

With the continuous $\tilde{A}$ and $\tilde{B}$ matrices extracted from the discrete model, we have the desired LOES in state space form:

$$\dot{x} = \tilde{A}x + \tilde{B}u \qquad (63)$$
$$y = \tilde{C}x$$

where $\tilde{A} \in R^n$, $\tilde{B} \in R^m$, and $\tilde{C}$ is chosen to give the desired output y. Note that n equals the number of states and m equals the number of inputs for the LOES.

The final step is to obtain the desired LOES transfer functions ($\dot{\theta}/F_s$, n_z/F_s, etc) from the transfer function matrix $\tilde{H}(s)$:

$$\tilde{H}(s) = Y(s)/U(s) = \tilde{C}(sI - \tilde{A})^{-1}\tilde{B} \qquad (64)$$

The order of the least squares LOES is determined by the number of columns of the X matrix (see equations 43 and 44) which are made up of the observed inputs u(k) and outputs y(k). The column size of this matrix determines the size of the resulting

parameter vector $\hat{\beta}_{LS}$ which in turn determines the order of the final LOES transfer function.

Optimal Input for System Identification:

The studies by Astrom and Bohlin (23) have shown that the choice of the input excitation u is an important consideration in time response matching techniques. In general, it can be said that if the input fails to "excite" all the dynamics of the plant it will be difficult or even impossible to identify the plant correctly. As discussed in the previous section, Astrom and Bohlin have defined an input to be "persistently exciting" if the matrix X^TX (which depends only on u(k)) is nonsingular. During the least squares matching of this study the inputs used to excite the plant were persistently exciting by this definition. The question arose, however, as to what the optimal input would be. That is, of the types of inputs that qualify as "persistently exciting" are there some that will excite the plant better than others and thereby achieve a better identification of the plant?

To determine the optimal input excitation to be used for the least squares matching a variety of ramp inputs were used. Variations were made in the rise time, amplitude, and sinusoidal components of the input to determine the effect of each of these on the quality of the least squares match. Figure 31 illustrates two of the inputs used and the corresponding plant responses. Note that 100 discrete input and output data points were used throughout the LS matching (i.e. N = 100 in equations 40-52).

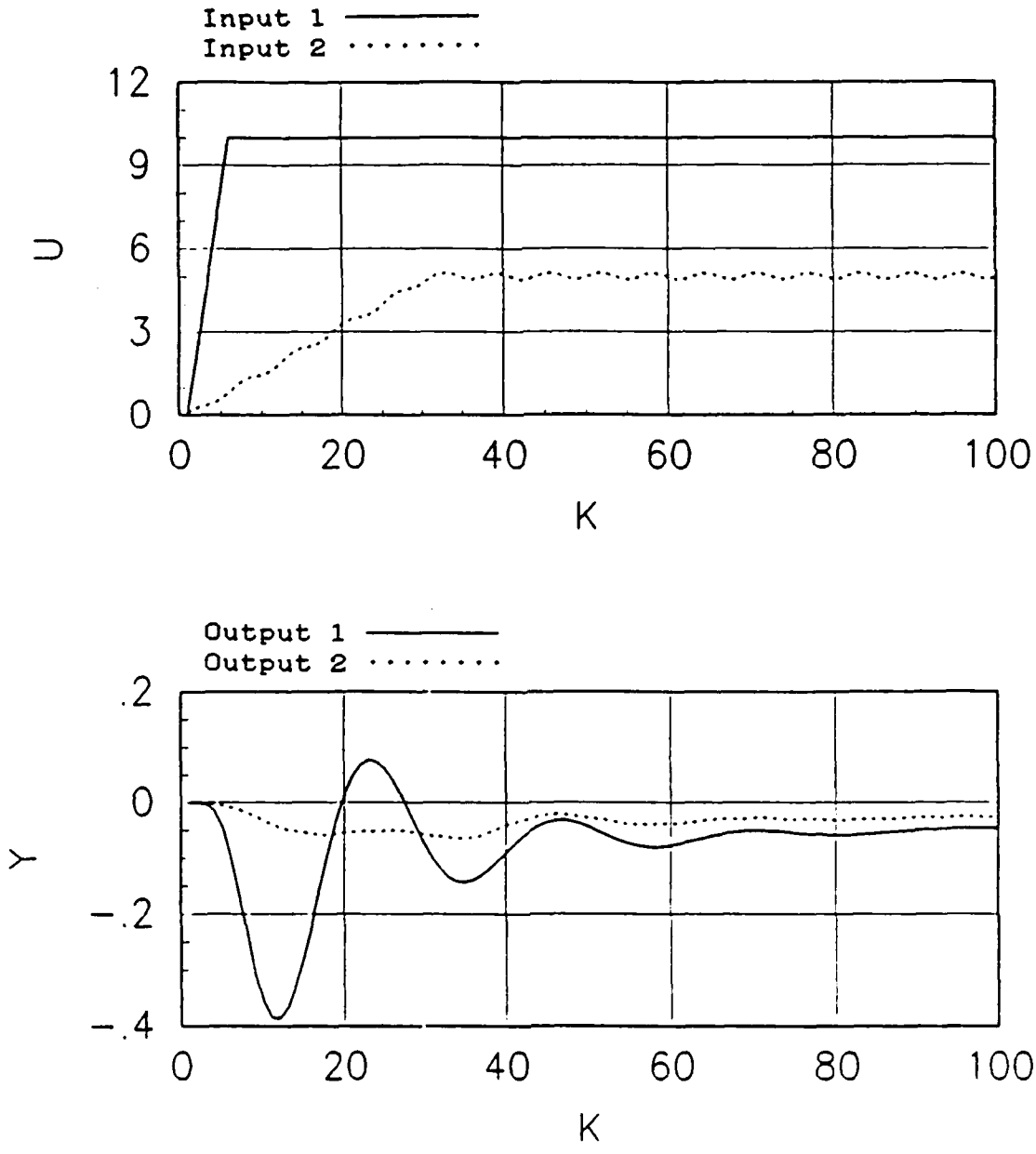

Figure 31. Sample Inputs u(k) and Corresponding Outputs y(k)

(The HOS dynamics are for an A-4D at 35,000 Ft, 0.70 Mach, ω_{sp} = 2.77 rps, ζ_{sp} = 0.225. The control system has a servo-actuator (13/s+13) and a second order feel system with ω_{fs} = 18.5 rps and ζ_{fs} = 1.0).

The range of rise times used varied from N = 0 (step input) to N = 50. Since the time step T = 0.1 sec, this corresponds to a variation in rise time of 0 to 5.0 seconds. The amplitude of the ramp input was varied from 0.1745 to 10.0 and the sinusoidal component was varied from 0 to 0.1667sin(10t). (The sinusoidal frequency was held constant at 10 rad/sec while the sinusoidal amplitude was varied).

As the rise time, amplitude, and sinusoidal components of the input were varied, corresponding changes in the frequency domain and time domain cost functions ($cost_f$ and $cost_t$) were used to determine the quality of the match. The input which produced the lowest mismatch as defined by these functions was considered to be the "optimal" input. To investigate the effects of rise time, amplitude, and sinusoidal components one of the three elements was varied while the other two were held constant (i.e. rise time was varied from 0 to 5.0 seconds while the amplitude and sinusoidal components were held constant at some value, etc.). In general, it was found that variations in amplitude and sinusoidal components had little effect on the quality of the LS match. Changes in the rise time, however, resulted in significant changes in the cost functions. Figure 32 shows the variation in $cost_f$ and $cost_t$ as a function of rise time (for an A-4D HOS) and indicates that there is indeed an optimal rise time associated with this type of least squares matching.

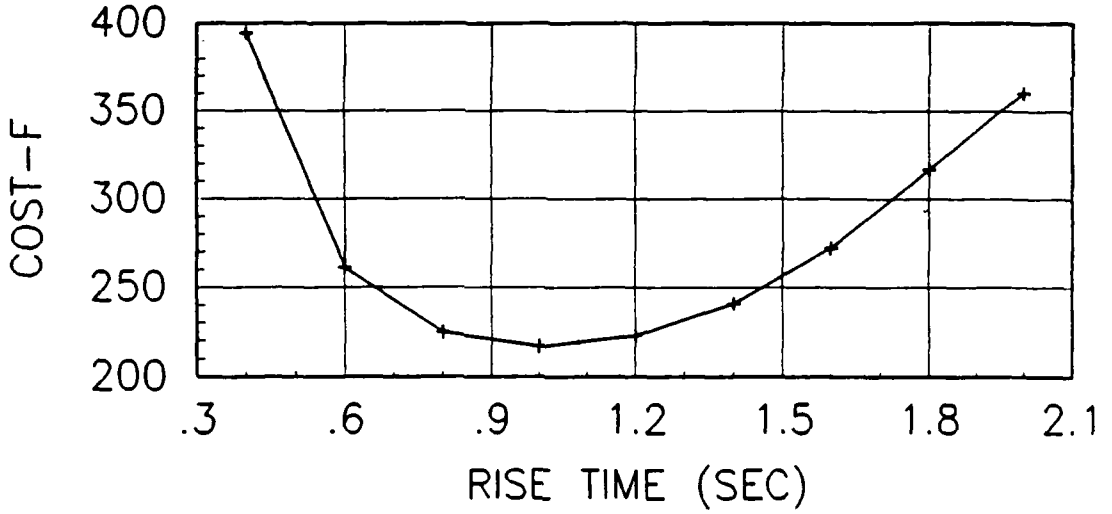

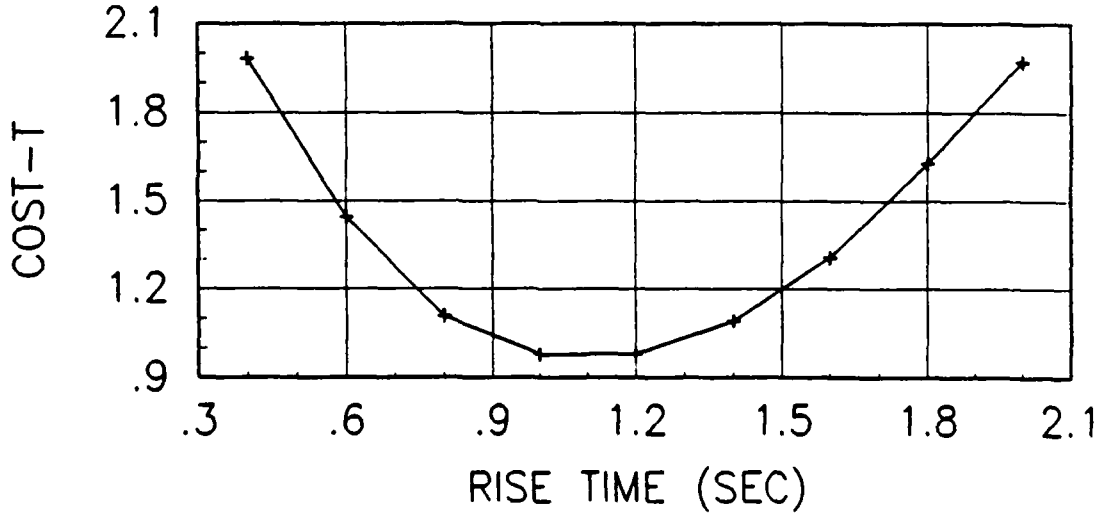

Figure 32. Optimal Rise Time for Least Squares Matching

(The cost functions shown are for the A-4D HOS described in Figure 31).

The fact that there is an optimal rise time for the LS matching technique can perhaps be explained by second-order dynamic response theory. Craig (25), shows that a second-order system will respond quite differently to ramp inputs depending on the rise time. Figure 33 shows the dynamic response of a second order system using rise times of $t_r = 0.2T_n$ and $t_r = 1.5T_n$ where T_n is the undamped natural period. The dynamic effects can be ignored (and the load is considered "statically applied") if the rise time is longer than about $3T_n$.

It makes sense that if an input is "slowly applied" the dynamics of the plant will not be excited sufficiently to identify the system. On the other hand, it has been shown by Franklin and Powell (22) that for extremely small rise times (i.e. step input) the dynamics of the plant are also not excited sufficiently for system identification (see equation 52 and associated discussion). With these considerations in mind, it makes sense that there would be an optimal rise time between the two extremes.

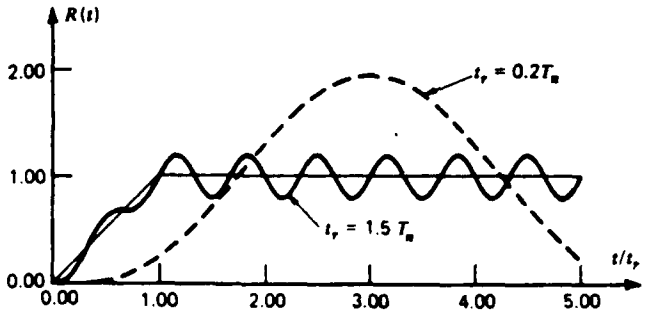

Figure 33. Response of Second Order System to Ramp Inputs (Reference 25)

Calculation of Required LOES Parameters:

Once the LOES transfer function (equation 64) is obtained, the equivalent parameters L_α, ζ_{sp}, ω_{sp}, and τ_θ are extracted and compared with the corresponding parameters obtained from the frequency response matching. The extraction of the parameters L_α, ζ_{sp}, and ω_{sp} is straightforward since these are just the roots of the LOES numerator and denominator. The determination of equivalent time delay τ_θ however is somewhat more complicated. Since there is not a straightforward method for this in the time domain; τ_θ was determined by iteration in the frequency domain. This was accomplished by using the HOS and LOES transfer functions to calculate phase_{HOS} and phase_{LOS}. The iteration was done by subtracting $57.29578*\omega_j*\tau_j$ from phase_{LOS} on each iteration until the cost_f function was minimized. (Note that this iteration has no effect on the gain component of the cost function). The change in phase before and after this iteration in time delay is shown in Figure 34 for an aircraft configuration used in the flight test program (explained in chapter V).

Least Squares Matching Results

To compare the time response matching results of this chapter with the frequency response matching results of chapter III, the LS technique was used to identify low-order equivalent systems for the 12 $\dot{\theta}/F_s$ high-order systems used in chapter III. In the frequency response matching, the 12 $\dot{\theta}/F_s$ HOS configurations (derived by varying ω_{fs} from 6.0 to 31.0 rad/sec for flight

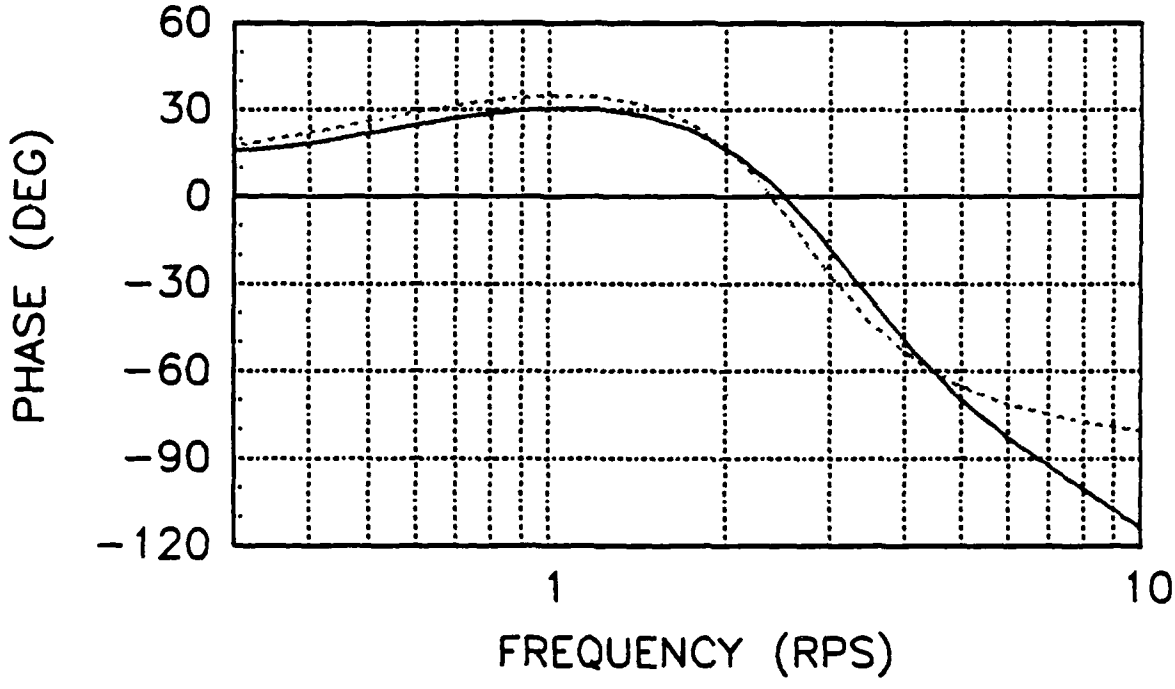

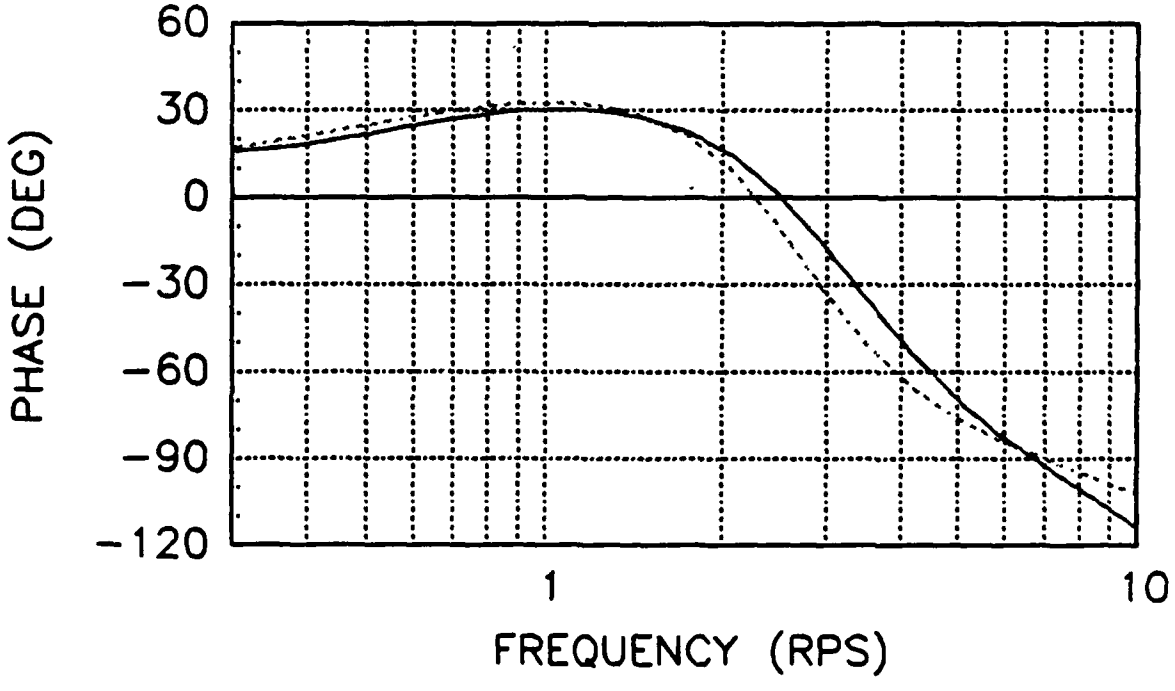

Figure 34. Calculation of Equivalent Time Delay (Configuration 3-1)

conditions 1 and 2) were all matched with L_α fixed and free resulting in a total of 24 LOES. The LS matching is done in the time domain, however, and there is no way to fix L_α at a specified value. Thus, only the L_α-free LOES configurations will be compared between the two matching techniques.

Based on the analysis of "optimal" LS input excitations (previous section) a ramp input was used with a rise time of 1.1 sec for the flight condition 1 matching and a rise time of 0.5 sec for the flight condition 2 matching. The amplitude of the ramp input was 5.0 and there was no sinusoidal component. The results of the LS matching are presented in tabular format in Appendix A and various graphical results are presented in this discussion. Analysis of the cost function data (Figures 35 and 36) shows that the LS matching generally had less mismatch in the time domain (lower $cost_t$) but greater mismatch in the frequency domain (higher $cost_f$) when compared to the LONFIT results. This makes sense intuitively since the LS match is performed using HOS time response data and the LONFIT match is performed using HOS frequency response data. It makes sense, therefore, that the LS match is closer in the time domain and the LONFIT match is closer in the frequency domain. A visual comparison of the frequency domain and time domain mismatch for HOS_1 and HOS_3 is shown in Figures 37-39 and can be compared with the corresponding LONFIT results in chapter III.

Comparison of the equivalent parameters (Figures 40-43) show that both the LS and LONFIT parameters approach their

corresponding basic aircraft values as ω_{fs} is increased. This is expected as the control system dynamics are made faster. As ω_{fs} is increased, the effects of the control system become less significant and the HOS behaves more like the basic aircraft (see the discussion on the effects of control system dynamics in chapter III). Figures 40-43 show that the LS parameters are closer to the basic aircraft values for L_α and τ_θ while the LONFIT parameters are closer for ω_{sp} and ζ_{sp}. The LS equivalent control anticipation parameters (CAP) are closer to the basic aircraft values for flight condition 1 but the LONFIT results are closer for flight condition 2 (Figure 44).

These comparisons between the Least Squares time response matching program and the LONFIT frequency response matching program have shown favorable results for the LS program. These comparisons primarily focused on the equivalent parameters generated by the two programs for a given high order system. The equivalent parameters were numerically similar between the two programs and approached the basic aircraft values as the feel system natural frequency was increased. This is consistent with equivalent systems theory. In the next chapter the Least Squares program will be further validated and compared to the well-accepted "Bandwidth" method (described in Appendix H) by predicting flying qualities of higher order systems. This comparison will be made based on the ability of the different techniques to accurately predict the handling quality levels of higher order systems using present MIL-STD-1797 guidance.

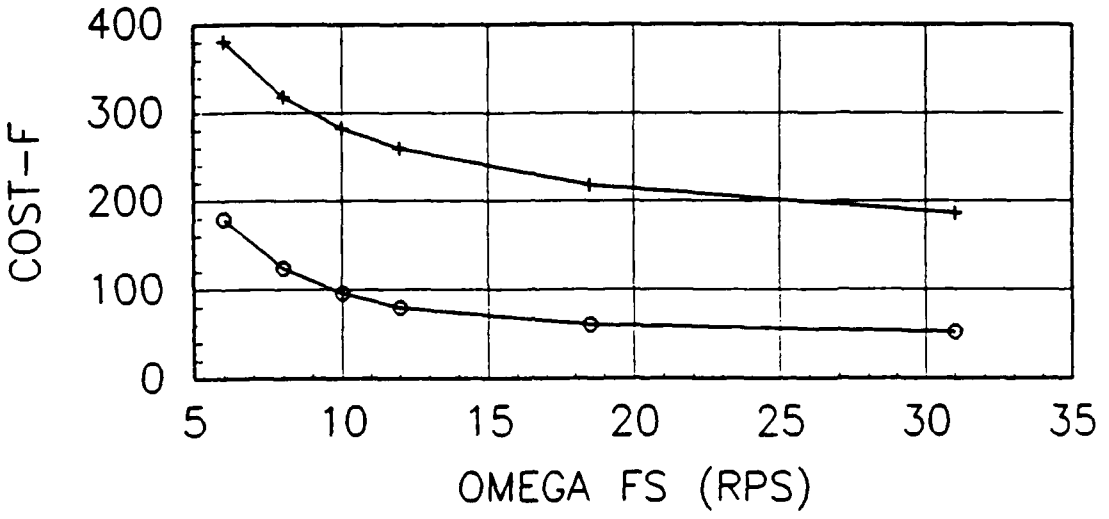

(a) Frequency Domain Cost Functions

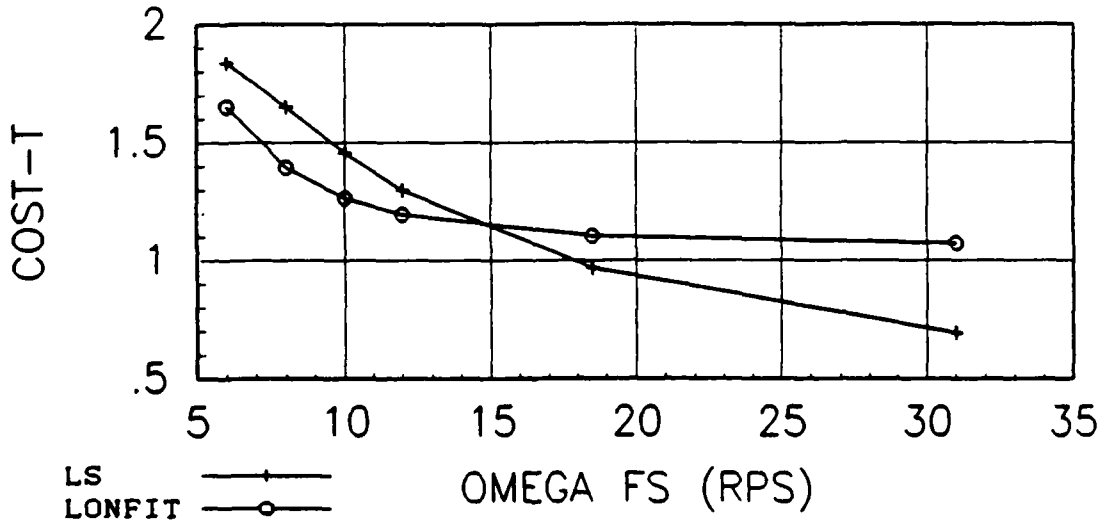

(b) Time Domain Cost Functions

Figure 35. Cost Functions versus ω_{fs} for HOS_1 Matching (Least Squares/LONFIT Comparison)

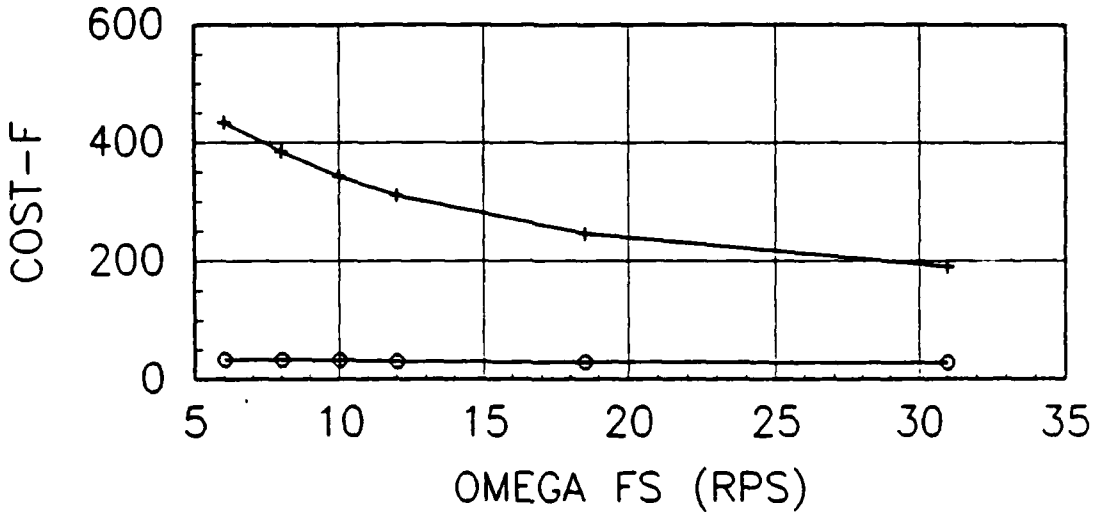

(a) Frequency Domain Cost Functions

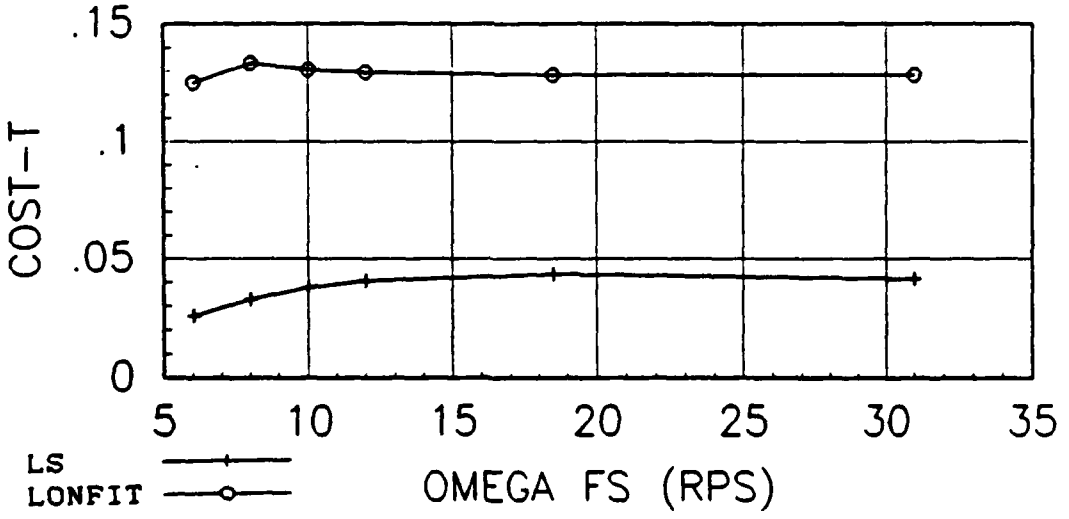

(b) Time Domain Cost Functions

Figure 36. Cost Functions versus w_{fs} for HOS_3 Matching (Least Squares/LONFIT Comparison)

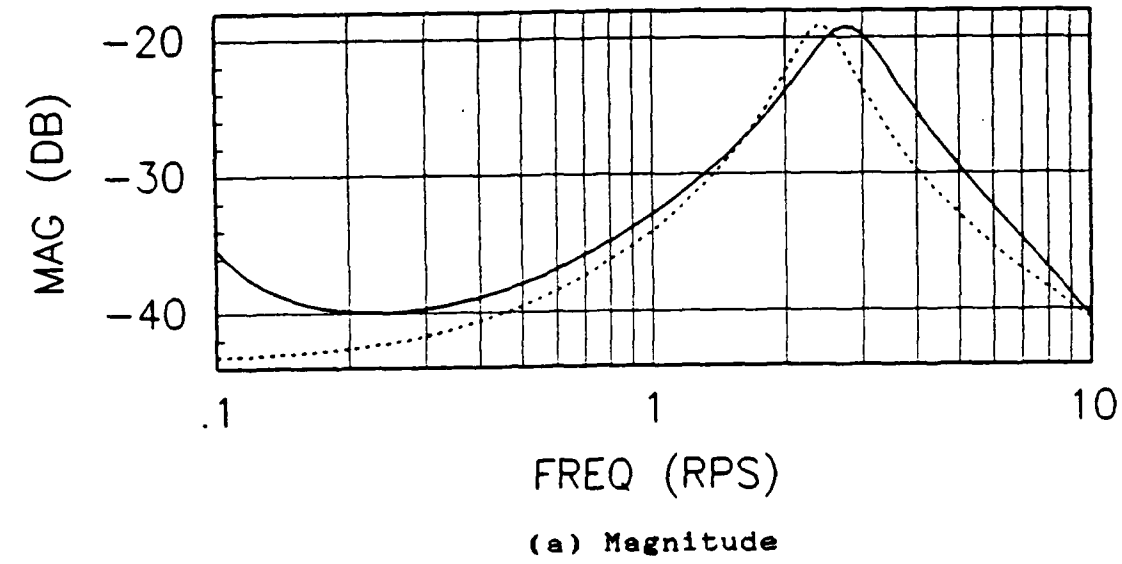

(a) Magnitude

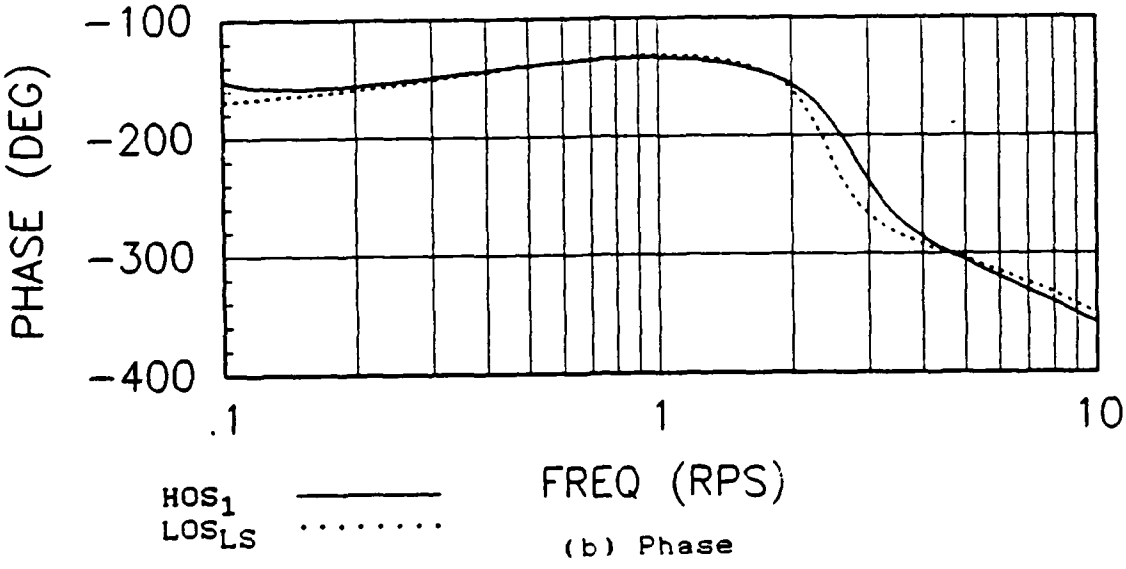

(b) Phase

Figure 37. Frequency Response Comparison, HOS_1 vs LOS_{LS} ($Cost_f$ = 218)

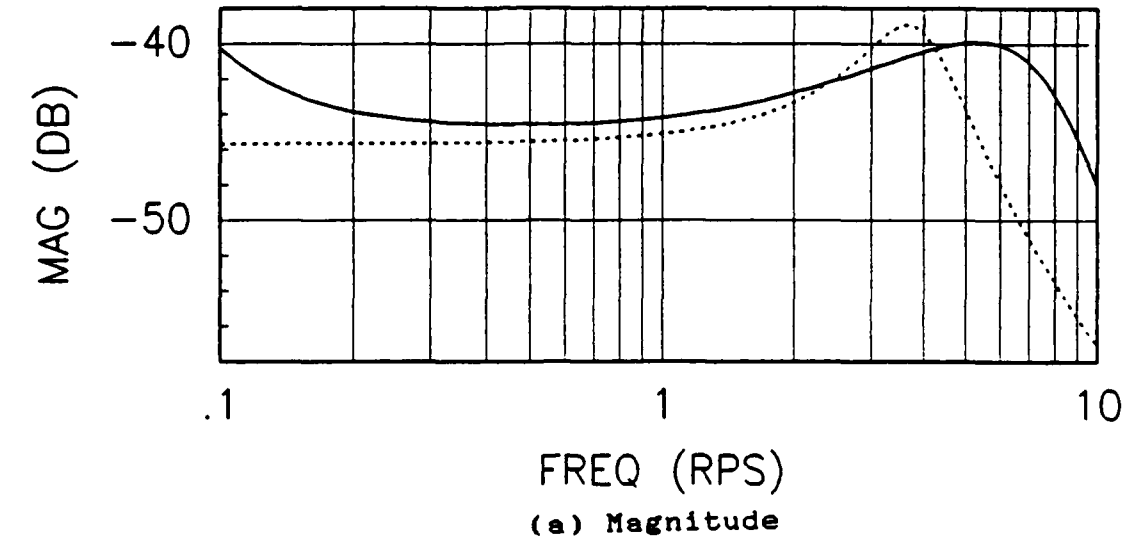

(a) Magnitude

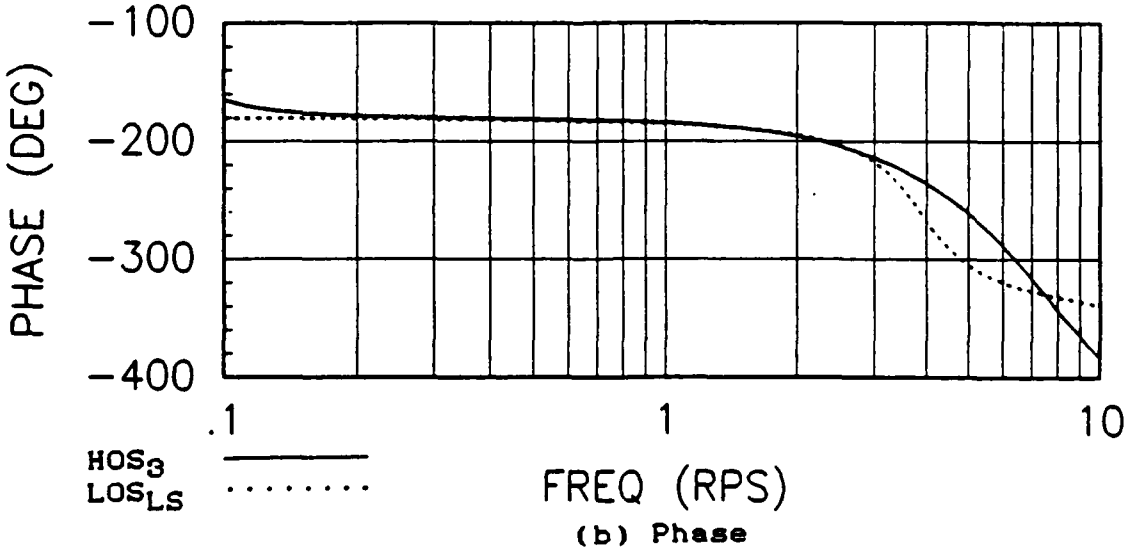

(b) Phase

Figure 38. Frequency Response Comparison, HOS_3 vs LOS_{LS} ($Cost_f$ = 433)

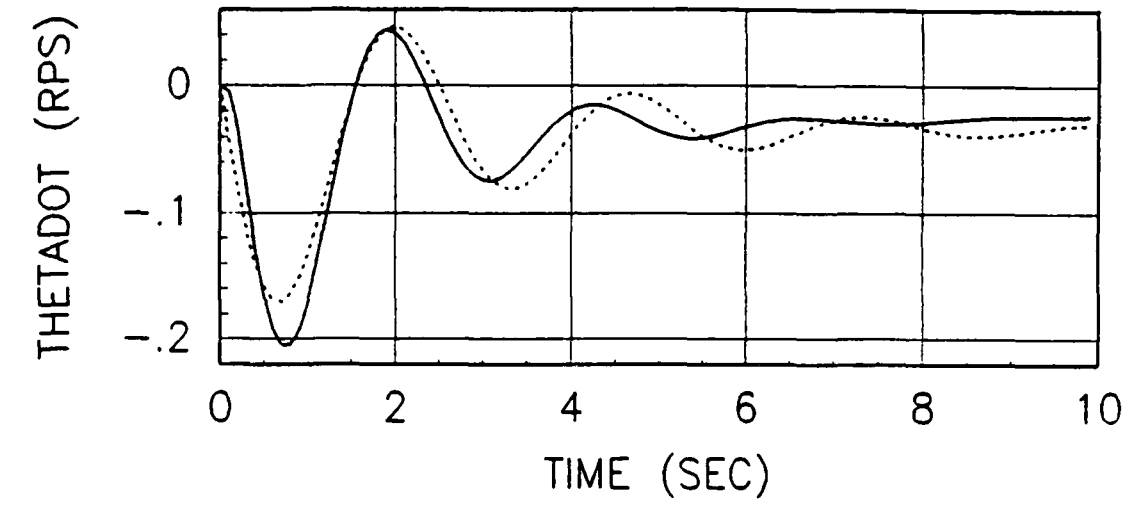

(a) HOS_1 vs LOS_{LS}

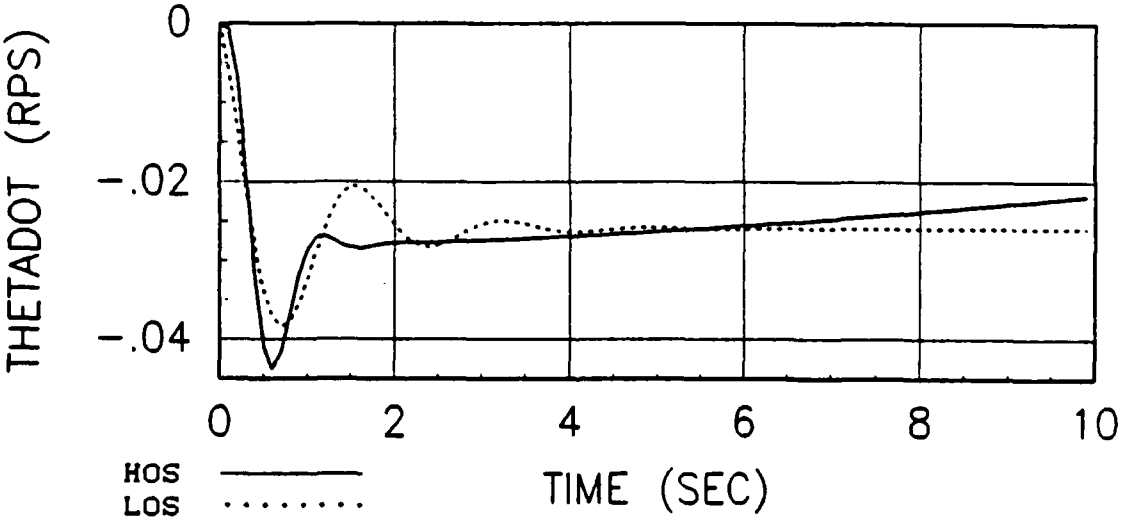

(b) HOS_3 vs LOS_{LS}

Figure 39. Time Response Comparisons (Step Input F_s = 5 lbs)

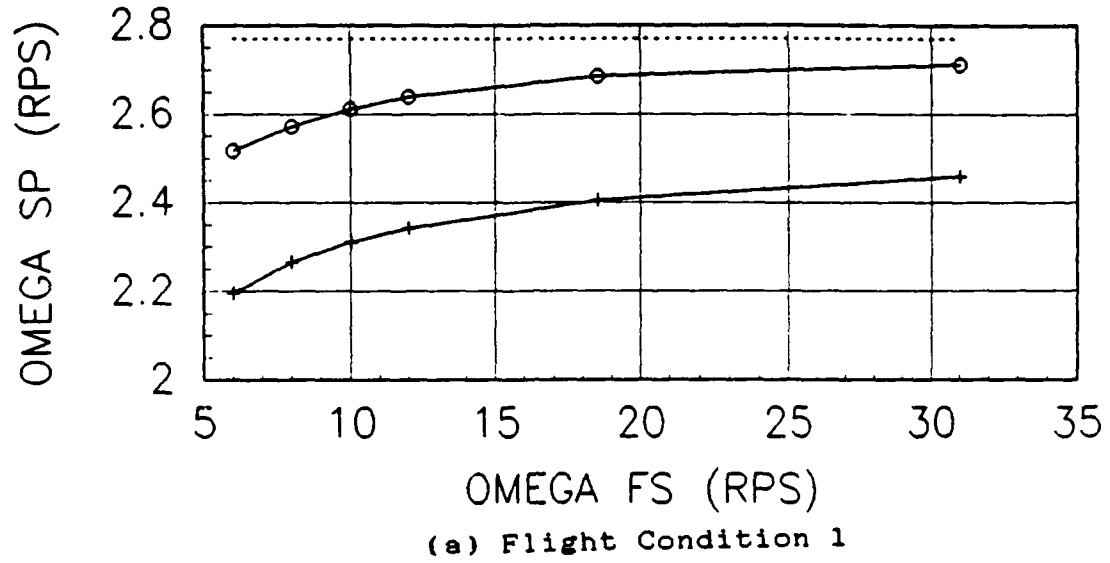

(a) Flight Condition 1

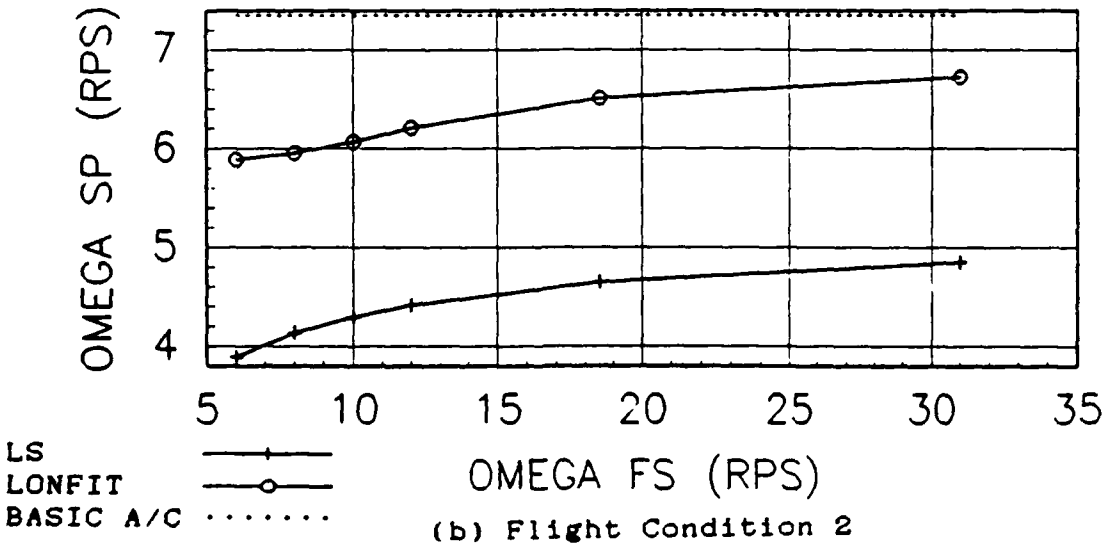

(b) Flight Condition 2

Figure 40. Equivalent ω_{sp} versus ω_{fs} (Least Squares/LONFIT Comparison)

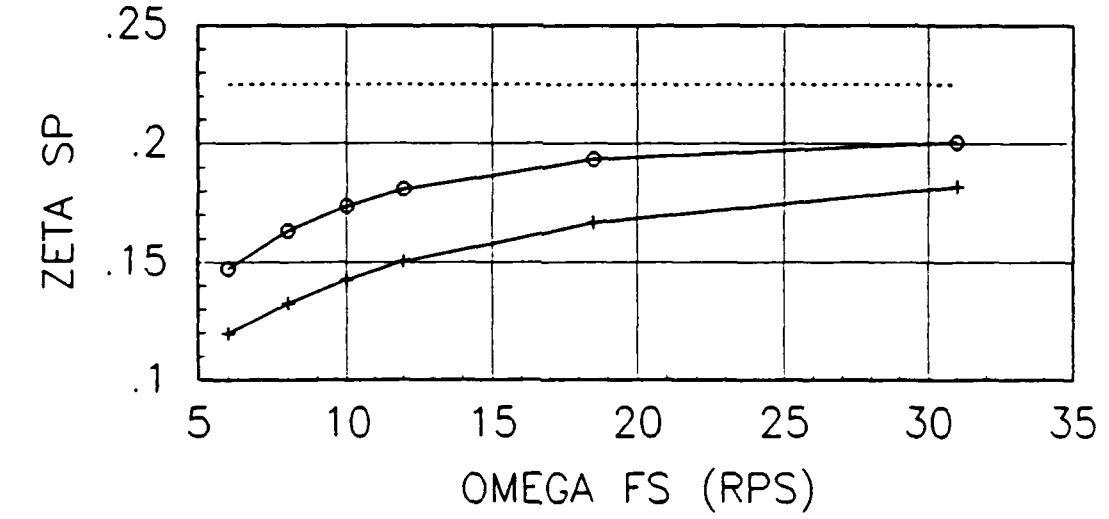

(a) Flight Condition 1

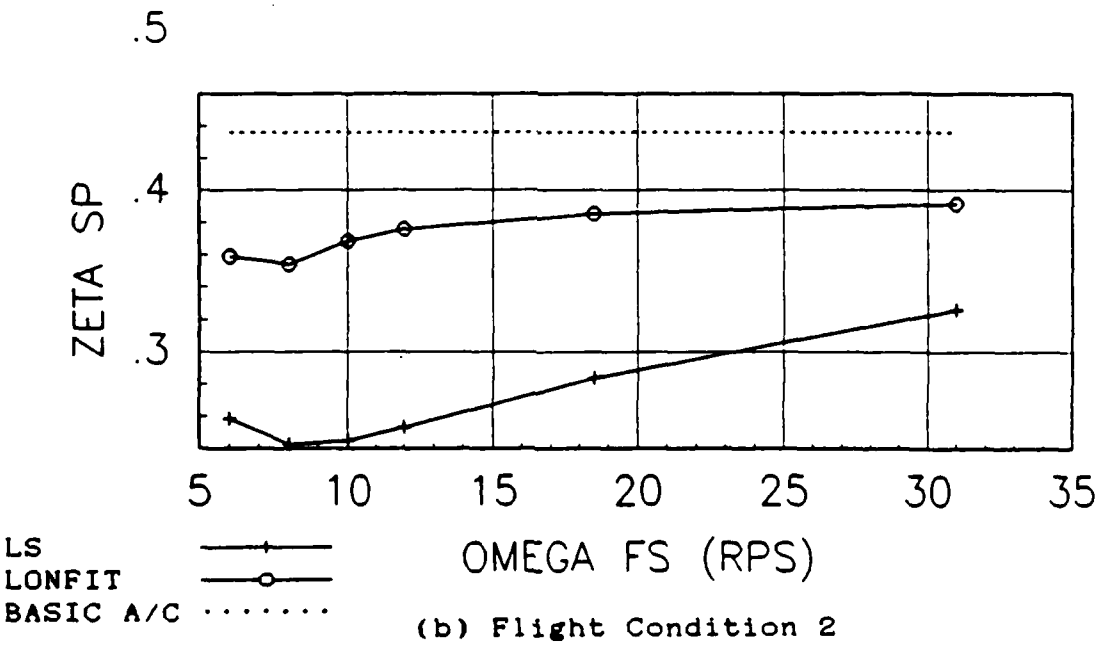

(b) Flight Condition 2

Figure 41. Equivalent ζ_{sp} versus ω_{fs} (Least Squares/LONFIT Comparison)

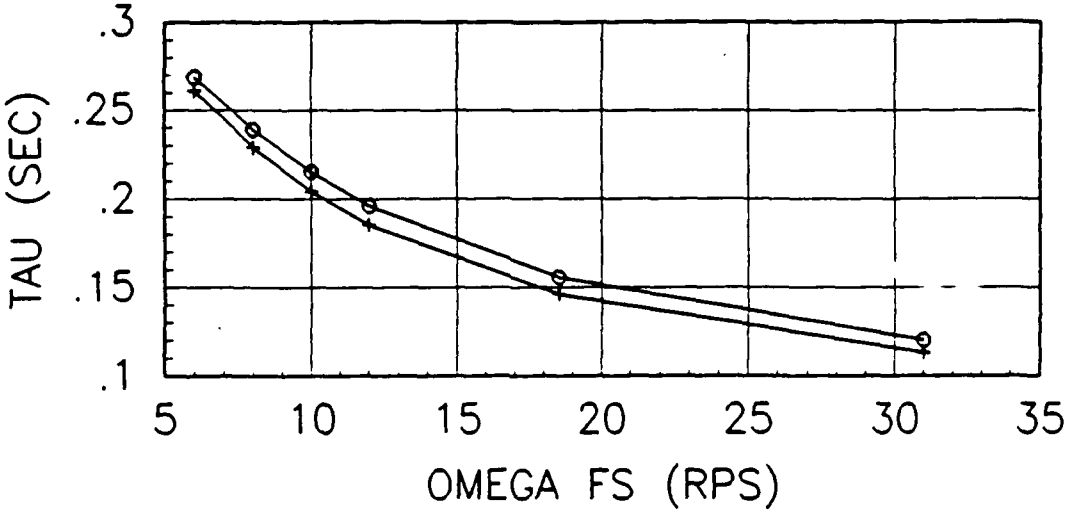

(a) Flight Condition 1

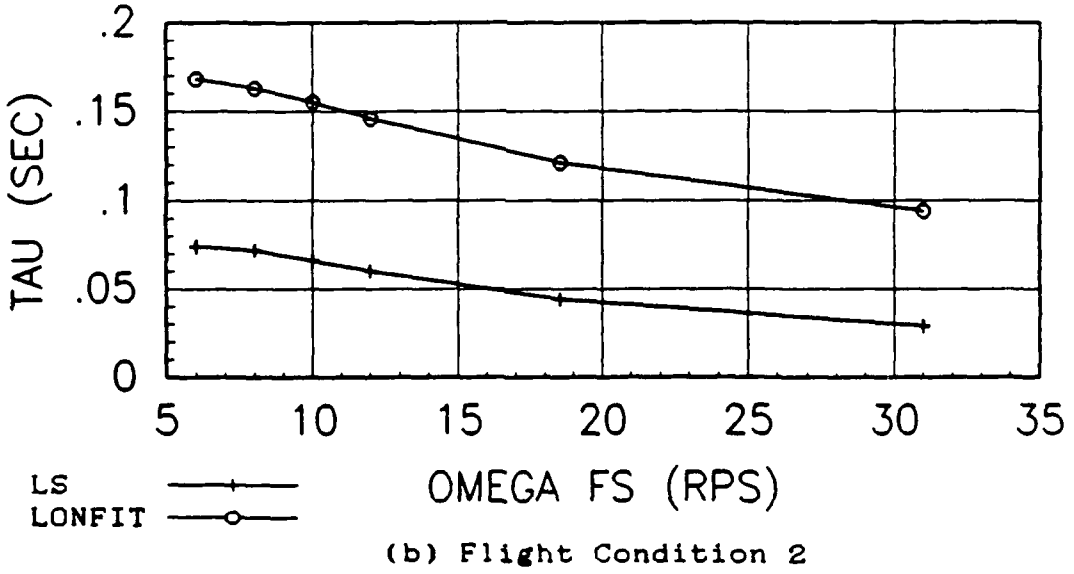

(b) Flight Condition 2

Figure 42. Equivalent Time Delay (τ_θ) versus ω_{fs} (Least Squares/LONFIT Comparison)

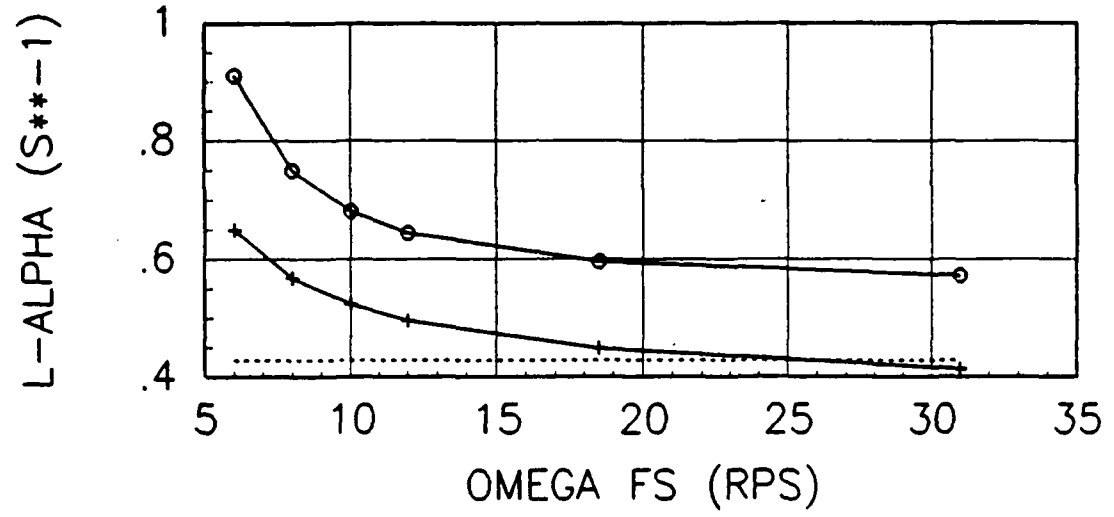

(a) Flight Condition 1

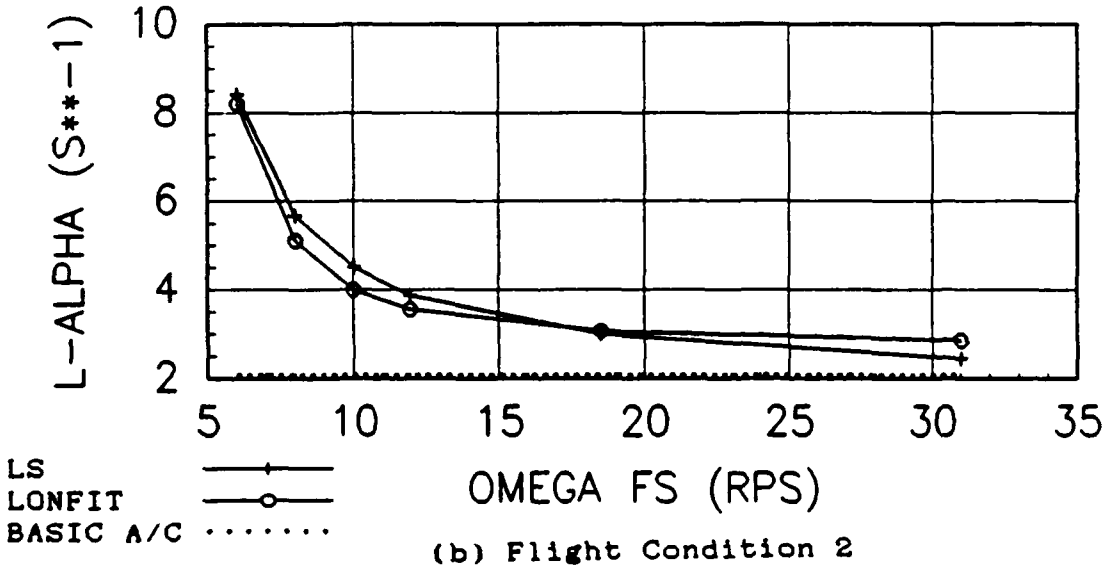

(b) Flight Condition 2

Figure 43. Equivalent L_α versus ω_{fs} (Least Squares/LONFIT Comparison)

4.11

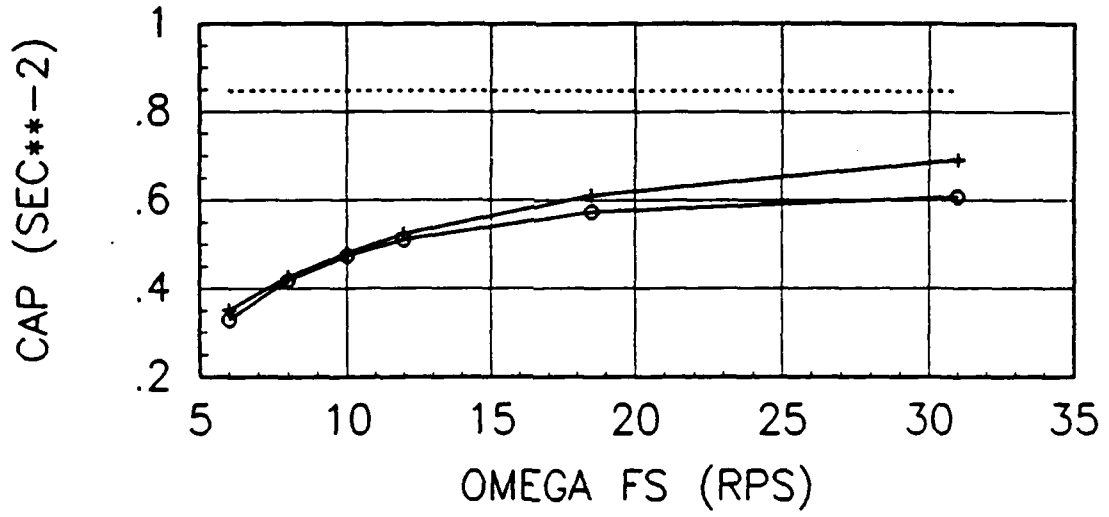

(a) Flight Condition 1

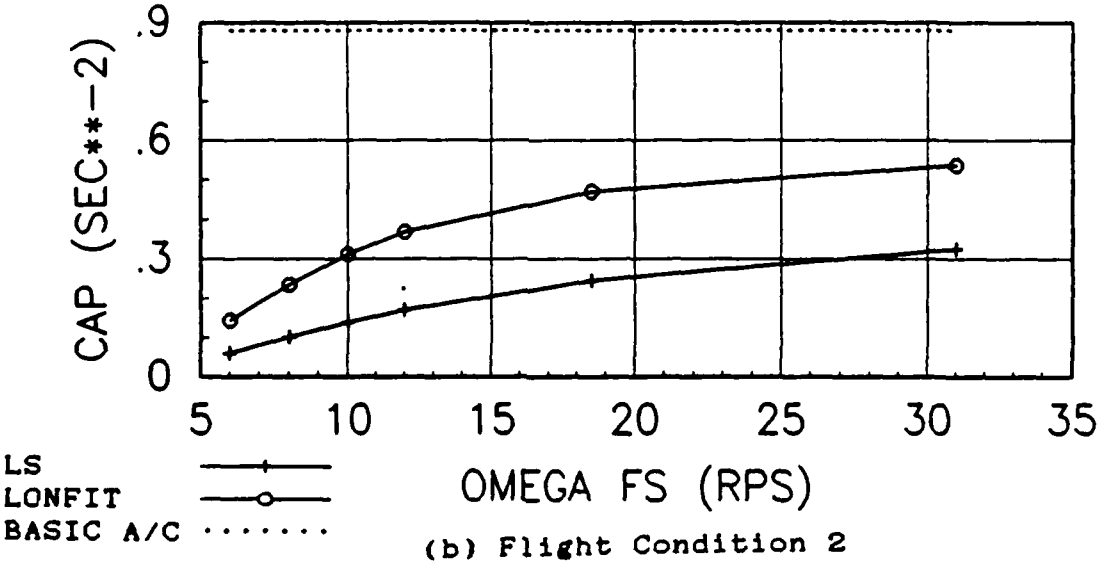

(b) Flight Condition 2

Figure 44. Equivalent CAP versus w_{fs} (Least Squares/LONFIT Comparison)

V. Flight Test Results

A limited flight test program was conducted at the Air Force Flight Test Center (AFFTC), Edwards Air Force Base, California, to evaluate the Least Squares system identification program developed in this thesis and to evaluate an additional AFIT thesis project involving the prediction of PIOs and handling qualities using the Optimal Control Model (OCM). The Commandant, USAF Test Pilot School (USAFTPS) directed the test program in partial fulfillment of the USAFTPS curriculum requirements. Three pilots and two engineers from USAFTPS Class 89A comprised the test team. The USAFTPS Special Projects Division acted as the System Program Office. Twenty-five sorties totaling 27.8 flight hours were flown between 12 September and 16 October 1989. A sortie summary is given in Appendix C.

The conclusions of the test team regarding the Least Squares Lower Order Equivalent System matching results will be summarized in this chapter. A more complete description of the flight test program can be found in the NT-33 HAVE CONTROL final flight test report (26).

Objectives

The objectives of the HAVE CONTROL flight test program pertaining to the Least Squares LOES technique were:

1. Determine if the LOES time response matching technique is suitable for flight test applications. This evaluation included ease of application and comparison with Hoh's Bandwidth Method.

2. Determine the optimal ramp input rise time for the LOES time response matching program.

3. Determine the effects of control system root location on system identification using the LOES method.

Test Aircraft Description

The NT-33A variable stability test aircraft, S/N 51-4120, was a modified, two seat jet trainer operated by the CALSPAN Corporation, Buffalo, New York and owned by the Flight Dynamics Laboratory, Wright-Patterson AFB, Ohio (27,28). The aircraft was capable of variable dynamic response and control system characteristics (29). The Variable Stability System (VSS) modified the static and dynamic responses of the basic NT-33A by commanding control surface positions through full authority electro-hydraulic servos. A programmable analog computer, associated aircraft response sensors, control surface servos, and an electro-hydraulic force-feel system provided the total simulation capability. The instructor/safety pilot varied the computer gains through controls located in the rear cockpit, allowing changes in airplane dynamics and control system characteristics during the flight. Appendix D contains additional information concerning the aircraft systems, capabilities, and safety provisions.

The front cockpit AVQ-7 Heads Up Display (HUD) displayed several flight parameters, including airspeed, altitude, angle of

attack, pitch attitude, heading, and the velocity vector. The HUD was used during the test to closely simulate a representative fighter aircraft.

Instrumentation and Data Reduction

The NT-33 test instrumentation system contained the following items:

1. An on-board Ampex AR 700 magnetic tape recording system with 2.25 hours recording capability. This system was used to record aircraft flight conditions, flight control positions, pilot voice, and aircraft states from the aircraft data acquisition system (DAS).

2. An AN/ANH-2 voice recorder was used to record interphone and UHF radio communications.

3. A HUD video recorder was used to record all approaches and landings.

The project pilot operated the HUD and on-board voice recorder system. The instructor/safety pilot operated the magnetic tape system and the HUD camera. The AFFTC photographic branch provided ground videotape coverage of each landing task.

Following each NT-33 mission, the project pilots reviewed the HUD video and tape recorder audio and summarized their comments for each configuration flown. Project pilot comments were used to qualitatively describe the aircraft PIO tendencies and handling qualities during the approach and landing task (this task is

defined in the next section). In addition, pilot comments were used to ensure project pilots used similar criteria when assigning pilot handling qualities ratings (PHQR). These pilot ratings were given in accordance with the Cooper-Harper scale as described in reference 30. The PHQRs for each configuration flown are tabulated in the results and analysis section of this chapter.

In accordance with the Cooper-Harper scale, the PHQRs were used to form three levels of flying qualities. Level 1 consisted of all PHQR values from one to three. Level 2 consisted of PHQRs from four to six. Level 3 consisted of PHQRs from seven to ten. The flying qualities levels assigned by the pilots were compared to the levels predicted prior to flight by the Least Squares LOES and Bandwidth methods. The purpose of using the two prediction methods (Least Squares LOES and Bandwidth) was primarily to compare results of the two methods and also to verify level boundaries as contained in MIL-STD-1797.

After each flight, the NT-33A AR-700 magnetic tape data was used to accomplish LOES matching using actual flight test data. The results of this matching were compared to the actual pilot ratings to evaluate the suitability of the LOES program to accomplish equivalent system matching using flight test data.

Test Methods and Conditions

The landing longitudinal PIO tendencies, flying qualities, and the Least Squares LOES identification technique were evaluated at three pairs of short period natural frequencies and damping

ratios. All short period dynamics met MIL-STD-1797 Level 1 requirements for the landing approach (Category C). The three pairs of baseline dynamics are depicted in Figure 45 and listed in Table VIII. Also shown in Table VIII are the first and second order filters that were used to vary the configuration dynamics. The dynamics were varied to achieve predicted handling qualities to span the spectrum from Level 1 to Level 3. Table VIII shows the OCM predicted handling qualities for each of the 13 configurations tested.

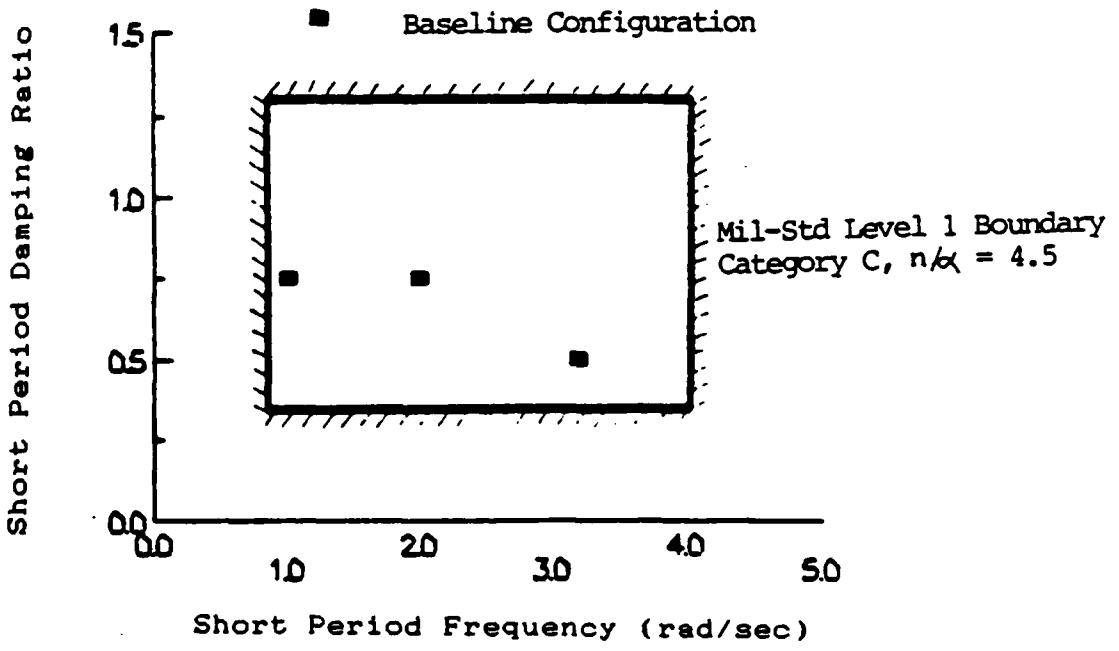

Figure 45. NT-33A Baseline Dynamics

The configuration dynamics were verified by the HAVE CONTROL test team and by the CALSPAN Corporation. These verifications are shown in Appendix E. Only the short period and filter dynamics

Table VIII

HAVE CONTROL Flight Test Configurations

Primary Config	ζ_{sp}	$\omega_{n_{sp}}$	K	τ_1	τ_2	ζ_1	ω_{n_1}	Predicted HQ Level
1-1	0.75	1.0	1.0	--	--	--	--	1
1-3			4.0	--	4	--	--	2
1-10			16.0	--	--	0.7	4	3(8)*
2-1	0.75	2.0	1.0	--	--	--	--	1
2-D			0.5	20	10	--	--	2
2-2			10.0	--	10	--	--	2
2-5			1.0	--	1	--	--	3(8)
2-7			144.0	--	--	0.7	12	2
3-1	0.50	3.2	1.0	--	--	--	--	1
3-3			4.0	--	4	--	--	2
3-5			1.0	--	1	--	--	2
3-6			256.0	--	--	0.7	16	2
3-8			81.0	--	--	0.7	9	2

* Numbers in parentheses indicate the OCM predicted handling qualities rating.

First Order Filters: $\dfrac{K(s+\tau_1)}{(s+\tau_2)}$

Second Order Filters: $\dfrac{K}{s^2+2\zeta_1\omega_{n_1}s+\omega_{n_1}{}^2}$

were varied to produce different aircraft handling qualities. The phugoid, lateral-directional, servo-actuator, and feel system dynamics were held constant. These parameters are shown in Appendix F.

After takeoff, the project pilot took control of the aircraft, and climbed to 5000 feet pressure altitude on a North turnout. The instructor/safety pilot set the short period and filter dynamics by adjusting the appropriate variable stability gain control in the rear cockpit. The project pilot established the landing configuration and accomplished the auto-step and auto-ramp inputs and the hand-step and hand-ramp inputs used for the system identification task. Further discussion of the system identification task is presented in the next section.

After accomplishing the open-loop tasks, the project pilot established a 1000 feet per minute descent in the landing configuration. Then at 50 feet above a 4000 feet mean sea level target altitude, the pilot simulated a landing task by an aggressive level off. As a safety precaution, if the configuration exhibited a divergent PIO or other Level 3 characteristics, that configuration was not tested any further.

After the simulated landing was accomplished, the project pilot returned to the pattern and flew the approach and landing without an offset. After touching down, the instructor/safety pilot disengaged the VSS and performed the takeoff. The project pilot then made preliminary comments on the configuration while the instructor/safety pilot flew the aircraft on an extended

downwind (South re-entry). If, during the straight in approach, a divergent PIO occurred or adequate performance could not be achieved, then the offset landing task was not attempted. Two visual approaches with a lateral offset were then flown, with one offset to each side of the runway. After the first offset approach, the project pilot added to his preliminary comments. After the second offset approach, the project pilot summarized his overall comments and assigned a PIO rating and a PHQR for that configuration. If the evaluation pilot felt confident enough to make an overall evaluation based on only two approaches he was allowed to eliminate the third approach. The evaluation pilot was allowed to assign separate ratings for the approach and flare if he deemed it necessary.

The landing task was a visual approach with a lateral offset and a correction to centerline prior to touchdown. The size of the lateral offset was approximately 150 feet. Since the width of the main runway at Edwards is 300 feet, the 150 foot offset to the left was made by aligning with the left edge of the runway, and the 150 foot offset to the right was made by aligning with the right edge of the runway. The aircraft was flown on glidepath using the instrument landing system until the beginning of the overrun. The correction to centerline was initiated at 100 feet above ground level. The safety pilot assisted in maintaining a constant offset correction between the three project pilots.

The touchdown zone was 1000 feet long starting at 500 feet past the threshold. The touchdown aimpoint was 1000 feet from the

threshold and within 5 feet of centerline. Each landing was treated as a "must land" situation, unless the instructor/safety pilot and/or project pilot determined that safety of flight would be compromised in an attempt to land. Table IX summarizes the performance criteria used to assign PHQRs to this visual landing task.

Table IX

Offset Landing Task Performance Standards	
Desired	Adequate
No PIOs	
Touchdown within 5 feet of centerline (main wheels on centerline)	Touchdown within 25 feet of centerline (tip tank on centerline)
Touchdown aimpoint +/- 250 ft	Touchdown aimpoint +/- 500 ft
Approach airspeed +/- 5 kts	Approach airspeed +10/-5 kts

System Identification Tasks

The dynamics of each configuration flown in the approach and landing task were verified using the Least Squares Lower Order Equivalent System matching technique. This required a ramp input with an optimal rise time. The optimal rise time, a function of aircraft dynamics and flight condition, was calculated for each configuration prior to conducting the flight tests. To investigate the effect of rise time on the matching technique, several auto-ramp and hand-ramp elevator inputs with varying rise times were used for each change in aircraft dynamics. In addition, auto-step and hand-step inputs were used for each set of

aircraft dynamics. The step inputs were used in the Least Squares program as low rise time ramp inputs because in actual test data a step input has a finite rise time.

The ramp and step inputs were accomplished with the aircraft trimmed for straight and level flight. The hand-step input was done by the project pilots by first trimming the aircraft for straight and level flight, then running the trim nose down (approximately 5 lbs F_s), and releasing the stick. The hand-ramp input was accomplished like the hand step input except that the stick was eased slowly to the trim condition using a predetermined (one or two second) rise time. The pilots were instructed that the exact rise time was not as critical as accomplishing a smooth release of the stick.

The instructor/safety pilot ran the data acquisition system (DAS) during these inputs. The longitudinal control force, and pitch rate response (obtained from the DAS) were used in the Least Squares LOES program to extract a lower order equivalent system model. The results of the LOES matching using the actual flight test data were then compared to results obtained prior to the flights based on the theoretical configuration dynamics. These results are presented in the remaining sections of this chapter.

Results and Analysis

The Least Squares system identification program was used to accomplish lower order equivalent system (LOES) matching with the 13 aircraft configurations shown in Table VIII. The matching was conducted prior to the actual flights using the known NT-33A phugoid, short period, servo-actuator, feel system, and filter dynamics. Only the short period and filter dynamics were varied from one configuration to another. The pre-flight matching results were used to predict handling qualities based on MIL-STD guidance and compared with the actual pilot ratings given during the offset landing task. These results were also compared to results obtained using Hoh's Bandwidth technique (described in Appendix H) and to the LOES results using actual flight test data.

The Bandwidth method was used so that the Least Squares LOES program could be compared with a well-accepted handling qualities estimation technique. The comparison between the two techniques was based primarily on the number of configurations correctly predicted (compared with the pilot's actual ratings). The results of the actual flight test LOES matching were important to verify the analytical LOES results and demonstrate the ability of the program to work using discrete flight test data.

Pre-Flight Matching Results

The Least Squares LOES matching technique (described in detail in chapter IV) was used to produce a least squares match to the higher order aircraft dynamics. The higher order dynamics

were represented by the aircraft's pitch rate time response excited by a ramp input. After the program accomplished the time response matching, frequency response lower order transfer functions were extracted in the form shown in equation 15.

Time responses and frequency responses of the LOES model were compared to the corresponding responses of the higher order system to determine the closeness of the match. These comparisons were made in terms of cost functions which mathematically define the quality of the match. The frequency domain and time domain cost functions that were used to analyze the quality of the LOES matching are shown in equations 17 and 18.

For a given aircraft configuration, the rise time of the ramp input and the length of the matching interval were varied until the best identification of the system (defined by low cost functions and realistic values of L_α) had been achieved. In general, higher cost functions were accepted in order to keep L_α fixed at the basic aircraft value (approx. 0.70 sec^{-1}). This technique produced reasonable results for all the LOES parameters whereas the opposite technique (i.e. freeing L_α to reduce the cost functions) resulted in unrealistic values for some LOES parameters.

The estimation of flying qualities levels was based on the criteria for equivalent ζ_{sp}, ω_{sp} and τ_θ given in MIL-STD-1797 (3). The requirements for time delay (τ_θ) and short period damping (ζ_{sp}) are specified as follows:

Level	Allowable Delay	Allowable ζ_{sp} Limits
1	0.10 (sec)	0.35-1.30
2	0.20 (sec)	0.25-0.35 or 1.30-2.00
3	0.25 (sec)	< 0.25 or > 2.00

The requirements for equivalent short period natural frequency (ω_{sp}) are given in terms of the control anticipation parameter (CAP) defined as CAP = $\omega_{sp}^2/(n/\alpha)$ where n/α = $(V/g)(1/T_{\theta 2})$. The requirements on CAP are listed below.

Level	Allowable CAP Limits ($g^{-1}sec^{-1}$)
1	0.16-3.60
2	0.05-0.16 or 3.60-10.00
3	< 0.05 or > 10.00

The requirements shown above are for Category C (approach, landing, and takeoff) flight phases. The results of the LOES matching including the LOES parameters, cost functions, and predicted flying qualities based on the above criteria are shown in Table X. Graphical results are presented in Appendix G.

Table X

Least Squares LOES Matching Results (Analytical Data)

CONFIG	LEVEL	$1/T_{\theta 2}$ (1/sec)	K_θ (rps/lb)	ζ_{sp}	ω_{sp} (rps)	τ_θ (sec)	CAP (1/gsec)	$cost_f$	$cost_t$
1-1	1	0.708	0.012	0.599	0.922	0.056	0.189	45.37	0.005
1-3	2	0.706	0.007	0.396	0.769	0.185	0.131	156.25	0.062
1-10	3	0.707	0.006	0.335	0.718	0.340	0.115	459.62	0.117
2-1	1	0.690	0.015	0.574	1.751	0.044	0.682	74.33	0.008
2-D	1	0.709	0.013	0.543	1.609	0.070	0.575	108.24	0.009
2-2	2	0.715	0.011	0.471	1.518	0.107	0.512	186.35	0.019
2-5	3	0.719	0.003	0.383	0.894	0.205	0.177	250.02	0.015
2-7	2	0.700	0.010	0.444	1.461	0.143	0.474	343.43	0.027
3-1	1	0.710	0.032	0.420	2.711	0.038	1.634	107.92	0.026
3-3	2	0.696	0.014	0.350	1.909	0.140	0.810	387.44	0.062
3-5	2	0.709	0.006	0.445	1.266	0.186	0.356	391.75	0.021
3-6	2	0.704	0.022	0.344	2.341	0.105	1.218	381.30	0.067
3-8	2	0.706	0.018	0.293	2.159	0.168	1.036	548.45	0.095

The cost functions give a mathematical measure of the "goodness" of the match. As a general rule of thumb, MIL-STD-1797 states that a frequency domain mismatch function of 200 or less will produce LOES dynamics that are similar enough to the high order system that pilots, in general, will not be able to tell them apart (3).

The matching results in Table X show that $cost_f$ was less than 200 for only 6 of the 13 configurations. A $cost_f$ greater than 200, however, does not mean that the LOES does not approximate the HOS well. The MIL-STD gives 200 as a guideline above which pilots may be able to tell some difference between the HOS and LOES dynamics. Additionally, the fact that the HOS does not match well to the LOES is an indication in itself that the flying qualities will not be "conventional". That is, the LOES is in the conventional short period form, and a HOS that can't match this form is already suspect of having poor flying qualities. Table X, for example, shows that the configurations with $cost_f$ greater than 200 all predicted Level 2 or 3 flying qualities. The flight test results, presented in Table XI, in general, agreed with these predictions.

Note that the "Actual Level" presented in Table XI was generally determined by averaging the pilot ratings from only two evaluations. Even though the data scatter between pilot ratings was small, this was a limited sample and the following discussions are presented with this consideration in mind.

Table XI

LOES Predicted Handling Qualities and Flight Test Pilot Ratings

Configuration	Predicted Level	Pilot Ratings	Actual Level
1-1	1	2/4	1
1-3	2	7/7	3
1-10	3	10	3
2-1	1	3/2	1
2-D	1	4.5/3	2
2-2	2	4/2	1
2-5	3	8/10	3
2-7	2	4.5/5	2
3-1	1	2/3	1
3-3	2	3/3	1
3-5	2	6/5	2
3-6	2	5/6	2
3-8	2	3/7/4/4	2

Table XI shows that the LOES matching technique correctly predicted the flying qualities for 9 of the 13 configurations (69 percent correct). Of the four that were incorrect, three were on the "borderline" in some sense. Configuration 2-2 for example was only 7 milliseconds above the Level 1 boundary for time delay (and thus rated Level 2 by the criteria). The pilot ratings were also on the borderline between Level 1 and 2 for configuration 2-2 (i.e. pilot ratings of 2 and 4 could actually be considered as

Level 1 or Level 2, especially when considering the "noise" level of plus or minus 1 pilot rating often cited as normal data scatter). With these considerations in mind, the LOES technique apparently correctly identified a "borderline" aircraft response for configuration 2-2.

Similar results were seen with configurations 1-3 and 2-D. Configuration 1-3 was 15 milliseconds below the Level 3 boundary for equivalent time delay and received pilot ratings of 7/7. Configuration 2-D was 30 milliseconds below the Level 2 boundary and received pilot ratings of 4.5/3. If these three configurations are considered as correctly predicting borderline cases instead of incorrectly predicting the flying quality level, 12 of the 13 configurations were correctly predicted by the LOES technique. This means 92 percent were correctly predicted.

These results do not suggest that the LOES criteria need to be changed. The problem of predicting flying qualities for "borderline" cases will always be there. Therefore it is important to test configurations that are borderline in nature to better define what the boundaries should be. The recommendation of the HAVE CONTROL test team was to conduct more flight testing using configurations that are borderline in equivalent time delay, equivalent damping, or CAP to better identify LOES boundaries.

With regard to borderline configurations, it should be recognized that the flying qualities of different aircraft can't always be categorized into three distinct levels but are better described by a continuous spectrum. The "bottom line" should be

to communicate to the pilot or the design engineer the expected flying qualities of the aircraft before the actual flight. Therefore, borderline configurations should be identified as such. This is especially important in cases such as configuration 1-3 which was predicted to be Level 2 (actually on the borderline between Level 2 and 3) and rated Level 3 by the pilots.

Bandwidth Method Correlation

Hoh's bandwidth method was used to compare flying qualities prediction results with the LOES method. The bandwidth technique predicts levels of handling qualities based on phase delay and system bandwidth. Large phase delays within the pilot's bandwidth of control (0.1 to 10 rad/sec) indicate the presence of higher order lag dynamics. In general, poor handling qualities are associated with low bandwidths and large phase delays.

Figure 46 presents Hoh's proposed Level 1, 2, and 3 boundaries based on phase delay and bandwidth. Also shown are the test configurations along with their associated actual pilot ratings. A detailed discussion of the bandwidth method and the graphical results for each configuration are shown in Appendix H. The bandwidth results are summarized and compared with the actual pilot ratings in Table XII.

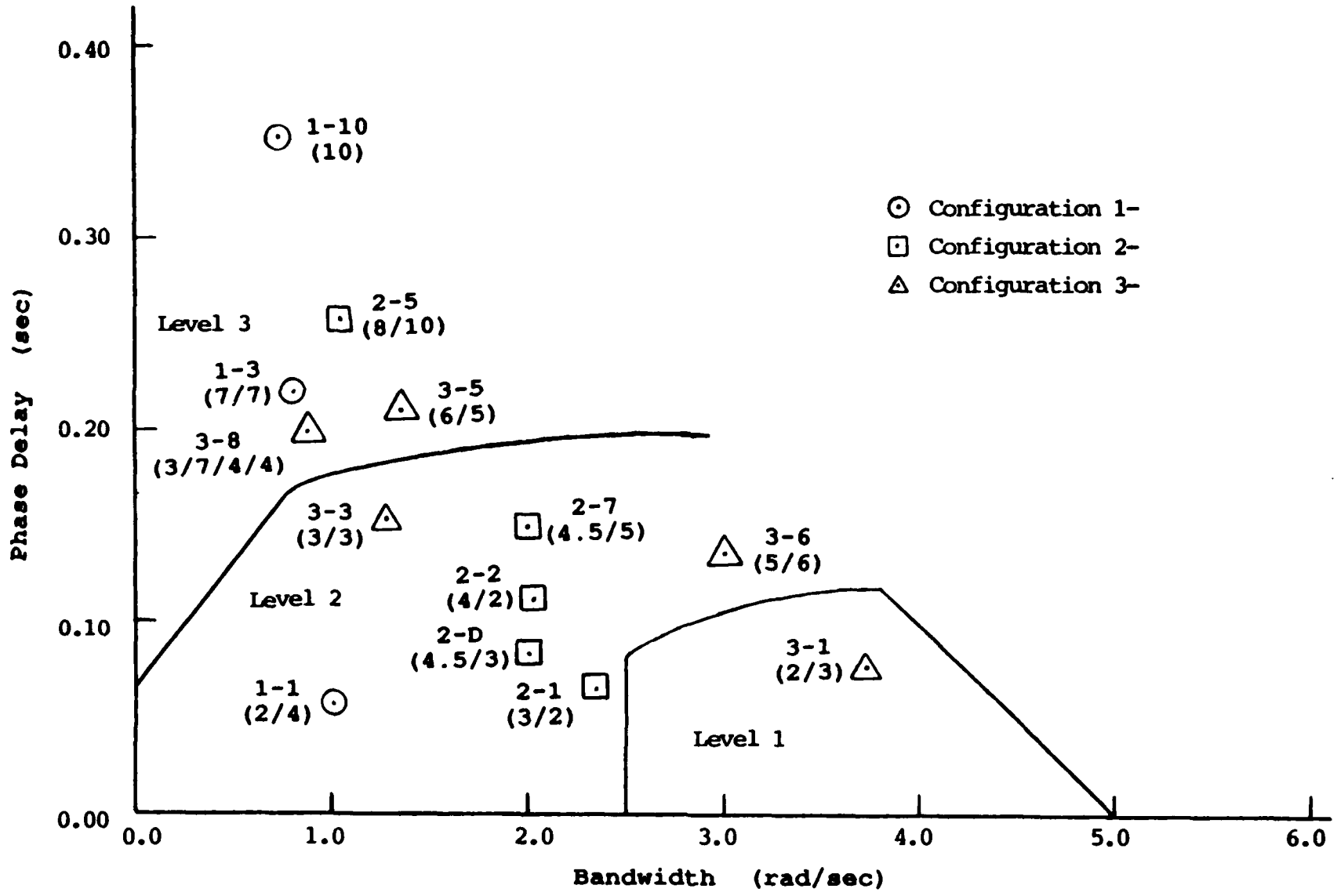

Figure 46. Handling Qualities Prediction Based on Hoh's Bandwidth Criteria

Table XII

Bandwidth Predicted Handling Qualities and Flight Test Pilot Ratings

Configuration	Predicted Level	Pilot Ratings	Actual Level
1-1	2	2/4	1
1-3	3	7/7	3
1-10	3	10	3
2-1	2	3/2	1
2-D	2	4.5/3	2
2-2	2	4/2	1
2-5	3	8/10	3
2-7	2	4.5/5	2
3-1	1	2/3	1
3-3	2	3/3	1
3-5	3	6/5	2
3-6	2	5/6	2
3-8	3	3/7/4/4	2

Hoh's theory correctly predicted the level of handling qualities for 7 of the 13 configurations (54 percent). Two of the configurations which were not correctly predicted were close to the Level 2 boundary (configurations 3-5 and 3-8). If the boundary was shifted up slightly, these configurations would have been correctly predicted. Additionally, shifting the Level 2 boundary up brings configuration 3-3 more into the heart of the Level 2 boundary which makes sense. Configuration 3-3 was rated

Level 1 by the pilots but close to the Level 2 boundary (almost rated Level 3) by the bandwidth criteria.

Shifting up the Level 2 boundary is further justified by the fact that τ_p was higher than τ_θ for 12 of the 13 configurations tested (a comparison between τ_p and τ_θ is made in the following section). Since the Level 2 limit for τ_θ has been set at 200 msec, and τ_p tends to be higher than τ_θ for a given configuration, it is reasonable to set the Level 2 limit for τ_p to 200 msec as well. Based on this limited flight test data, Figure 47 presents the HAVE CONTROL test team's suggested Level 2 boundary change for Hoh's bandwidth criteria. Using the new boundary, the bandwidth method would have correctly predicted 9 of the 13 configurations (69 percent).

The purpose of using the bandwidth method in this study was to compare the results to the Least Squares LOES technique. With the limited flight test data and associated considerations presented in this discussion, the LOES technique correctly predicted the handling qualities for 92 percent of the configurations tested compared with only 69 percent correctly predicted by the bandwidth criteria. The Least Squares LOES computer program performed very well compared to the well-accepted bandwidth method. Application of the LOES program was somewhat more involved than using the simple bandwidth method, but the results were more correct. Further comparisons between the two methods including a comparison between the time delay parameters (τ_p and τ_θ) will be made in the following section.

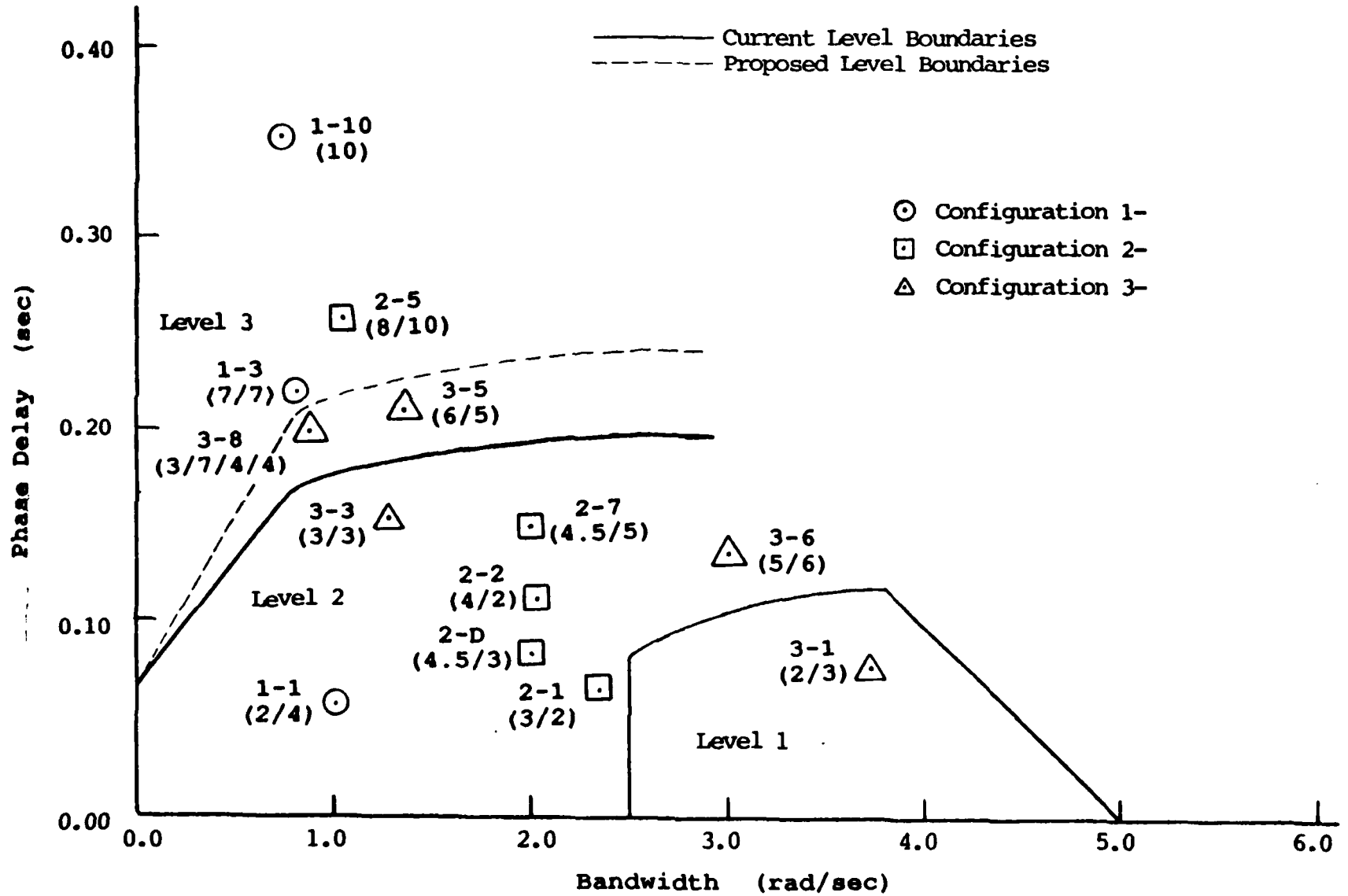

Figure 47. Proposed Boundary Changes for Hoh's Bandwidth Criteria

Flight Test Matching Results

To verify the analytical LOES matching, the actual stick force inputs and pitch rate response outputs were used to produce lower order equivalent matches for each configuration. The results of this matching, including the LOES parameters, the cost function ($cost_t$), and the predicted flying qualities based on the MIL-STD-1797 criteria are shown in Table XIII. Graphical results are shown in Appendix G.

Table XIII

Least Squares LOES Matching Results (Flight Test Data)

CONFIG	LEVEL	$1/T_{\theta 2}$ (1/sec)	K_θ (rps/lb)	ζ_{sp}	ω_{sp} (rps)	TD (sec)	CAP (1/gsec)	$cost_t$
1-1	2	4.023	0.084	1.000	0.863	0.100	0.166	0.030
1-3	2	7.846	0.010	0.876	2.270	0.180	1.145	0.024
1-10*	3	-	-	-	-	-	-	-
2-1	2	0.744	0.031	1.000	1.267	0.120	0.357	0.020
2-D	2	0.694	0.041	1.000	0.800	0.100	0.142	0.030
2-2	2	0.643	0.032	1.000	0.888	0.180	0.175	0.030
2-5	3	-2.616	-0.041	1.000	1.994	0.200	0.884	0.004
2-7	2	3.959	0.010	0.384	2.675	0.140	1.590	0.051
3-1	1	0.493	0.067	0.959	3.032	0.040	2.042	0.056
3-3	2	0.694	0.028	0.752	2.264	0.120	1.140	0.024
3-5	2	0.518	0.026	1.000	0.720	0.160	0.115	0.018
3-6	2	0.718	0.038	0.675	2.680	0.100	1.597	0.019
3-8	2	0.946	0.027	0.508	2.493	0.160	1.381	0.031

* Configuration 1-10 was not flown in landing approach due to uncontrollability during level off task

The results presented in Table XIII demonstrate some of the problems that were encountered during the flight test matching. One of the problems was that the ramp input rise time and/or the length of the match time could not be varied as easily as was done in the analytical matching. During the analytical matching, these inputs could be varied continuously until the best match was

achieved. This is how the parameter L_α was fixed at the basic aircraft value and how the cost functions were minimized.

Because of the difficulties involved in precisely varying the input rise time and the length of available match time some configurations did not match well using the flight test data and realistic values of L_α were not achieved in every case. A realistic value of L_α is important because this generally effects the accuracy of the other equivalent parameters. Table XIII shows that four of the configurations (1-1, 1-3, 2-5, and 2-7) had unrealistic values of $1/T_{\theta 2}$ (and therefore L_α).

In the cases where a poor match was achieved, generally the rise time of the ramp input was "close enough" based on analytical predictions but not enough data was collected. That is, the length of available pitch rate response data was insufficient to identify the system dynamics. Depending on the configuration, anywhere from 3 to 10 seconds of data were generally required to make a good match. The problem was that to get a good response from the aircraft, a fairly large stick force input (about 5 lbs) was required. This much input, however, caused a large pitch rate up that had to be recovered before the nose was too high. So, there was a trade off between getting a good response from the aircraft and getting enough data to make the system identification.

Additional problems included noise and/or turbulence effects. In some cases, the rise time was correct and there was enough data to make the match, but noise in the data or turbulence made the data unusable. These problems were minimized however because the

flights were conducted early in the morning in smooth air.

Despite the problems mentioned, the overall results of the flight test data matching were encouraging. Table XIV compares the predicted handling qualities with the actual pilot ratings. These results show that 8 of the 13 configurations were correctly predicted by the flight test matching (62 percent correct). Of the 5 that were incorrect, 4 were on the "borderline" in time delay as was discussed previously with regard to the analytical matching results.

Table XIV

Flight Test Matching Results and Flight Test Pilot Ratings

Configuration	Predicted Level	Pilot Ratings	Actual Level
1-1	2	2/4	1
1-3	2	7/7	3
1-10	3	10	3
2-1	2	3/2	1
2-D	2	4.5/3	2
2-2	2	4/2	1
2-5	3	8/10	3
2-7	2	4.5/5	2
3-1	1	2/3	1
3-3	2	3/3	1
3-5	2	6/5	2
3-6	2	5/6	2
3-8	2	3/7/4/4	2

The overall results of the flight test matching show that good results can be obtained when large enough inputs are flown in smooth air and an adequate amount of data is collected before the pitch up is terminated. In addition, it was found that the pilots could fly the ramp and step inputs precisely enough by hand to be used in the LOES program. In fact, the hand-ramp inputs were used in several of the configuration matches tabulated in Table XIII because the inputs worked as well or better than the auto-ramp inputs. This is an important finding because it means that the LOES system identification program can be used on virtually any instrumented test aircraft since an auto-input capability is not required. All that is required is a DAS that can measure stick force input and pitch rate output.

Using the flight test data an additional time delay measurement was made which will be referred to as "TD" to be distinguished from phase delay (τ_p) and equivalent time delay (τ_e or τ_θ). TD was found by measuring the delay between the first onset of stick force and the resulting response in pitch rate. These measurements are shown graphically in Appendix G.

Figure 48 gives a comparison between τ_e, τ_p, and TD which shows them to be numerically similar. As was discussed earlier, τ_p tends to be higher than τ_e for a given configuration. Despite this fact, the bandwidth criteria are more restrictive on allowable τ_p than the LOES criteria are on τ_e. This was one of the reasons for the recommendation to change the bandwidth criteria.

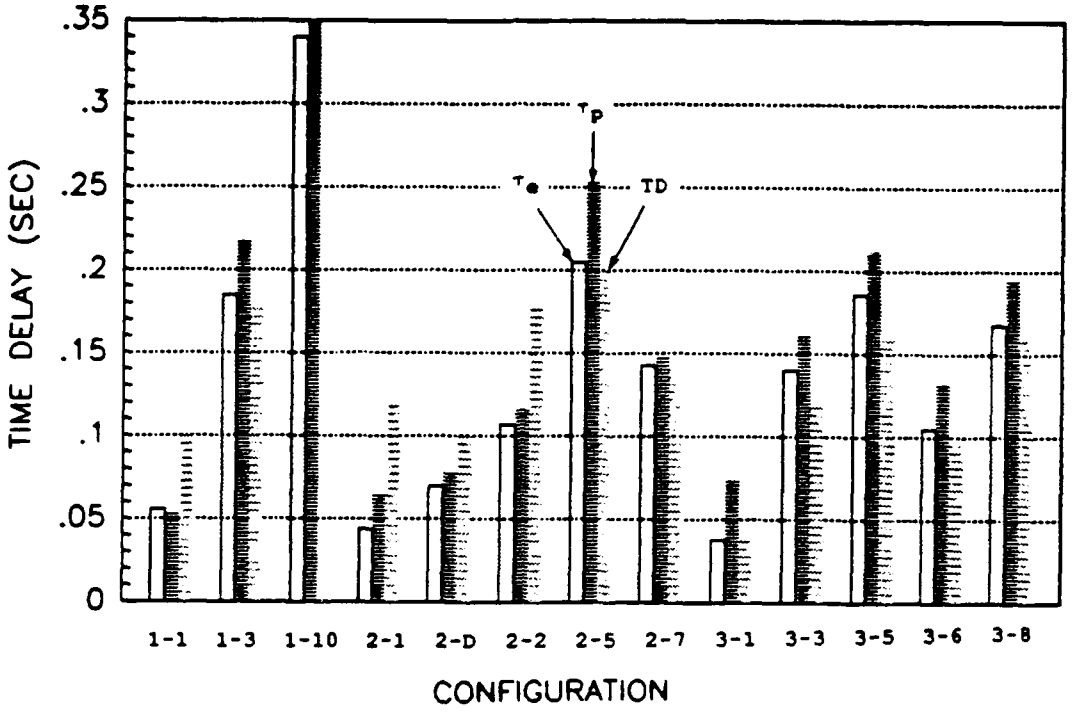

Figure 48. Comparison of Time Delay Parameters

Figure 48 provides a good illustration of the importance of time delay as a flying qualities parameter. Configuration 1-10, for example, had significantly higher values of time delay than the other configurations and was also the worst flying configuration (1-10 was not evaluated in the landing task because it was uncontrollable at altitude). In general, the handling quality predictions were largely determined by time delay (rather than ζ_{sp} or ω_{sp}). Configurations with lower time delay were generally predicted to have good handling qualities and

configurations with higher time delay were predicted to have poor handling qualities. The flight test results, in general, agreed with these predictions.

The overall results of the analytical and flight test matching have shown that the Least Squares program is well suited to perform lower order equivalent systems matching and predict handling qualities. The results of the LOES predictions compared favorably with the Bandwidth results and with the actual pilot ratings. These results are summarized in Table XV.

Table XV

Flight Test Handling Quality Prediction Results
(Percent Correctly Predicted)

	Actual MIL-STD Boundaries	Borderline Cases Correct
Bandwidth (Pre-Flight)	54	69
LS LOES (Pre-Flight)	69	92
LS LOES (Flight Data)	62	92

VI. Conclusions and Recommendations

A program has been developed for matching the time response of high-order aircraft systems with lower-order equivalent systems. The lower-order equivalent systems are extracted in the form of the short period pitch rate transfer function to take advantage of the "classical" aircraft data base in MIL-STD-1797. The attractive aspects of the Least Squares LOES program are its simplicity and its adaptability to flight test parameter identification requirements.

Comparisons between the Least Squares program and LONFIT have shown that both programs give numerically similar LOES parameters for a given high-order system. The LOES parameters derived from both programs were found to approach the corresponding basic aircraft values as the control system dynamics were made "faster" compared to the aircraft dynamics. That is, as the control system dynamics became more "transparent", the equivalent parameters predicted that the aircraft would have a classical low-order response. This is consistent with LOES theory.

During the flight test program the Least Squares technique correctly predicted the flying qualities levels of 92 percent of the aircraft configurations tested compared with only 69 percent correctly predicted by Hoh's Bandwidth method. Additionally, the Bandwidth method's time delay parameter (τ_p) was found to be higher than the LOES time delay parameter (τ_e) for 12 of the 13 configurations tested. Despite this fact, the MIL-STD-1797 Level 2 boundary for τ_p is lower than the Level 2 boundary for τ_e.

These findings resulted in a recommendation by the test team to change the Level 2 Bandwidth boundary.

It was found that the short period numerator term, L_α, could be fixed at the basic aircraft value by varying the rise time of the ramp input and/or the length of the overall match time. Fixing L_α was the preferred method of matching since this gave more realistic values for all LOES parameters and also gave the most correct flying qualities predictions.

Fixing L_α during the analytical matching was easy since the rise time and length of match time could be varied as needed. These inputs could not be varied as easily with the actual flight test data however. Generally the rise time of the input could be controlled adequately but the problem was in getting enough data. There was a trade off between getting a good response out of the airplane (which required a fairly large stick force input) and getting enough data before the resulting rapid pitch up had to be recovered.

An important finding during the flight test matching was that the pilots could hand fly the required stick force ramp inputs. One of the reasons the NT-33A aircraft was used for the test program was to take advantage of the auto-input capability. It was thought that the pilots could not fly the ramp inputs with the precision required by the Least Squares program. In actual flight test applications however, it was found that a smooth ramp input of approximately 1 second was adequate. The pilots were instructed that the smoothness of the input was more important

than the actual rise time. The results showed that in many cases the hand-flown inputs worked as well or better than the auto-inputs. This is an important finding because it means the Least Squares program can be used with any DAS instrumented aircraft.

Despite the problems already mentioned with the actual flight test matching, 9 of the 13 configurations were matched well (with L_α close to the basic aircraft value) and 12 out of 13 were correctly predicted (92 percent). These results are encouraging and the recommendation is to conduct more flight testing with the Least Squares LOES program to determine how the problems can be solved. The program has been run at the Air Force Flight Test Center (AFFTC) Simulation Facility on $Matrix_X$ and can be applied to almost any flight test mission using only about 5-10 minutes of actual flight time. The test aircraft must have a data acquisition system capable of recording stick force input and pitch rate output at 10 samples per second.

Parameter identification techniques will soon be a part of the curriculum at the USAF Test Pilot School and this may be a good program to use. Potential starting points for an AFIT/TPS thesis project could be refining the overall technique to work better using flight test data, modifying the program to simultaneously match pitch rate and normal acceleration, modifying the program to identify lateral-directional equivalent parameters, and conducting comparisons with MMLE or other LOES programs regarding pre-flight flying qualities predictions.

The overall test results of the Least Squares LOES program have shown that it works well in comparisons with LONFIT, Hoh's Bandwidth method, and actual pilot ratings. The recommendation is to use the Least Squares LOES program in applications requiring flight test parameter identification and handling qualities predictions.

APPENDIX A. FREQUENCY AND TIME RESPONSE MATCHING RESULTS

This appendix contains the equivalent parameters, CAP, and the cost functions obtained from the freqency domain matching (LONFIT) and the time domain matching (LEAST SQUARES) techniques. The data is presented for the LONFIT results, the LEAST SQUARES results, and finally a comparison between the two is given in tabular format. Graphical comparisons of this data are presented in the discussion (chapters III and IV).

TABLE A1

LONFIT FREQUENCY RESPONSE MATCHING RESULTS
FLIGHT CONDITION 1*

ω_{fs}	L_α	L_α	K_θ	ζ_{sp}	ω_{sp}	τ_θ	CAP	$cost_f$	$cost_t$
(rps)	-	(s^{-1})	(rps/lb)	-	(rps)	(sec)	1/(g*s)	-	-
6.0	Fix	0.428	-0.092	0.245	2.270	0.287	0.569	264.62	1.017
6.0	Free	0.909	-0.073	0.147	2.517	0.269	0.329	179.08	1.652
8.0	Fix	0.428	-0.106	0.236	2.404	0.252	0.638	178.29	0.851
8.0	Free	0.750	-0.090	0.163	2.572	0.239	0.417	123.79	1.393
10.0	Fix	0.428	-0.116	0.235	2.481	0.226	0.680	135.16	0.745
10.0	Free	0.681	-0.101	0.174	2.612	0.215	0.473	95.21	1.263
12.0	Fix	0.428	-0.122	0.235	2.529	0.206	0.706	111.56	0.688
12.0	Free	0.644	-0.108	0.181	2.640	0.196	0.511	79.50	1.193
18.5	Fix	0.428	-0.133	0.238	2.601	0.164	0.747	81.80	0.626
18.5	Free	0.595	-0.120	0.193	2.686	0.156	0.572	59.95	1.102
31.0	Fix	0.428	-0.139	0.240	2.640	0.127	0.769	69.36	0.612
31.0	Free	0.572	-0.127	0.201	2.712	0.120	0.607	52.12	1.071

*Flight condition 1 is at M = 0.70, Alt = 35,000 feet, V_{To} = 681 fps, and q = 171 psf. The basic aircraft short period dynamics for the A-4D at this flight condition are L_α = 0.428 sec^{-1}, ζ_{sp} = 0.225, and ω_{sp} = 2.77 rad/s.

TABLE A2

LONFIT FREQUENCY RESPONSE MATCHING RESULTS
FLIGHT CONDITION 2*

ω_{fs}	L_α	L_α	K_θ	ζ_{sp}	ω_{sp}	τ_θ	CAP	$cost_f$	$cost_t$
(rps)	-	(s^{-1})	(rps/lb)	-	(rps)	(sec)	1/(g*s)	-	-
6.0	Fix	2.080	-0.059	0.720	4.524	0.220	0.333	57.908	0.069
6.0	Free	8.197	-0.027	0.359	5.887	0.168	0.143	33.290	0.125
8.0	Fix	2.080	-0.078	0.654	5.192	0.201	0.439	50.142	0.073
8.0	Free	5.111	-0.044	0.354	5.949	0.163	0.235	32.878	0.133
10.0	Fix	2.080	-0.091	0.613	5.631	0.185	0.516	45.050	0.077
10.0	Free	3.989	-0.059	0.368	6.065	0.155	0.312	31.650	0.130
12.0	Fix	2.080	-0.102	0.587	5.930	0.172	0.573	41.742	0.079
12.0	Free	3.546	-0.069	0.376	6.204	0.146	0.368	30.648	0.129
18.5	Fix	2.080	-0.120	0.549	6.433	0.141	0.674	36.734	0.085
18.5	Free	3.059	-0.088	0.386	6.508	0.121	0.469	29.051	0.128
31.0	Fix	2.080	-0.133	0.529	6.739	0.112	0.740	34.157	0.088
31.0	Free	2.853	-0.101	0.391	6.726	0.094	0.537	28.263	0.128

*Flight condition 2 is at M = 0.85, Alt = 0 feet, V_{To} = 950 fps, and q = 945 psf. The basic aircraft short period dynamics for the A-4D at this flight condition are L_α = 2.08 sec^{-1}, ζ_{sp} = 0.436, and ω_{sp} = 7.35 rad/s.

TABLE A3

LEAST SQUARES TIME RESPONSE MATCHING RESULTS
FLIGHT CONDITION 1

ω_{fs}	L_α	L_α	K_θ	ζ_{sp}	ω_{sp}	τ_θ	CAP	$cost_f$	$cost_t$
(rps)	-	(s^{-1})	(rps/lb)	-	(rps)	(sec)	1/(g*s)	-	-
6.0	Free	0.649	-0.053	0.120	2.196	0.261	0.351	380.76	1.835
8.0	Free	0.568	-0.063	0.133	2.265	0.229	0.427	317.82	1.648
10.0	Free	0.523	-0.071	0.143	2.310	0.204	0.482	282.33	1.456
12.0	Free	0.495	-0.076	0.150	2.342	0.185	0.524	259.24	1.296
18.5	Free	0.448	-0.087	0.167	2.405	0.146	0.611	218.04	0.965
31.0	Free	0.413	-0.097	0.182	2.459	0.113	0.691	185.80	0.691

TABLE A4

LEAST SQUARES TIME RESPONSE MATCHING RESULTS
FLIGHT CONDITION 2

ω_{fs}	L_α	L_α	K_θ	ζ_{sp}	ω_{sp}	τ_θ	CAP	$cost_f$	$cost_t$
(rps)	-	(s^{-1})	(rps/lb)	-	(rps)	(sec)	1/(g*s)	-	-
6.0	Free	8.416	-0.009	0.258	3.890	0.074	0.061	433.24	0.026
8.0	Free	5.674	-0.016	0.243	4.133	0.072	0.102	384.44	0.033
10.0	Free	4.504	-0.021	0.245	4.294	0.066	0.139	342.09	0.038
12.0	Free	3.874	-0.026	0.253	4.411	0.060	0.170	309.61	0.041
18.5	Free	2.987	-0.037	0.283	4.644	0.044	0.245	245.06	0.043
31.0	Free	2.451	-0.050	0.326	4.854	0.029	0.326	190.27	0.041

TABLE A5

LONFIT AND LEAST SQUARES COMPARISON
FLIGHT CONDITION 1*

ω_{fs}	Type of	L_α	K_θ	ζ_{sp}	ω_{sp}	τ_θ	CAP	$cost_f$	$cost_t$
(rps)	-	(s^{-1})	(rps/lb)	-	(rps)	(sec)	1/(g*s)	-	-
6.0	Lon	0.909	-0.073	0.147	2.517	0.269	0.329	179.08	1.652
6.0	LS	0.649	-0.053	0.120	2.196	0.261	0.351	380.76	1.835
8.0	Lon	0.750	-0.090	0.163	2.572	0.239	0.417	123.79	1.393
8.0	LS	0.568	-0.063	0.133	2.265	0.229	0.427	317.82	1.648
10.0	Lon	0.681	-0.101	0.174	2.612	0.215	0.473	95.21	1.263
10.0	LS	0.523	-0.071	0.143	2.310	0.204	0.482	282.33	1.456
12.0	Lon	0.644	-0.108	0.181	2.640	0.196	0.511	79.	1.193
12.0	LS	0.495	-0.076	0.150	2.342	0.185	0.524	259.24	1.296
18.5	Lon	0.595	-0.120	0.193	2.686	0.156	0.572	59.95	1.102
18.5	LS	0.448	-0.087	0.167	2.405	0.146	0.611	218.04	0.965
31.0	Lon	0.572	-0.127	0.201	2.712	0.120	0.607	52.12	1.071
31.0	LS	0.413	-0.097	0.182	2.459	0.113	0.691	185.80	0.691

*L_α free for all configurations

TABLE A6

LONFIT AND LEAST SQUARES COMPARISON
FLIGHT CONDITION 2*

ω_{fs} (rps)	Type of -	L_α (s^{-1})	K_θ (rps/lb)	ζ_{sp} -	ω_{sp} (rps)	τ_θ (sec)	CAP 1/(g*s)	$cost_f$ -	$cost_t$ -
6.0	Lon	8.197	-0.027	0.359	5.887	0.168	0.143	33.290	0.125
6.0	LS	8.416	-0.009	0.258	3.890	0.074	0.061	433.24	0.026
8.0	Lon	5.111	-0.044	0.354	5.949	0.163	0.235	32.878	0.133
8.0	LS	5.674	-0.016	0.243	4.133	0.072	0.102	384.44	0.033
10.0	Lon	3.989	-0.059	0.368	6.065	0.155	0.312	31.650	0.130
10.0	LS	4.504	-0.021	0.245	4.294	0.066	0.139	342.09	0.038
12.0	Lon	3.546	-0.069	0.376	6.204	0.146	0.368	30.648	0.129
12.0	LS	3.874	-0.026	0.253	4.411	0.060	0.170	309.61	0.041
18.5	Lon	3.059	-0.088	0.386	6.508	0.121	0.469	29.051	0.128
18.5	LS	2.987	-0.037	0.283	4.644	0.044	0.245	245.06	0.043
31.0	Lon	2.853	-0.101	0.391	6.726	0.094	0.537	28.263	0.128
31.0	LS	2.451	-0.050	0.326	4.854	0.029	0.326	190.27	0.041

*L_α free for all configurations

APPENDIX B. LEAST SQUARES MATRIX$_x$ PROGRAMS

The computer programs used for the least squares matching, the extraction of continuous state space matrices from the discrete matrices, and the calculation of the LOES parameters and cost functions were all written for MATRIX$_x$ (31). The MATRIX$_x$ programs were written as main programs with subroutines. The subroutines are executable files and are preceded by the command "exec" (meaning execute). The first program, called COST.FREQ, was used to calculate cost$_f$, cost$_t$, and CAP given the results from the LONFIT (frequency domain) matching.

To run COST.FREQ on MATRIX$_x$ an input variable "in" must exist in the MATRIX$_x$ memory where in = <lalpha gain zeta omega tau>. The vectors "numhos" and "denhos" must also be defined where numhos is the numerator of the HOS transfer function and denhos is the denominator of the HOS transfer function. The program uses the input vector, which contains the low-order equivalent parameters from the frequency domain matching, and forms the LOES transfer function. The LOES and HOS transfer functions are then used to calculate cost$_f$ and cost$_t$. The LOES parameters are also used to calculate CAP, the control anticipation parameter (defined in chapter I).

COST.FREQ

```
exec('costf.freq')
exec('costt.freq')
v=681;
cap=(32.174*in(4)**2)/(v*in(1));
out=<in cap costf costt>
return
```

'costf.freq' - (subroutine used to calculate $cost_f$)

```
num=in(2)*<1 in(1)>;
den=<1 2*in(3)*in(4) in(4)**2>;
<o,dbhos,phhos>=bode(numhos,denhos,.1,10,21);
<o,dblos,phlos>=bode(num,den,.1,10,21);
if abs(phhos(1)-phlos(1)) > 180,...
     for i=1:21,phlos(i)=phlos(i)-360;end
for i=1:21,phlos(i)=phlos(i)-57.29578*o(i)*in(5);
cost=0;
for i=1:21,...
cost=cost+(dbhos(i)-dblos(i))**2 + 0.01745*(phhos(i)-
phlos(i))**2;
costf=(20/21)*cost
return
```

'costt.freq' - (subroutine used to calculate $cost_t$)

```
for i=1:100,u5(i)=5;end
<t,yhos>=lsim(numhos,denhos,u5,.1);
<t,ylos>=lsim(num,den,u5,.1);
costt=0;
for i=1:100,...
costt=costt + (57.29578*yhos(i) - 57.29578*ylos(i))**2;end
costt=costt/100
return
```

The next main program is called LEAST.SQUARES and was used to perform the time domain matching for comparison with LONFIT. To run LEAST.SQUARES on $MATRIX_x$ the variable "shos" must be defined and exist in the $MATRIX_x$ memory. "shos" is the system matrix of the HOS defined as:

$$shos = \begin{bmatrix} A_{HOS} & B_{HOS} \\ C_{HOS} & D_{HOS} \end{bmatrix}$$

where A_{HOS}, B_{HOS}, C_{HOS}, and D_{HOS} represent the state space form of the high-order system. LEAST.SQUARES forms the input vector u depending on the desired rise time (various rise times were used but the version shown below is for a rise time of 1.1 sec). The

input u and corresponding output y (found from the HOS time response to u) are used to perform the least squares matching. Note that within the subroutine 'ls.tr11' is another subroutine 'extract.ab' which is used to extract the continuous A and B matrices from the discrete F and G forms. The extraction programs are shown last (the Sinha and Lastman technique and the variation of this technique which uses the power series expansion of e^{AT} as explained in chapter IV).

LEAST.SQUARES

```
exec('ls.tr11')
exec('roots')
exec('tau')
exec('costf.time')
exec('costt.time')
v=681;
cap=(32.174*omega**2)/(v*lalpha);
out=<lalpha gain zeta omega tau cap costf costt>
return
```

```
'ls.tr11' - (performs the least squares matching using the
             discrete input u and corresponding output y;
             "tr11" refers to the rise time of 1.1 sec)

t=<.1:.1:10>';
u(1)=0;
for i=1:11,u(i+1)=u(i)+0.4545455;end
for i=13:100,u(i)=5.0;end
ns=7;
<t,y>=lsim(shos,ns,u,.1);
for i=3:100,x(i-2,:)=<y(i-1) y(i-2) u(i-1) u(i-2)>;
for i=3:100,capy(i-2,1)=y(i,1);
theta=x capy
yout=x*theta;
dnum2=<theta(3) theta(4)>
dden2=<1 -theta(1) -theta(2)>
ns=2;
<sd,ns>=sform(dnum2,dden2);
c=sd(3,:);
n=10;
exec('extract.ab;2');
b=real(b);
```

```
sc=<a,b;c>;
<num,den>=tform(sc,ns)
<o,dls,pls>=bode(num,den,.1,10,21);
for i=1:100,u5(i)=5;end
<t,yls>=lsim(num,den,u5,.1);
return


'roots' - (the equivalent parameters lalpha, zeta, omega, and
           gain are calculated from "num" and "den" - the output
           of the ls.tr11 program)

rd=roots(den);
sigma=abs(real(rd(1)));
omega=abs(rd(1));
zeta=sigma/omega;
rn=roots(num);
lalpha=-rn;
gain=num(1);
return


'tau' - (the equivalent time delay tau is calculated by iteration
         in the frequency domain)

ns=7;
<o,d,p>=bode(shos,ns,.1,10,21);
<o,d1,p1>=bode(num,den,.1,10,21);
if abs(p(1)-p1(1)) > 180,...
     for i=1:21,p1(i)=p1(i)-360;end
pplot=<p p1>;
plot(o,pplot,'logx')
tau=nt;
diff=1.0;
while diff > 0,...
ssp1=0;...
ssp2=0;...
plos=p1;...
for i=1:21,plos(i)=plos(i)-57.29578*o(i)*tau;end,...
for i=1:21,ssp1=ssp1 + 0.01745*(p(i)-plos(i))**2;end,...
tau=tau + 0.001;...
plos=p1;...
for i=1:21,plos(i)=plos(i)-57.29578*o(i)*tau;end,...
for i=1:21,ssp2=ssp2 + 0.01745*(p(i)-plos(i))**2;end,...
diff=ssp1-ssp2;
pplot2=<p plos>;
plot(o,pplot2,'logx')
tau
return
```

'costf.time' - (calculates $cost_f$)

```
ns=7;
<o,dbhos,phhos>=bode(shos,ns,.1,10,21);
<o,dblos,phlos>=bode(num,den,.1,10,21);
if abs(phhos(1)-phlos(1)) > 180,...
     for i=1:21,phlos(i)=phlos(i)-360;end
for i=1:21,phlos(i)=phlos(i)-57.29578*o(i)*tau;end
cost=0;
for i=1:21,...
cost=cost+(dbhos(i)-dblos(i))**2 + 0.01745*(phhos(i)-
phlos(i))**2;
costf=(20/21)*cost
return
```

'costt.time' - (calculates $cost_t$)

```
for i=1:100,u5(i,1)=5;end
ns=7;
<t,yhos>=lsim(shos,ns,u5,.1);
<t,ylos>=lsim(num,den,u5,.1);
costt=0;
for i=1:100,...
costt=costt + (57.29578*yhos(i) - 57.29578*ylos(i))**2;end
costt=costt/100;
return
```

'extract.ab;1' - (performs Sinha and Lastman extraction technique of the continuous A and B matrices from the discrete F and G forms)

```
T=0.1;
<F,G,H,I>=SPLIT(SD,NS);
AT=0.5*(F-INV(F));
FOR I=1:3,...
FSTAR=EXP(AT);...
AT=AT+INV(F)*(F-FSTAR);END
A=AT/T
Q=INV(A)*(EXP(AT)-EYE);
B=INV(Q)*G
RETURN
```

'extract.ab;2' - (performs Sinha and Lastman extraction for the A matrix and the power series extraction for the B matrix)

```
T=0.1;
<F,G,H,I>=SPLIT(SD,NS);
AT=0.5*(F-INV(F));
FOR I=1:3,...
```

```
FSTAR=EXP(AT);...
AT=AT+INV(F)*(F-FSTAR);END
A=AT/T;
FACT=1.0;
Q=ONES(2)-ONES(2);
FOR J=0:N,...
L=J;...
FACT=FACT*(L+1);...
K=((A**L)*(T**(L+1)))/FACT;...
Q=Q+K;END
FACT
K
A
B=INV(Q)*G
RETURN
```

The next program was used to conduct the analytical matching prior to the flight test matching. The results were used to predict flying qualities levels based on MIL-STD-1797 guidance for equivalent LOES parameters. The version presented here is called LS.SOF (Least Squares Second Order Filter). The program builds the basic aircraft transfer function for configuration 3 (in this case) and then adds the high-order dynamics by adding a second order pre-filter (pre-filter dynamics are for configuration 3-8 in this case).

After the HOS transfer function is completed ("numhos" and "denhos" exist in the $MATRIX_X$ memory) the program accomplishes the least squares matching, extracts the LOES parameters, and computes the cost functions similar to the LEAST.SQUARES program although there are some differences. The most important difference is that this version is interactive, allowing the user to specify rise time, match time, and initial estimates for time delay. This interaction speeds up the overall time required to achieve the best match since several combinations of rise time and match time

must be tried. The "best match" was defined by L_α fixed at the aircraft value while simultaneously achieving the lowest possible cost functions.

LS.SOF

```
inquire tr 'ENTER RISE TIME IN SEC:'
inquire tm 'ENTER MATCH TIME IN SEC:'
inquire nt 'ENTER INITIAL TIME DELAY IN SEC:'
exec('config.3')
exec('nd.sof')
exec('ls.match')
exec('roots.')
exec('tau.')
exec('costf.time')
exec('costt.time')
v=205;
cap=(omega**2)/4.5;
out=<alpha gain zeta omega tau cap costf costt>
return
```

```
'config.3' - (builds the basic aircraft transfer function by
              reading in the appropriate stability derivatives
              and using them to build "numac" and "denac")

XU=-0.041;
XW=0.11;
XQ=0;
XDE=0.0032;
ZU=-0.25;
ZW=-0.87625;
ZQ=0;
ZDE=1.1;
MU=0;
MW=-0.04098;
MQ=-2.32375;
MDE=0.33685;
AN=MDE;
BN = XDE*MU + ZDE*MW - MDE*(XU + ZW);
CN = XDE*(ZU*MW-MU*ZW) + ZDE*(XW*MU-XU*MW) + MDE*(ZW*XU-XW*ZU);
NUMAC1=<AN BN CN>;
TTH1=MIN(ABS(ROOT(NUMAC1)))
TTH2=MAX(ABS(ROOT(NUMAC1)))
N1=<1 TTH1>;
N2=<1 TTH2>;
AC2=CONVOLVE(N1,N2);
NUMAC=MDE*1.1*AC2
```

```
Uo=205;
W=25;
G=32.174;
CTHO=COS(0.0785398);
STHO=SIN(0.0785398);
AD = -MQ -ZW -ZU;
BD = XU*(MQ+ZW) + MQ*ZW - Uo*MW - XW*ZU + W*MU;
CD = -XU*(ZW*MQ-Uo*MW)+ZU*(XW*MQ+W*MW)-MU*(Uo*XW+W*ZW-G*CTHO)+G*MW*STHO
DD = G*CTHO*(ZU*MW-MU*ZW) - G*XU*MW*STHO;
DENAC=<1 AD BD CD DD>;
RTS=ROOT(DENAC);
OMEGAP=MIN(ABS(RTS));
OMEGASP=MAX(ABS(RTS));
SIGMAP=MIN(ABS(REAL(RTS)));
SIGMASP=MAX(ABS(REAL(RTS)));
ZETAP=SIGMAP/OMEGAP;
ZETASP=SIGMASP/OMEGASP;
OUTAC=<ZETAP OMEGAP ZETASP OMEGASP>;
ZETASP=0.50;
OMEGASP=3.20;
RETURN
```

```
'nd.sof' - (builds the second order filter transfer function,
            the feel system and actuator transfer functions,
            and the HOS transfer function "numhos" and "denhos")

kfilt=81;
z1=0.7;
wn1=9;
numfilt=kfilt;
denfilt=<1 2*(z1)*(wn1) wn1**2>;
numfs=84.5;
denfs=<1 31.2 676>;
numserv=75**2;
denserv=<1 105 75**2>;
a=conv(numfilt,numfs);
b=conv(numserv,numac);
numhos=conv(a,b);
s=<1 0>;
numhos=conv(s,numhos);
e=conv(denfilt,denfs);
d1=<1 2*(zetap)*(omegap) omegap**2>;
d2=<1 2*(zetasp)*(omegasp) omegasp**2>;
denac=conv(d1,d2);
f=conv(denserv,denac);
denhos=conv(e,f);
return
```

'ls.match' - (conducts the least squares matching using the time response of the HOS and outputs the LOES transfer function "num" and "den")

```
tm=tm*10;
tr=tr*10;
tinc=5/tr;
u(1)=0;
for i=1:tr,u(i+1)=u(i)+tinc;end
for i=(tr+2):tm,u(i)=5.0;end
<t,y>=lsim(numhos,denhos,u,.1);
for i=3:tm,x(i-2,:)=<y(i-1) y(i-2) u(i-1) u(i-2)>;
for i=3:tm,capy(i-2,1)=y(i,1);
theta=x\capy
yout=x*theta;
dnum2=<theta(3) theta(4)>
dden2=<1 -theta(1) -theta(2)>
ns=2;
<sd,ns>=sform(dnum2,dden2);
c=sd(3,:);
n=10;
exec('extract.ab');
b=real(b);
sc=<a,b;c>;
<num,den>=tform(sc,ns)
for i=1:tm,u5(i)=5;end
<t,yls>=lsim(num,den,u5,.1);
<t,yhos>=lsim(numhos,denhos,u5,.1);
ycomp=<yhos yls>;
plot(t,ycomp)
return
```

Note that 'extract.ab' and 'roots' are identical to 'extract.ab;2' and 'roots' which were already presented as subroutines of the LEAST.SQUARES program. Therefore these are not repeated here.

'tau' - (the equivalent time delay tau is calculated by iteration in the frequency domain)

```
<o,d,p>=bode(numhos,denhos,.3,10,21);
<o,d1,p1>=bode(num,den,.3,10,21);
if abs(p(1)-p1(1)) > 180,...
    for i=1:21,p1(i)=p1(i)-360;end
pplot=<p p1>;
plot(o,pplot,'logx')
tau=nt;
diff=1.0;
```

```
while diff > 0,...
ssp1=0;...
ssp2=0;...
plos=p1;...
for i=1:21,plos(i)=plos(i)-57.29578*o(i)*tau;end,...
for i=1:21,ssp1=ssp1 + 0.01745*(p(i)-plos(i))**2;end,...
tau=tau + 0.001;...
plos=p1;...
for i=1:21,plos(i)=plos(i)-57.29578*o(i)*tau;end,...
for i=1:21,ssp2=ssp2 + 0.01745*(p(i)-plos(i))**2;end,...
diff=ssp1-ssp2;
pplot2=<p plos>;
plot(o,pplot2,'logx')
tau
return
```

'costf.time' - (calculates $cost_f$)

```
<o,dbhos,phhos>=bode(numhos,denhos,.3,10,21);
<o,dblos,phlos>=bode(num,den,.3,10,21);
if abs(phhos(1)-phlos(1)) > 180,...
      for i=1:21,phlos(i)=phlos(i)-360;end
for i=1:21,phlos(i)=phlos(i)-57.29578*o(i)*tau;end
cost=0;
for i=1:21,...
cost=cost+(dbhos(i)-dblos(i))**2 + 0.01745*(phhos(i)-phlos(i))**2;
costf=(20/21)*cost
dcomp=<dbhos dblos>;
pcomp=<phhos phlos>;
return
```

'costt.time' - (calculates $cost_t$)

```
<t,yhos>=lsim(numhos,denhos,u5,.1);
<t,ylos>=lsim(num,den,u5,.1);
costt=0;
for i=1:tm,...
costt=costt + (57.29578*yhos(i) - 57.29578*ylos(i))**2;end
costt=costt/tm;
return
```

The next program (LS.FLT) was used to conduct the least squares matching using the actual flight test (DAS) data. In this case the input vector "u" and the output vector "y" are not calculated from the HOS transfer function but must already exist

in the $MATRIX_x$ memory. Getting "u" and "y" from the aircraft's data tape into the $MATRIX_x$ memory was a trick in itself! To do this consult the local expert on the data acquisition system and computer system you're using!

The subroutines in LS.FLT are very similar to the subroutines already presented and are therefore presented below without explanation. Note that for the actual flight test matching, the HOS was not modeled in the frequency domain and therefore $cost_f$ is not calculated.

LS.FLT

```
INQUIRE TM 'INPUT MATCH TIME IN SEC:'
exec('ls.fltmat')
exec('roots.')
exec('costt.flt')
v=205;
cap=(omega**2)/4.5;
out=<lalpha gain zeta omega 0.000 cap costt>
return
```

```
 'ls.fltmat'

tm=tm*10
for i=3:tm,x(i-2,:)=<y(i-1) y(i-2) u(i-1) u(i-2)>;
for i=3:tm,capy(i-2,1)=y(i,1);
theta=x\capy
yout=x*theta;
dnum2=<theta(3) theta(4)>
dden2=<1 -theta(1) -theta(2)>
ns=2;
<sd,ns>=sform(dnum2,dden2);
c=sd(3,:);
n=10;
exec('extract.ab');
b=real(b);
sc=<a,b;c>;
<num,den>=tform(sc,ns)
```

```
um=u(1:tm,1);
<t,ylos>=lsim(num,den,um,.1);
yhos=y(1:tm,1);
ycomp=<yhos ylos>;
plot(t,ycomp)
return
```

```
'roots'
rd=root(den);
sigma=abs(real(rd(1)));
omega=abs(rd(1));
zeta=sigma/omega;
rn=root(num);
lalpha=-rn;
gain=num(1);
return
```

```
'costt.flt'
costt=0;
for i=1:tm,...
costt=costt + (57.29578*yhos(i) - 57.29578*ylos(i))**2;end
costt=costt/tm;
return
```

The final program presented is called DATA.SMOOTH and was used to smooth the flight test data. This was done by taking 50 samples/second and averaging every five data points to get 10 samples a second. The least squares program worked very well with only 10 samples/second but required smooth data. Therefore this program was used throughout the flight test matching.

```
DIM
INQUIRE M 'ENTER COLUMN LENGTH:'
PR=PITCHX01';
SF=LNGLSB01';
T=<0:.02:(M*.02)-.02>';
PLOT(T,SF,'CHART 5 95 55 100')
PLOT(T,PR,'CHART 5 95 0 45')
INQUIRE T1 'ENTER T1:'
INQUIRE T2 'ENTER T2:'
PR2=PR(T1/.02:T2/.02,1);
SF2=SF(T1/.02:T2/.02,1);
T2=<0:.02:T2-T1>';
PLOT(T2,SF2,'CHART 5 95 55 100')
PLOT(T2,PR2,'CHART 5 95 0 45')
```

```
DIM
INQUIRE M2 'ENTER COLUMN LENGTH (DIV BY 5):'
FOR I=1:(M2/5),...
   J=I*5;...
   U(I,1)=(SF2(J-4)+SF2(J-3)+SF2(J-2)+SF2(J-1)+SF2(J))/5;...
   Y(I,1)=(PR2(J-4)+PR2(J-3)+PR2(J-2)+PR2(J-1)+PR2(J))/5;END
T3=<0:.1:(M2/5-1)*.1>';
PLOT(T3,U,'CHART 5 95 55 100')
PLOT(T3,Y,'CHART 5 95 0 45')
ESF=U(1,1);
EPR=Y(1,1);
FOR I=1:(M2/5),...
   U(I,1)=U(I,1)-ESF;...
   Y(I,1)=-0.0174533*(Y(I,1)-EPR);END
PLOT(T3,U,'CHART 5 95 55 100')
PLOT(T3,Y,'CHART 5 95 0 45')
RETURN
```

APPENDIX C. SORTIE SUMMARY AND PROJECT PILOT EXPERIENCE

Twenty-five flights totaling 27.8 hours were flown in support of this project. A buildup approach was used for familiarizing the team with the task and test aircraft. Eight T-38A sorties were flown to practice the offset landing task. Five NT-33A HUD flights were then used for familiarization with the test aircraft and at the same time fullfill a TPS curriculum requirement. Lastly, twelve NT-33A data sorties were flown in direct support of this project.

TABLE C1

SORTIE SUMMARY

DATE	A/C	CREW	MISSION	HOURS
12 SEP 89	T-38	LINDSEY/RUNYON	OFFSET LAND	1.2
13 SEP 89	T-38	THOMAS/RUNYON	OFFSET LAND	1.2
13 SEP 89	T-38	BAUM/RUNYON	OFFSET LAND	1.2
15 SEP 89	T-38	LINDSEY/RUNYON	OFFSET LAND	1.1
18 SEP 89	T-38	THOMAS/RUNYON	OFFSET LAND	1.2
19 SEP 89	NT-33	THOMAS/EASTER	HUD EVAL	1.6
20 SEP 89	NT-33	THOMAS/EASTER	DATA 1	1.0
20 SEP 89	T-38	BAUM/RUNYON	OFFSET LAND	1.2
20 SEP 89	NT-33	BAUM/EASTER	HUD EVAL	1.4
21 SEP 89	NT-33	THOMAS/EASTER	DATA 2	0.9
21 SEP 89	NT-33	LINDSEY/EASTER	HUD EVAL	1.5
22 SEP 89	NT-33	BAUM/EASTER	DATA 3	0.8
22 SEP 89	NT-33	MANNING/EASTER	HUD EVAL	1.6
25 SEP 89	NT-33	LINDSEY/EASTER	DATA 4	1.0
25 SEP 89	NT-33	LIU/EASTER	HUD EVAL	1.7
25 SEP 89	T-38	MANNING/RUNYON	OFFSET LAND	1.0
26 SEP 89	NT-33	LINDSEY/EASTER	DATA 5	0.9
3 OCT 89	NT-33	BAUM/BALL	DATA 6	0.8
3 OCT 89	NT-33	THOMAS/BALL	DATA 7	0.8
4 OCT 89	NT-33	LINDSEY/BALL	DATA 8	0.9
4 OCT 89	NT-33	LINDSEY/BALL	DATA 9	1.0
5 OCT 89	NT-33	BAUM/BALL	DATA 10	0.8
10 OCT 89	NT-33	BAUM/BALL	DATA 11	0.9
10 OCT 89	NT-33	THOMAS/BALL	DATA 12	0.9
16 OCT 89	T-38	LIU/RUNYON	OFFSET LAND	1.2

TOTAL SORTIE COUNT

	SORTIES	HOURS
T-38 TRAINING	8	9.3
NT-33 TRAINING	5	7.8
NT-33 DATA	12	10.7
	TOTAL HOURS	27.8

TABLE C2

PROJECT PILOT EXPERIENCE

Pilot	Aircraft	Hours
A	C-141	2500
B	F/RF-4	1000
	T-39	50
C	B-52	2200
	T-37	150

APPENDIX D. AIRCRAFT DESCRIPTION AND TEST INSTRUMENTATION

The NT-33A variable stability airplane, shown in Figure D1, is a T-33 jet trainer modified with a Variable Stability System. The VSS can be divided into two independent parts. The first part, the variable feel system, provides a variety of stick and rudder pedal forces, gradients, and displacements. The variable feel is provided by disconnecting the elevator, aileron, and rudder controls in the front cockpit from their respective control surfaces and connecting the controls to separate servomechanisms. The second part of the VSS is the response feedback flight control system. This part augments the normal T-33 dynamics to represent those of the vehicle being simulated.

Figure D1. NT-33A Variable Stability Aircraft

The augmentation is accomplished by connecting the elevator, aileron, and rudder control surfaces to individual servos. These individual servos can be driven by a number of different inputs, such as the aircraft's artificial feel system (pilot's commands, position or force), attitude and rate gyros, accelerometers, dynamic pressure pickups, angle of attack vane and sideslip

probe. This arrangement, through a response-feedback system, allows the normal T-33 derivatives to be augmented to simulate the handling qualities of existing or hypothetical aircraft. A block diagram of the VSS is shown in Figure D2.

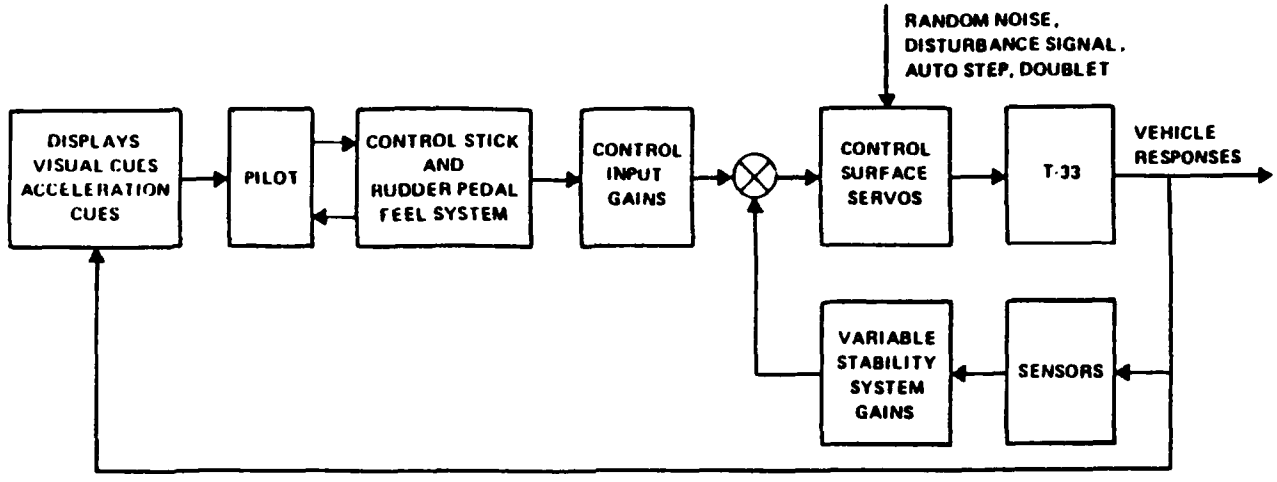

Figure D2. Variable Stability NT-33A Block Diagram

The original T-33 nose section has been replaced with the larger nose of an F-94 to provide the volume required for the electronic components of the response-feedback system and recording equipment. The physical layout of the control system is shown in Figure D3. Each control surface has an electro-hydraulic position servo which is actuated by inputs from the VSS. The servos operate in parallel with the normal T-33 control surface's actuating mechanisms. Each of the surface position actuators has a hydraulic limiting circuit which limits the maximum hinge moment which can be generated by the flight control system. The rear cockpit controls have a direct mechanical connection to the aircraft control surfaces at all times.

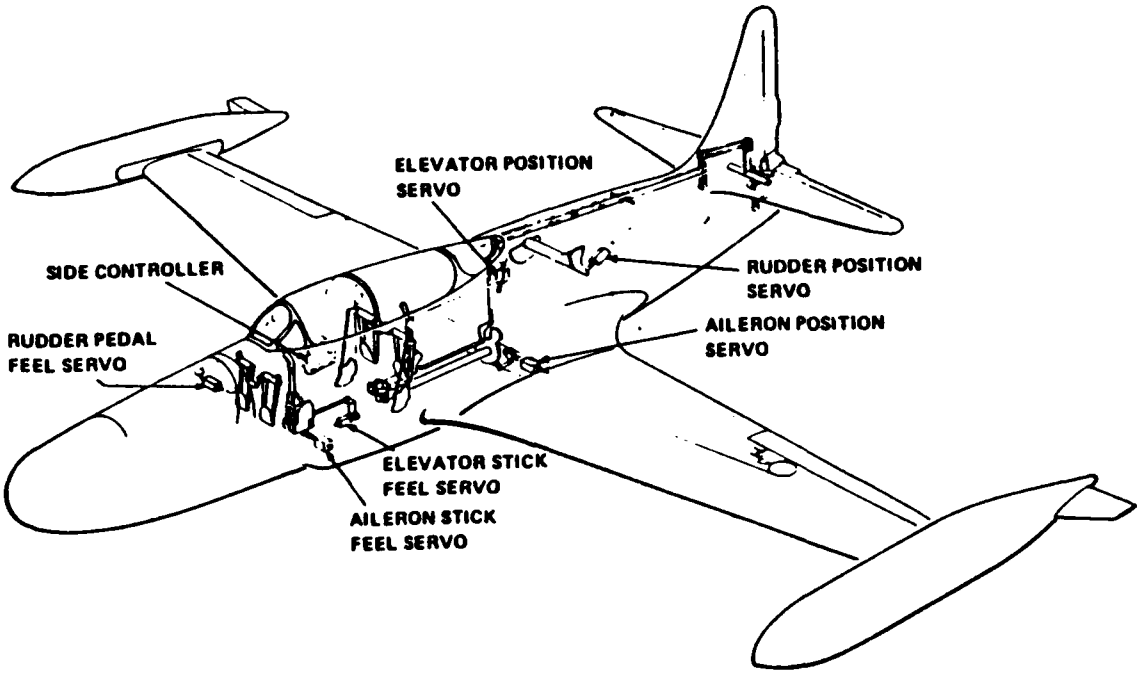

Figure D3. Control System Layout

NT-33 SAFETY FEATURES

The primary safety feature in the airplane is the safety pilot; however, the NT-33A also has numerous safety provisions designed into the variable stability equipment.

Control Interlock System: The control buttons and switches for the various functions of the VSS are wired so that the proper sequence of operation of these controls must be observed to energize the various parts of the VSS. No action will result from a button or switch activated out of sequence. For example, interlocking circuits prevent servo engagement prior to auto balance engage.

Automatic Safety Trips: The automatic safety trip monitors the servovalve amplifier error signals and the normal and lateral accelerometer output signals. If these signals exceed preset values, the VSS is automatically shut off. Safety trip accelerometer limits have been set as follows:

a. n_z Pushover (- 0.3g on the g meter)

b. n_z Pullout (+ 4.8g on g meter)

c. n_y ($\pm$ 0.25g)

Audio-visual VSS Shut-off Warning System: When the VSS has been disengaged either automatically or manually, red lights will flash in both cockpits and a "beep, beep" will be heard in the interphone.

Special Aircraft Limitation: The variable stability NT-33A is limited to 375 KIAS with a never exceed speed of 400 KIAS.

Special Pilot Emergency Procedures: In addition to normal NT-33A emergency procedures, the following pertain specifically to the variable stability NT-33A:

-Manual VSS trip: The project pilot can manually disengage the VSS from the control surfaces and return control of the aircraft to the safety pilot. Disengage switches are located on both the centerstick and the sidestick.

-In the event of safety pilot incapacitation, the project pilot can fly the aircraft back to the base via his fly-by-wire controls with normal T-33 characteristics. This is accomplished by actuating the red guarded safety trip bypass switch located on the left side of the VSS engage panel and sequentially depressing the adjacent four buttons starting from the left. Subsequent buttons are pressed after the light below the previously pressed button is lit.

-If a feel system hardover should occur, the project pilot can activate the feel system hydraulic bypass switch and move the control stick out of the way to ensure non-interference during ejection.

TABLE D1

NT-33A DIGITAL TAPE PARAMETERS

DIGITAL CHANNEL NUMBER	RECORDED VARIABLE	ENGINEERING UNITS
1	Pressure Altitude	feet
2	Normal Acceleration	g's
3	Velocity (Indicated)	knots
4	Pitch Rate	degrees/second
5	Pitch Angle	degrees
6	Yaw Rate	degrees/second
7	Elevator Stick Deflection	inches
8	Angle of Sideslip	degrees
9	Event Mark	N/A
10	Radar Altitude	feet
11	Pitch Error	degrees
12	Roll Rate	degrees/second
13	Roll Angle	degrees
14	Longitudinal Acceleration	g's
15	Roll Error	degrees
16	Elevator Deflection	degrees
17	Lateral Acceleration	g's
18	Elevator Stick Force	pounds
19	Vertical Velocity	feet/second
20	Rudder Deflection	degrees
21	Total Aileron Deflection	degrees
22	Change in Heading	degrees
23	Lateral Stick Deflection	inches
24	Angle of Attack	degrees
25	Aileron Stick Force	pounds
26	Rudder Pedal Deflection	inches
27	Rudder Pedal Force	pounds
28	Time Rate of AOA Change	degrees/second

APPENDIX E. AIRCRAFT CONFIGURATION IDENTIFICATION

The plots in this appendix demonstrate the fidelity between the computer generated data and the actual flight test data. That is, these plots show how close the theoretical data (i.e. the estimate of how the aircraft will fly) agrees with how the aircraft actually flies. This is important since the prediction of flying qualities and the verification of the Least Squares LOES program were dependent on the analytical data.

The CALSPAN Corporation accomplished configuration verifications for the three baseline configurations (1-1, 2-1, and 3-1). These verifications are shown in Figures E1-E3. The first plot on these pages shows the theoretical input (δ_e in degrees) compared to the actual input (F_s in pounds). The next two plots show the corresponding theoretical and actual responses in pitch rate and angle of attack.

The remaining configurations were verified as part of the flight test program and are shown in Figures E4-E16. The first plot in these figures shows the actual stick force input. The second plot shows the corresponding actual pitch rate output compared to the theoretical pitch rate output. The theoretical output in these figures was computed using the actual input. This was possible because $MATRIX_x$ (31) can accept arbitrary inputs. Note that the agreement between the theoretical and actual aircraft responses was very good for both the CALSPAN and $MATRIX_x$ verifications. This indicates that the analytical models were adequate.

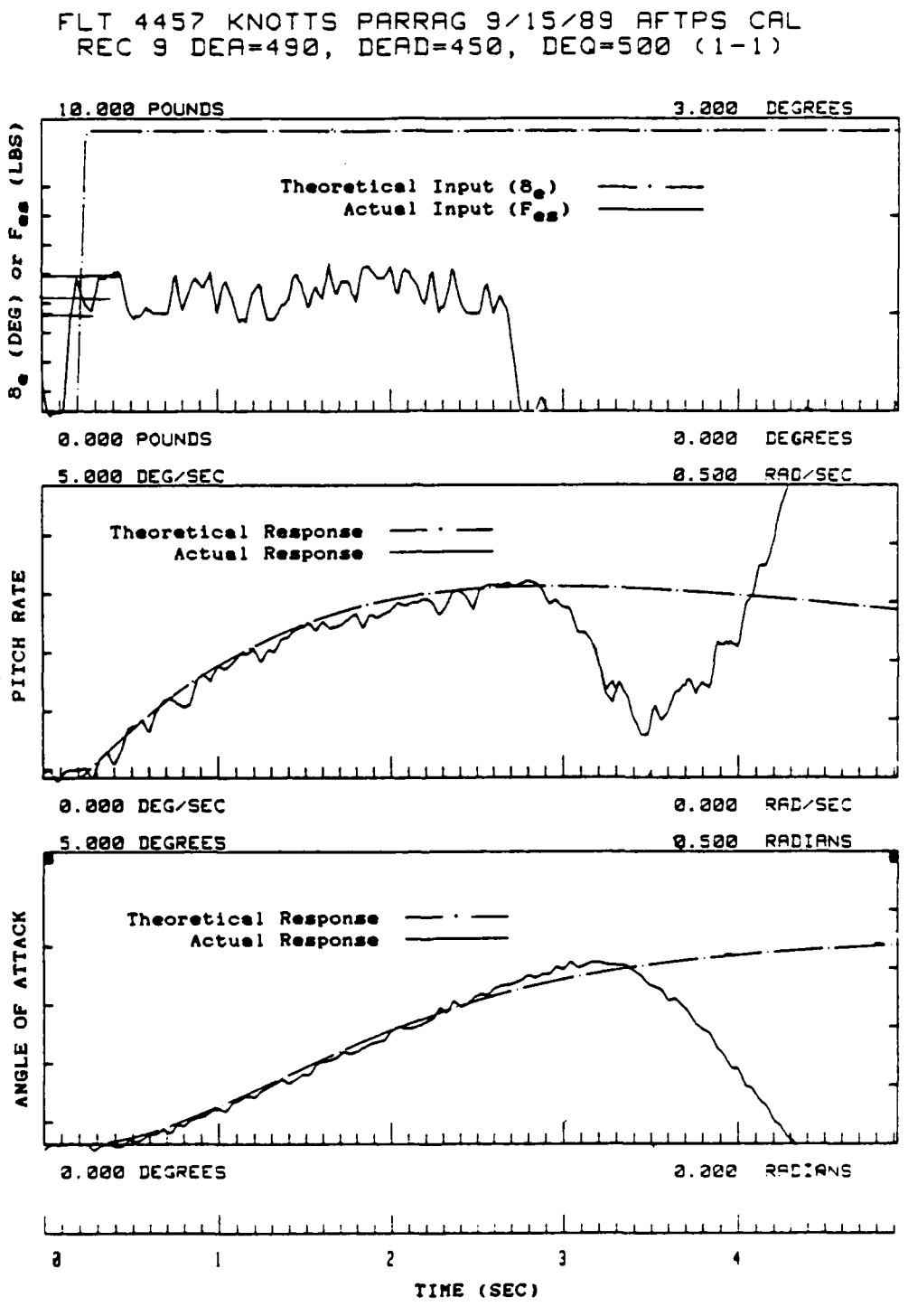

Figure E1. System Verification by CALSPAN - Configuration 1-1

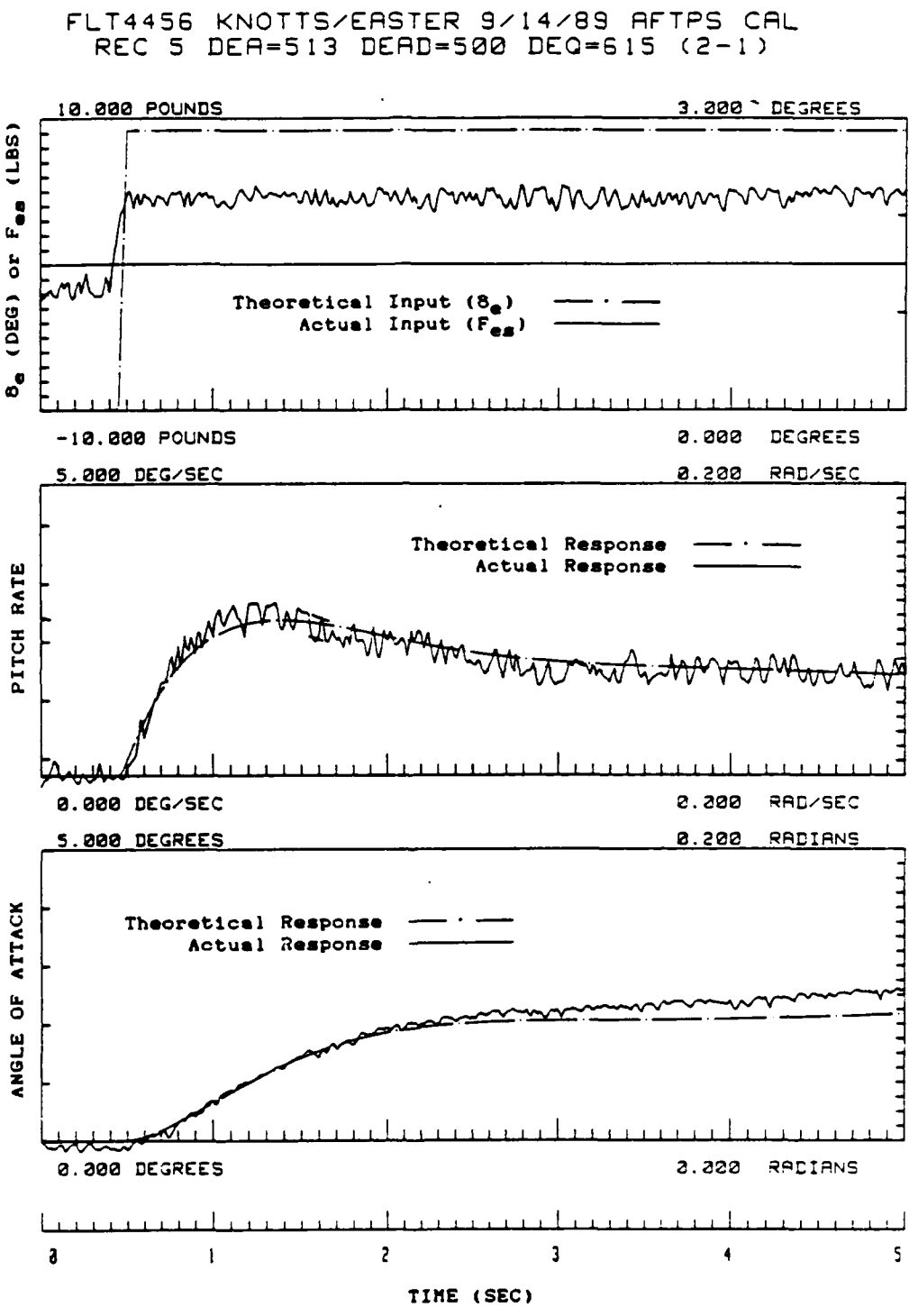

Figure E2. System Verification by CALSPAN - Configuration 2-1

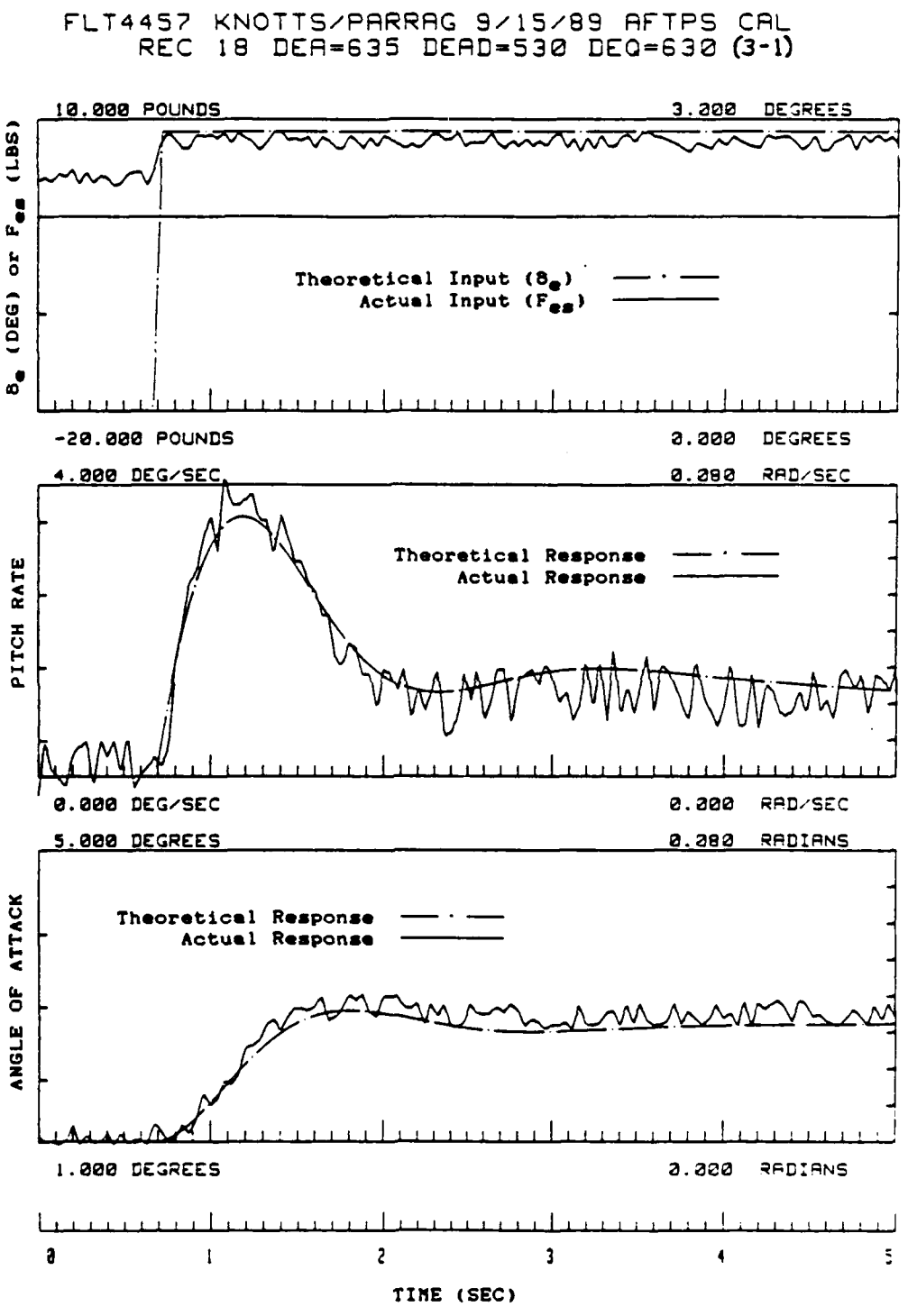

Figure E3. System Verification by CALSPAN - Configuration 3-1

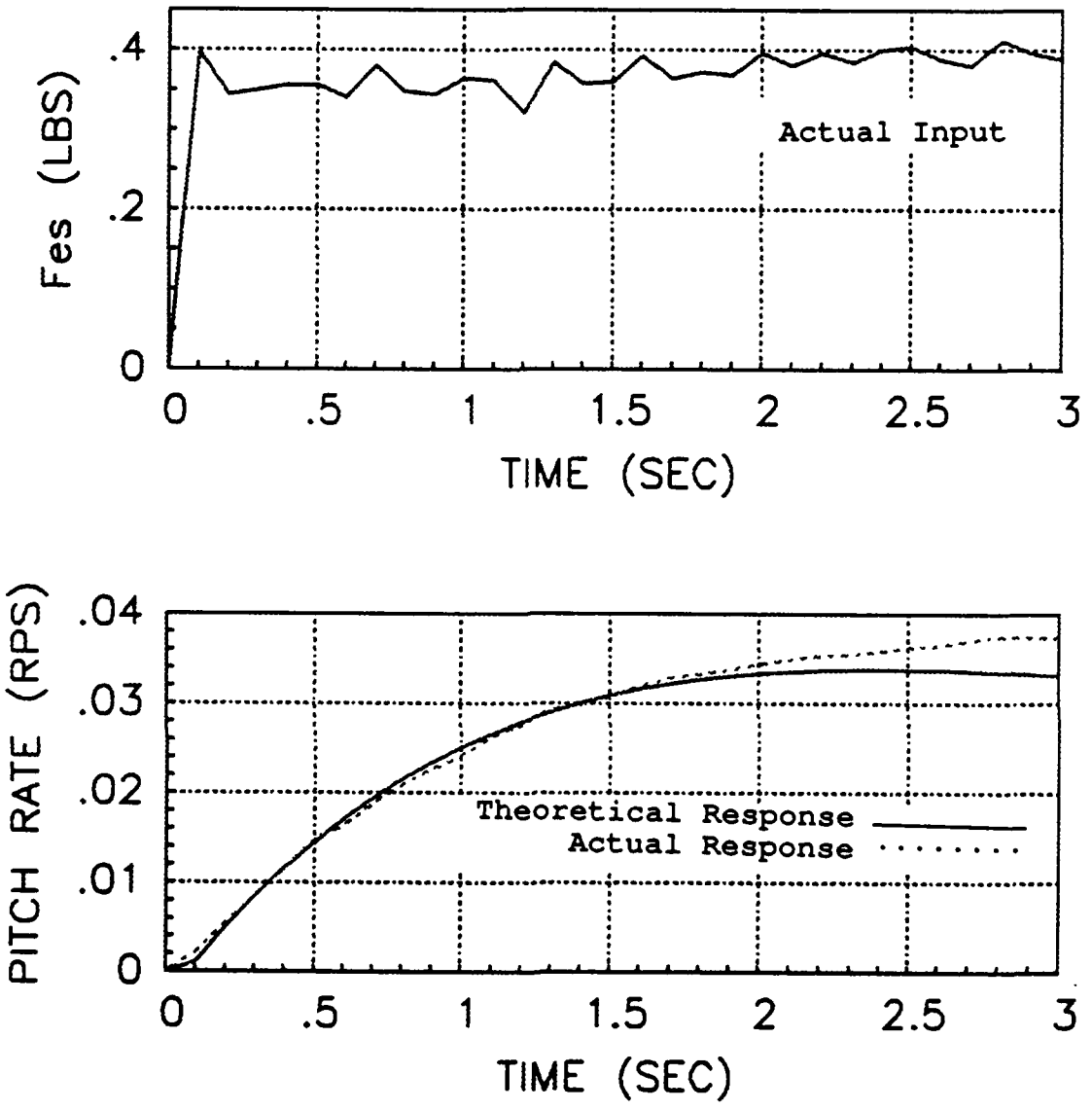

Figure E4. System Verification - Configuration 1-1

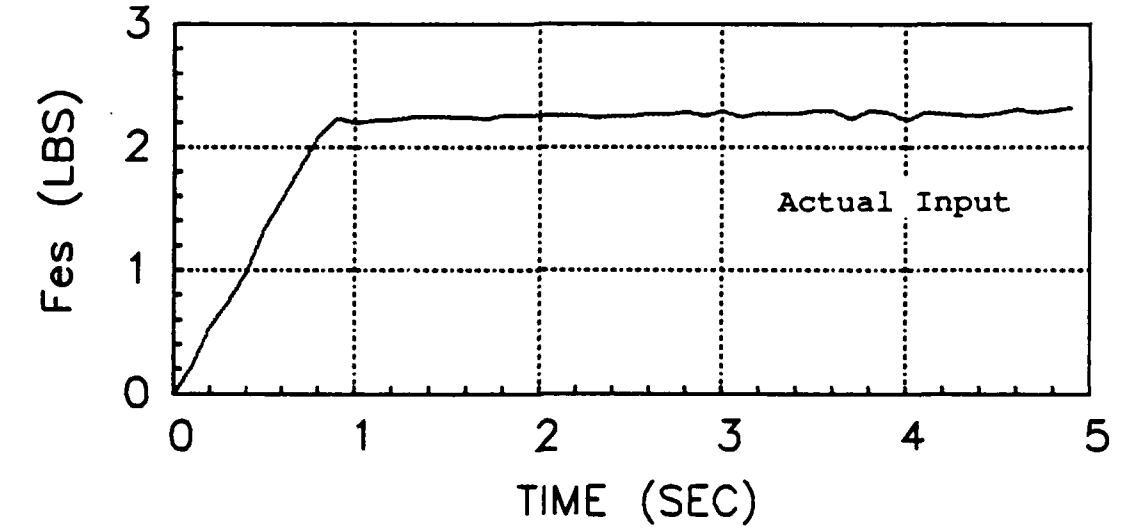

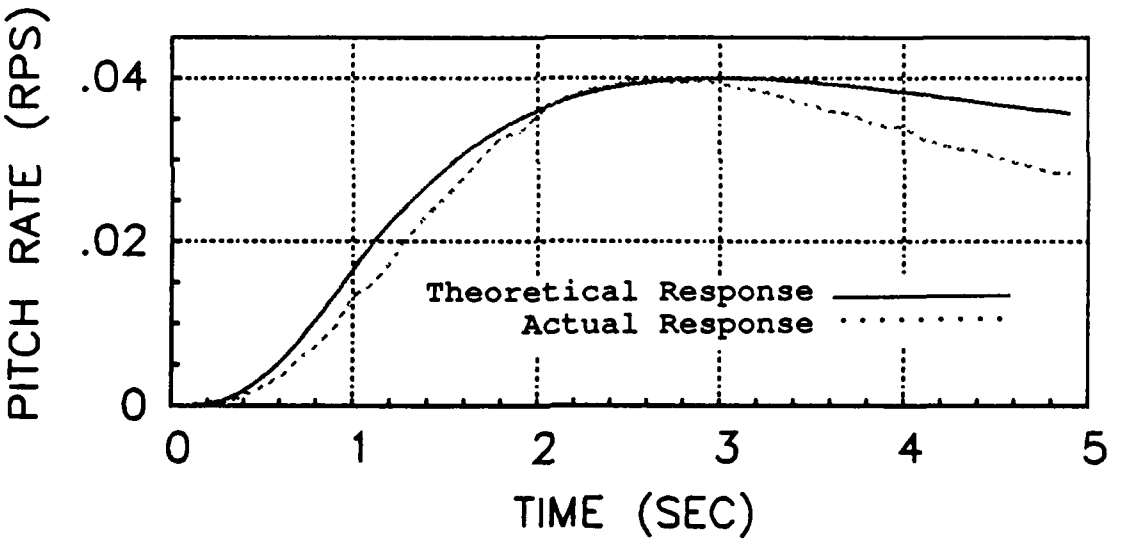

Figure E5. System Verification - Configuration 1-3

Configuration 1-10 was not flown in the landing evaluation because it was highly uncontrollable at altitude. Therefore, there was no data collected for system verification

Figure E6. System Verification - Configuration 1-10

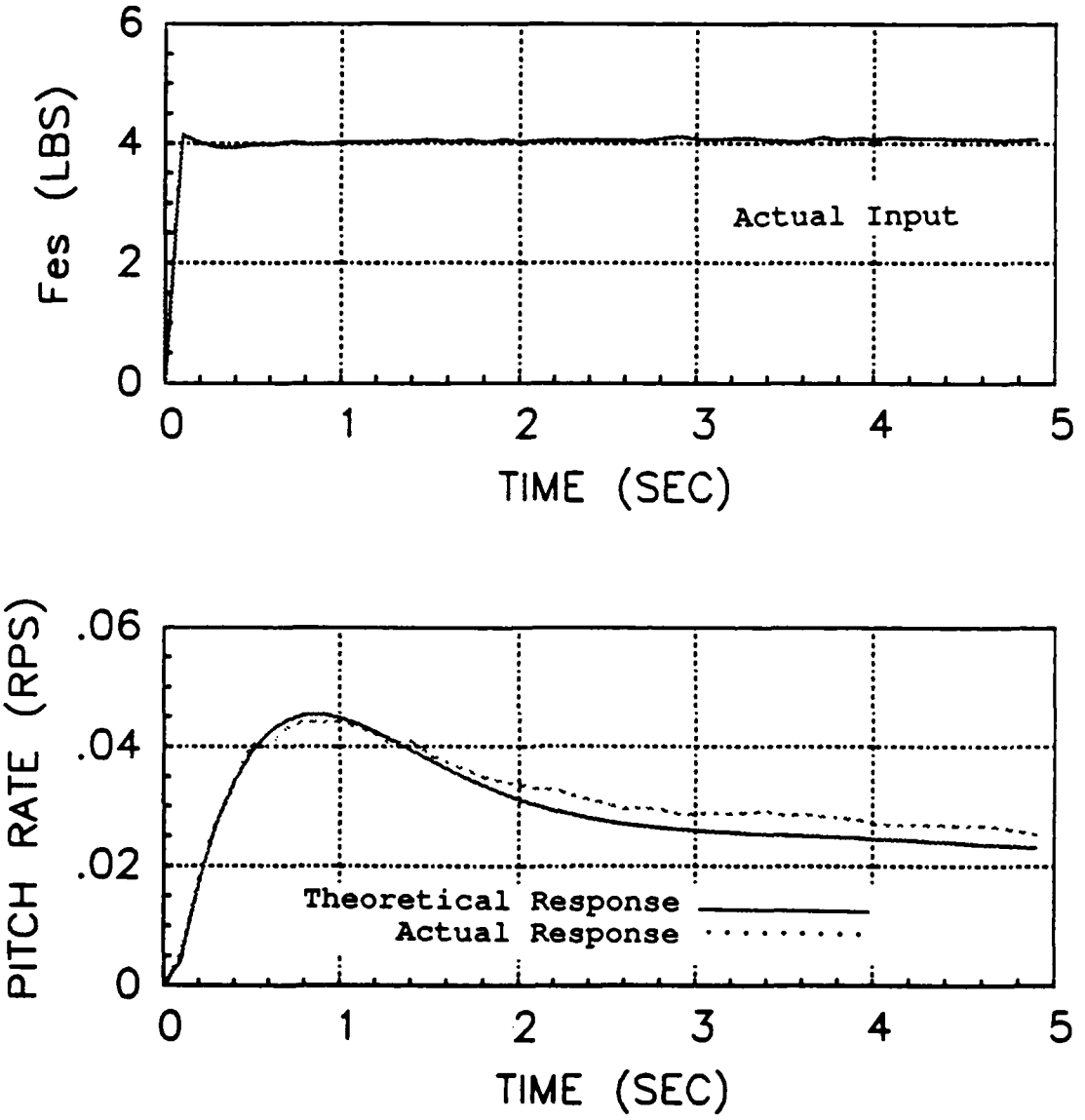

Figure E7. System Verification - Configuration 2-1

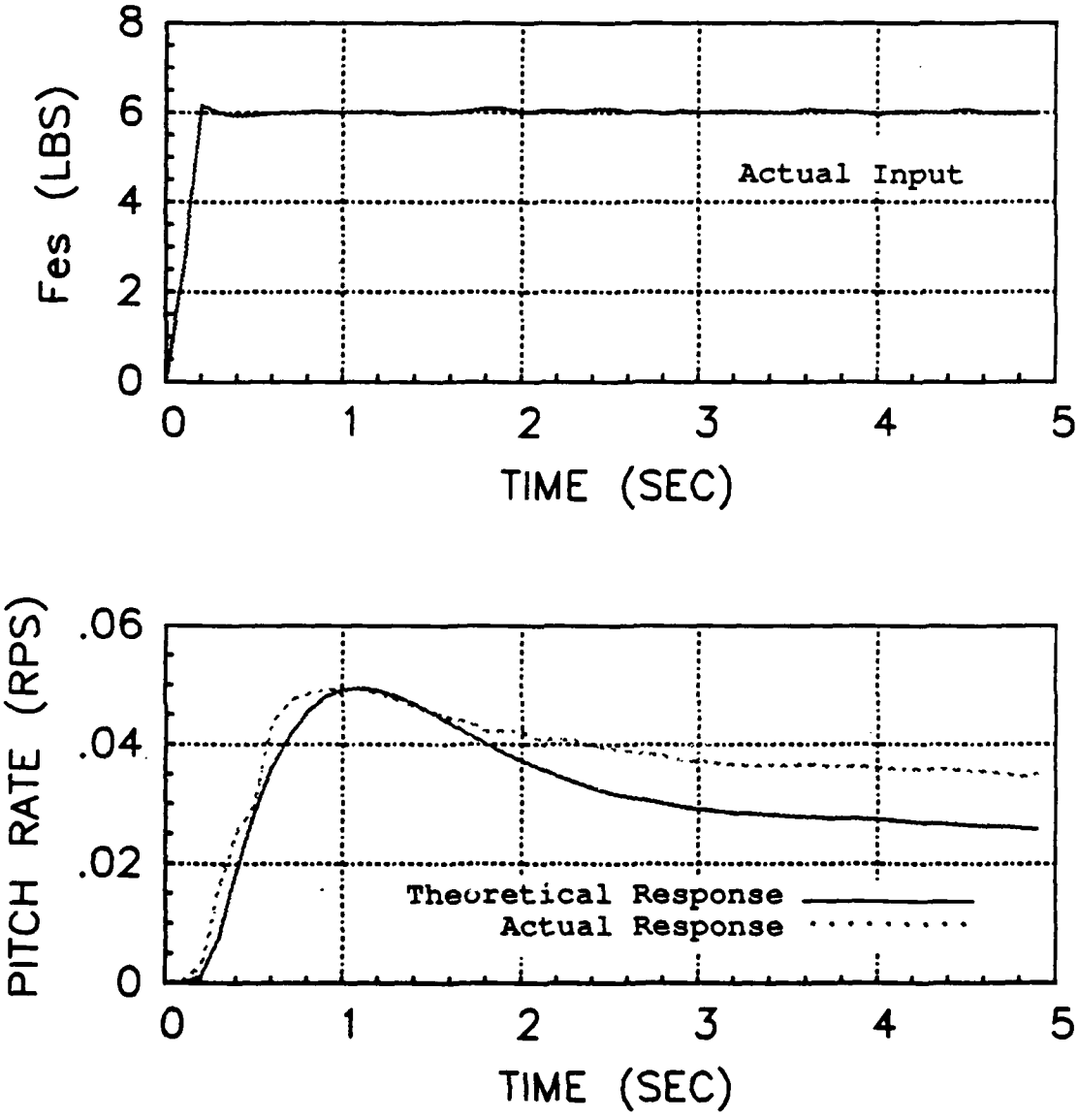

Figure E8. System Verification - Configuration 2-D

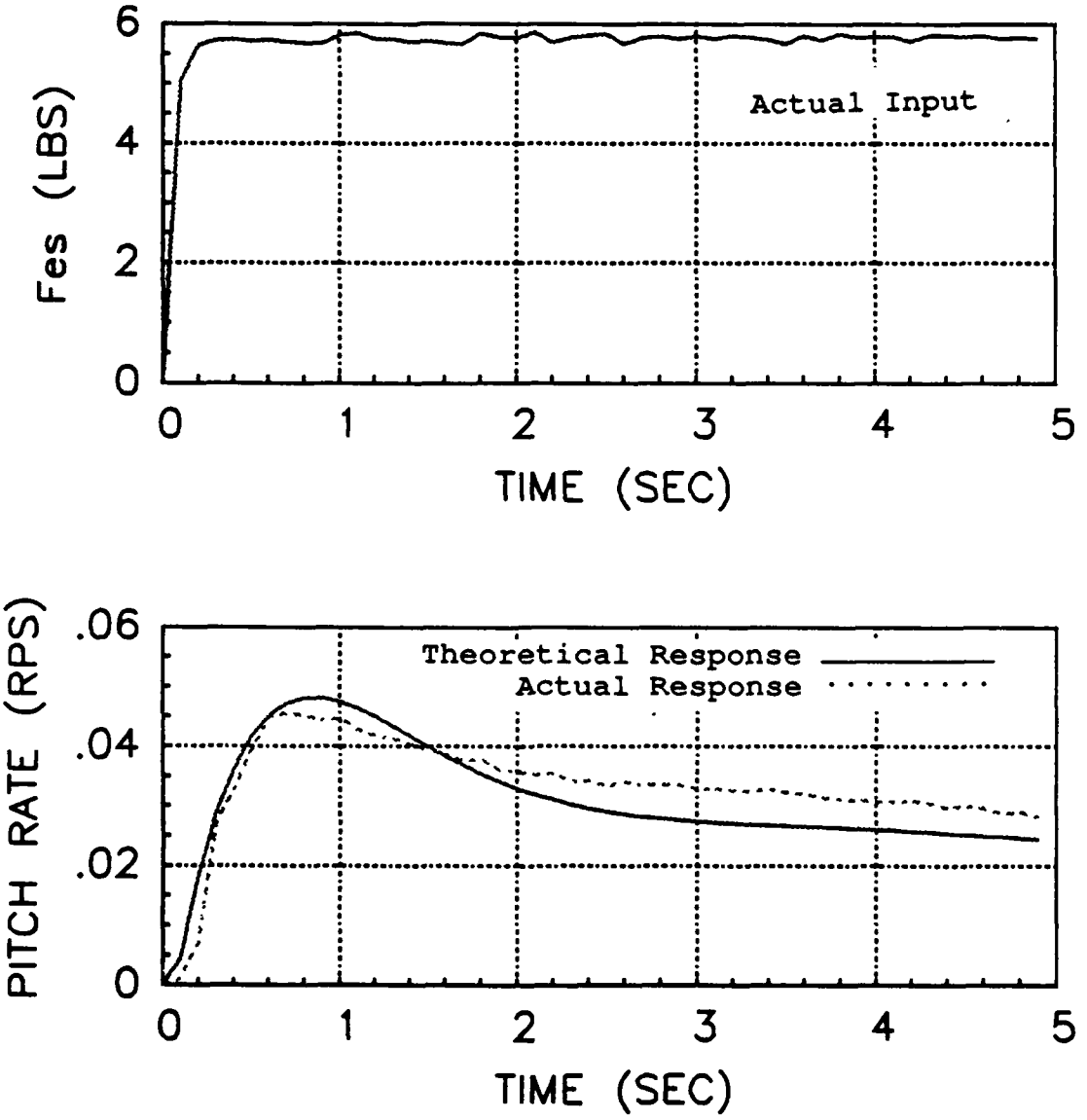

Figure E9. System Verification - Configuration 2-2

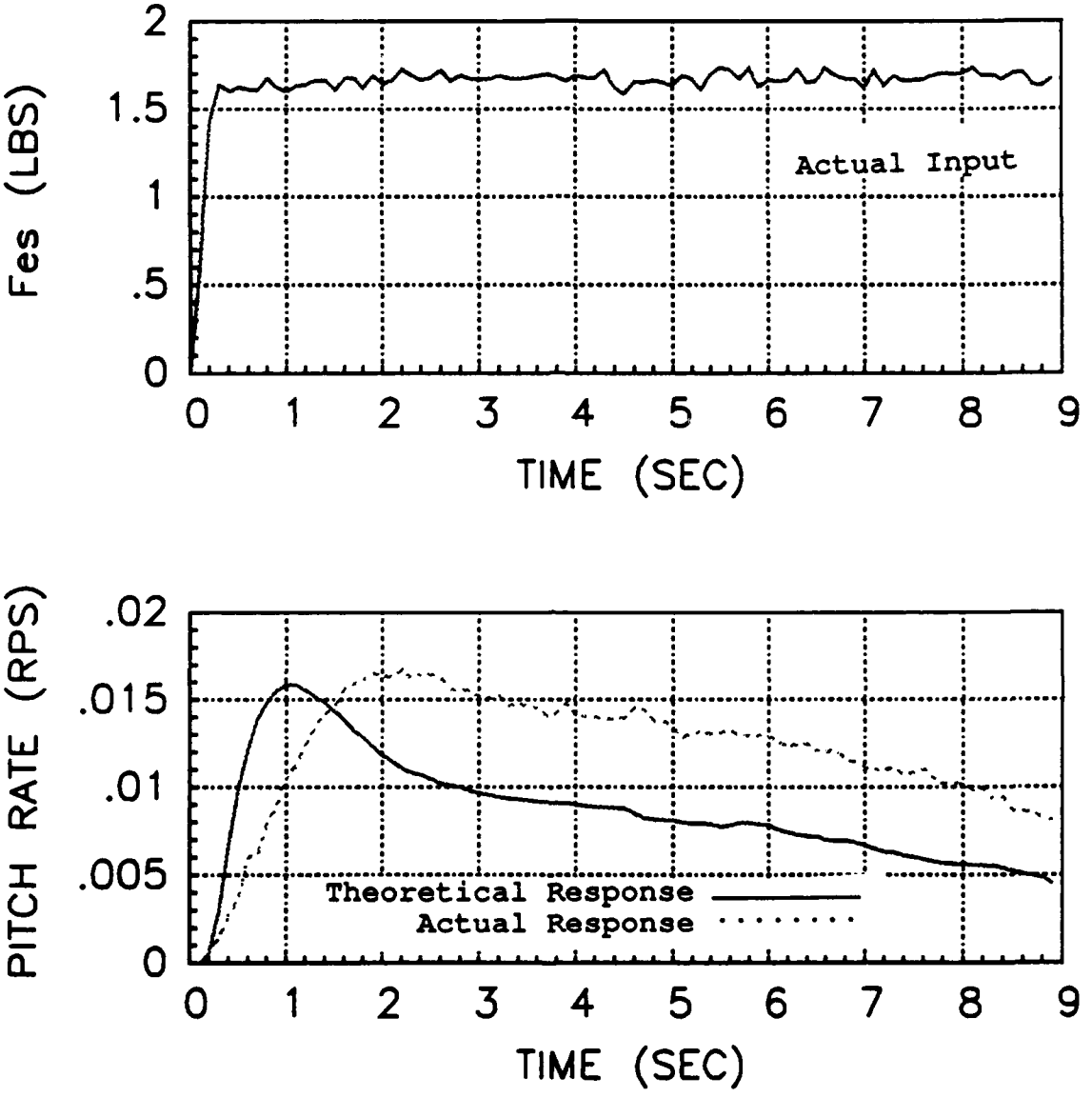

Figure E10. System Verification - Configuration 2-5

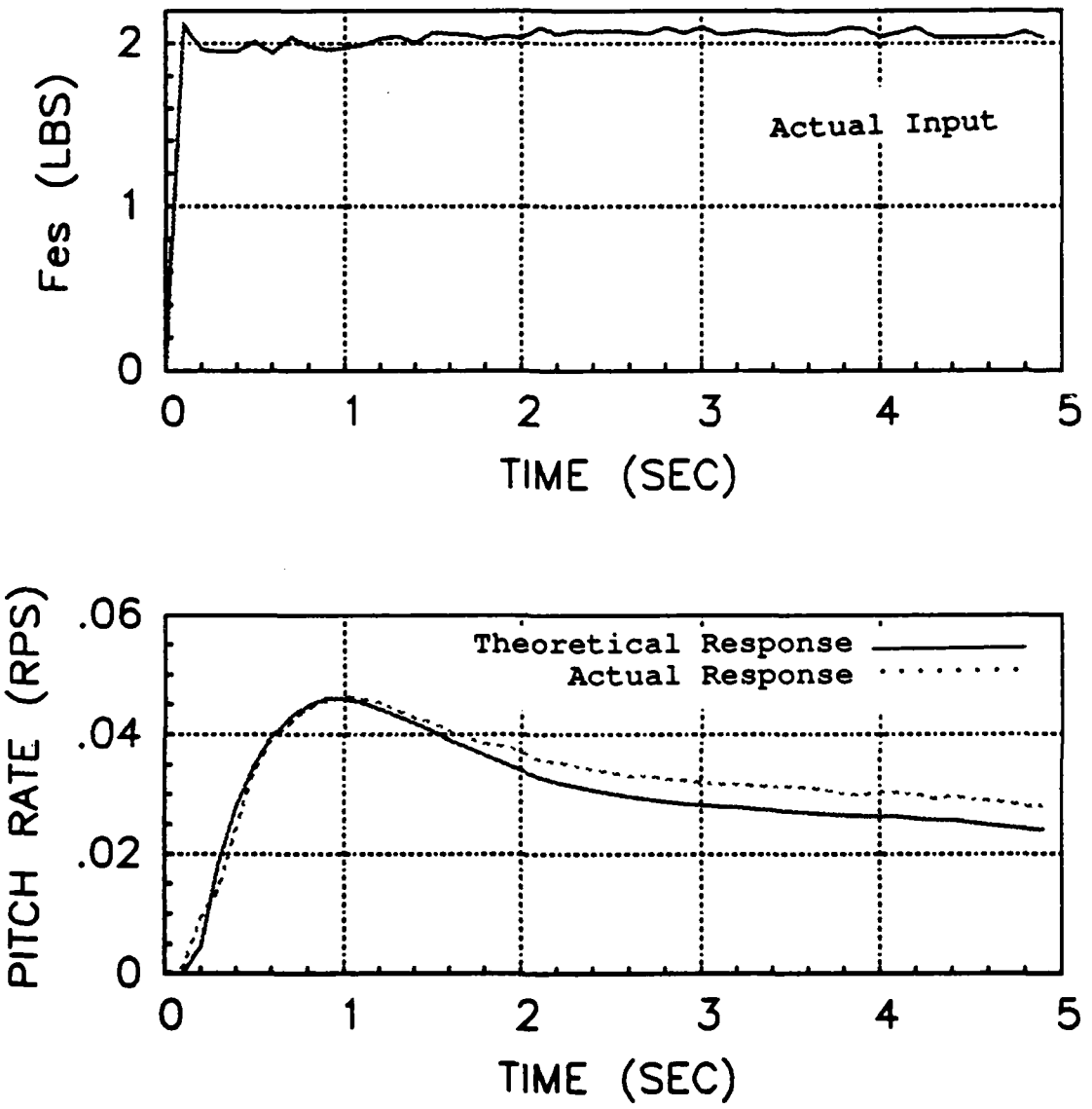

Figure E11. System Verification - Configuration 2-7

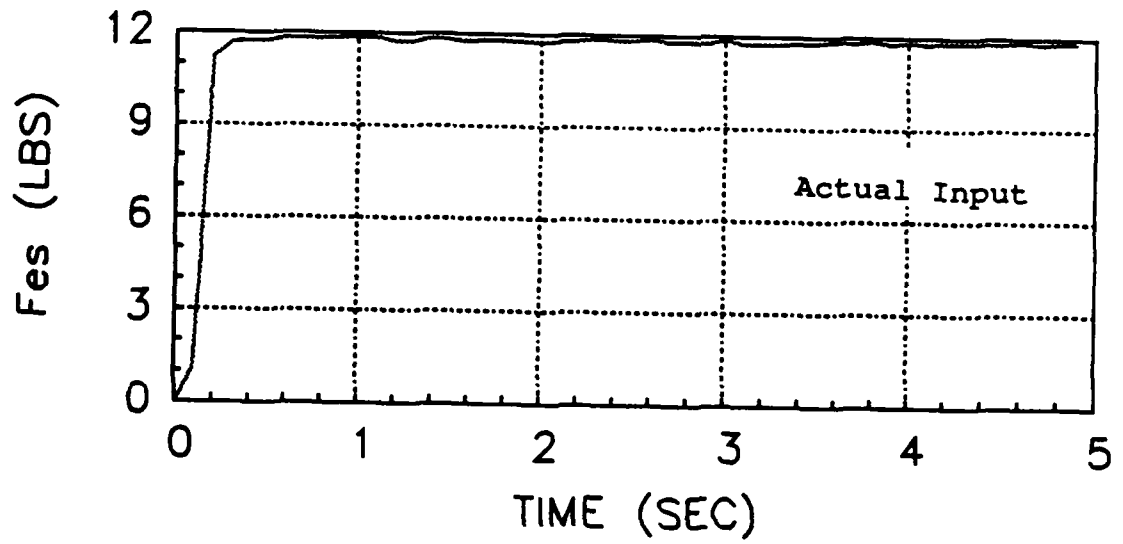

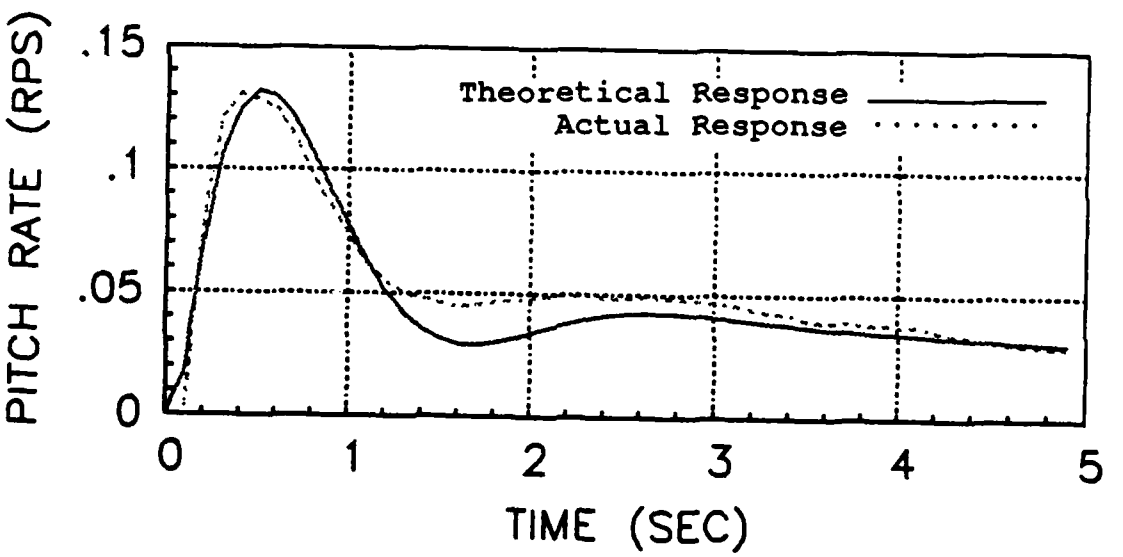

Figure E12. System Verification - Configuration 3-1

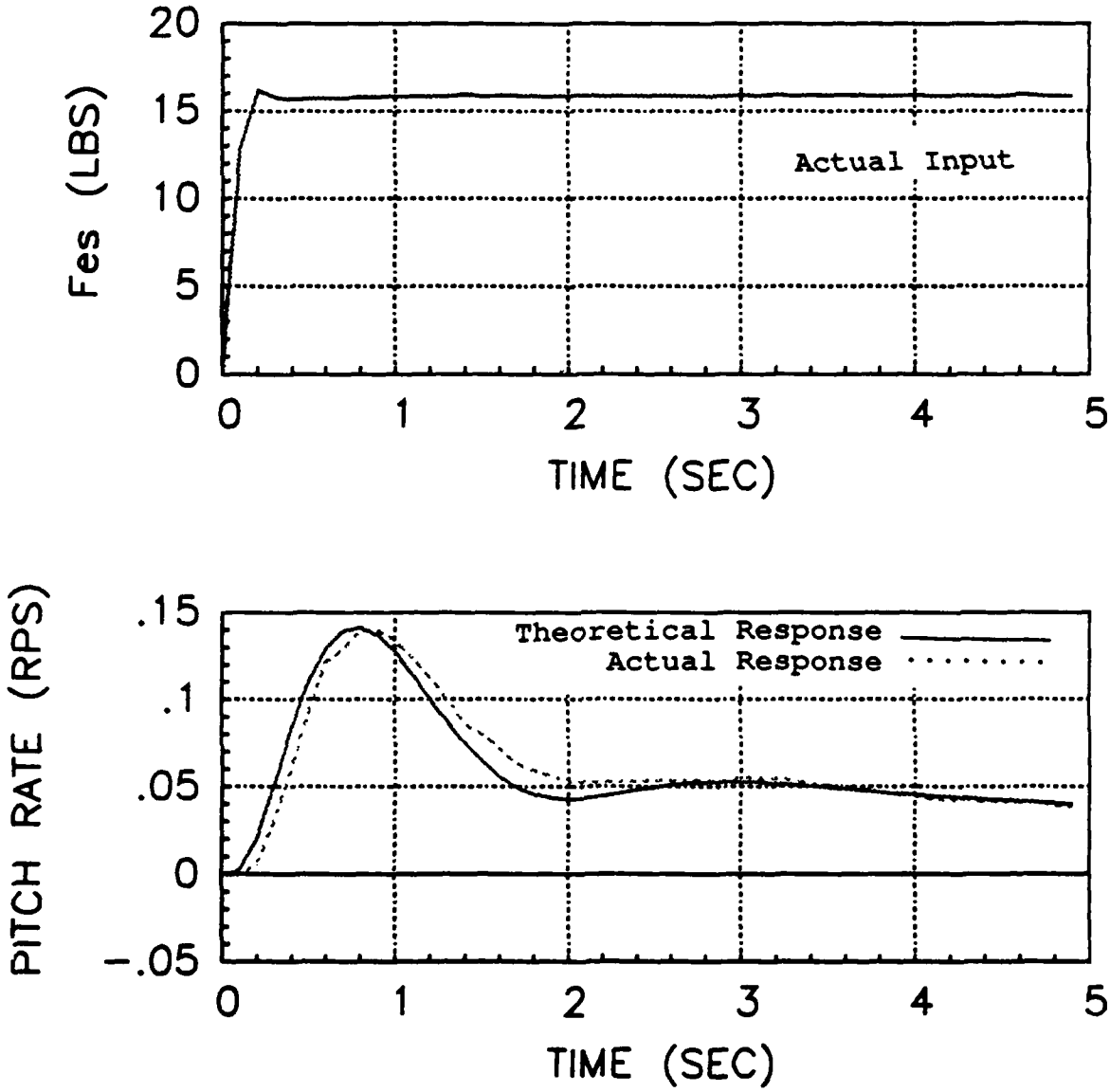

Figure E13. System Verification - Configuration 3-3

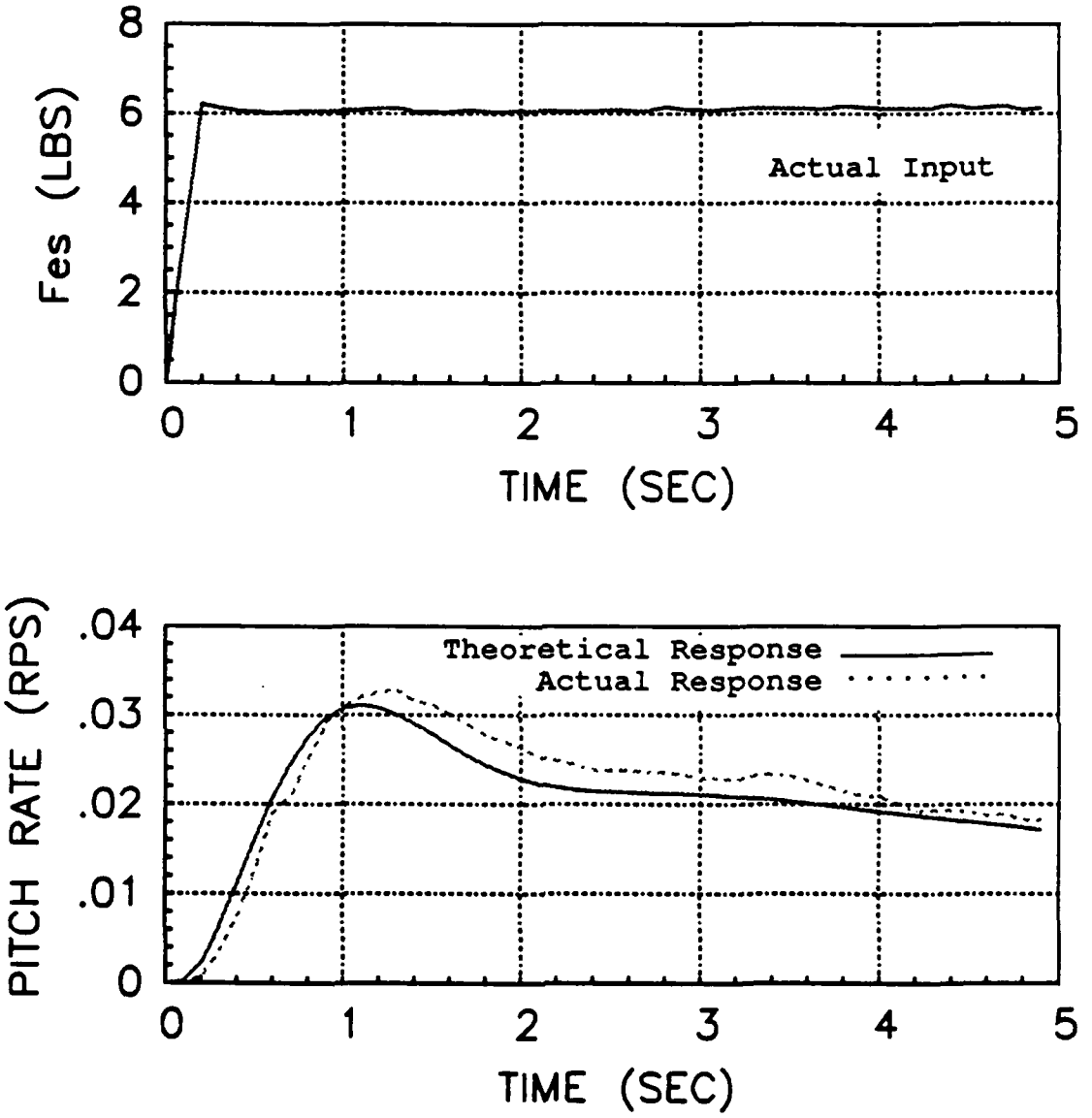

Figure E14. System Verification - Configuration 3-5

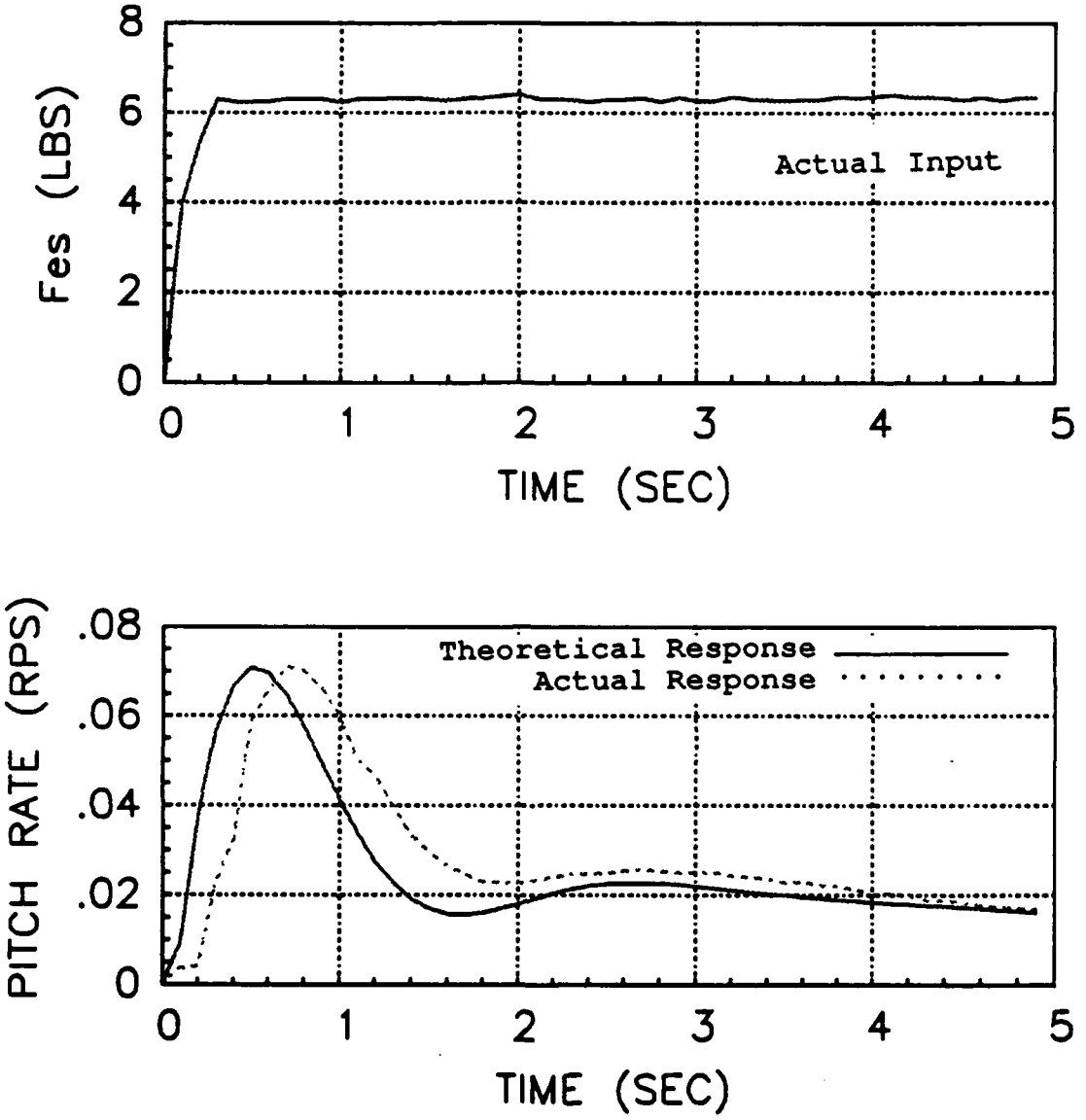

Figure E15. System Verification - Configuration 3-6

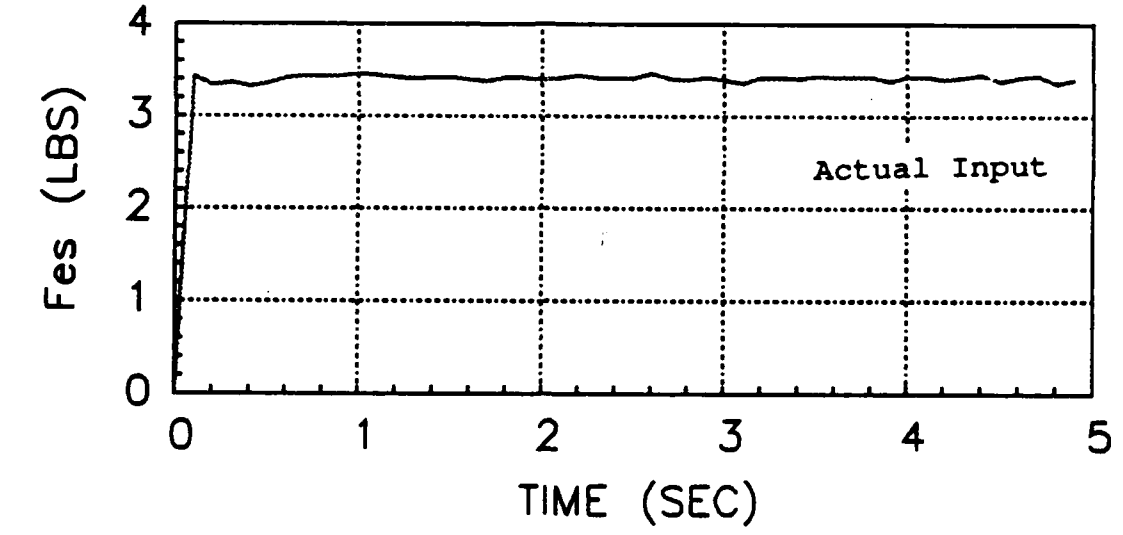

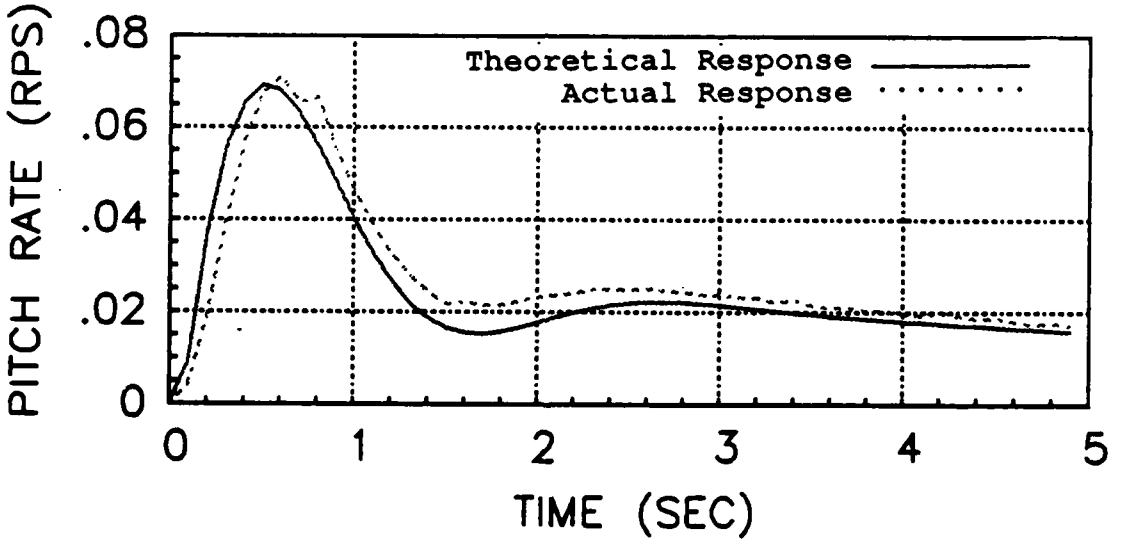

Figure E16. System Verification - Configuration 3-8

APPENDIX F. AIRCRAFT PARAMETERS AND STABILITY DERIVATIVES

This appendix contains the NT-33A longitudinal and lateral parameters, feel system and actuator parameters, and stability derivatives. Table F1 shows the longitudinal and lateral dynamics. Note that ω_{sp} and ζ_{sp} were varied to produce the different flying qualities. The only other variable between configurations was the pre-filter dynamics (shown in Chapter V, Table VIII). Table F1 also shows the feel system and actuator dynamics which were held constant throughout the flight test program. Table F2 shows the stability derivatives for the three baseline configurations (1-1, 2-1, and 3-1).

TABLE F1

NT-33A PARAMETERS

PARAMETER	VALUE
ω_{nsp} (rad/sec)	variable
ζ_{sp}	variable
n/α (g/rad)	4.50
$1/T_{\theta 2}$ (1/sec)	0.70
ω_{np} (rad/sec)	0.17
ζ_p	0.15
$1/T_{\theta 1}$ (1/sec)	0.08
ω_{nd} (rad/sec)	1.30
ζ_d	0.20
φ/β	1.50
τ_r (sec)	0.30
F_{es}/in (lbs/in)	6.50
F_{as}/in (lbs/in)	3.00

Feel systems: $\dfrac{A}{s^2 + 2(.6)(26)s + 26^2}$ (in/lb)

Elevator: A = 84.50
Aileron: A = 169.00
Rudder: A = 11.47

Actuators: $\dfrac{75^2}{s^2 + 2(.7)(75)s + 75^2}$ (deg/in)

Table F2

NT-33A Flight Test Stability Derivatives

Parameter	1-1	2-1	3-1
ω_{sp}	1.00	2.00	3.20
ζ_{sp}	0.75	0.75	0.50
X_u	-0.041	-0.041	-0.041
X_w	0.11	0.11	0.11
X_q	0	0	0
X_{δ_e}	0.0032	0.0032	0.0032
Z_u	-0.25	-0.25	-0.25
Z_w	-0.74939	-0.77925	-0.87625
Z_q	0.0	0.0	0.0
Z_{δ_e}	1.1	1.1	1.1
M_u	0.0	0.0	0.0
M_w	-0.002134	-0.01128	-0.04098
M_q	-0.75061	-2.22075	-2.32375
M_{δ_e}	0.33685	0.33685	0.33685
θ_0	4.5	4.5	4.5

APPENDIX G. LEAST SQUARES LOES MATCHING RESULTS

This appendix contains the Least Squares matching results from the flight test program. The analytical (pre-flight) results are shown in Figures G1-G13. These results were obtained using computer generated HOS data based on the known NT-33A dynamics. The HOS and LOES time responses were then matched using the Least Squares program. The first plot on each page shows a comparison between these time responses. The next two plots show a comparison between the HOS and LOES frequency responses. The corresponding LOES parameters and cost functions are tabulated at the bottom of each page. Also, the predicted handling quality level (based on MIL-STD-1797 guidance for equivalent parameters) is listed for each configuration.

The flight test results (Figures G14-G25) differ from the analytical results in that the HOS pitch rate response was taken from actual flight test data instead of computer generated data. The Least Squares program was then used to match the HOS and LOES time responses (shown on the first plot for each configuration). The next two plots show how the "actual" time delay (referred to as TD to distinguish it from equivalent time delay τ_e) was measured. The frequency responses (and therefore τ_e) were not measured during the actual flight test program. A detailed comparison between the analytical and flight test results is given in Chapter V.

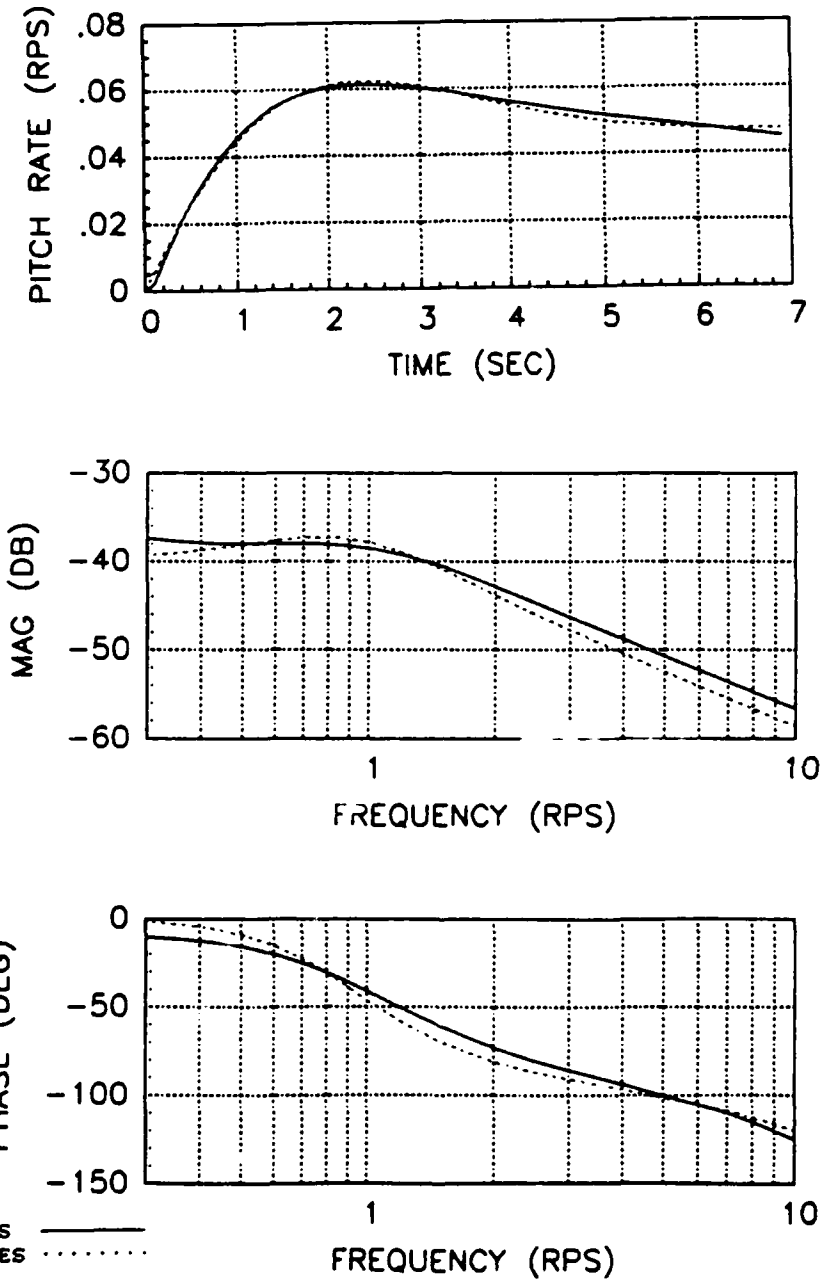

CONFIG	LEVEL	$1/T_{\theta 2}$ (1/sec)	K_θ (rps/lb)	ζ_{sp}	ω_{sp} (rps)	τ_θ (sec)	CAP (1/gsec)	$cost_f$	$cost_t$
1-1	1	0.708	0.012	0.599	0.922	0.056	0.189	45.37	0.005

Figure G1. Least Squares LOES Matching Results (Analytical Data)
Configuration 1-1

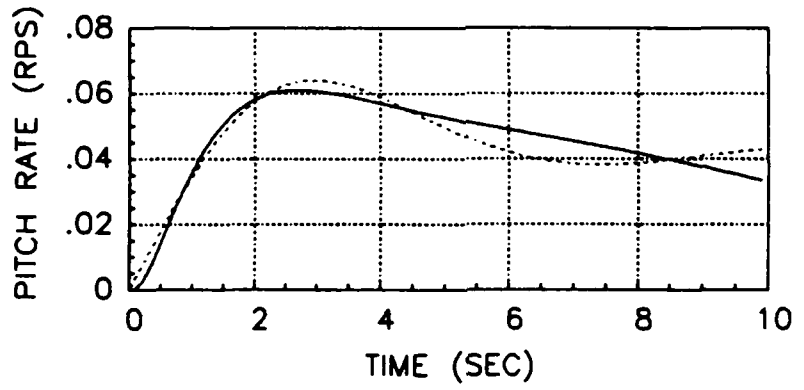

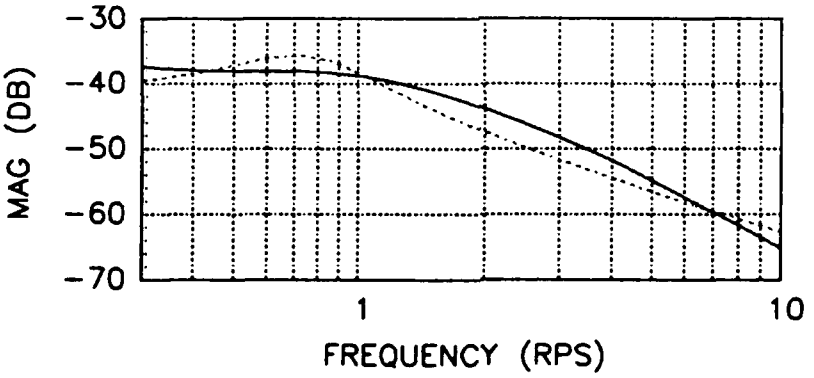

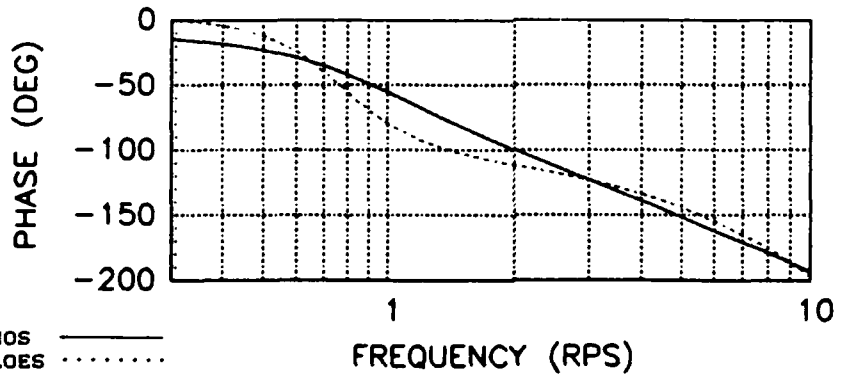

CONFIG	LEVEL	$1/T_{\theta 2}$ (1/sec)	K_θ (rps/lb)	ζ_{sp}	ω_{sp} (rps)	τ_θ (sec)	CAP (1/gsec)	$cost_f$	$cost_t$
1-3	2	0.706	0.007	0.396	0.769	0.185	0.131	156.25	0.062

Figure G2. Least Squares LOES Matching Results (Analytical Data)
Configuration 1-3

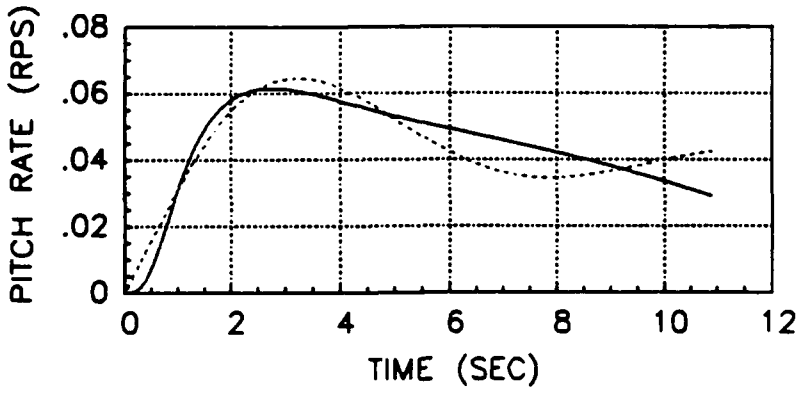

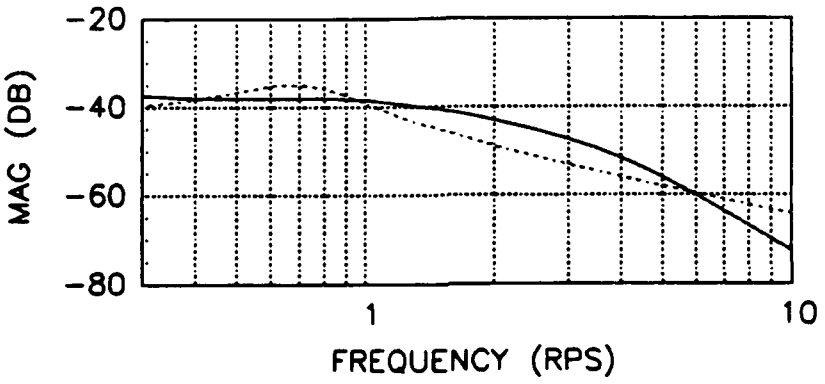

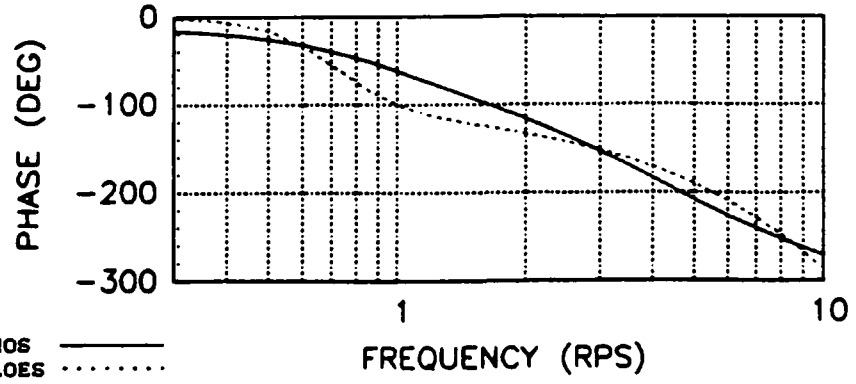

HOS ———
LOES .....

CONFIG	LEVEL	$1/T_{\theta 2}$ (1/sec)	K_θ (rps/lb)	ζ_{sp}	ω_{sp} (rps)	τ_θ (sec)	CAP (1/gsec)	$cost_f$	$cost_t$
1-10	3	0.707	0.006	0.335	0.718	0.340	0.115	459.62	0.117

Figure G3. Least Squares LOES Matching Results (Analytical Data)
Configuration 1-10

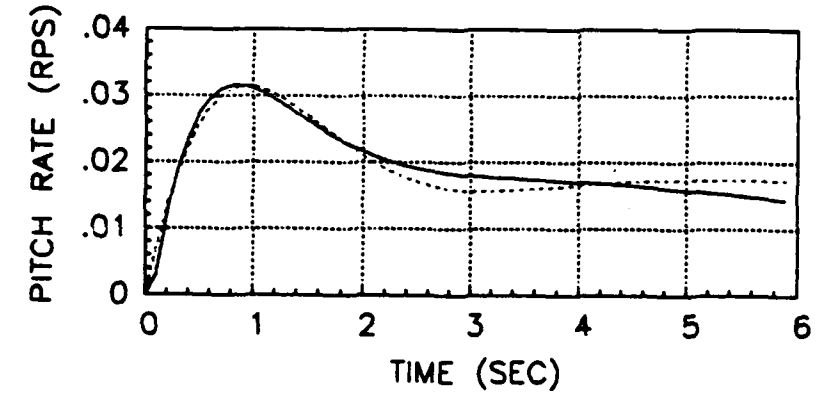

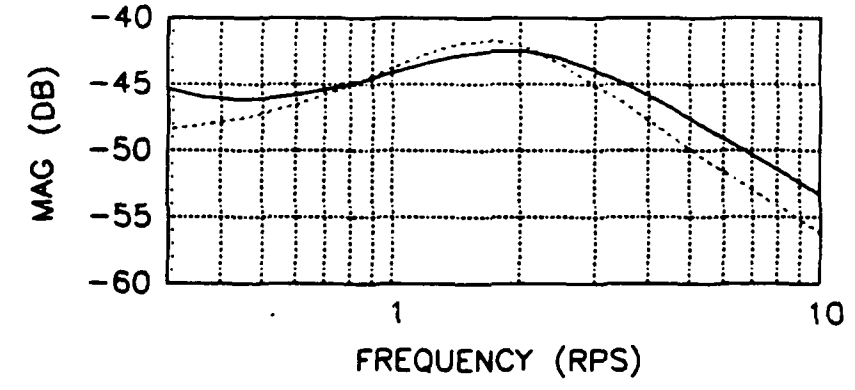

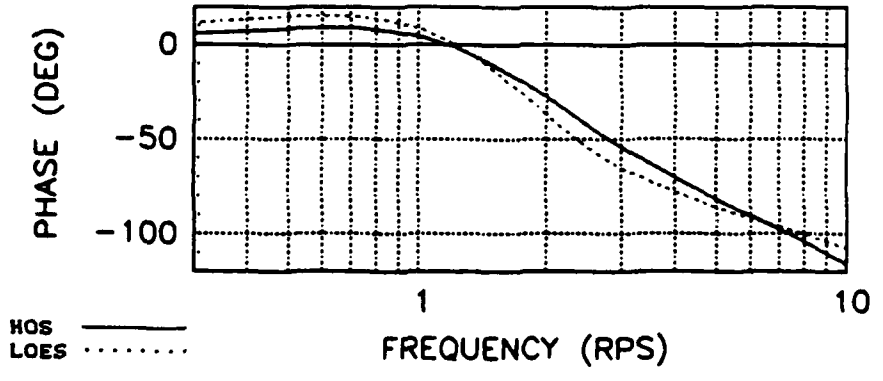

CONFIG	LEVEL	$1/T_{\theta 2}$ (1/sec)	K_θ (rps/lb)	ζ_{sp}	ω_{sp} (rps)	τ_θ (sec)	CAP (1/gsec)	$cost_f$	$cost_t$
2-1	1	0.690	0.015	0.574	1.751	0.044	0.682	74.33	0.008

Figure G4. **Least Squares LOES Matching Results (Analytical Data)**
Configuration 2-1

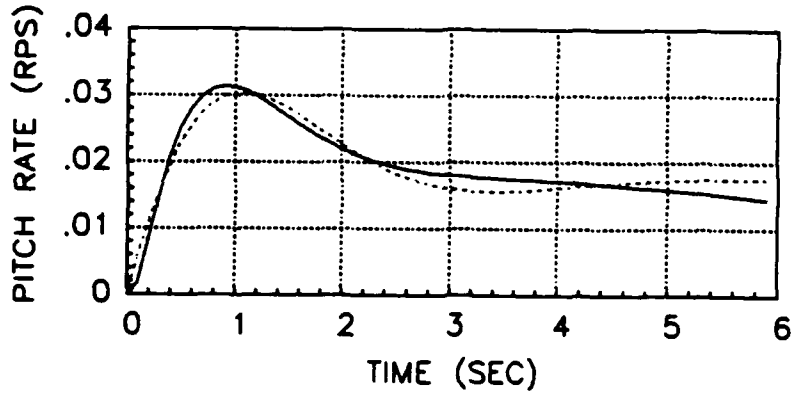

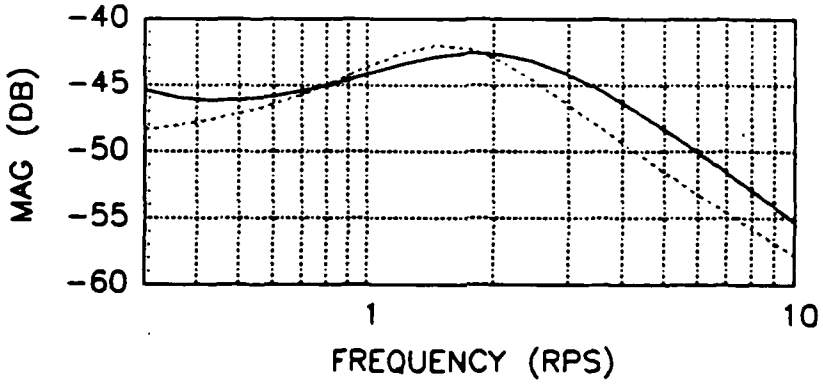

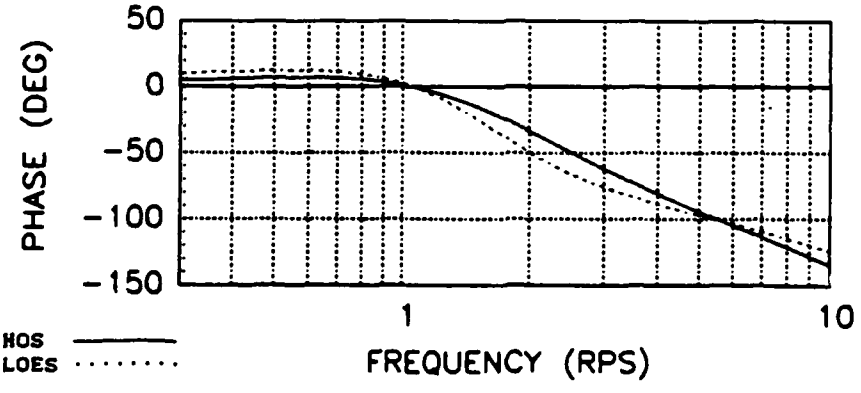

CONFIG	LEVEL	$1/T_{\theta 2}$ (1/sec)	K_θ (rps/lb)	ζ_{sp}	ω_{sp} (rps)	τ_θ (sec)	CAP (1/gsec)	$cost_f$	$cost_t$
2-D	1	0.709	0.013	0.543	1.609	0.070	0.575	108.24	0.009

Figure G5. Least Squares LOES Matching Results (Analytical Data)
Configuration 2-D

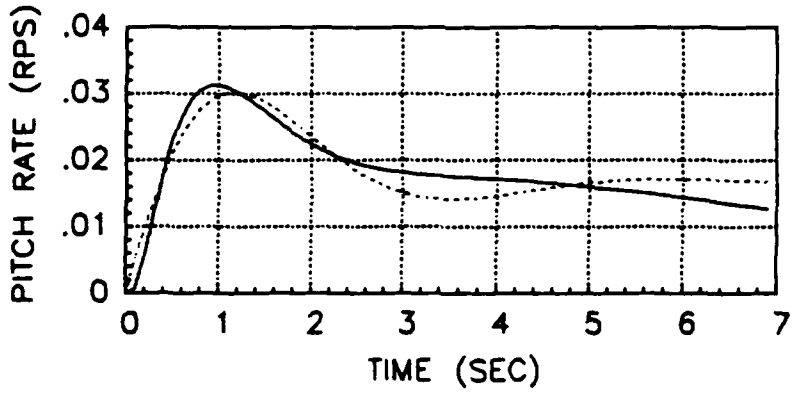

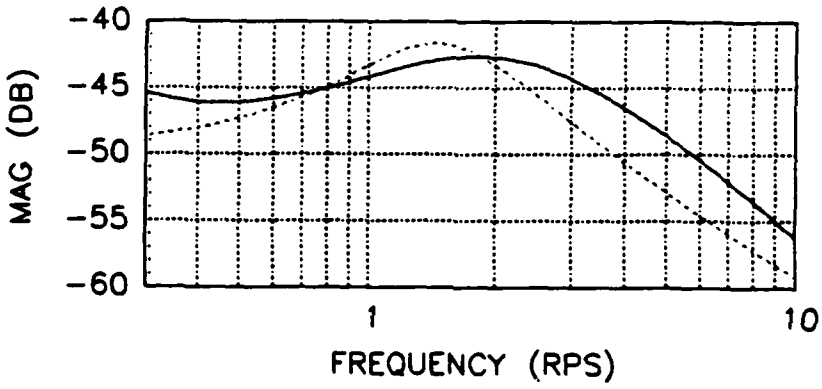

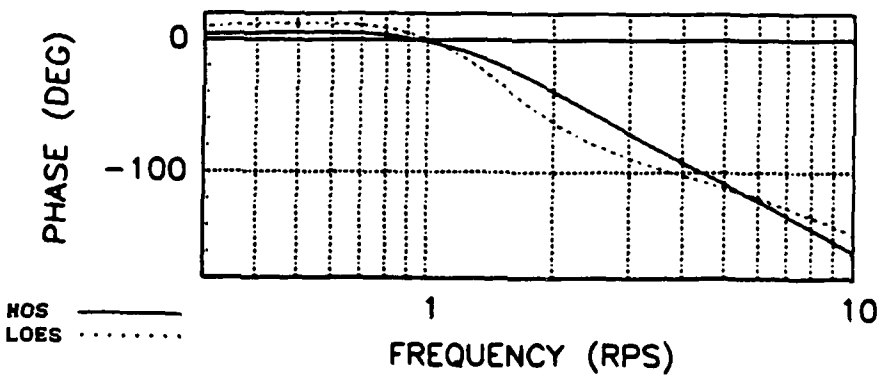

CONFIG	LEVEL	$1/T_{\theta 2}$ (1/sec)	K_θ (rps/lb)	ζ_{sp}	ω_{sp} (rps)	τ_θ (sec)	CAP (1/gsec)	$cost_f$	$cost_t$
2-2	2	0.715	0.011	0.471	1.518	0.107	0.512	186.35	0.019

Figure G6. **Least Squares LOES Matching Results (Analytical Data)**
Configuration 2-2

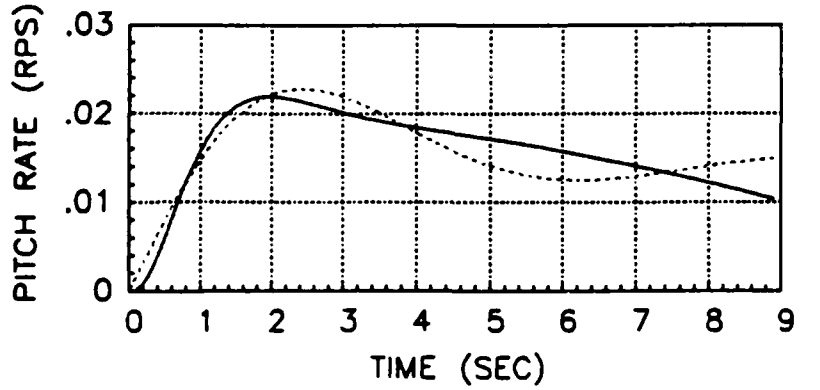

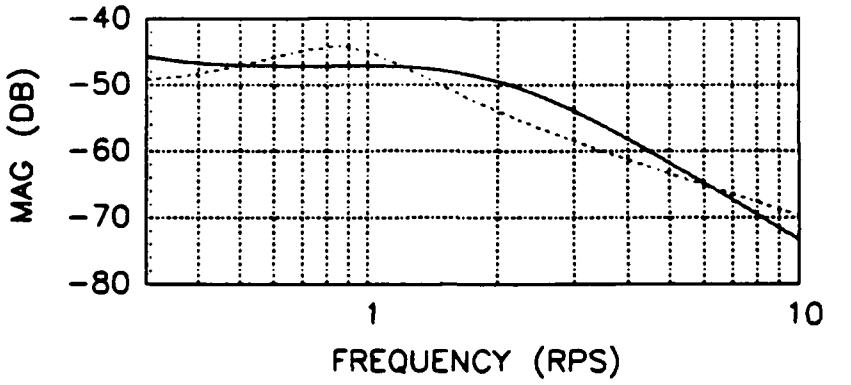

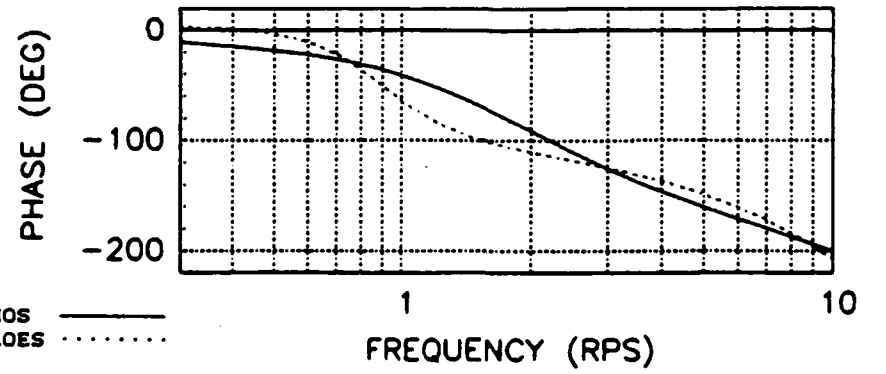

CONFIG	LEVEL	$1/T_{\theta 2}$ (1/sec)	K_θ (rps/lb)	ζ_{sp}	ω_{sp} (rps)	τ_θ (sec)	CAP (1/gsec)	$cost_f$	$cost_t$
2-5	3	0.719	0.003	0.383	0.894	0.205	0.177	250.02	0.015

Figure G7, Least Squares LOES Matching Results (Analytical Data)
Configuration 2-5

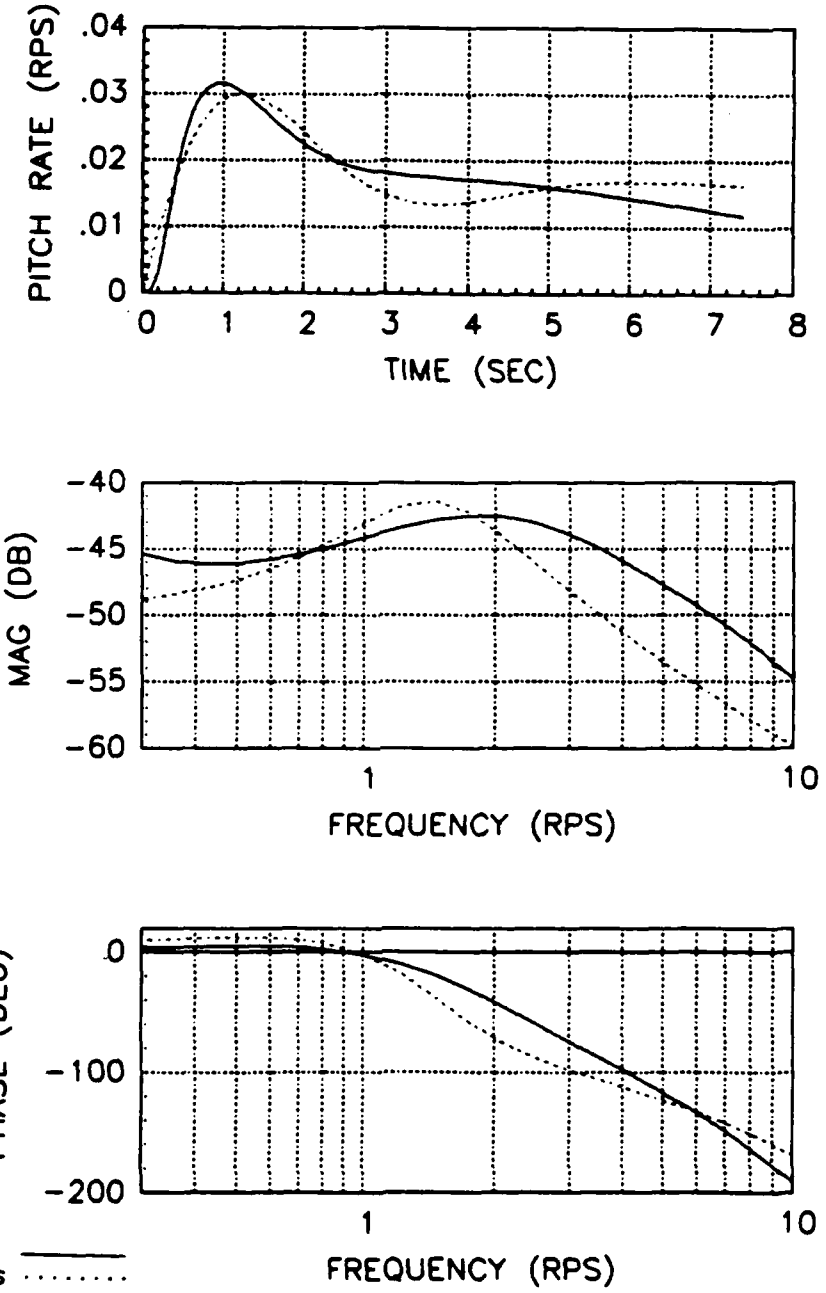

CONFIG	LEVEL	$1/T_{\theta 2}$ (1/sec)	K_θ (rps/lb)	ζ_{sp}	ω_{sp} (rps)	τ_θ (sec)	CAP (1/gsec)	$cost_f$	$cost_t$
2-7	2	0.700	0.010	0.444	1.461	0.143	0.474	343.43	0.027

Figure G8. Least Squares LOES Matching Results (Analytical Data)
Configuration 2-7

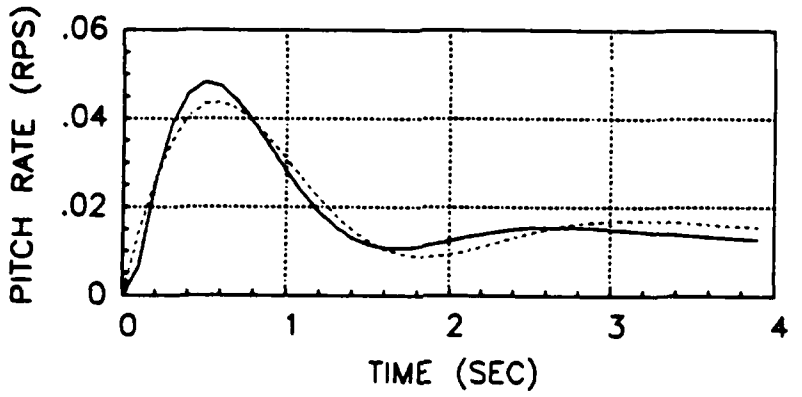

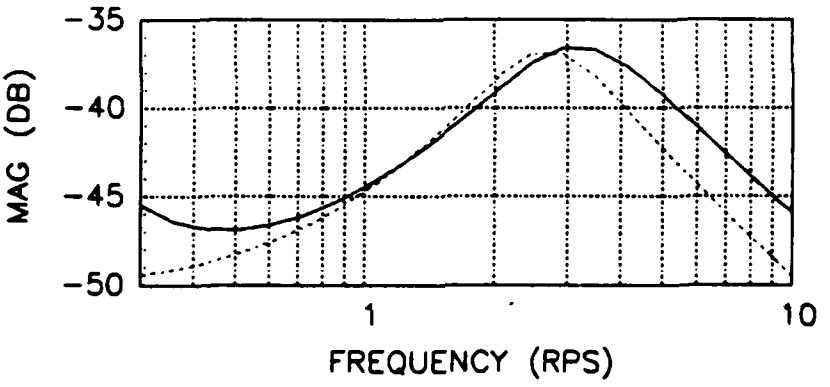

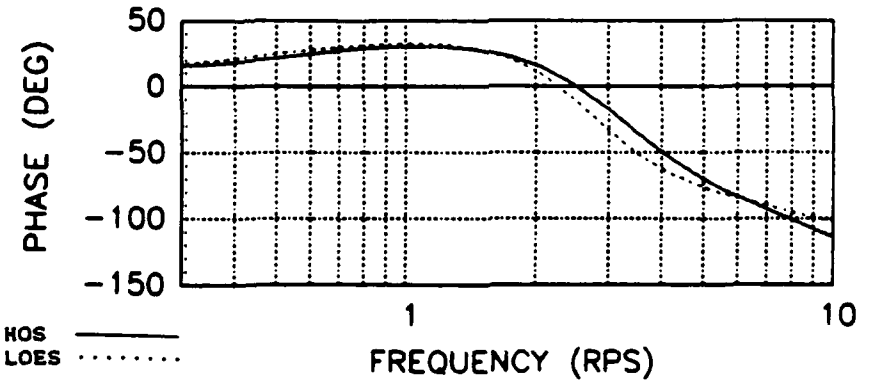

CONFIG	LEVEL	$1/T_{\theta 2}$ (1/sec)	K_θ (rps/lb)	ζ_{sp}	ω_{sp} (rps)	τ_θ (sec)	CAP (1/gsec)	$cost_f$	$cost_t$
3-1	1	0.710	0.032	0.420	2.711	0.038	1.634	107.92	0.026

Figure G9. Least Squares LOES Matching Results (Analytical Data)
Configuration 3-1

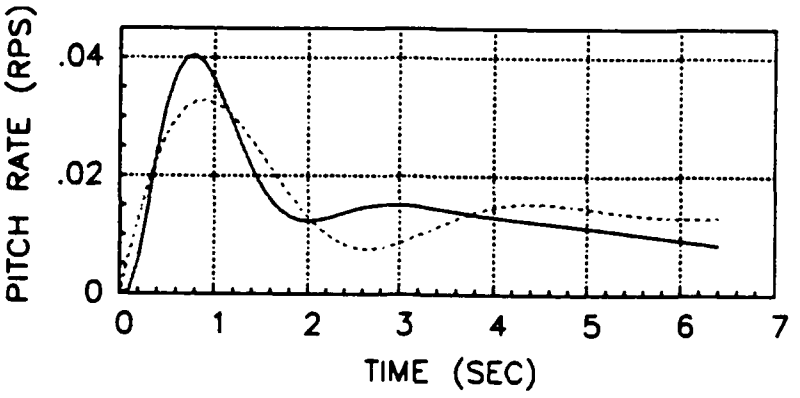

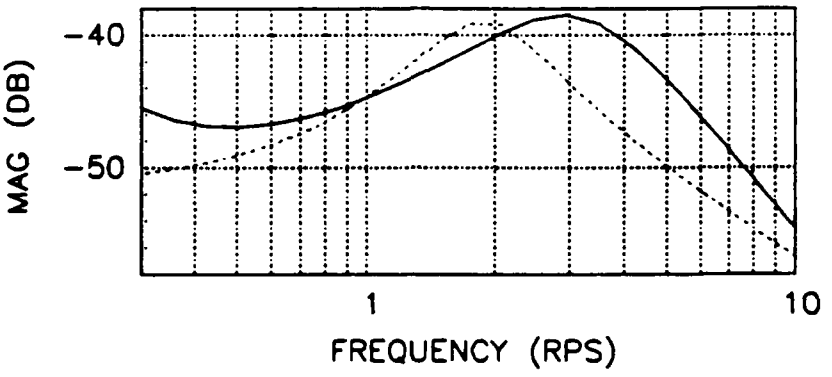

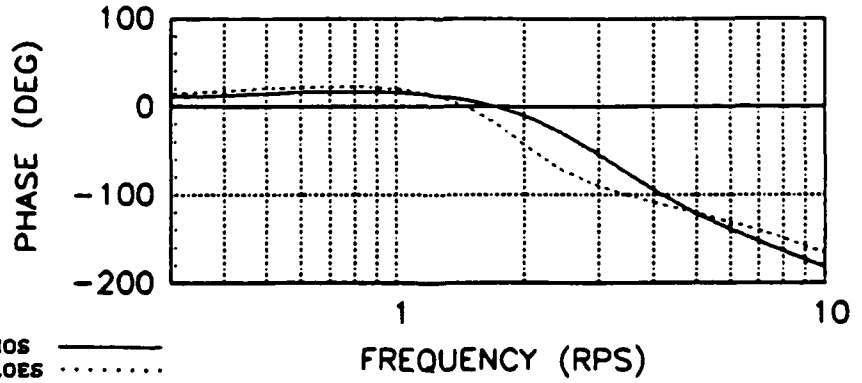

HOS ——————
LOES .....

CONFIG	LEVEL	$1/T_{\theta 2}$ (1/sec)	K_θ (rps/lb)	ζ_{sp}	ω_{sp} (rps)	τ_θ (sec)	CAP (1/gsec)	$cost_f$	$cost_t$
3-3	2	0.696	0.014	0.350	1.909	0.140	0.810	387.44	0.062

Figure G10. Least Squares LOES Matching Results (Analytical Data)
Configuration 3-3

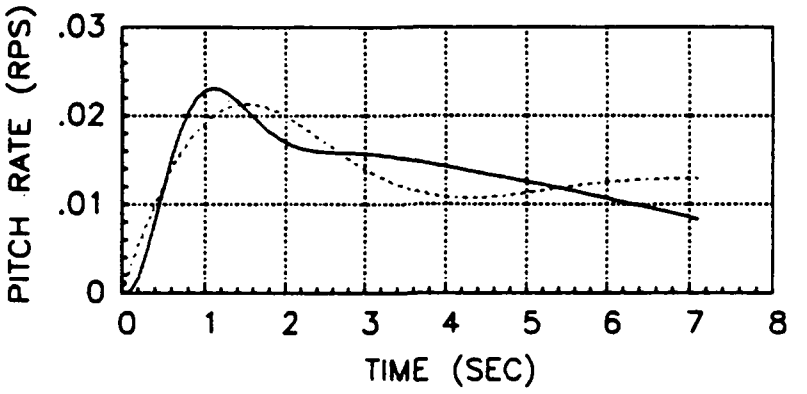

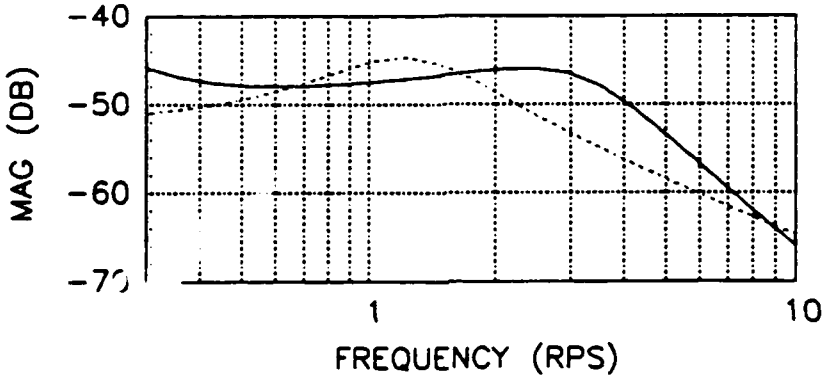

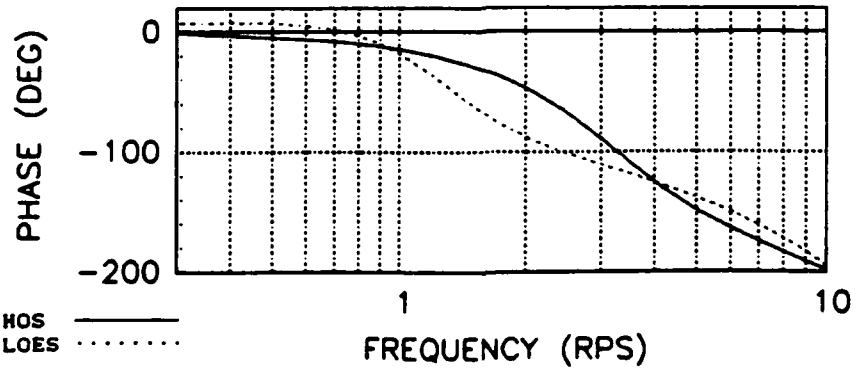

CONFIG	LEVEL	$1/T_{\theta 2}$ (1/sec)	K_θ (rps/lb)	ζ_{sp}	ω_{sp} (rps)	τ_θ (sec)	CAP (1/gsec)	$cost_f$	$cost_t$
3-5	2	0.709	0.006	0.445	1.266	0.186	0.356	391.75	0.021

Figure G11. Least Squares LOES Matching Results (Analytical Data)
Configuration 3-5

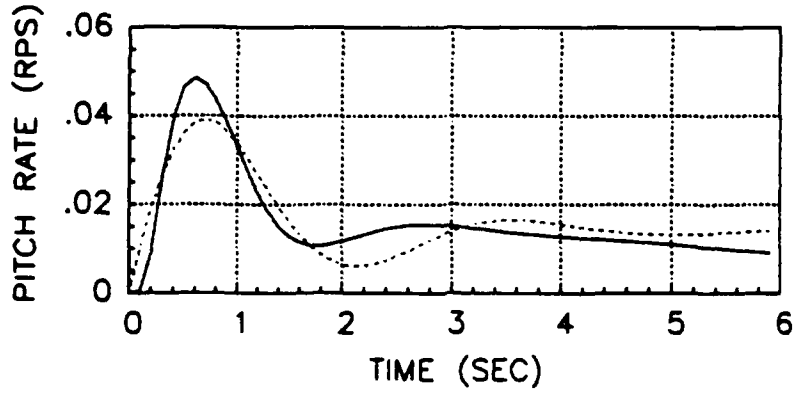

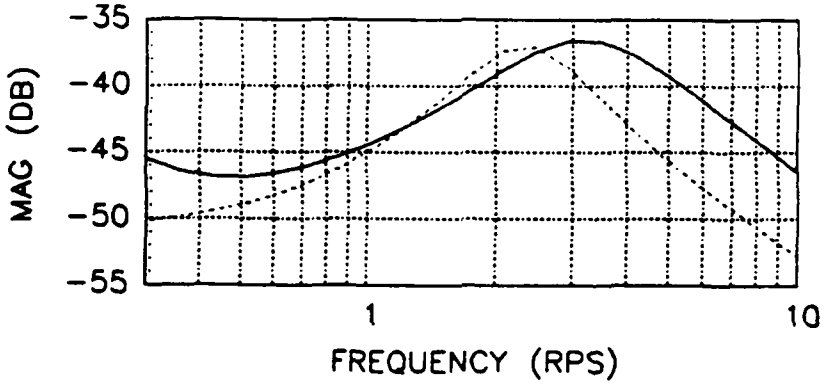

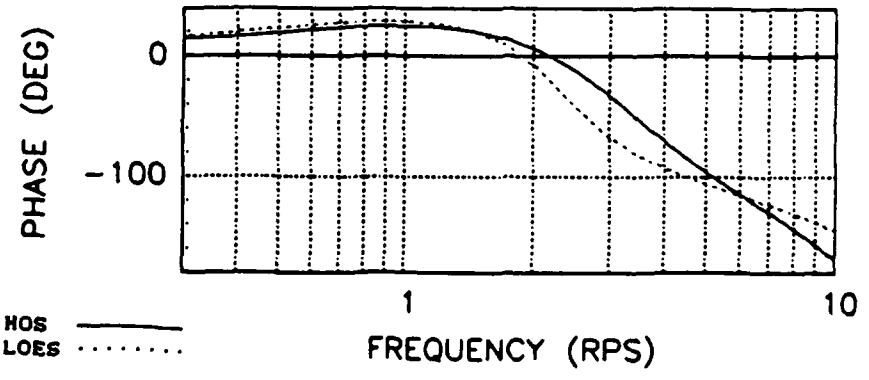

CONFIG	LEVEL	$1/T_{\theta 2}$ (1/sec)	K_θ (rps/lb)	ζ_{sp}	ω_{sp} (rps)	τ_θ (sec)	CAP (1/gsec)	$cost_f$	$cost_t$
3-6	2	0.704	0.022	0.344	2.341	0.105	1.218	381.30	0.067

Figure G12. Least Squares LOES Matching Results (Analytical Data)
Configuration 3-6

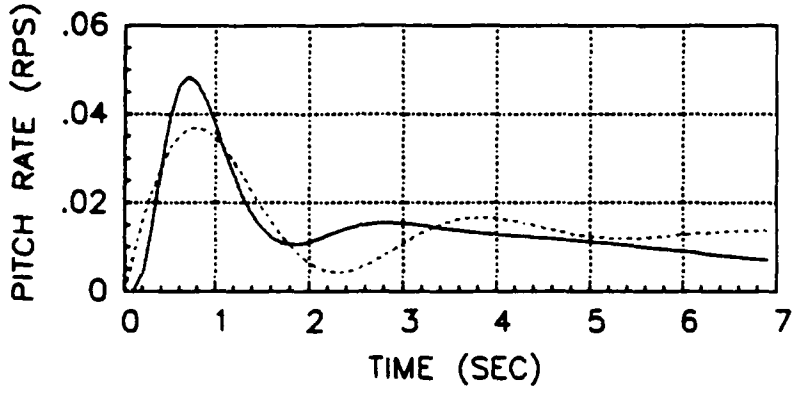

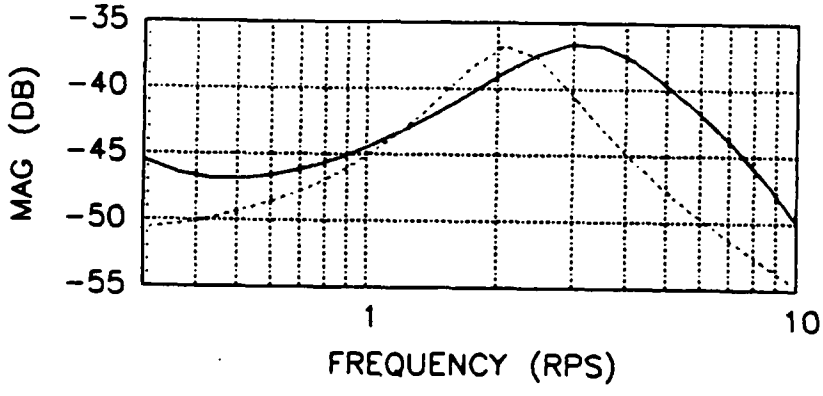

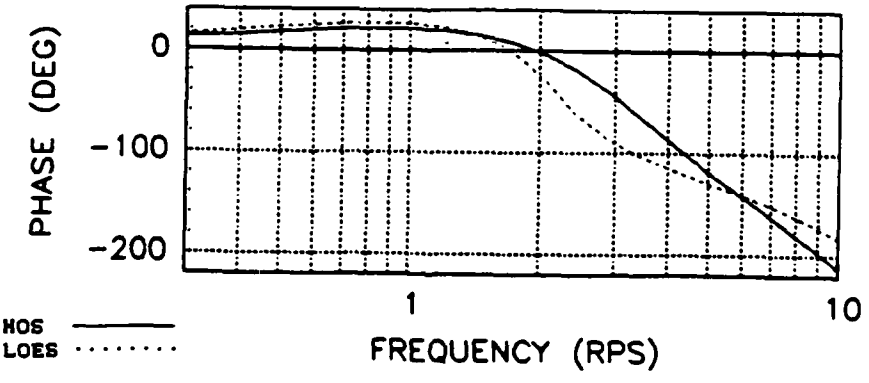

CONFIG	LEVEL	$1/T_{\theta 2}$ (1/sec)	K_θ (rps/lb)	ζ_{sp}	ω_{sp} (rps)	τ_θ (sec)	CAP (1/gsec)	$cost_f$	$cost_t$
3-8	2	0.706	0.018	0.293	2.159	0.168	1.036	548.45	0.095

Figure G13. Least Squares LOES Matching Results (Analytical Data)
Configuration 3-8

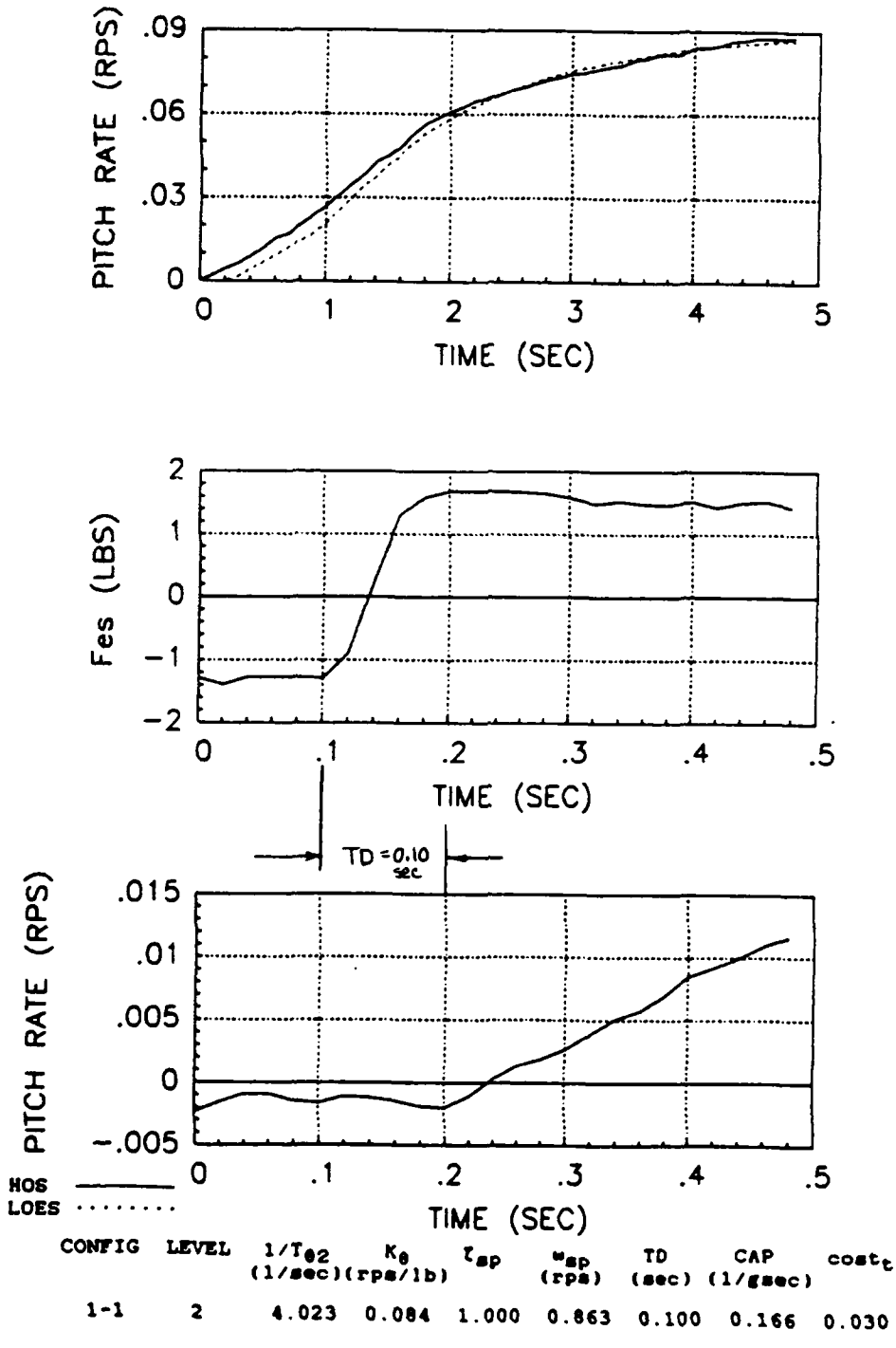

CONFIG	LEVEL	$1/T_{\theta 2}$ (1/sec)	K_θ (rps/lb)	τ_{sp}	ω_{sp} (rps)	TD (sec)	CAP (1/gsec)	$cost_t$
1-1	2	4.023	0.084	1.000	0.863	0.100	0.166	0.030

Figure G14. Least Squares LOES Matching Results (Flight Test Data)
Configuration 1-1

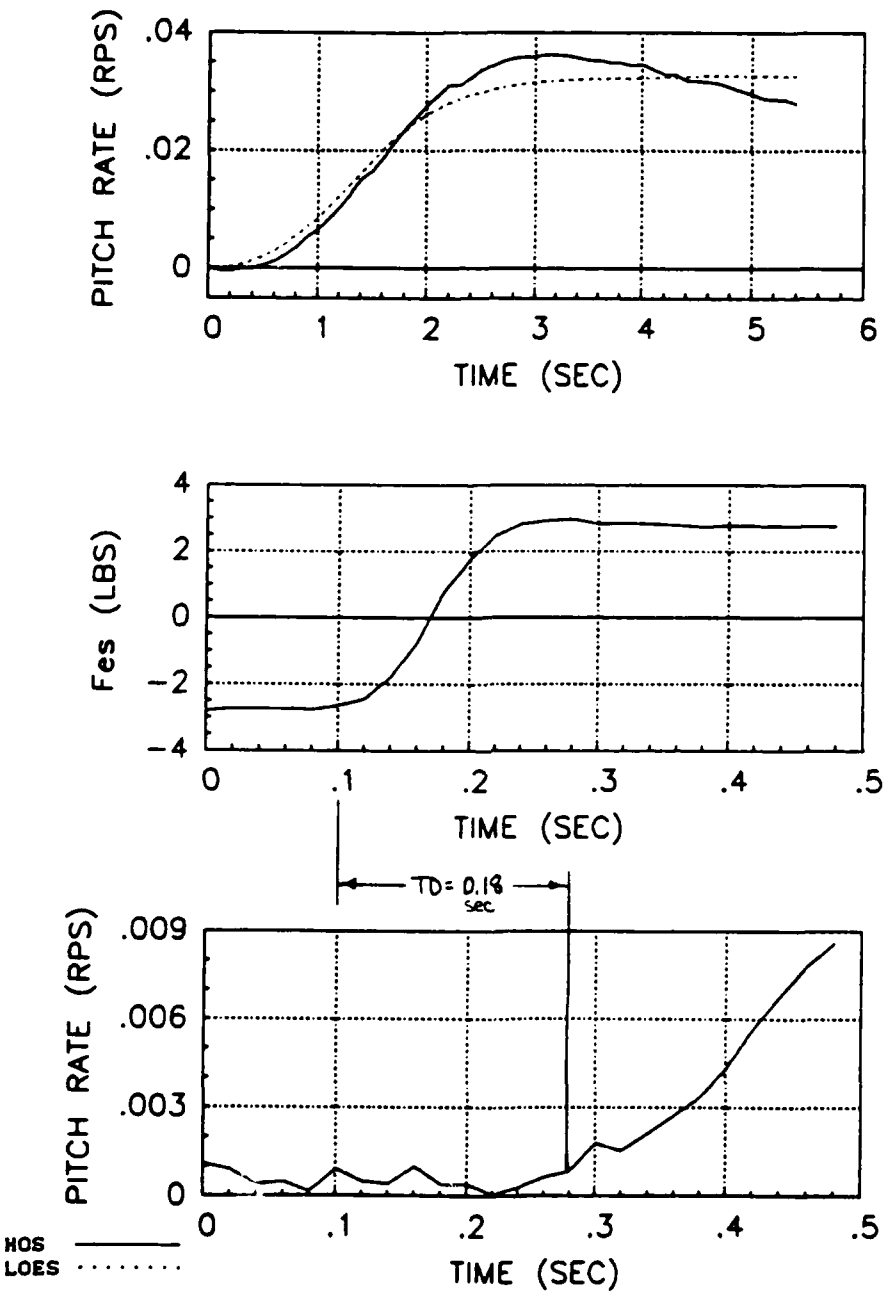

CONFIG	LEVEL	$1/T_{\theta 2}$ (1/sec)	K_θ (rps/lb)	ζ_{sp}	ω_{sp} (rps)	TD (sec)	CAP (1/gsec)	$cost_t$
1-3	2	7.846	0.010	0.876	2.270	0.180	1.145	0.024

Figure G15. Least Squares LOES Matching Results (Flight Test Data)
Configuration 1-3

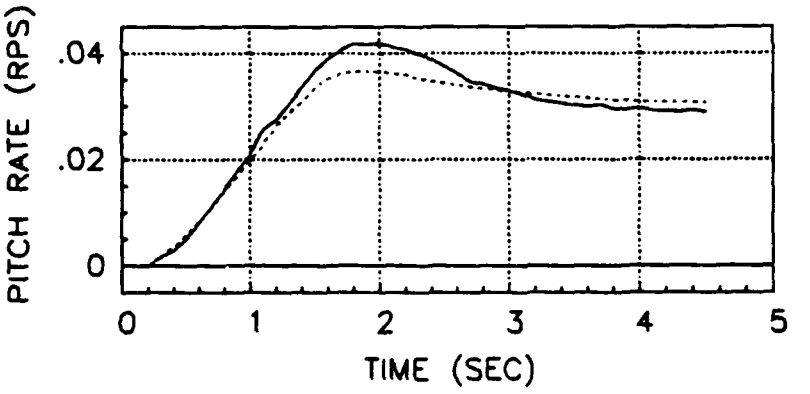

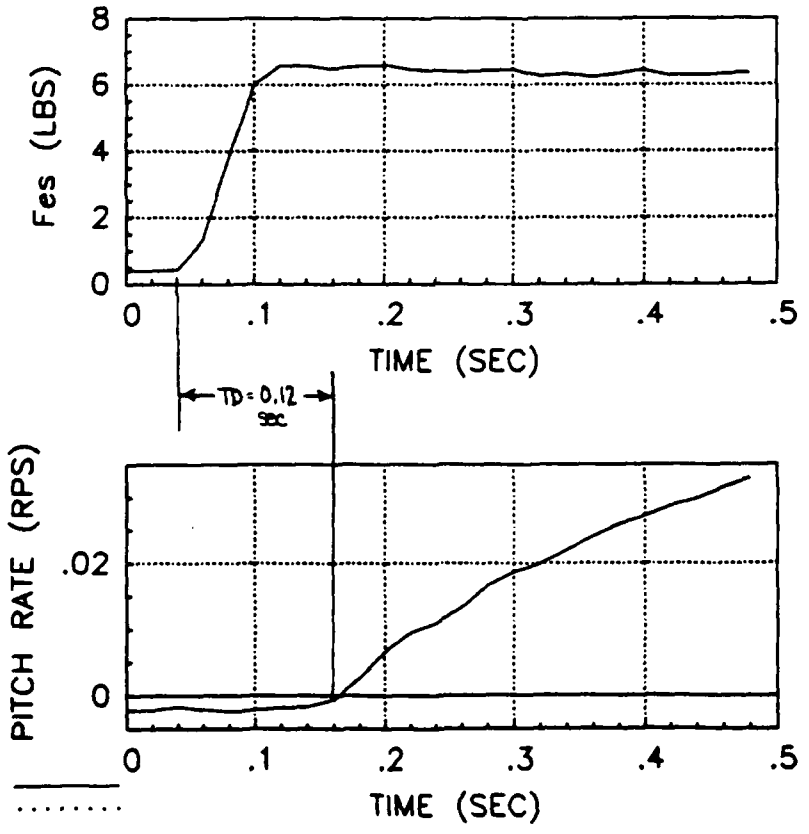

CONFIG	LEVEL	$1/T_{\theta 2}$ (1/sec)	K_θ (rps/lb)	ζ_{sp}	ω_{sp} (rps)	TD (sec)	CAP (1/gsec)	$cost_t$
2-1	2	0.744	0.031	1.000	1.267	0.120	0.357	0.020

Figure G16. Least Squares LOES Matching Results (Flight Test Data)
Configuration 2-1

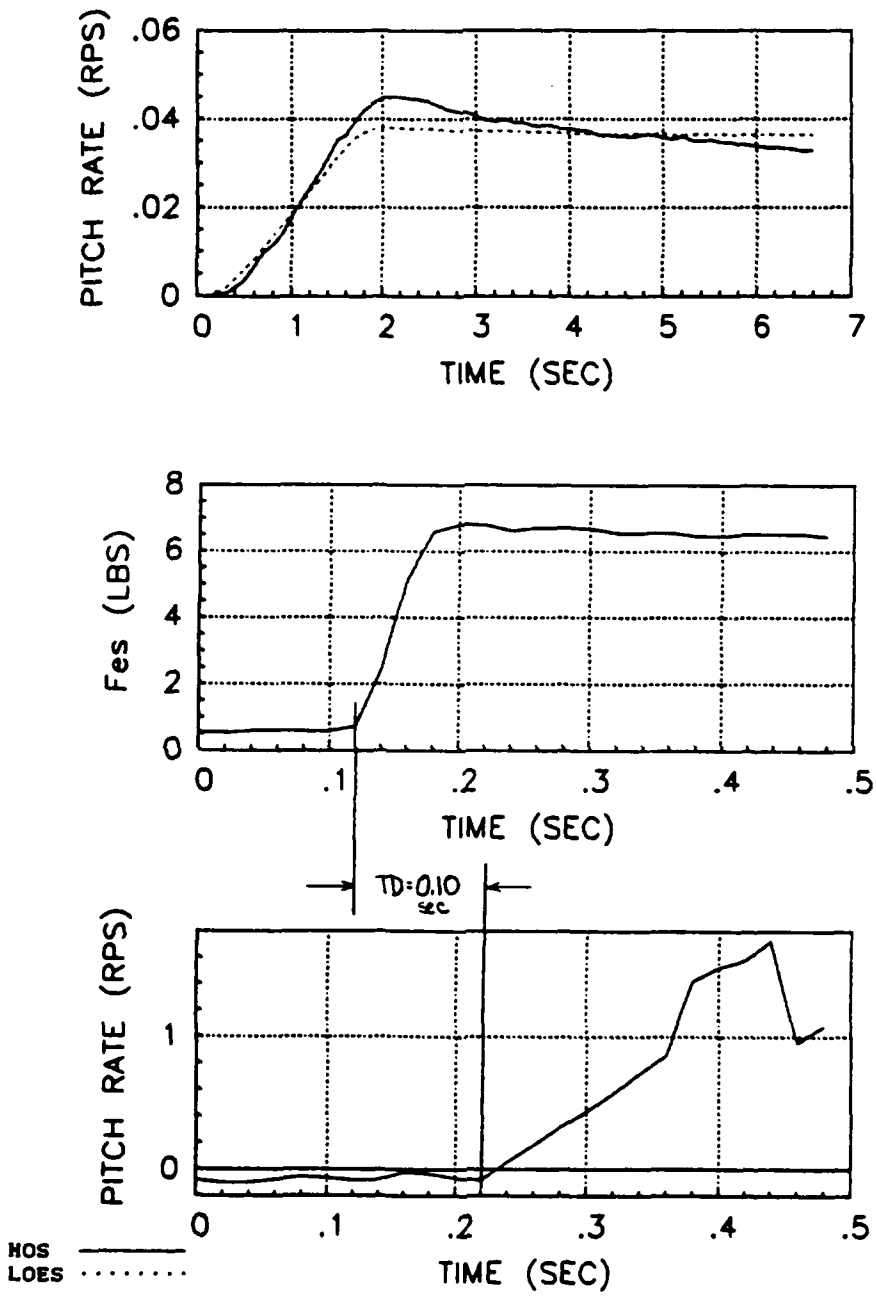

CONFIG	LEVEL	$1/T_{\theta 2}$ (1/sec)	K_θ (rps/lb)	ζ_{sp}	ω_{sp} (rps)	TD (sec)	CAP (1/gsec)	$cost_t$
2-D	2	0.694	0.041	1.000	0.800	0.100	0.142	0.030

Figure G17. Least Squares LOES Matching Results (Flight Test Data)
Configuration 2-D

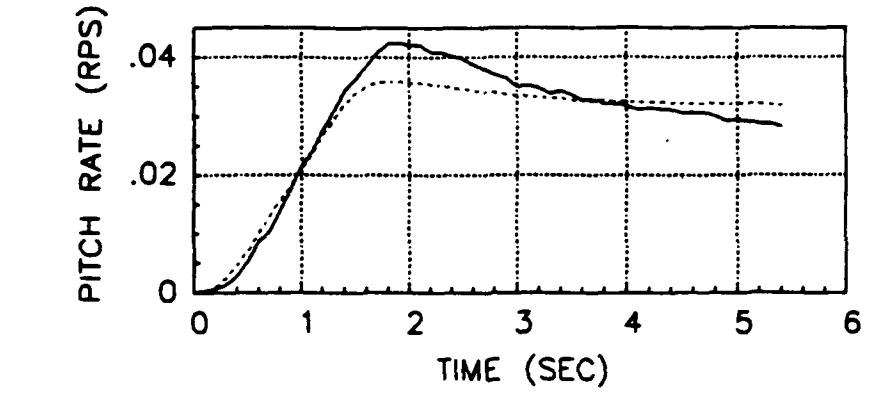

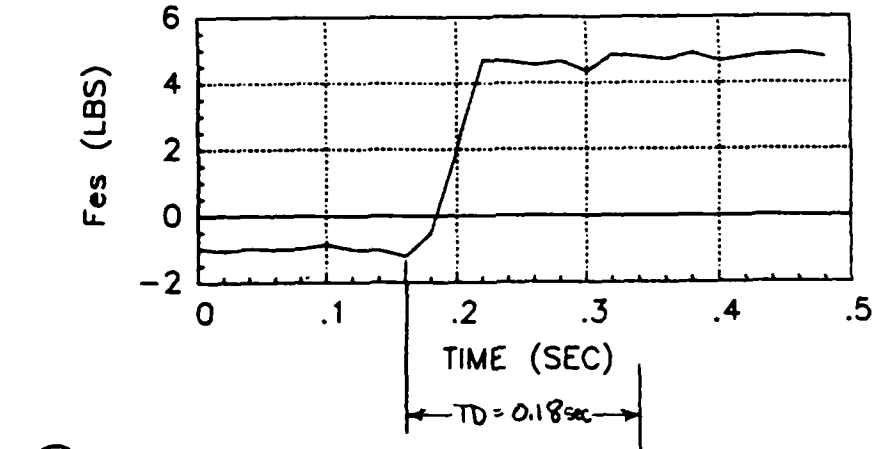

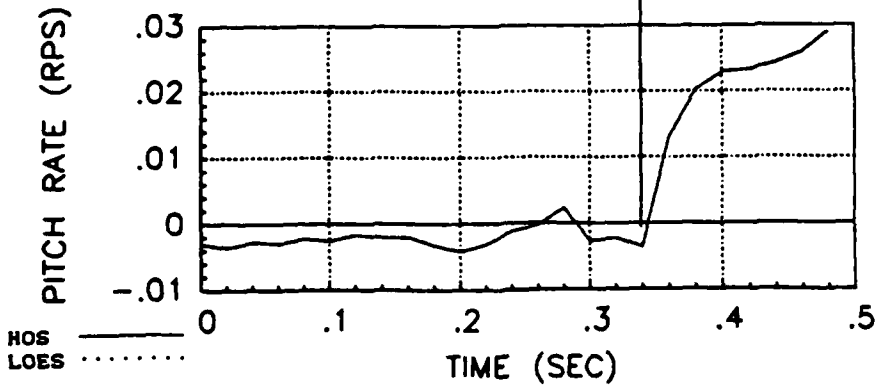

CONFIG	LEVEL	$1/T_{\theta 2}$ (1/sec)	K_θ (rps/lb)	ζ_{sp}	ω_{sp} (rps)	TD (sec)	CAP (1/gsec)	$cost_t$
2-2	2	0.643	0.032	1.000	0.888	0.180	0.175	0.030

Figure G18. **Least Squares LOES Matching Results (Flight Test Data)**
Configuration 2-2

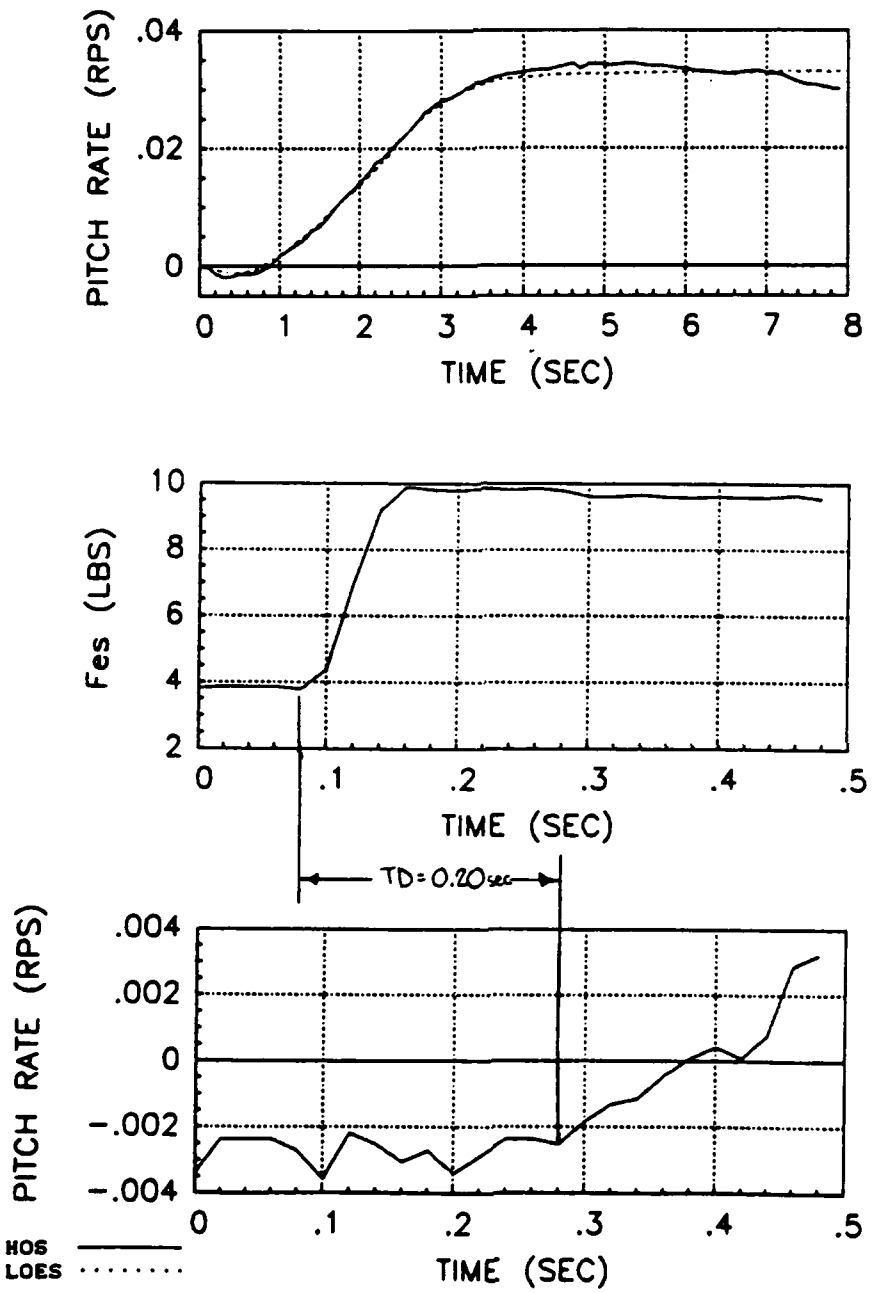

CONFIG	LEVEL	$1/T_{\theta 2}$ (1/sec)	K_θ (rps/lb)	ζ_{sp}	ω_{sp} (rps)	TD (sec)	CAP (1/gsec)	$cost_t$
2-5	3	-2.616	-0.041	1.000	1.994	0.200	0.884	0.004

Figure G19. Least Squares LOES Matching Results (Flight Test Data)
Configuration 2-5

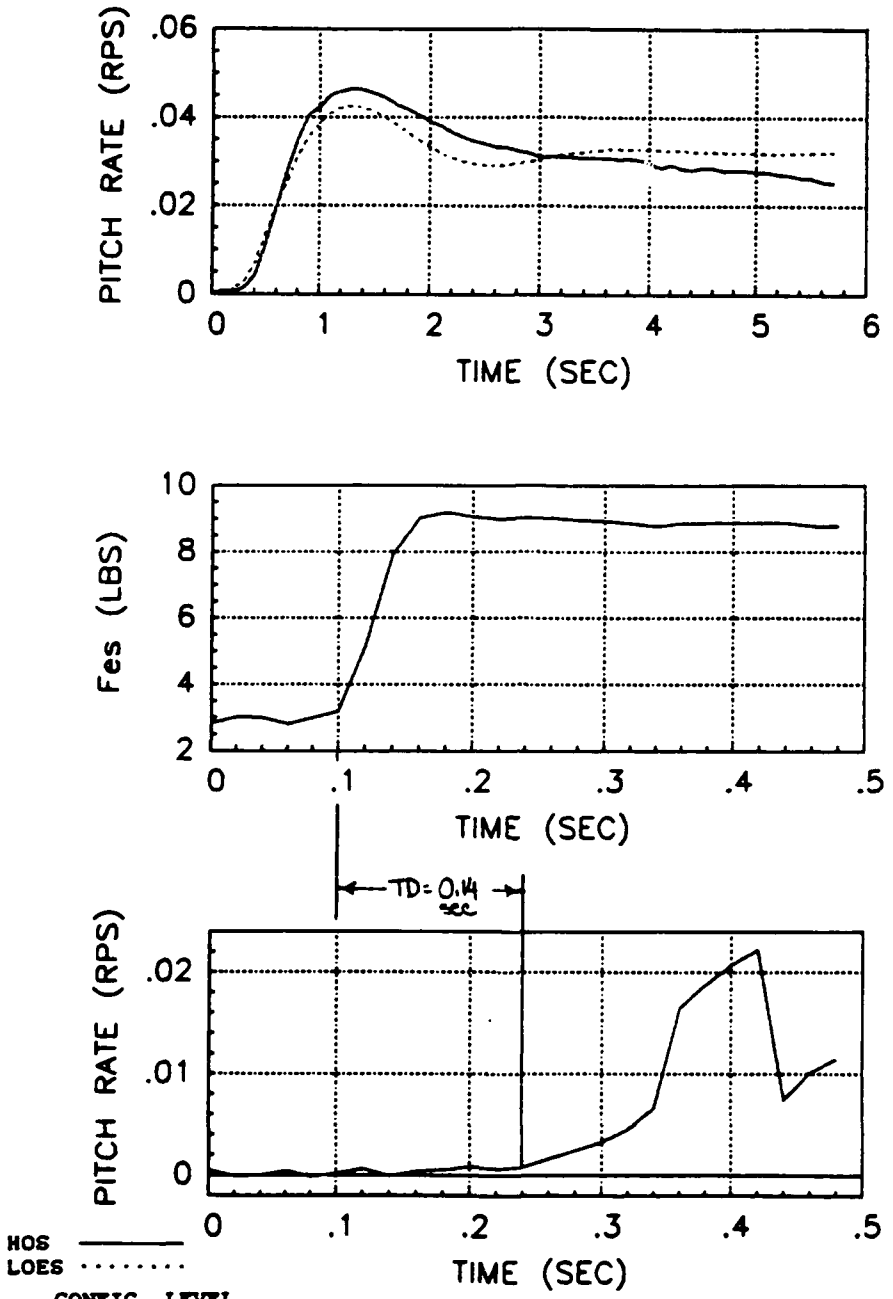

CONFIG	LEVEL	$1/T_{\theta 2}$ (1/sec)	K_θ (rps/lb)	ζ_{sp}	ω_{sp} (rps)	TD (sec)	CAP (1/gsec)	$cost_t$
2-7	2	3.959	0.010	0.384	2.675	0.140	1.590	0.051

Figure G20. Least Squares LOES Matching Results (Flight Test Data)
Configuration 2-7

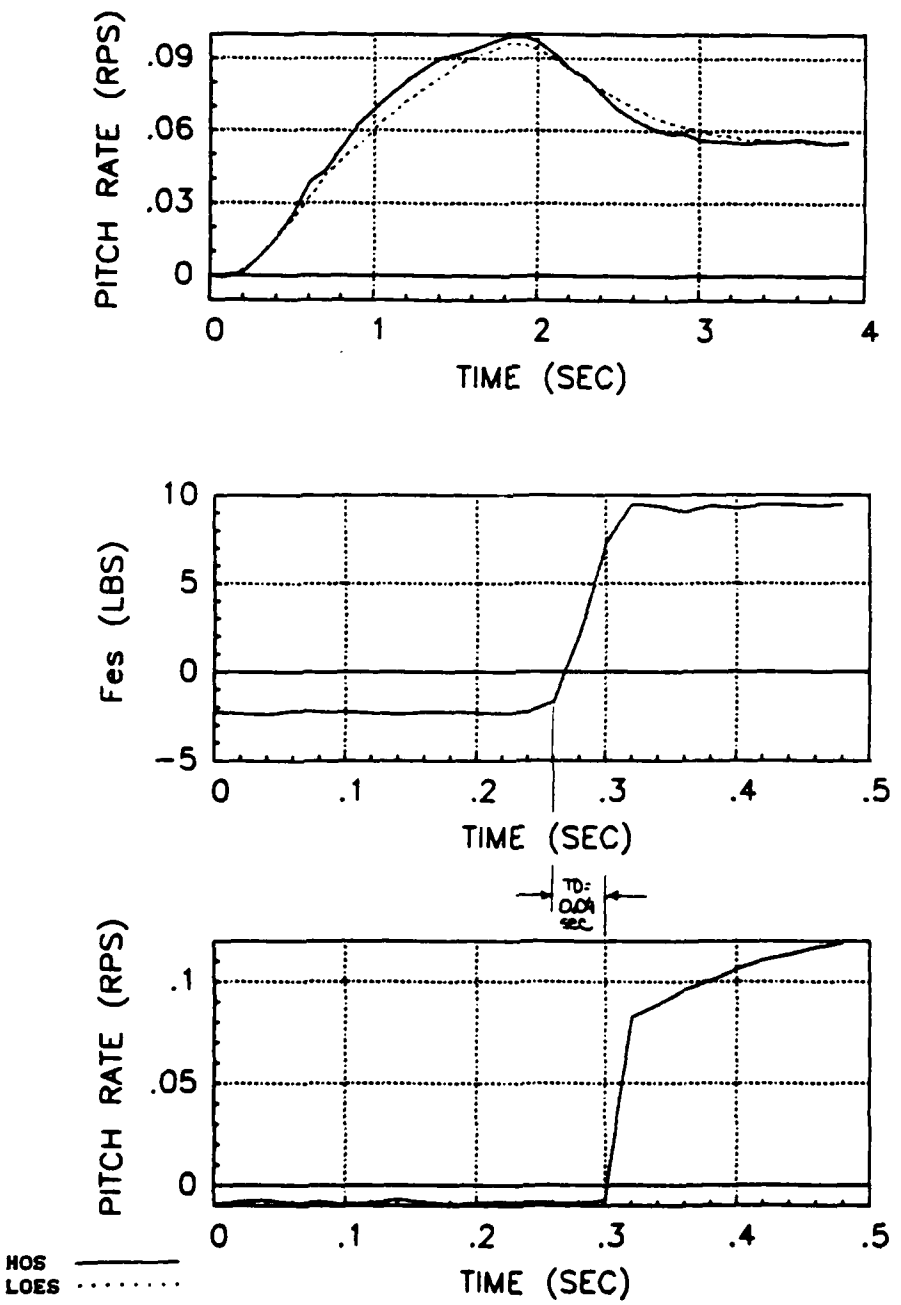

CONFIG	LEVEL	$1/T_{\theta 2}$ (1/sec)	K_θ (rps/lb)	ζ_{sp}	ω_{sp} (rps)	TD (sec)	CAP (1/gsec)	$cost_t$
3-1	1	0.493	0.067	0.959	3.032	0.040	2.042	0.056

Figure G21. Least Squares LOES Matching Results (Flight Test Data)
Configuration 3-1

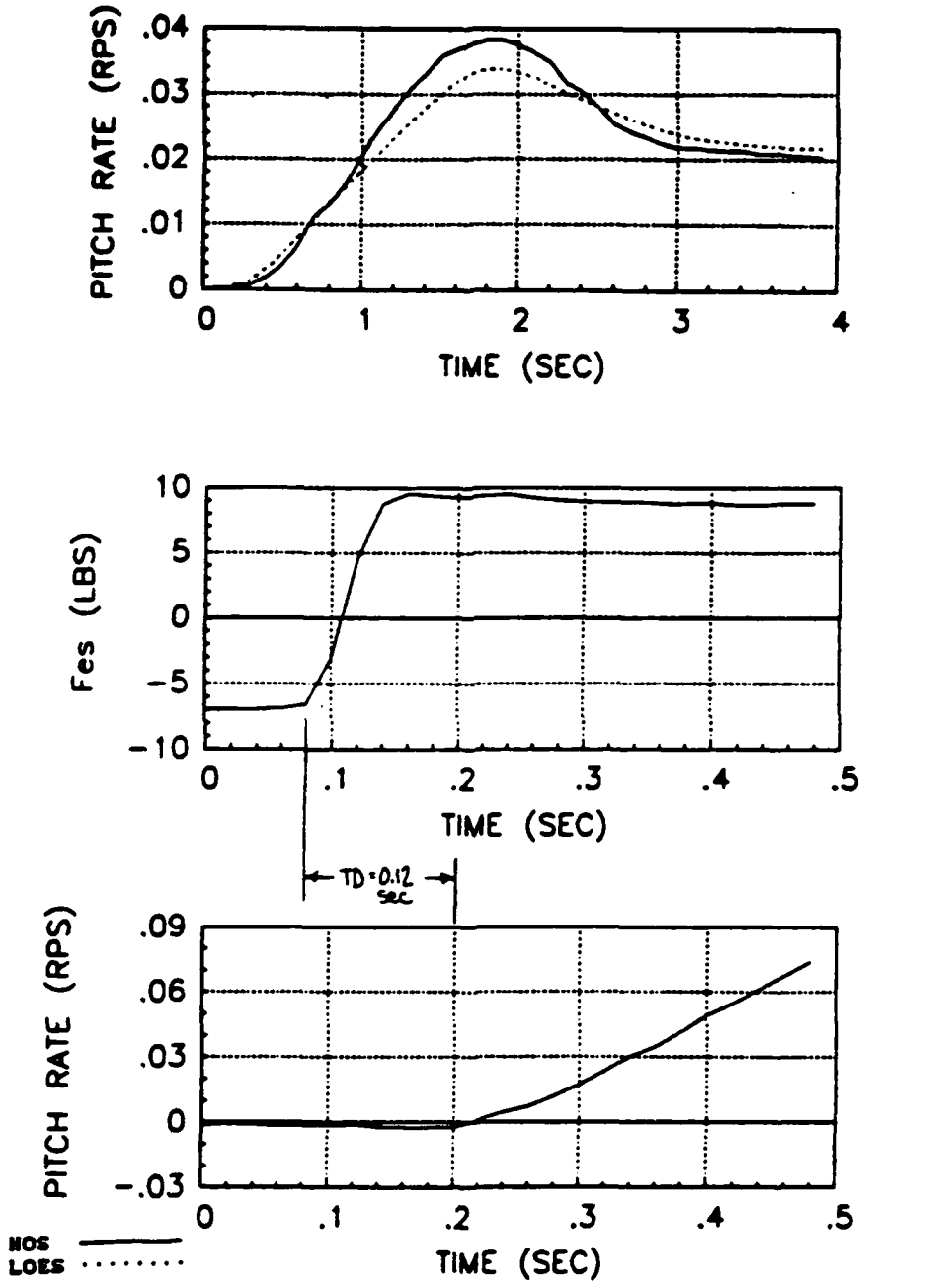

CONFIG	LEVEL	$1/T_{\theta 2}$ (1/sec)	K_θ (rps/lb)	ζ_{sp}	ω_{sp} (rps)	TD (sec)	CAP (1/gsec)	$cost_t$
3-3	2	0.694	0.028	0.752	2.264	0.120	1.140	0.024

Figure G22. **Least Squares LOES Matching Results (Flight Test Data)**
Configuration 3-3

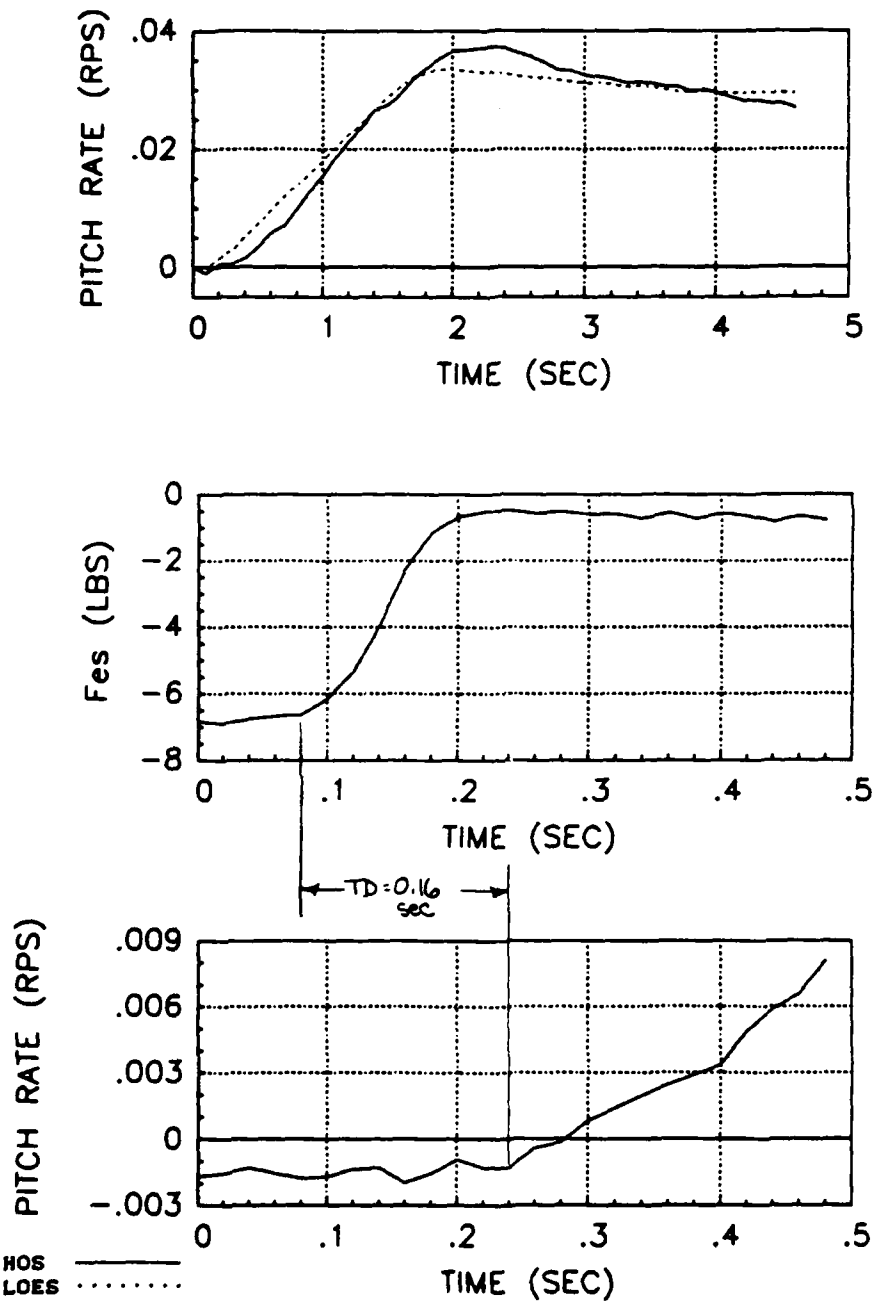

CONFIG	LEVEL	$1/T_{\theta 2}$ (1/sec)	K_θ (rps/lb)	ζ_{sp}	ω_{sp} (rps)	TD (sec)	CAP (1/gsec)	$cost_t$
3-5	2	0.518	0.026	1.000	0.720	0.160	0.115	0.018

Figure G23. **Least Squares LOES Matching Results (Flight Test Data)**
Configuration 3-5

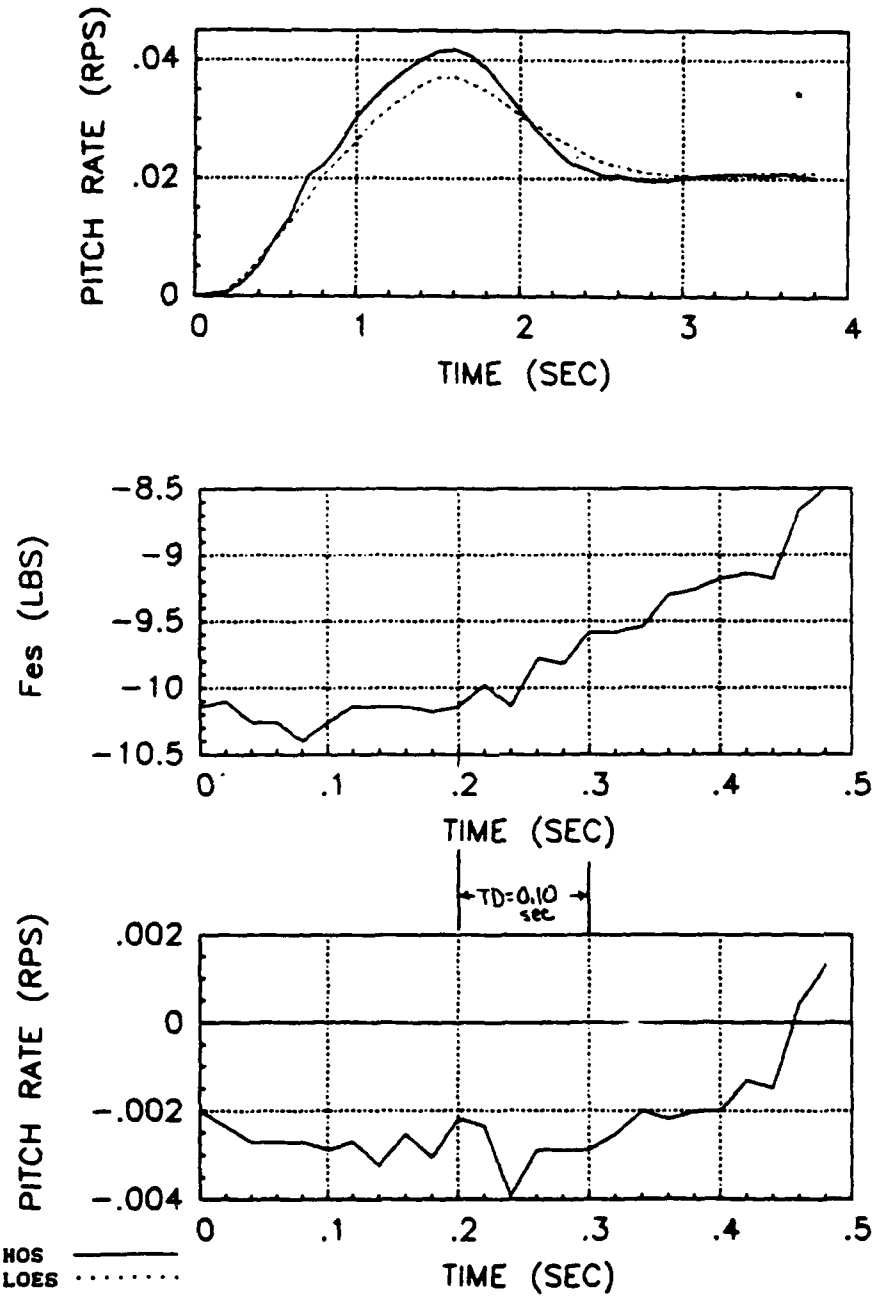

CONFIG	LEVEL	$1/T_{\theta 2}$ (1/sec)	K_θ (rps/lb)	ζ_{sp}	ω_{sp} (rps)	TD (sec)	CAP (1/gsec)	$cost_t$
3-6	2	0.718	0.038	0.675	2.680	0.100	1.597	0.019

Figure G24. Least Squares LOES Matching Results (Flight Test Data)
Configuration 3-6

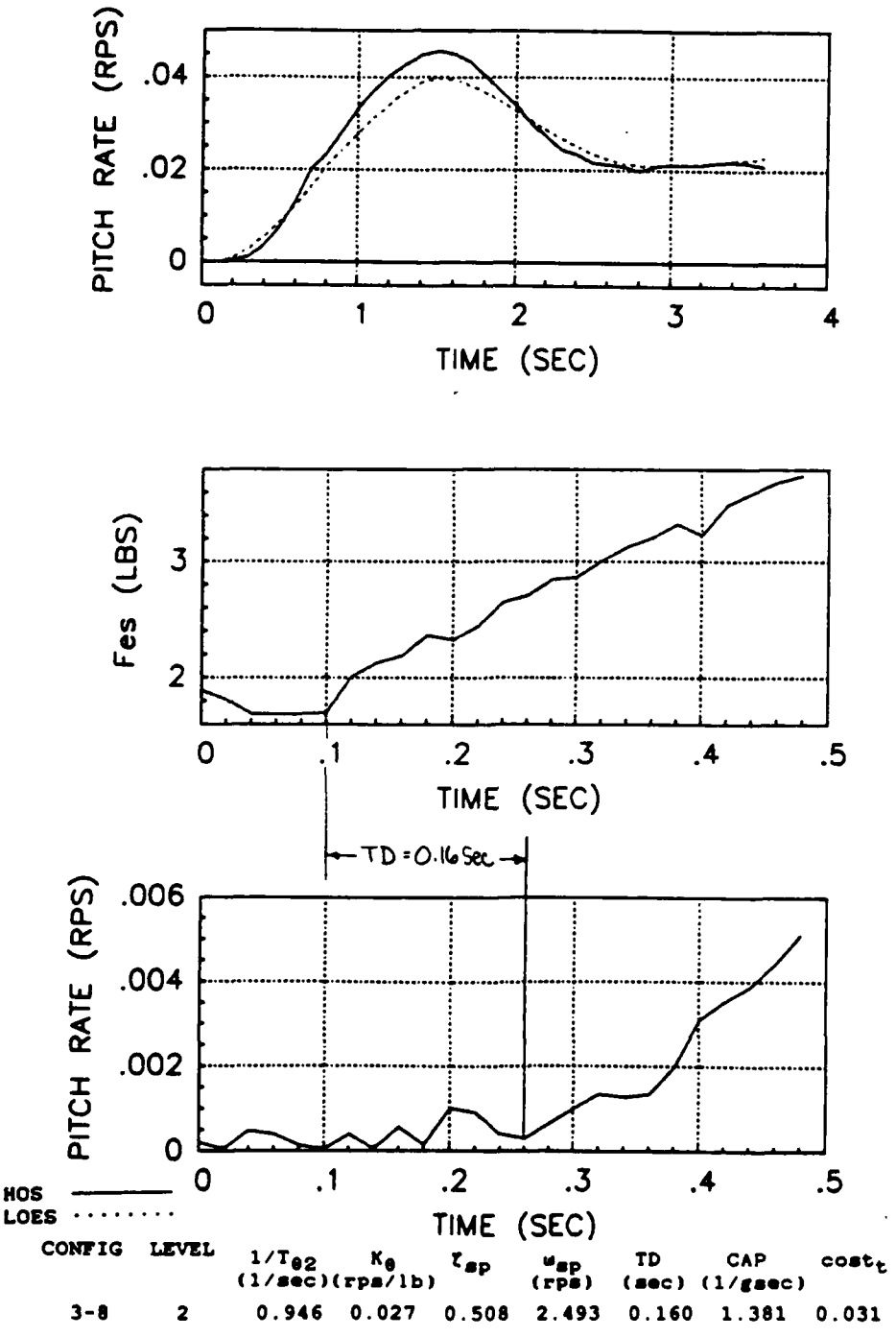

CONFIG	LEVEL	$1/T_{\theta 2}$ (1/sec)	K_θ (rps/lb)	ζ_{sp}	ω_{sp} (rps)	TD (sec)	CAP (1/gsec)	$cost_t$
3-8	2	0.946	0.027	0.508	2.493	0.160	1.381	0.031

Figure G25. Least Squares LOES Matching Results (Flight Test Data)
Configuration 3-8

APPENDIX H. BANDWIDTH THEORY AND PREDICTION RESULTS

The Bandwidth method has been proposed as a handling qualities requirement by MIL-STD-1797 (3). The Bandwidth method is simple to use because it assumes a "gain only" pilot model and involves only the use of open loop pitch to stick force (θ/F_s) Bode plots.

Bandwidth can be loosely defined as the maximum frequency at which closed loop compensatory tracking can take place without threatening the stability of the aircraft; i.e. the maximum open loop crossover frequency. Hence, a large value of bandwidth is generally desireable to achieve superior tracking performance.

The reason for including bandwidth in this study was to compare the results of the bandwidth predicted handling quality levels with the least squares LOES results. The bandwidth method sets up boundaries for Level 1, 2, and 3 handling qualities, and thus is well suited for a comparison with the LOES method. The bandwidth criteria are based on maximum crossover frequency and system phase delay, while the LOES method uses requirements for equivalent ζ_{sp}, ω_{sp}, and τ_θ. The approach taken in this study was to see how well the bandwidth boundaries and the phase delay parameter correlated with the LOES boundaries and equivalent time delay.

The following discussion of the bandwidth theory is taken from MIL-STD-1797 (3) and Hodgkinson (32). Crossover

frequency, directly determined by pilot gain, is a rough measure of the rapidity of the closed loop response. Physically, the pilot will increase his gain to track more rapidly moving targets with acceptable error. However, the pilot cannot indefinitely increase crossover frequency by increasing gain, because he will eventually lose closed loop stability (when the phase margin of the open loop system becomes negative). The pilot would like to choose a value of crossover frequency which allows him to double his gain and still provide adequate phase margin. A reasonable crossover frequency would then be one which provides at least 6 dB of gain margin and 45 degrees of phase margin.

The above crossover frequency is the bandwidth frequency (ω_{BW}) and is shown in Figure H1. To find ω_{BW} for a system, first find the frequency at which the phase shift is -135 degrees; this is $\omega_{BWphase}$. Then find the amplitude at which the phase shift is -180 degrees and add 6 dB. The frequency corresponding to this amplitude is ω_{BWgain}. The smaller of these two frequencies is ω_{BW}.

Handling qualities and pilot ratings are not dependent on bandwidth alone; the shape of the phase curve at frequencies above ω_{BW} becomes important as well. If the phase curve drops off rapidly at frequencies above ω_{BW}, the aircraft will generally receive poor pilot ratings, since an abrupt loss in stability margin is produced when the pilot attempts to increase the crossover frequency. One measure of rapid phase

equivalent system time delay, unlike ω_{BW}, cannot easily be measured by hand. Phase delay (τ_p), a parameter that measures phase rolloff by hand, is defined in Figure H1. Usually, τ_p is numerically similar to τ_e.

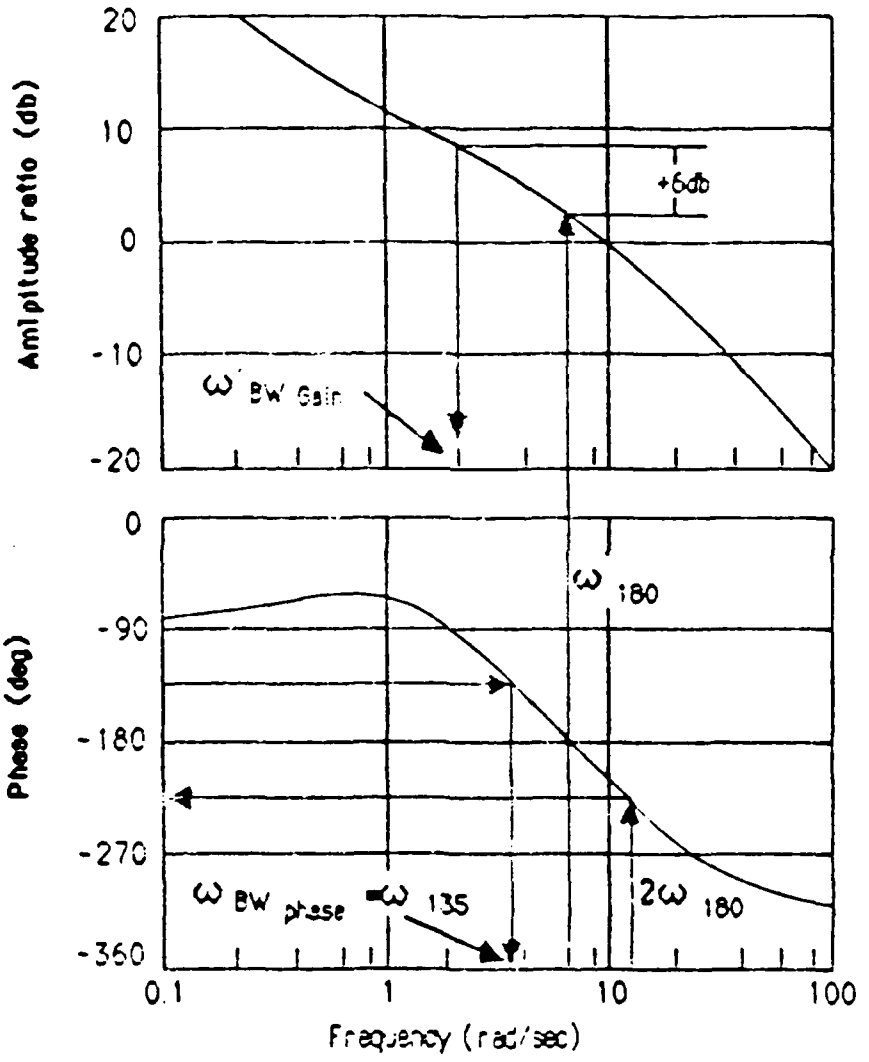

$$\omega_{BW} = \min[\omega_{BWphase}, \omega_{BWgain}]$$

$$\tau_p = -[\phi(2\omega_{180})+180]/[57.3x2\omega_{180}]$$

Figure H1. Definition of Bandwidth and Phase Delay Parameters

The bandwidth criteria suggests that systems with high attainable crossover frequencies and without rapid phase rolloffs should have good handling qualities. Figure H2 shows flying qualities boundaries based on bandwidth frequency and τ_p. The boundaries are referred to as the bandwidth criteria.

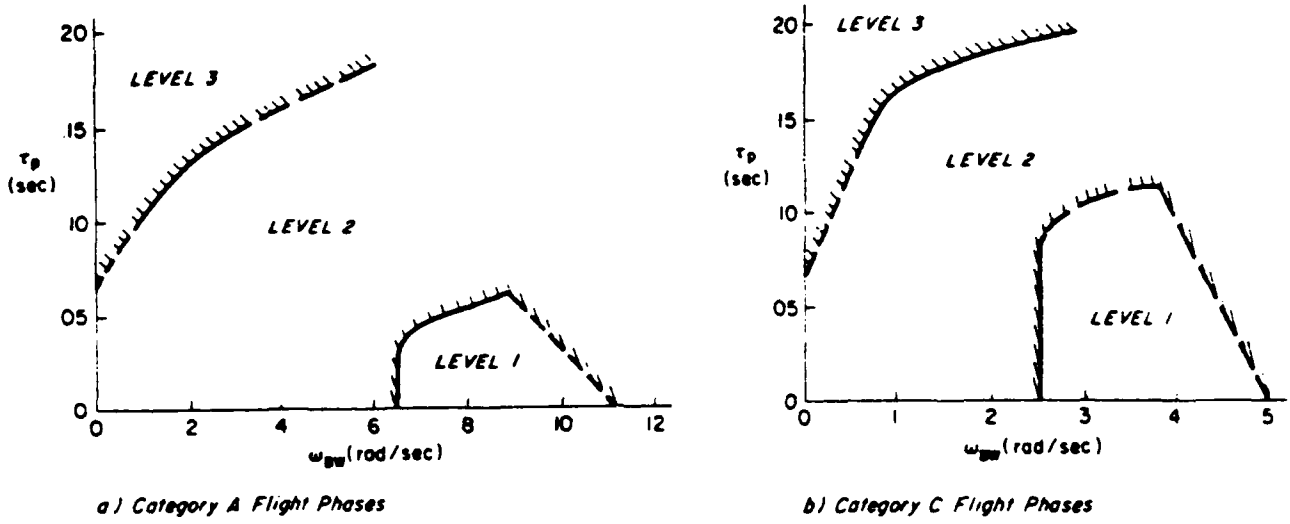

Figure H2. Bandwidth Requirements (MIL-STD-1797, Ref H1)

The bandwidth method can then be summarized as follows:

1. Determine ω_{180} from the Bode plot of θ/F_s.
2. Find $\omega_{BWphase}$ (freq where phase margin is 45 degrees).
3. Find magnitude θ/F_s at ω_{180} and add 6 dB.
4. Find ω_{BWgain} (freq where above magnitude occurs).
5. $\omega_{BW} = \min[\omega_{BWphase}, \omega_{BWgain}]$.
6. $\tau_p = -[\Phi(2\omega_{180})+180]/[57.3x2\omega_{180}]$.
7. Find τ_p and ω_{BW} on the τ_p vs ω_{BW} plot to determine the predicted level of handling qualities.

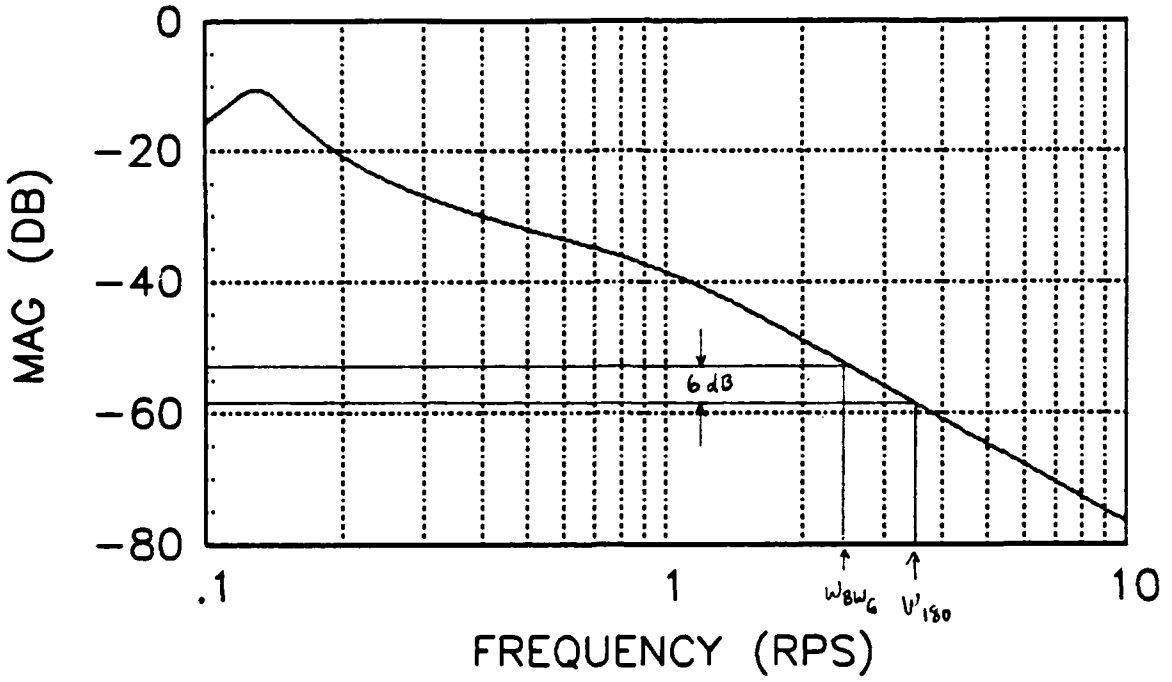

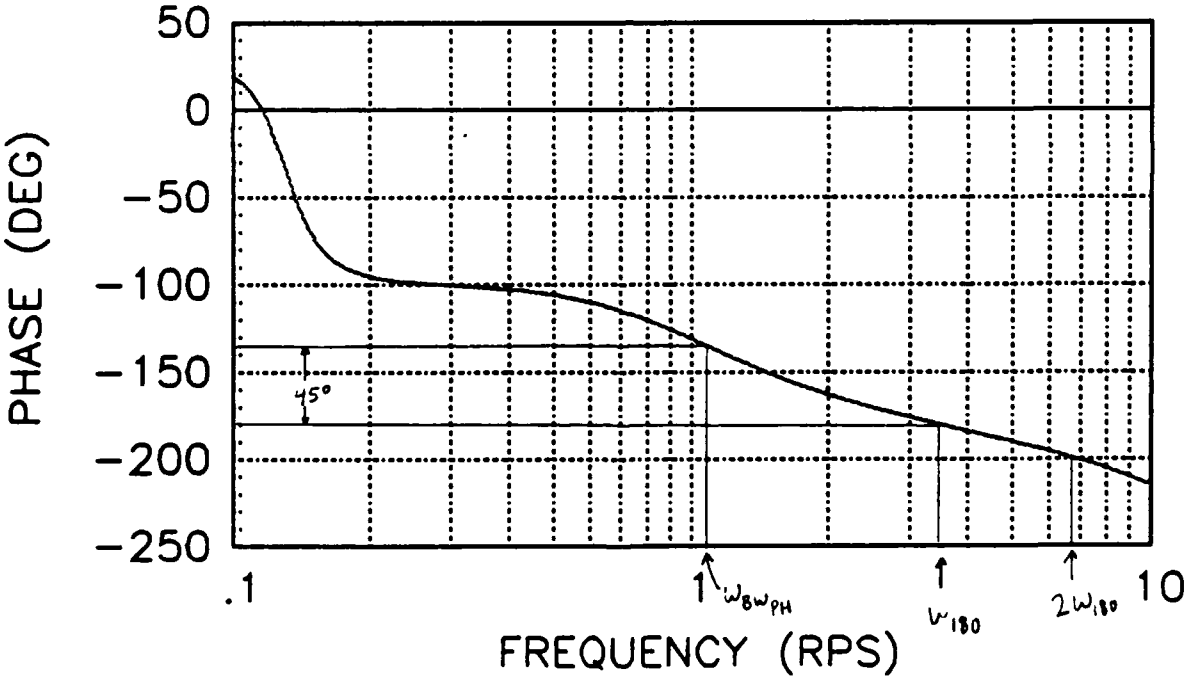

$\omega_{BW} = \min[\omega_{BW_{phase}}, \omega_{BW_{gain}}] = 1.02$ rps

$$\tau_p = -[\phi(2\omega_{180})+180]/[57.3 \times 2\omega_{180}]$$
$$= -[-200+180]/[2(3.3)(57.3)]$$
$$= 0.053 \text{ sec}$$

Predicted Flying Qualities - Level 2

Figure H3. Bandwidth Results for Configuration 1-1

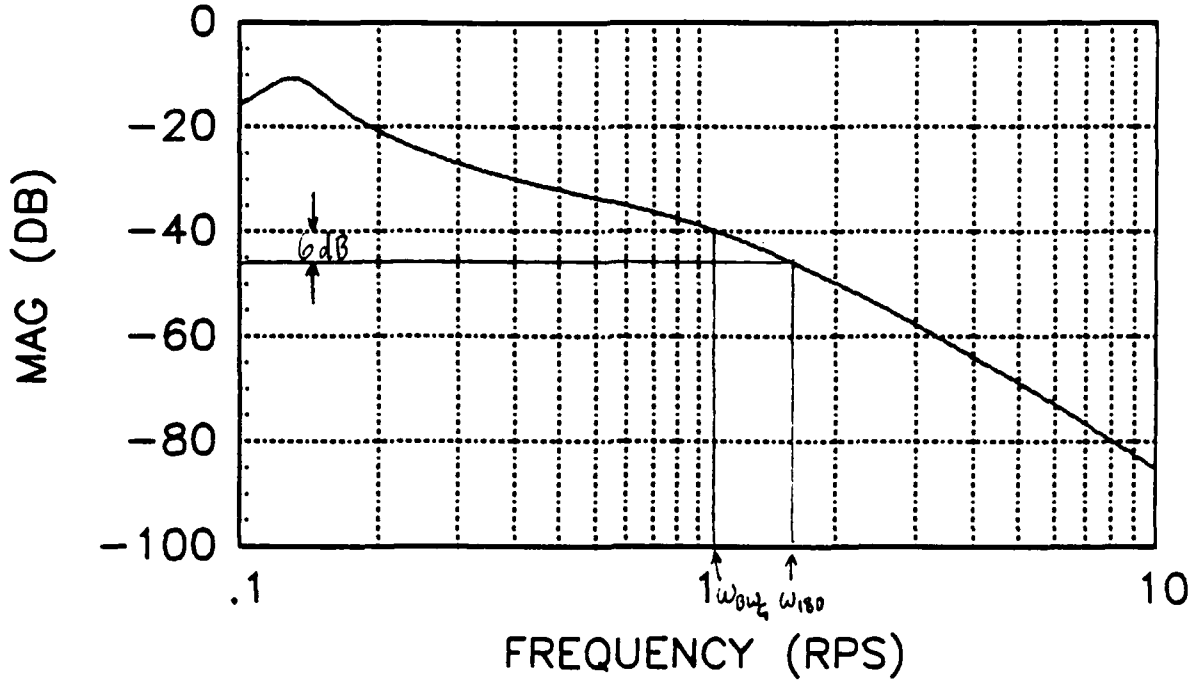

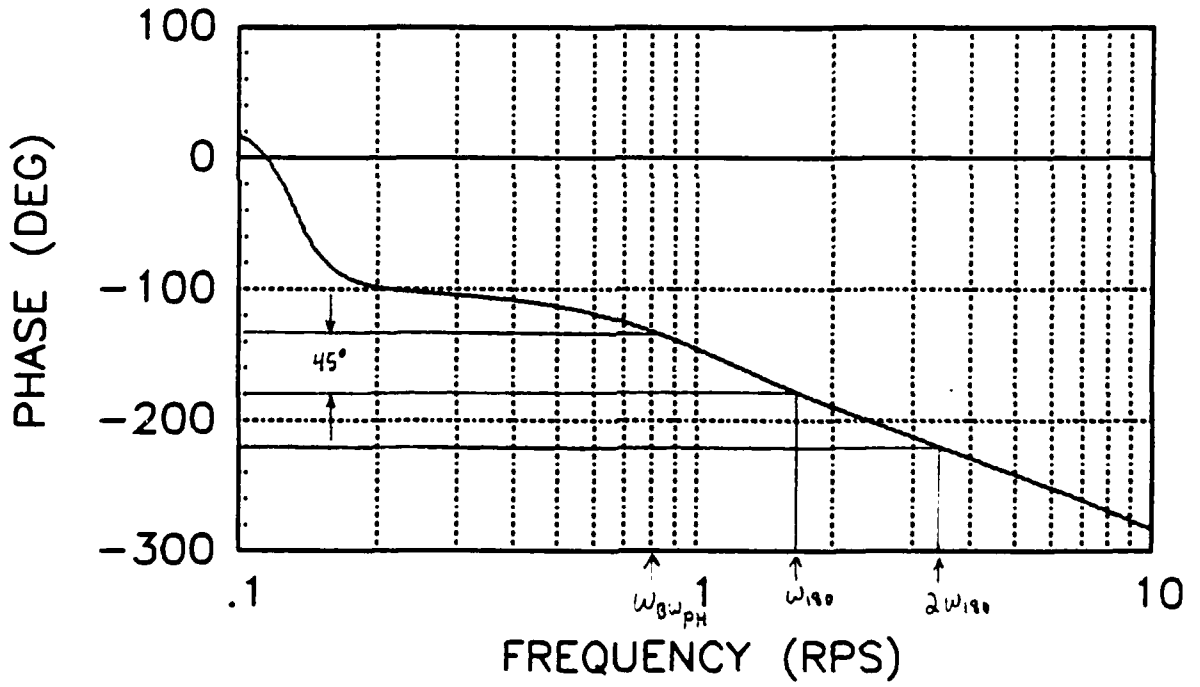

ω_{BW} = min[$\omega_{BWphase}$, ω_{BWgain}] = 0.80 rps

$$\tau_p = -[\phi(2\omega_{180})+180]/[57.3 \times 2\omega_{180}]$$
$$= -[-220+180]/[2(1.6)(57.3)]$$
$$= 0.218 \text{ sec}$$

Predicted Flying Qualities - Level 3

Figure H4. Bandwidth Results for Configuration 1-3

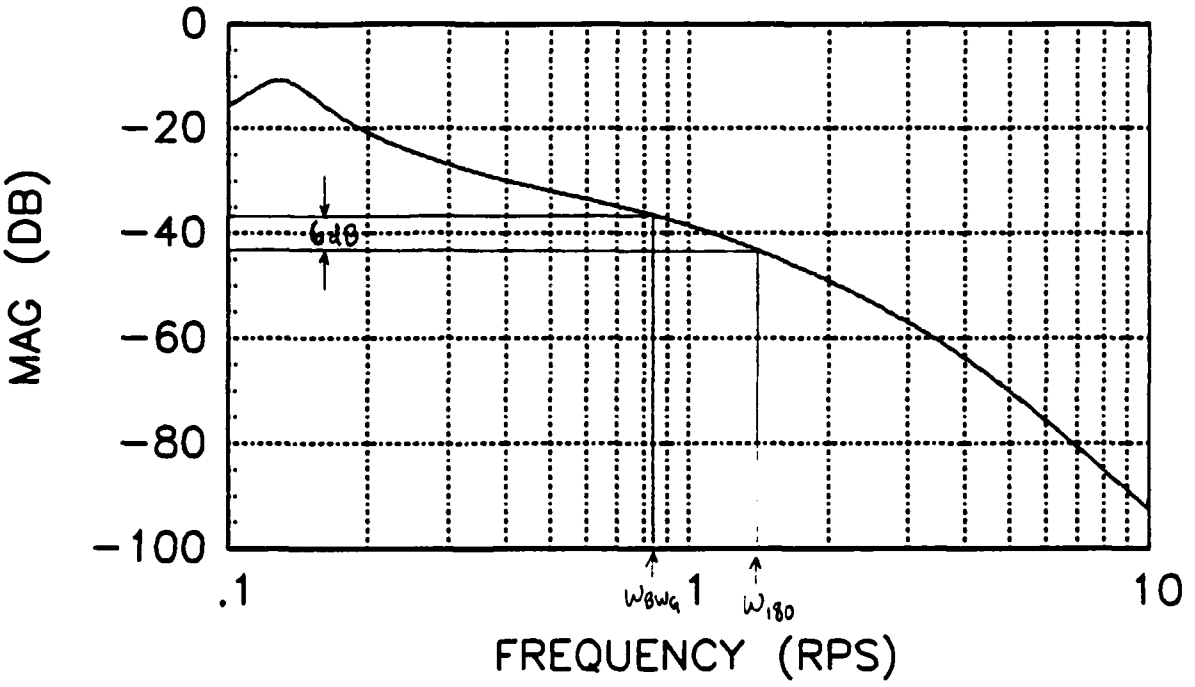

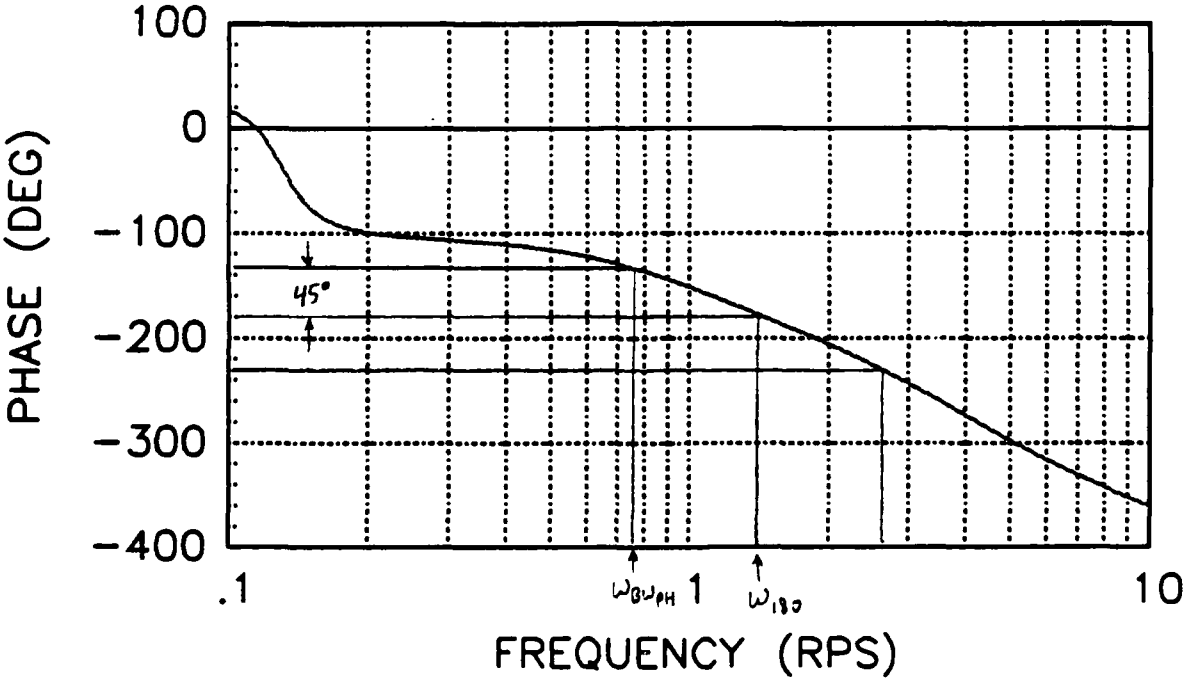

$\omega_{BW} = \min[\omega_{BWphase}, \omega_{BWgain}] = 0.76$ rps

$$\tau_p = -[\Phi(2\omega_{180})+180]/[57.3x2\omega_{180}]$$
$$= -[-232+180]/[2(1.3)(57.3)]$$
$$= 0.349 \text{ sec}$$

Predicted Flying Qualities - Level 3

Figure H5. Bandwidth Results for Configuration 1-10

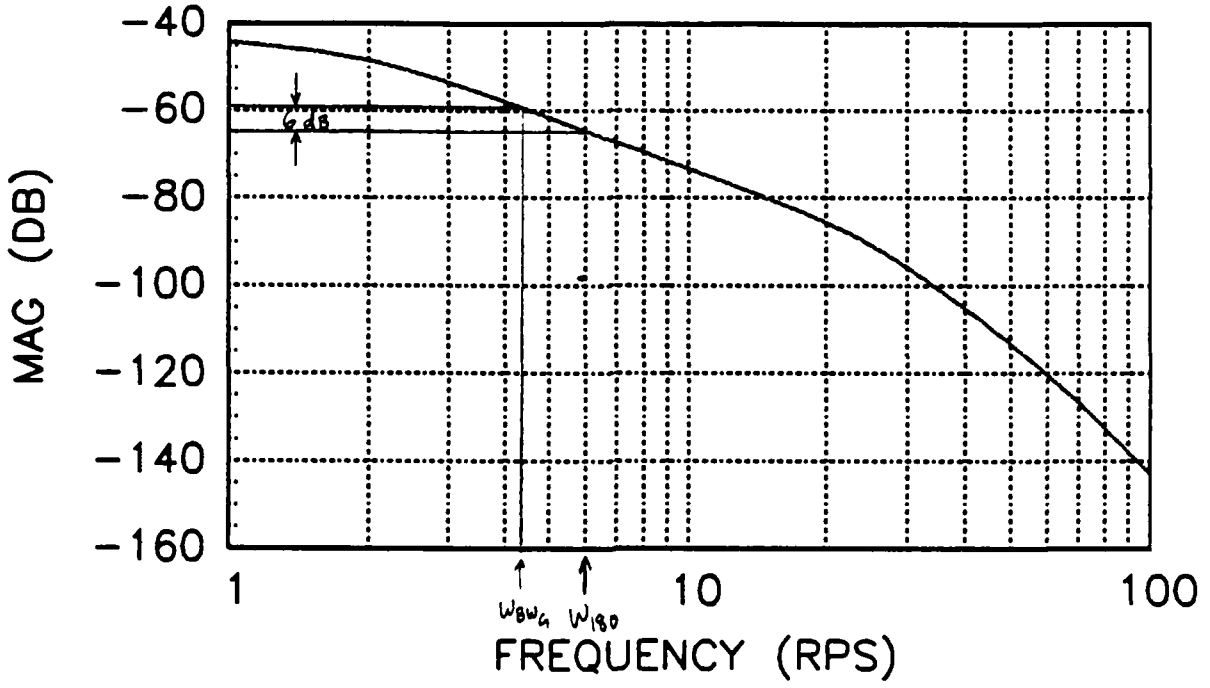

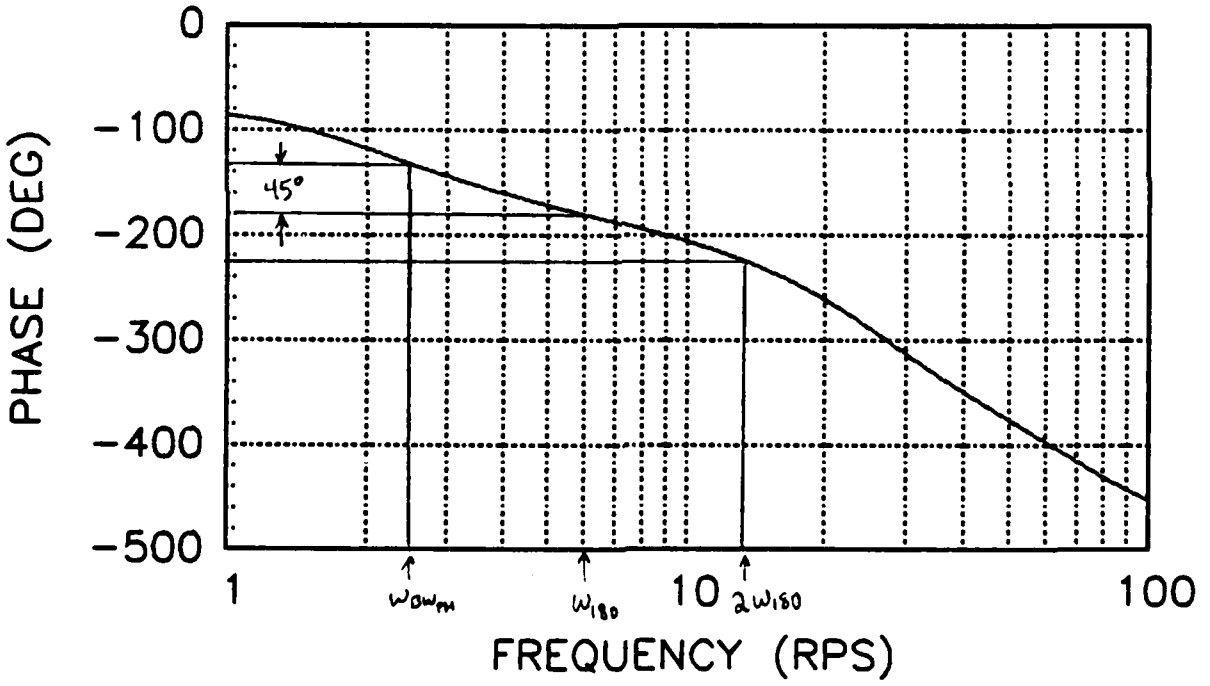

$\omega_{BW} = \min[\omega_{BWphase}, \omega_{BWgain}] = 2.30$ rps

$$\tau_p = -[\Phi(2\omega_{180})+180]/[57.3 \times 2\omega_{180}]$$
$$= -[-225+180]/[2(6.0)(57.3)]$$
$$= 0.065 \text{ sec}$$

Predicted Flying Qualities - Level 2

Figure H6. Bandwidth Results for Configuration 2-1

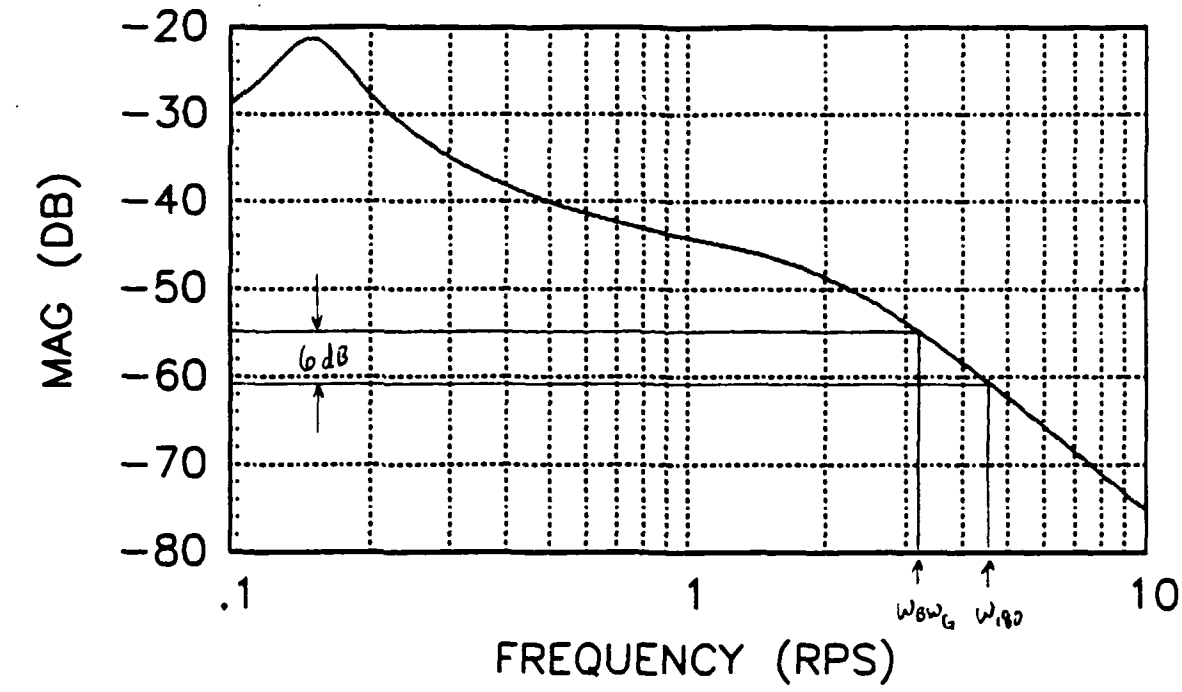

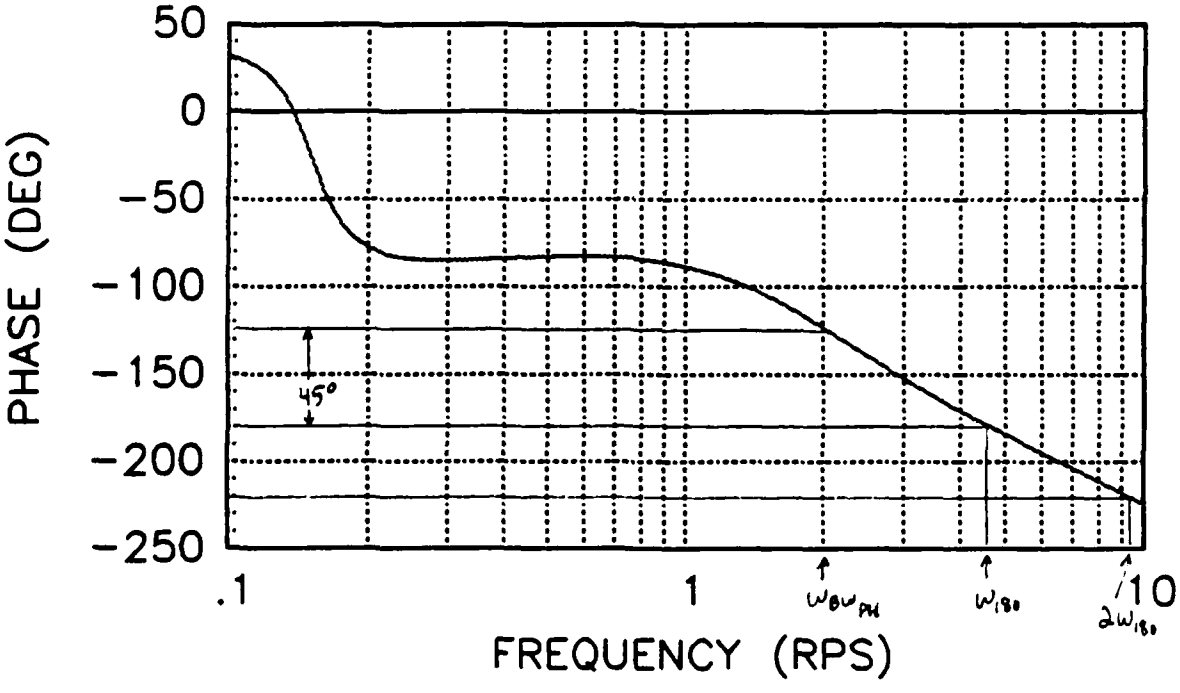

$\omega_{BW} = \min[\omega_{BWphase}, \omega_{BWgain}] = 2.00$ rps

$$\tau_p = -[\Phi(2\omega_{180})+180]/[57.3 \times 2\omega_{180}]$$
$$= -[-221+180]/[2(4.6)(57.3)]$$
$$= 0.078 \text{ sec}$$

Predicted Flying Qualities - Level 2

Figure H7. Bandwidth Results for Configuration 2-D

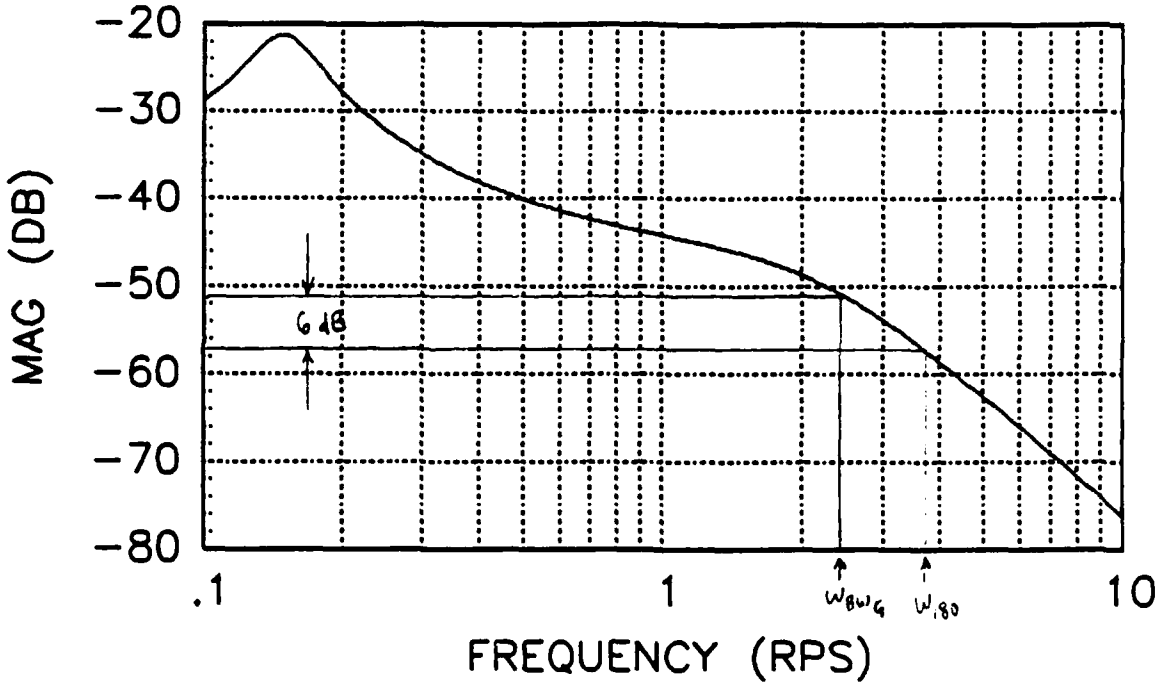

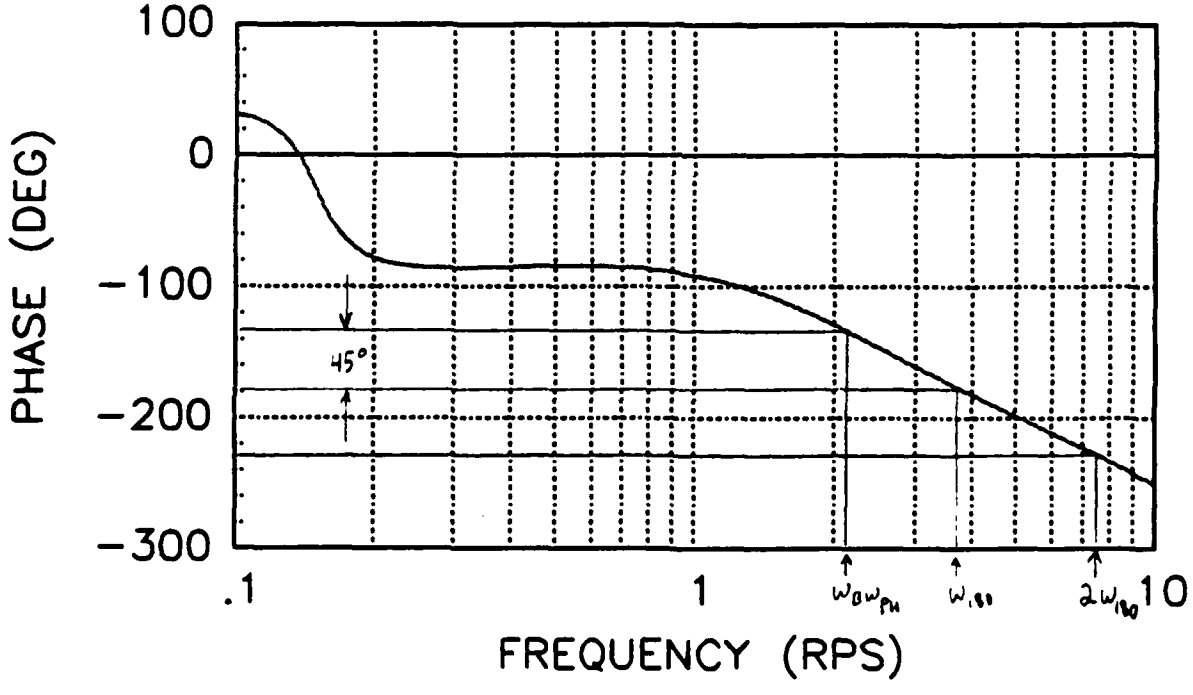

$\omega_{BW} = \min[\omega_{BWphase}, \omega_{BWgain}] = 2.05$ rps

$$\tau_p = -[\phi(2\omega_{180})+180]/[57.3 \times 2\omega_{180}]$$
$$= -[-229+180]/[2(3.7)(57.3)]$$
$$= 0.116 \text{ sec}$$

Predicted Flying Qualities - Level 2

Figure H8. Bandwidth Results for Configuration 2-2

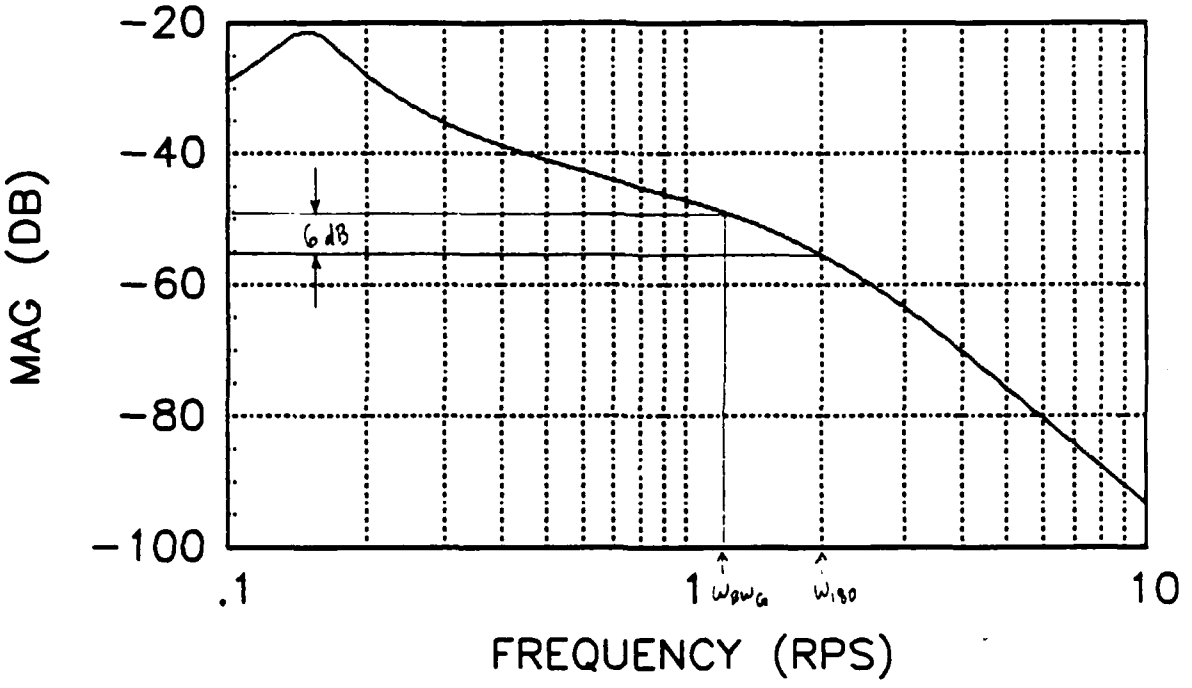

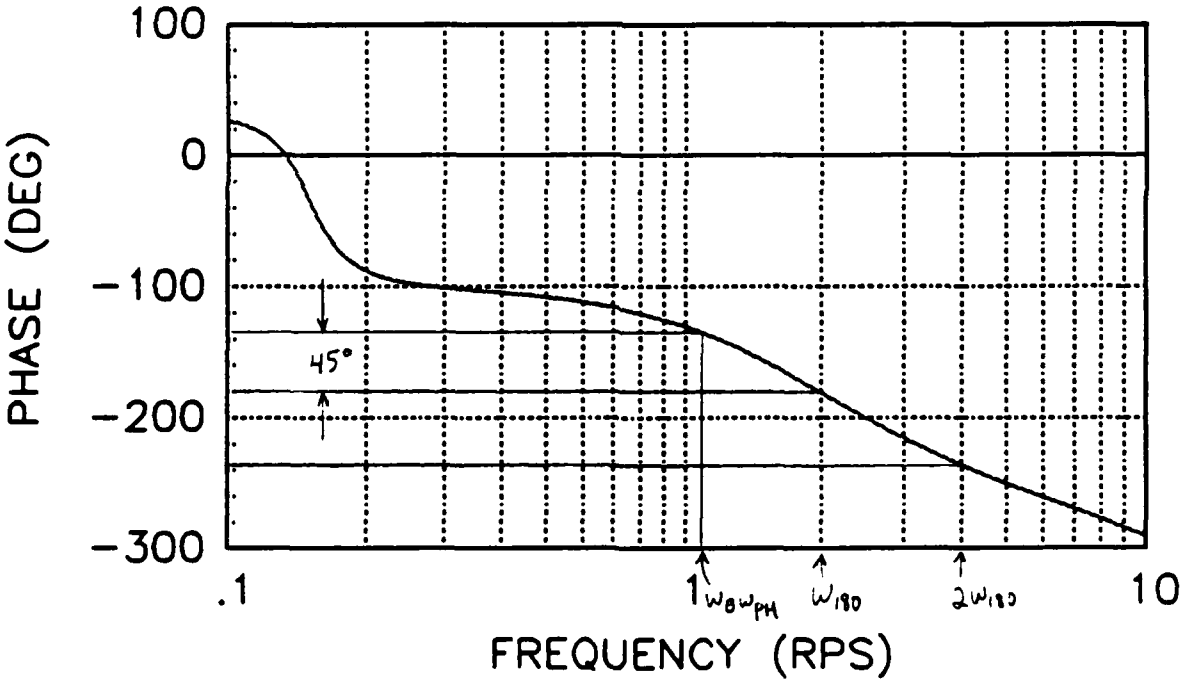

ω_{BW} = min[$\omega_{BWphase}$, ω_{BWgain}] = 1.05 rps

$$\tau_p = -[\phi(2\omega_{180})+180]/[57.3x2\omega_{180}]$$
$$= -[-238+180]/[2(2.0)(57.3)]$$
$$= 0.253 \text{ sec}$$

Predicted Flying Qualities - Level 3

Figure H9. Bandwidth Results for Configuration 2-5

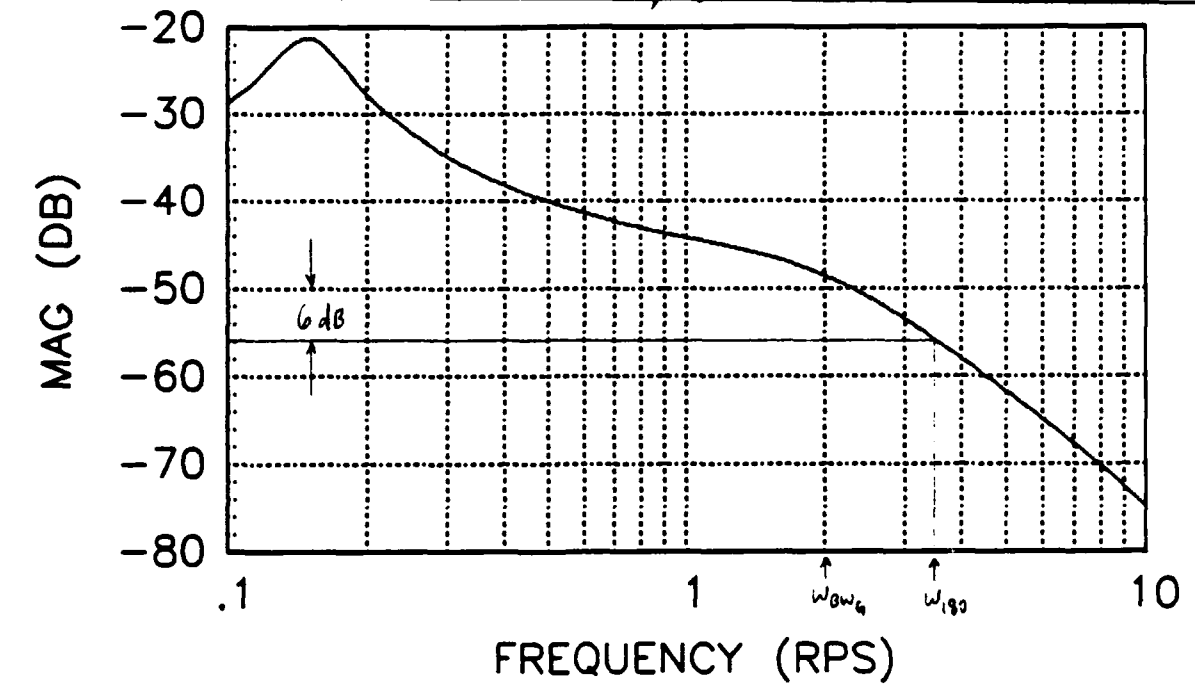

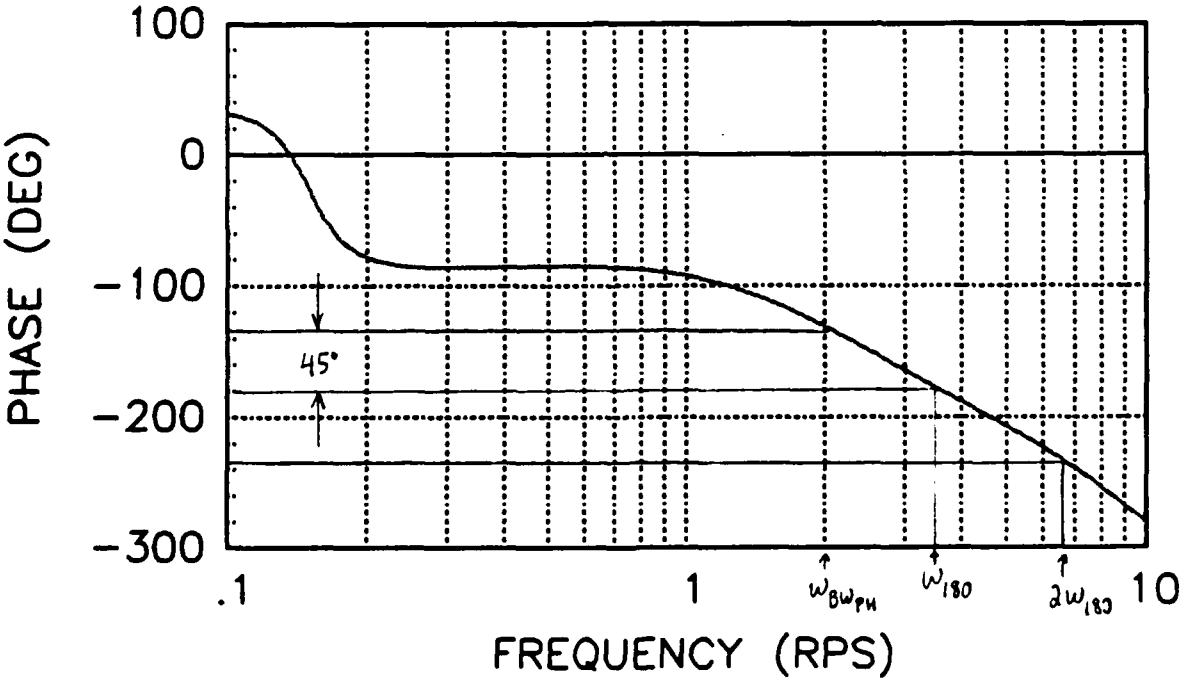

$\omega_{BW} = \min[\omega_{BWphase}, \omega_{BWgain}] = 2.00$ rps

$$\tau_p = -[\phi(2\omega_{180})+180]/[57.3 \times 2\omega_{180}]$$
$$= -[-235+180]/[2(3.25)(57.3)]$$
$$= 0.148 \text{ sec}$$

Predicted Flying Qualities - Level 2

Figure H10. Bandwidth Results for Configuration 2-7

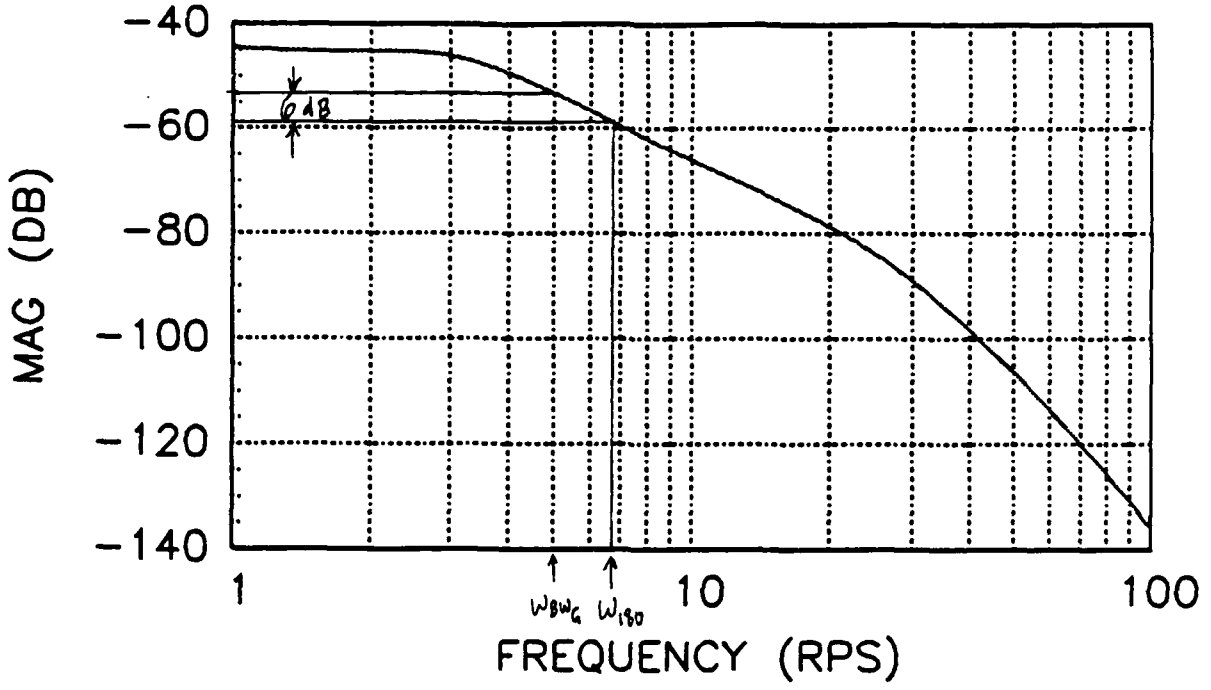

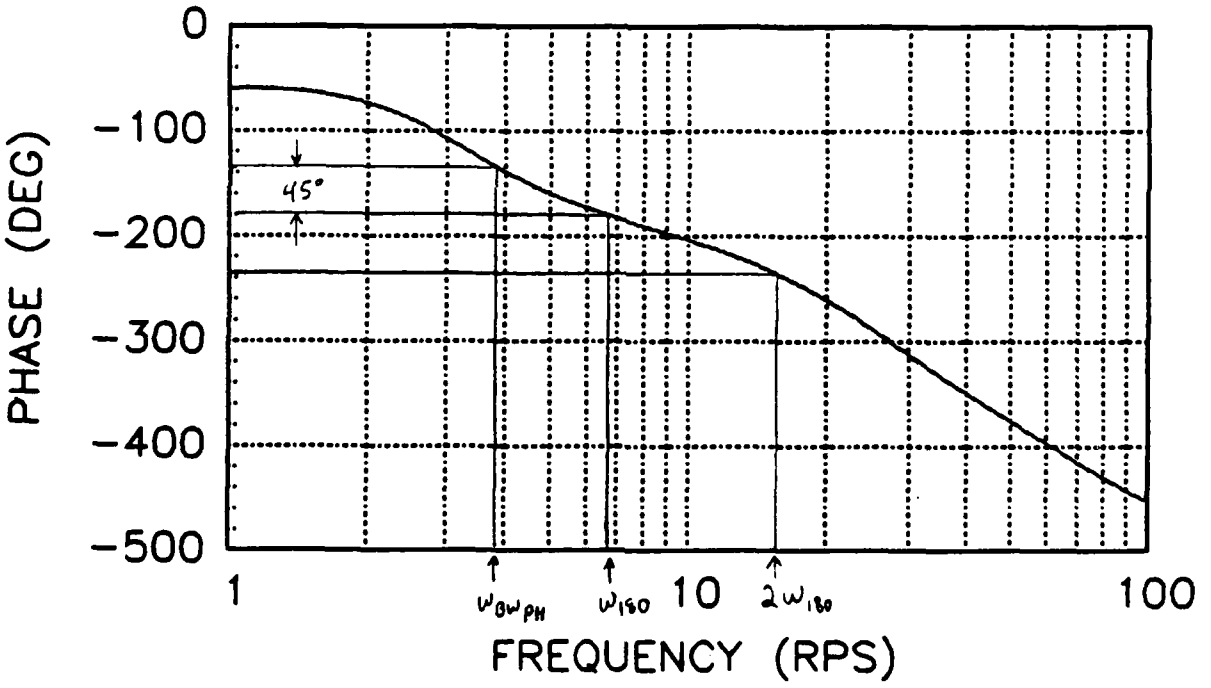

$\omega_{BW} = \min[\omega_{BWphase}, \omega_{BWgain}] = 3.80$ rps

$$\tau_p = -[\phi(2\omega_{180})+180]/[57.3 \times 2\omega_{180}]$$
$$= -[-237+180]/[2(6.7)(57.3)]$$
$$= 0.074 \text{ sec}$$

Predicted Flying Qualities - Level 1

Figure H11. Bandwidth Results for Configuration 3-1

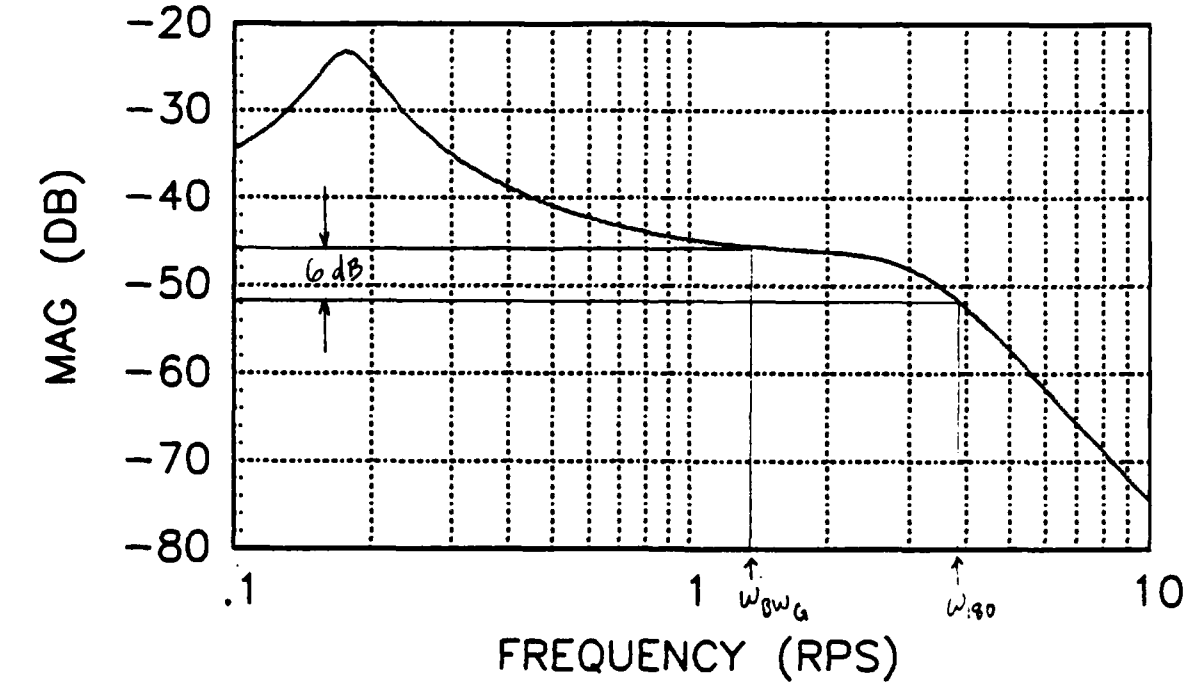

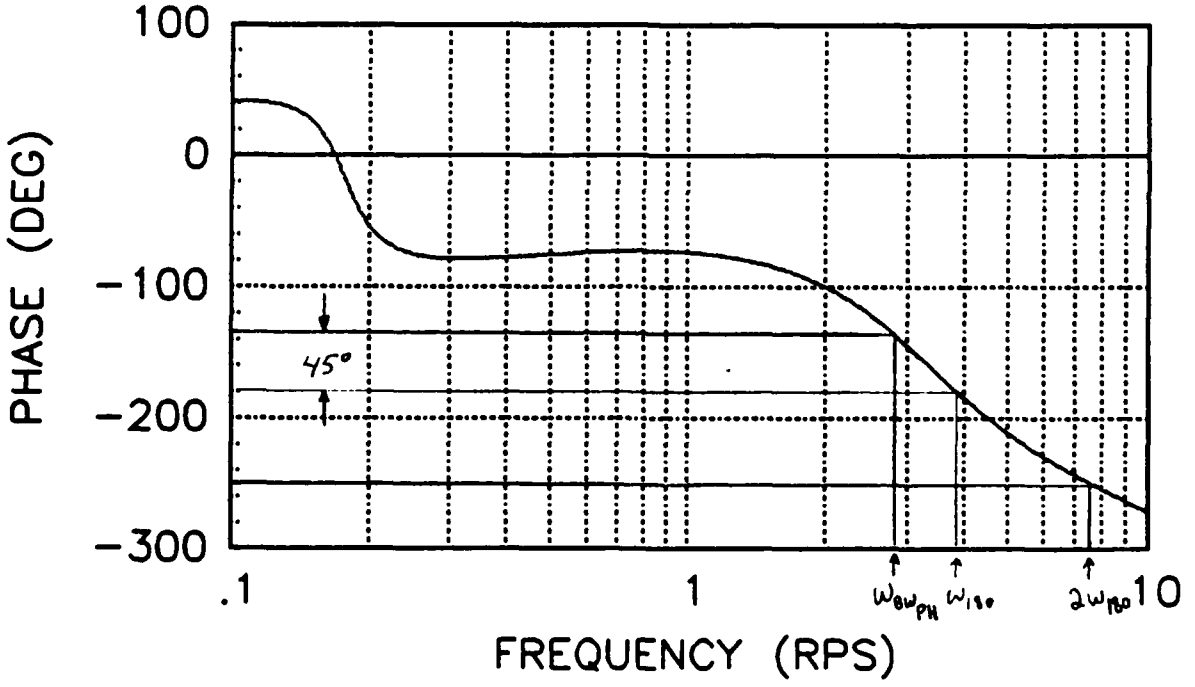

$\omega_{BW} = \min[\omega_{BWphase}, \omega_{BWgain}] = 1.25$ rps

$$\tau_p = -[\phi(2\omega_{180})+180]/[57.3 \times 2\omega_{180}]$$
$$= -[-250+180]/[2(3.8)(57.3)]$$
$$= 0.161 \text{ sec}$$

Predicted Flying Qualities - Level 2

Figure H12. Bandwidth Results for Configuration 3-3

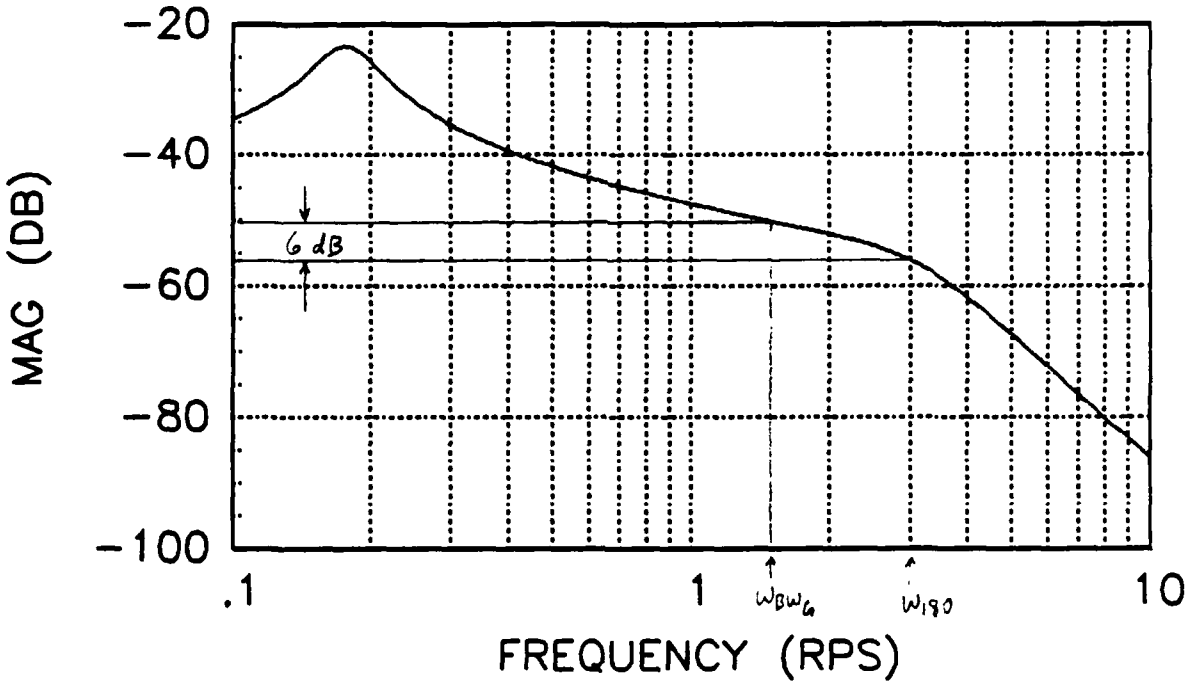

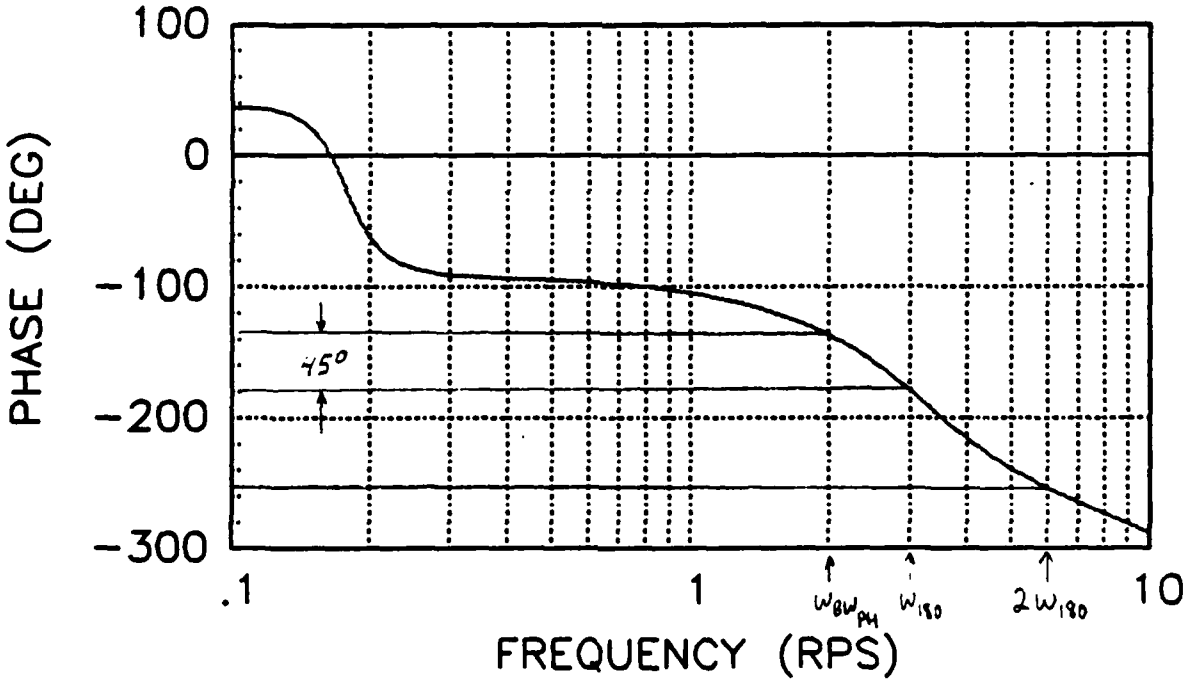

$\omega_{BW} = \min[\omega_{BW_{phase}}, \omega_{BW_{gain}}] = 1.30$ rps

$$\tau_p = -[\phi(2\omega_{180})+180]/[57.3 \times 2\omega_{180}]$$
$$= -[-253+180]/[2(3.0)(57.3)]$$
$$= 0.212 \text{ sec}$$

Predicted Flying Qualities - Level 3

Figure H13. Bandwidth Results for Configuration 3-5

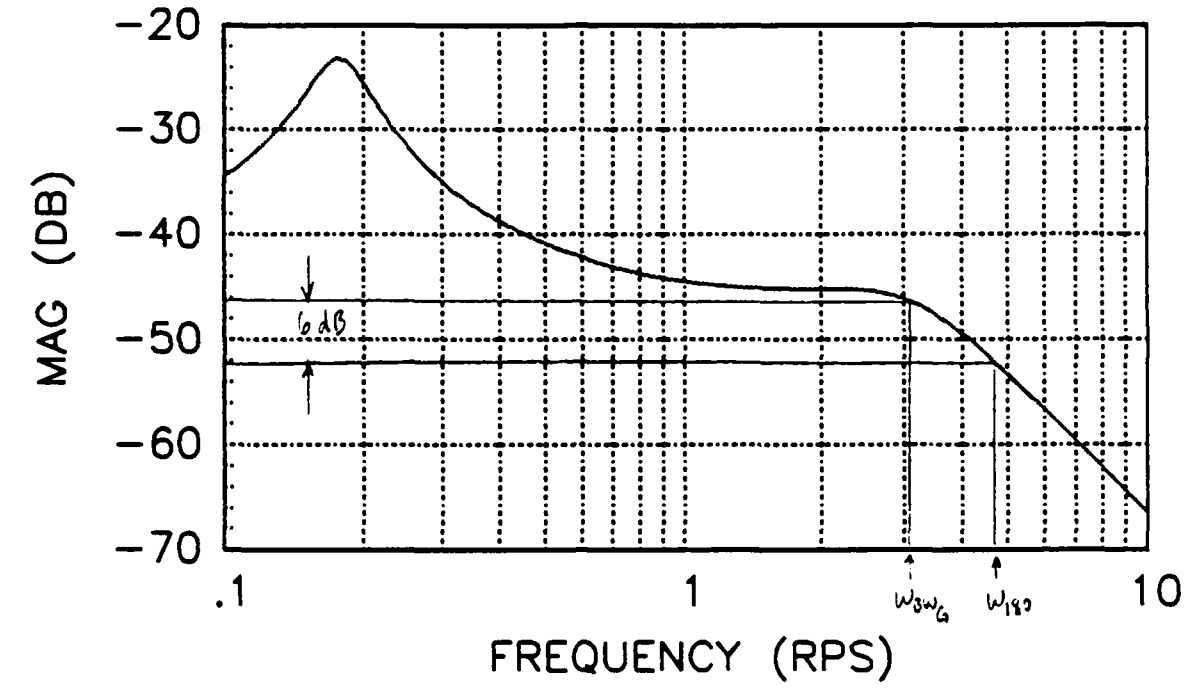

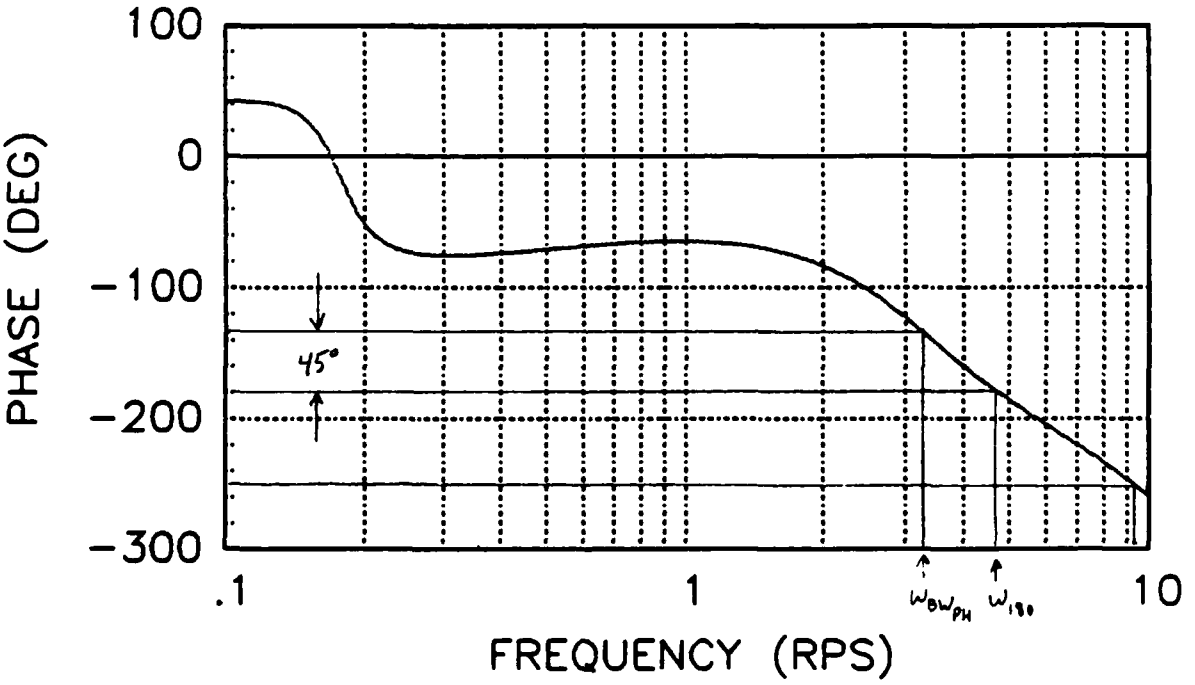

ω_{BW} = min[$\omega_{BWphase}$, ω_{BWgain}] = 3.02 rps

$$\tau_p = -[\Phi(2\omega_{180})+180]/[57.3x2\omega_{180}]$$
$$= -[-250+180]/[2(4.6)(57.3)]$$
$$= 0.133 \text{ sec}$$

Predicted Flying Qualities - Level 2

Figure H14. Bandwidth Results for Configuration 3-6

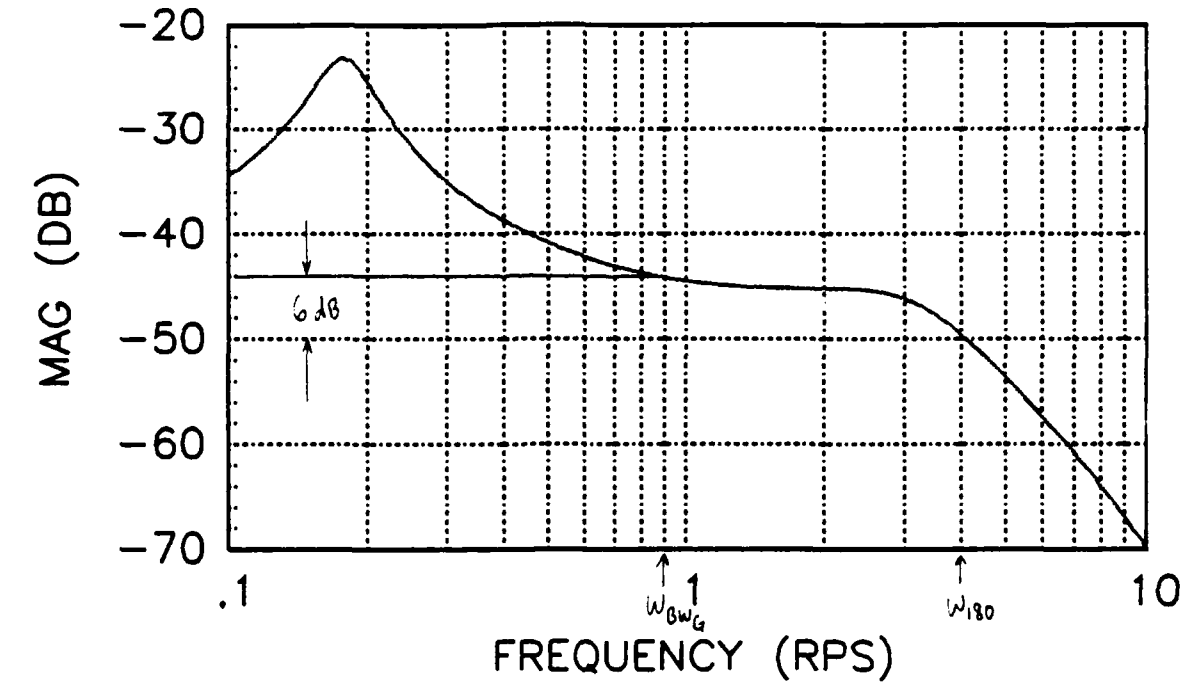

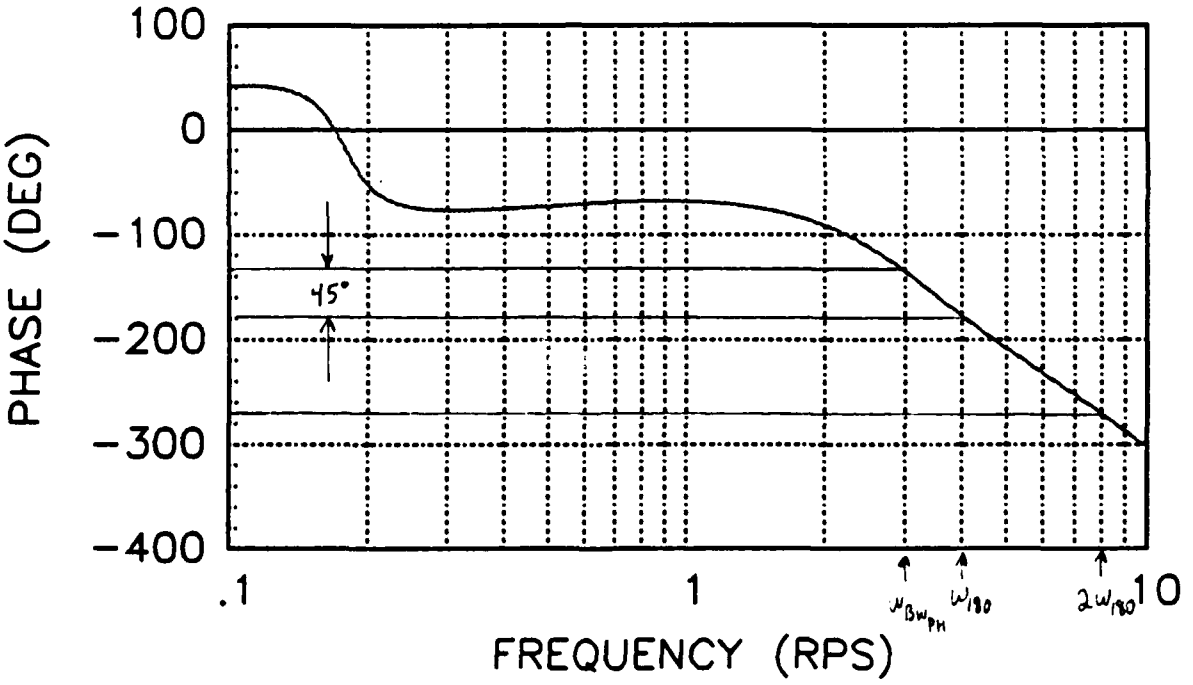

$\omega_{BW} = \min[\omega_{BW_{phase}}, \omega_{BW_{gain}}] = 0.90$ rps

$$\tau_p = -[\phi(2\omega_{180})+180]/[57.3 \times 2\omega_{180}]$$
$$= -[-270+180]/[2(4.0)(57.3)]$$
$$= 0.196 \text{ sec}$$

Predicted Flying Qualities - Level 3

Figure H15. Bandwidth Results for Configuration 3-8

Bibliography

1. Military Specification, Flying Qualities of Piloted Airplanes, MIL-F-8785B. August 1969.

2. Military Specification, Flying Qualities of Piloted Airplanes, MIL-F-8785C. November 1980.

3. Military Standard, Flying Qualities of Piloted Vehicles, MIL-STD-1797. April 1987.

4. Hodgkinson, J. "Equivalent Systems Criteria for Handling Qualities of Military Aircraft," Criteria for Handling Qualities of Military Aircraft. AGARD-CP-333. June 1982.

5. McRuer, Duane et al. Aircraft Dynamics and Automatic Control. Princeton, NJ: Princeton University Press. 1973.

6. Leggett, David. Flying Qualities Engineer. Personal Interview. Flying Qualities Group, FDL/AFWAL/FDCC, Wright-Patterson AFB OH. October 1988.

7. Hodgkinson, J. et al. "Equivalent System Verification and Evaluation of Augmentation Effects on Fighter Approach and Landing Flying Qualities," AFWAL-TR-81-3116, Volume 1. AFWAL/AFSC Wright-Patterson AFB OH. September 1981.

8. Hodgkinson, J. and K. A. Johnston. "Initial Results of an Inflight Simulation of Augmented Dynamics in Fighter Approach and Landing," AIAA paper 79-1783. August 1979.

9. Wood, J. R. and J. Hodgkinson. Definition of Acceptable Levels of Mismatch for Equivalent Systems of Augmented Aircraft. MDC Report A6792. 19 December 1980.

10. DiFranco, D. A. "In-Flight Investigation of the Effects of Higher-Order Control System Dynamics on Longitudinal Handling Qualities," AFFDL-TR-68-90. August 1968.

11. Neal, T. P. and R. E. Smith. "An In-Flight Investigation to Develop Control System Design Criteria for Fighter Airplanes," AFFDL-TR-70-74, Volume 1. December 1970.

12. Hodgkinson, J. et al. "Handling Qualities of Aircraft with Stability and Control Augmentation Systems - A Fundamental Approach," Aeronautical Journal. February 1976.

13. Smith, R. E. "Effects of Control System Dynamics on Fighter Approach and Landing Longitudinal Flying Qualities," AFFDL-TR-78-122, Volume 1 March 1978.

Bibliography (Continued)

14. Shafer, Mary F. "Low-Order Equivalent Models of Highly Augmented Aircraft Determined from Flight Data," AIAA paper 80-1627. August 1980.

15. Biezad, D. J. Systems Theory and Flight Test Techniques. USAF/TPS. Edwards AFB, CA.

16. Roskam, Jan. Airplane Flight Dynamics and Automatic Flight Controls. Ottawa Kansas: Roskam Aviation and Engineering Corp. 1982.

17. Gentry, Thomas A. and L. R. Pujara. "An Example of Preliminary Longitudinal flying Qualities Design Using a Frequency Matching Method,"

18. Hodgkinson, J. et al. "Longitudinal Short-Period Equivalent System Frequency Curve Fit (LONFIT) Users Guide," McDonnell Aircraft Company, McDonnell Douglas Corporation, St. Louis, MO. 25 October 1978.

19. Hodgkinson, J. and J. Buckley. "General Purpose Frequency Response Curve Fit (MACFIT) Users Guide," McDonnell Aircraft Company, McDonnell Douglas Corporation, St. Louis, MO. 25 October 1978.

20. Mitchell, D. G. and R. H. Hoh. "Low-Order Approaches to High-Order Systems: Problems and Promises," AIAA paper 82-4250. April 1982.

21. D Azzo, J. J. and C. H. Houpis. Linear Control System Analysis and Design. Third Edition. New York: McGraw-Hill Book Company. 1988.

22. Franklin, G. F. and J. D. Powell. Digital Control of Dynamic Systems. Reading, Mass: Addison-Wesley Publishing Company. 1980.

23. Astrom, K. J. and T. Bohlin. Numerical Identification of Linear Dynamical Systems from Normal Operating Records. New York: Plenum Press. 1966.

24. Sinha, N. and G. Lastman. "Identification of Continuous-Time Multivariable Systems from Sampled Data," International Journal of Control. 1982.

25. Craig, Roy R. Structural Dynamics an Introduction to Computer Methods. New York: John Wiley & Sons, Inc. 1981.

Bibliography (Concluded)

26. Lindsey, Steven W., Capt, et. al. NT-33A Evaluation of the Optimal Control Model and LOES Matching Technique. HAVE CONTROL Final Report. USAFTPS-TR-89A-TM1. USAF Test Pilot School, Edwards AFB CA. December 1989.

27. USAF Series T-33 Aircraft, T.O. 1T-33A-1. 31 January 1973, Change 7, 30 August 1976.

28. Partial Flight Manual. NT-33A S/N 51-4120.

29. Hall, G. W. and R. W. Huber. System Description and Performance Data for the USAF/CAL Variable Stability T-33 Airplane. AFFDL-TR-70-71. Cornell Aeronautical Laboratory, Inc. August 1970.

30. Cooper, G. E. and R. P. Harper Jr. The Use of Pilot Rating in the Evaluation of Aircraft Handling Qualities. NASA TN-D-5153. Dryden Flight Test Center: National Aeronautics and Space Administration. April 1969.

31. Integrated Systems, Inc. $Matrix_X$ Users Guide - Engineering Analysis and Control Design. Version 6.0. May 1986.

32. Hodgkinson, J., J. R. Wood and R. H. Hoh. An Alternative Method of Specifying Bandwidth for Flying Qualities. AIAA Paper 82-1609. New York, N.Y. 1982.

VITA

Captain Clarke O. Manning [redacted]. He received a Bachelor of Science degree in Zoology from Brigham Young University in April 1980. After graduation he attended the USAF Officer Training School (OTS) and was commissioned a Second Lieutenant in the United States Air Force. He then attended the Air Force Institute of Technology (AFIT) at Wright-Patterson Air Force Base, Ohio, where he earned a Bachelor of Science degree in Aeronautical Engineering. He completed AFIT as a distinguished graduate in April 1985 and was assigned to the Harry G. Armstrong Aerospace Medical Research Laboratory (AAMRL) at Wright-Patterson AFB. His duties at AAMRL included research, test, and development of crew protection and escape systems such as the advanced concept Crew Escape Technology (CREST) ejection seat and the Boeing/AAMRL hypervelocity escape capsule for the National Aerospace Plane (NASP). In 1987, Captain Manning was selected for the Joint Air Force Institute of Technology - Test Pilot School (AFIT/TPS) Program. He entered AFIT in September 1987 and after completing the course work at Wright-Patterson began the Flight Test Engineering course at the USAF Test Pilot School in January 1989. He graduated from the Test Pilot School in December 1989 and upon completion of the AFIT/TPS thesis project received a Master of Science degree in Aeronautical Engineering from the Air Force Institute of Technology. Captain Manning is now assigned as a flight test engineer to the 4950th Test Wing at Wright-Patterson AFB, Ohio.

SECURITY CLASSIFICATION OF THIS PAGE

REPORT DOCUMENTATION PAGE

Form Approved
OMB No. 0704-0188

1a. REPORT SECURITY CLASSIFICATION UNCLASSIFIED	1b. RESTRICTIVE MARKINGS
2a. SECURITY CLASSIFICATION AUTHORITY	3. DISTRIBUTION / AVAILABILITY OF REPORT Approved for public release; distribution unlimited
2b. DECLASSIFICATION / DOWNGRADING SCHEDULE	
4. PERFORMING ORGANIZATION REPORT NUMBER(S) AFIT/GAE/ENY/90M-02	5. MONITORING ORGANIZATION REPORT NUMBER(S)
6a. NAME OF PERFORMING ORGANIZATION School of Engineering 6b. OFFICE SYMBOL (If applicable) AFIT/ENY	7a. NAME OF MONITORING ORGANIZATION
6c. ADDRESS (City, State, and ZIP Code) Air Force Institute of Technology Wright-Patterson AFB, Ohio 45433	7b. ADDRESS (City, State, and ZIP Code)
8a. NAME OF FUNDING / SPONSORING ORGANIZATION USAF Test Pilot School 8b. OFFICE SYMBOL (If applicable) USAFTPS/CDR	9. PROCUREMENT INSTRUMENT IDENTIFICATION NUMBER
8c. ADDRESS (City, State, and ZIP Code) Edwards AFB, CA 93523	10. SOURCE OF FUNDING NUMBERS PROGRAM ELEMENT NO. / PROJECT NO. / TASK NO / WORK UNIT ACCESSION NO.
11. TITLE (Include Security Classification) See Box 19	
12. PERSONAL AUTHOR(S) Clarke O. Manning, B.S., Captain, USAF	
13a. TYPE OF REPORT M.S. Thesis 13b. TIME COVERED FROM _____ TO _____ 14. DATE OF REPORT (Year, Month, Day) 1990 March 15. PAGE COUNT 264	
16. SUPPLEMENTARY NOTATION	

17. COSATI CODES			18. SUBJECT TERMS (Continue on reverse if necessary and identify by block number)
FIELD	GROUP	SUB-GROUP	
01	04		Equivalent Systems, Parameter Identification, Flight Controls, Handling Qualities, NT-33

19. ABSTRACT (Continue on reverse if necessary and identify by block number)

Title: Development of a Least Squares Time Response Lower-Order Equivalent Systems Technique

Thesis Chairman: Major (Dr.) Daniel Gleason
Adjunct Assistant Professor of Aerospace Engineering

20. DISTRIBUTION / AVAILABILITY OF ABSTRACT ☒ UNCLASSIFIED/UNLIMITED ☐ SAME AS RPT ☐ DTIC USERS	21. ABSTRACT SECURITY CLASSIFICATION UNCLASSIFIED
22a. NAME OF RESPONSIBLE INDIVIDUAL Major (Dr.) Daniel Gleason	22b. TELEPHONE (Include Area Code) 805-277-4369 22c. OFFICE SYMBOL USAFTPS/CDR

DD Form 1473, JUN 86 *Previous editions are obsolete* SECURITY CLASSIFICATION OF THIS PAGE

The most widely accepted method for specifying flying qualities of highly-augmented aircraft is the low-order equivalent systems technique. This technique matches the frequency response of a high-order system (HOS) with a lower-order equivalent system (LOES). The LOES is generally in the form of a "classical" (unaugmented) aircraft so that comparisons with the classical data base can be made. Most LOES research has been accomplished using frequency response matching, however there are also methods available for matching the time responses of the HOS and LOES. Time response matching is an attractive option for flight test applications since all that is required is output versus input data.

This thesis develops and tests a Least Squares LOES time response matching program. The program was tested analytically at the Air Force Institute of Technology, Wright-Patterson AFB, OH. During the analytical testing, a HOS was modeled using an A-4D aircraft with servo-actuator and feel system dynamics. Lower order equivalent parameters were calculated using the Least Squares program and the results were compared to those obtained using a frequency response matching program (LONFIT). Various flight conditions and feel system dynamics were used to change the HOS dynamics and the effects of these changes on the two matching techniques were investigated.

The Least Squares LOES program was also tested during a flight test program the the USAF Test Pilot School, Edwards AFB, CA. During this test, a variable stability NT-33A aircraft operated by the CALSPAN Corporation was used to model the higher-order aircraft dynamics. Thirteen configurations were tested using system identification and offset landing tasks. The configurations were chosen to span Level 1, 2, and 3 flying qualities by varying the short period natural frequency, the short period damping ratio, and pre-filter dynamics. The LOES Least Squares program was used to predict the flying qualities of the configurations based on MIL-STD-1797 guidance for equivalent time delay, short period natural frequency, and short period damping ratio. Parameter identification was also accomplished using the actual flight test output versus input data. The results of the flying qualities predictions were compared to predictions given by Hoh's Bandwidth method for specifying flying qualities.